Structural Engineering Report No. 109

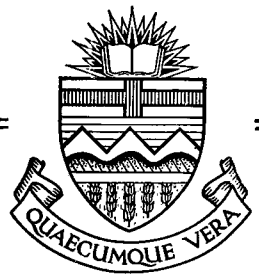

TESTS OF REINFORCED CONCRETE DEEP BEAMS

by

D. M. ROGOWSKY

J. G. MacGREGOR

S. Y. ONG

November, 1983

TESTS OF REINFORCED CONCRETE DEEP BEAMS

by

D.M. Rogowsky

J.G. MacGregor

S.Y. Ong

Structural Engineering Report #109

Department of Civil Engineering
The University of Alberta
Edmonton, Alberta, Canada

September, 1983

Abstract

The construction and testing of 23 reinforced concrete deep beams is described and the test data is presented. The beams consisted of 6 simple span beams and 17 two span continuous beams, each span being 2 m in length. The shear span to depth ratios ranged from 1 to 2.5. Various arrangements and amounts of web reinforcement were used including: no web reinforcement, minimum and maximum horizontal web reinforcement, and minimum and maximum vertical web reinforcement. The beams were supported and loaded by columns cast monolithically with the beams. The loads were applied through columns to the top of the beams at midspan.

Measurements made during each test included applied loads and reactions, midspan deflections, and concrete and steel strains. The strains were measured over 2 and 5 inch gage lengths. Cracks were marked and photographed at each load step.

The beams generally failed in shear, exhibiting a wide range in behavior, ranging from very brittle to very ductile, depending on the amount and arrangement of the web reinforcement, and the shear span to depth ratio.

ACKNOWLEDGEMENTS

The assistance and cooperation of the many staff of the I. F. Morrison Laboratory, University of Alberta, in conducting the experimental program is gratefully acknowledged.

This study was made possible by Grant A1673 from the Natural Sciences and Engineering Research Council of Canada.

Thanks are extended to Darlene Rogowsky for her arduous task of typing the text and numerous diagrams.

Table of Contents

Chapter		Page
1.	Introduction	1
	1.1 Overview of Deep Beam Study	1
	1.2 Object and Scope of Test Series	2
2.	Test Specimens	4
	2.1 Introduction	4
	2.2 Details of Specimens	6
3.	Materials and Material Properties	19
	3.1 Reinforcement	19
	3.1.1 Steel Properties	19
	3.1.2 Assembly of Reinforcement	21
	3.2 Concrete	26
	3.2.1 Ingredients and Mix Proportions	26
	3.2.2 Concrete Strength Properties	30
4.	Instrumentation	33
	4.1 Overview	33
	4.2 Loads and Reactions	33
	4.3 Steel Strains	35
	4.4 Concrete Strains	36
	4.5 Displacements	37
	4.6 Crack Observations	39
5.	Testing	41
	5.1 Test Set-Up	41
	5.2 Testing Procedure	41
	5.3 Support Settlement	44
6.	Test Results	48

6.1 Presentation of Results 48
6.2 Failure Loads 48
6.3 Deflections and Support Settlements 52
6.4 Mode of Data Presentation 52
6.5 Beam 1/1.0 61
6.6 Beam 2/1.0 69
6.7 Beam 3/1.0 74
6.8 Beam 4/1.0 80
6.9 Beam 5/1.0 80
6.10 Beam 6/1.0 91
6.11 Beam 7/1.0 97
6.12 Beam 1/1.5 103
6.13 Beam 2/1.5 108
6.14 Beam 3/1.5 113
6.15 Beam 4/1.5 113
6.16 Beam 5/1.5 113
6.17 Beam 6/1.5 121
6.18 Beam 7/1.5 121
6.19 Beam 8/1.5 127
6.20 Beam 1/2.0 127
6.21 Beam 2/2.0 133
6.22 Beam 3/2.0 138
6.23 Beam 4/2.0 138
6.24 Beam 5/2.0 147
6.25 Beam 6/2.0 152
6.26 Beam 7/2.0 157
6.27 Beam 5/2.5 157

7. Summary and Conclusions 167

List of Tables

Table		Page
2.1	Reinforcement Details of Specimens	7
2.2	Geometric Details of Specimens	8
3.1	Steel Stress-Strain Analysis	20
3.2	Mix Design for 8 Cubic Foot Batch	28
3.3	Concrete Properties	31
6.1	Experimental Loads and Reactions	49
6.2	Balanced Loads and Reactions	50
6.3	Ultimate Shear Strengths	51

List of Figures

Figure		Page
2.1	Typical Test Series	5
2.2	Overall Dimension of Specimens	9
2.3	Beam 1/1.0 and 2/1.0 Reinforcement Details	10
2.4	Beam 3/1.0 and 4/1.0 Reinforcement Details	11
2.5	Beam 5/1.0, 6/1.0, and 7/1.0 Reinforcement Details	12
2.6	Beam 1/1.5 and 2/1.5 Reinforcement Details	13
2.7	Beam 3/1.5, 4/1.5, 5/1.5, 6/1.5, and 7/1.5 Reinforcement Details	14
2.8	Beam 1/2.0 and 2/2.0 Reinforcement Details	15
2.9	Beam 3/2.0, 4/2.0, 5/2.0, 6/2.0, and 7/2.0 Reinforcement Details	16
2.10	Beam 5/2.5 Reinforcement Details	17
3.1	Steel Force-Strain Curves 15M, 20M, and 25M Bars	22
3.2	Steel Force-Strian Curves 10M and 6mm Bars	23
3.3	Welding and Brazing Effects on 10M Bars	25
3.4	Grain Size Analysis of Aggregates	29
4.1	Typical Concrete Strain Gage Layout	38
5.1	Loading Frame and Test Set-Up	42
6.1	Beam 1/1.0, 2/1.0, 3/1.0, and 4/1.0 Load Deflection Curves	53
6.2	Beam 5/1.0, 6/1.0, and 7/1.0 Load Deflction Curves	54
6.3	Beam 1/1.5, 2/1.5, 3/1.5, and 4/1.5 Load-Deflection Curves	55
6.4	Beam 5/1.5, 6/1.5, 7/1.5, and 8/1.5 Load-Deflection Curves	56
6.5	Beam 1/2.0 and 2/2.0 Load-Deflection Curves	57

Figure Page

6.6 Beam 3/2.0 and 4/2.0 Load-Deflection Curves.....58

6.7 Beam 5/2.0 and 6/2.0 Load-Deflection Curves.....59

6.8 Beam 7/2.0 and 5/2.5 Load-Deflection Curves.....60

6.9 Beam 1/1.0 Crack Patterns.....62

6.10 Beam 1/1.0 Horizontal Concrete Compressive Strains.....63

6.11 Beam 1/1.0 Concrete Compressive Strains.....64

6.12 Beam 1/1.0 Retest Concrete Compressive Strains.....65

6.13 Beam 1/1.0 Steel Strains.....66

6.14 Beam 1/1.0 Load vs. Steel Strains.....67

6.15 Beam 2/1.0 Crack Patterns.....70

6.16 Beam 2/1.0 Concrete Compressive Strains.....71

6.17 Beam 2/1.0 Steel Strains.....72

6.18 Beam 2/1.0 Load vs. Steel Strains.....73

6.19 Beam 3/1.0 Crack Patterns - West Face.....75

6.20 Beam 3/1.0 Crack Patterns - East Face (Reversed)....76

6.21 Beam 3/1.0 Concrete Compressive Strains.....77

6.22 Beam 3/1.0 Steel Strains.....78

6.23 Beam 3/1.0 Load vs. Steel Strain.....79

6.24 Beam 4/1.0 Crack Pattern - West Face.....81

6.25 Beam 4/1.0 Crack Pattern - East Face (Reversed).....82

6.26 Beam 4/1.0 Concrete Compressive Strains.....83

6.27 Beam 4/1.0 Steel Strains.....84

6.28 Beam 4/1.0 Load vs. Steel Strains.....85

6.29 Beam 5/1.0 Crack Pattern - West Face.....86

6.30 Beam 5/1.0 Crack Pattern - East Face (Reversed).....87

Figure Page

6.31 Beam 5/1.0 Concrete Compressive Strains.....88
6.32 Beam 5/1.0 Steel Strains.....89
6.33 Beam 5/1.0 Load vs. Steel Strain.....90
6.34 Beam 6/1.0 Crack Pattern - West Face.....92
6.35 Beam 6/1.0 Crack Pattern - East Face (Reversed).....93
6.36 Beam 6/1.0 Concrete Compressive Strains.....94
6.37 Beam 6/1.0 Steel Strains.....95
6.38 Beam 6/1.0 Load vs. Steel Strain.....96
6.39 Beam 7/1.0 Crack Pattern - West Face.....98
6.40 Beam 7/1.0 Crack Pattern - East Face (Reversed).....99
6.41 Beam 7/1.0 Concrete Compressive Strains.....100
6.42 Beam 7/1.0 Steel Strains.....101
6.43 Beam 7/1.0 Load vs. Steel Strain.....102
6.44 Beam 1/1.5 Crack Patterns.....104
6.45 Beam 1/1.5 Concrete Compressive Strains.....105
6.46 Beam 1/1.5 Steel Strains.....106
6.47 Beam 1/1.5 Load vs. Steel Strain.....107
6.48 Beam 2/1.5 Crack Patterns.....109
6.49 Beam 2/1.5 Concrete Compressive Strains.....110
6.50 Beam 2/1.5 Steel Strains.....111
6.51 Beam 2/1.5 Load vs. Steel Strain.....112
6.52 Beam 3/1.5 Crack Patterns.....114
6.53 Beam 4/1.5 Crack Patterns.....115
6.54 Beam 5/1.5 Crack Patterns.....116
6.55 Beam 5/1.5 Concrete Compressive Strains.....117

Figure Page

6.56 Beam 5/1.5 Steel Strains.....118

6.57 Beam 5/1.5 Load vs. Steel Strain.....119

6.58 Beam 6/1.5 Crack Patterns.....122

6.59 Beam 6/1.5 Concrete Compressive Strains.....123

6.60 Beam 6/1.5 Steel Strains.....124

6.61 Beam 6/1.5 Load vs. Steel Strains.....125

6.62 Beam 7/1.5 Crack Patterns.....126

6.63 Beam 8/1.5 Crack Patterns.....128

6.64 Beam 1/2.0 Crack Patterns.....129

6.65 Beam 1/2.0 Concrete Compressive Strains.....130

6.66 Beam 1/2.0 Steel Strains.....131

6.67 Beam 1/2.0 Load vs. Steel Strain.....132

6.68 Beam 2/2.0 Concrete Crack Patterns.....134

6.69 Beam 2/2.0 Concrete Compressive Strains.....135

6.70 Beam 2/1.0 Steel Strains.....136

6.71 Beam 2/1.0 Load vs. Steel Strain.....137

6.72 Beam 3/2.0 Crack Patterns.....139

6.73 Beam 3/2.0 Concrete Compressive Strains.....140

6.74 Beam 3/2.0 Steel Strains.....141

6.75 Beam 3/2.0 Load vs. Steel Strain.....142

6.76 Beam 4/2.0 Crack Patterns.....143

6.77 Beam 4/2.0 Concrete Compressive Strains.....144

6.78 Beam 4/2.0 Steel Strains.....145

6.79 Beam 4/2.0 Load vs. Steel Strain.....146

6.80 Beam 5/2.0 Crack Patterns.....148

Figure Page

6.81 Beam 5/2.0 Concrete Compressive Strains.....149

6.82 Beam 5/2.0 Steel Strains.....150

6.83 Beam 5/2.0 Load vs. Steel Strain.....151

6.84 Beam 6/2.0 Crack Patterns.....153

6.85 Beam 6/2.0 Concrete Compressive Strains.....154

6.86 Beam 6/2.0 Steel Strains.....155

6.87 Beam 6/2.0 Load vs. Steel Strain.....156

6.88 Beam 7/2.0 Crack Patterns.....158

6.89 Beam 7/2.0 Concrete Compressive Strains.....159

6.90 Beam 7/2.0 Steel Strains.....160

6.91 Beam 7/2.0 Load vs. Steel Strain.....161

6.92 Beam 5/2.5 Crack Patterns.....162

6.93 Beam 5/2.5 Concrete Compressive Strains.....163

6.94 Beam 5/2.5 Steel Strains.....164

6.95 Beam 5/2.5 Load vs. Steel Strain.....165

1. Introduction

1.1 Overview of Deep Beam Study

The use of reinforced concrete deep beams has become more prevelant in recent years. Deep beams often appear in form of transfer girders in highrise buildings as well as pilecaps, foundation walls, tanks, bins, folded plate roof structures, floor diaphrams, shear walls, and brackets or corbels. They are characterized as being relatively short and deep, having a thickness that is small relative to their span or depth, and being primarily loaded in the plane of the member. They are "two dimensional" members in a state of plate stress in which shear is a dominant feature. The internal stresses cannot be determined by ordinary beam theory, and ordinary design procedures for determining strength do not apply.

There have been numerous two dimensional linearly elastic studies of homogenous and isotropic deep beams. Unfortunately reinforced concrete deep beams are far from being linearly elastic or homogeneous and isotropic when the ultimate load is reached and hence such studies are only of moderate value. There have also been extensive experimental investigations of simply supported deep beams, but few if any tests of continuous deep beams.

Design procedures for reinforced concrete deep beams are poorly defined. The current ACI Code design provisions for deep beams, which evolved from simply supported deep

beam studies, are not directly applicable to continuous deep beams. When using the shear capacity equation, one is faced with the mathematical impossibility of dividing by a parameter which can approach zero. There is a need for rational design procedures for deep beams in general, and continuous deep beams in particular.

1.2 Object and Scope of Test Series

This report describes a systematic experimental investigation of reinforced concrete continuous deep beams. This study is intended to provide the basis for a rational physical model which will explain the behavior of deep beams, with the eventual goal being the formulation of safe and rational design procedures for continuous and simply supported deep beams. This report describes the experimental investigation and presents the significant test data. The development of a rational model and rational design recommendations will be considered in a doctoral thesis to follow.

The scope of the test series is limited to the investigation of four prime parameters:

1) shear span to depth ratio
2) amount of vertical web reinforcement (stirrups)
3) amount of horizontal web reinforcement
4) statical conditions i.e. simple shear span vs. continuous shear span

The nominal shear span to depth ratios ranged from 1.0 to

2.5 while the web reinforcement included three levels: none, a low amount (approximately the minimum reinforcement required by the ACI Code), and a large amount (approximately the maximum amount allowed by the ACI Code). A comparable simple span beam was tested for most of the continuous beams in the series. The variation in concrete strengths as actually obtained ranged from 14.5 to 46.8 MPa and hence concrete strength is a fifth parameter in the study.

The main flexural steel and reinforcement details were chosen to preclude failure in modes other than shear.

2. Test Specimens

2.1 Introduction

The standard series of specimens at each shear span to depth ratio consisted of 7 beams as shown schematically in Fig. 2.1. Beams 1 and 2 were simply supported and contained identical flexural reinforcements. Stirrups were provided at only one end of each beam giving a total of 4 different web reinforcement conditions in the 4 simply supported shear spans. The remaining beams in the series were two span continuous beams which had the geometry of two simple spans end to end. All of the continuous beams in a series had the same main flexural reinforcement, and were symmetrical so that 5 different web reinforcement conditions in the continuous shear span were considered.

The identification number for each beam consists of an integer number corresponding to its place in the test series as shown in Fig. 2.1, followed by a "/" and a real number which indicates the nominal shear span to depth ratio, followed by "N" or "S" indicating the north or south shear span. Hence, BM 2/1.0N conceptually has the same basic type of reinforcement, and is directly comparable to BM 2/1.5N and BM 2/2.0N. A suffix of "T1" indicates that the data is for the first test of the beam, (virgin test) while a suffix of "T2" indicates that the data is for the retest of the beam after the initial failure was externally reinforced.

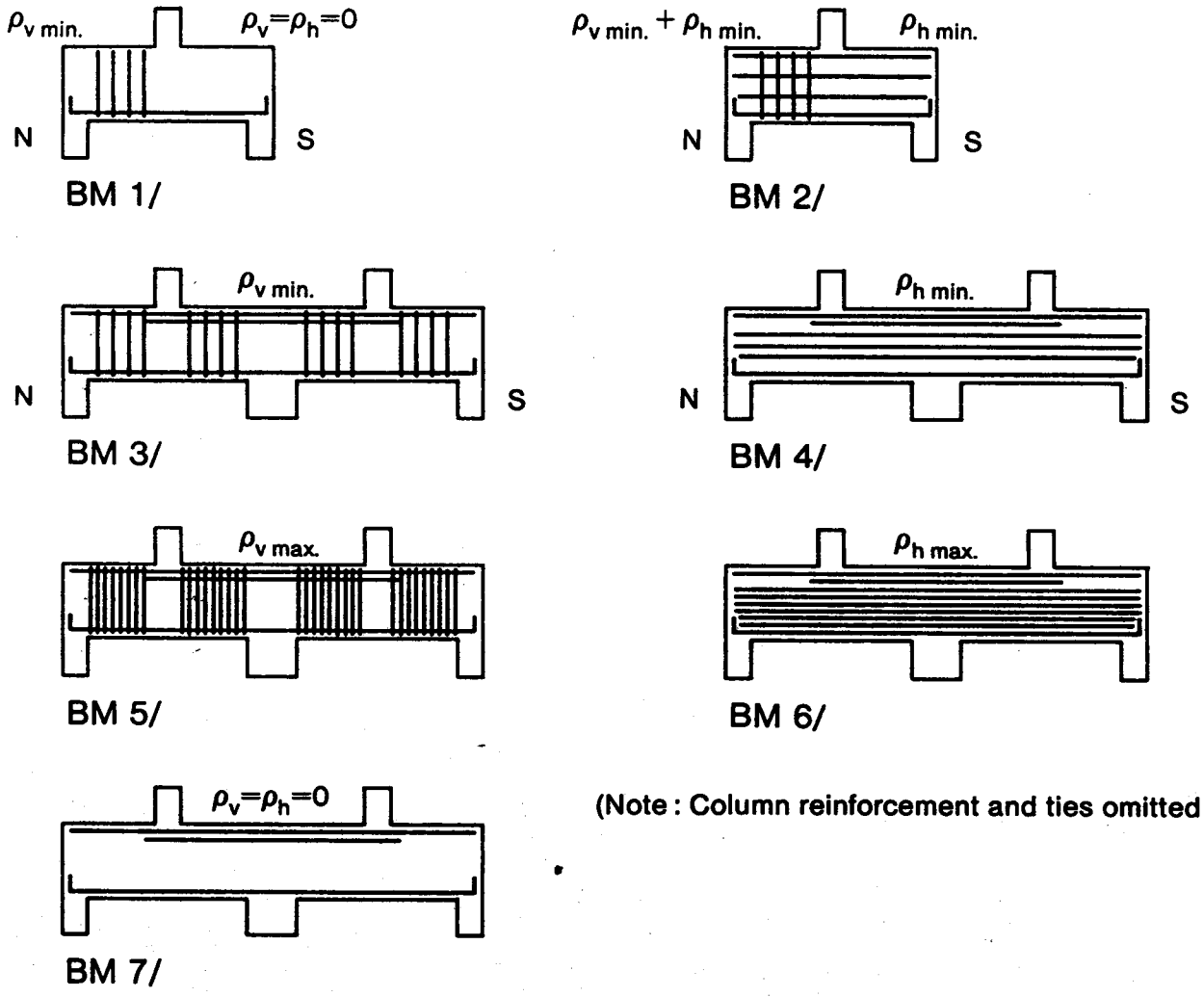

(Note : Column reinforcement and ties omitted for clarity).

Figure 2.1 Typical Test Series

The location of the centre lines of the loads and reactions was the same for all beams tested. Only the beam depth and size of loading column were varied to obtain the desired shear span to depth ratios. The beams were loaded and supported through column stubs cast integrally with the beam to load and support the beam in a realistic manner.

2.2 Details of Specimens

All specimens were concreted in the same forms and differed only in overall depths and number of spans. The overall dimensions are given in Fig. 2.2. The details of the reinforcement for each beam are given in Tables 2.1 and 2.2, and Figures 2.3 to 2.10. In all cases the beam reinforcement passed inside the vertical column bars. The clear cover to the column ties and the top and bottom of the stirrups was 10 mm. The clear side cover to the stirrups was 25 mm. The side clear cover to the outside longitudinal bars was 35 mm except in beams 1, 2, 3 and 4, of the X/1.0 series in which it was 45 mm.

All bottom flexural reinforcement extended the full length of the beam. Both ends of the bars had standard hooks located within the exterior column cages. All column steel extended at least one compression development length into the beam. Horizontal stirrups were anchored at each end with standard hooks. All vertical stirrups were closed stirrups anchored at the top with 135 degree hooks around a main flexural bar or, in the case of simple spans, around a

TABLE 2.1 Reinforcement Details of Specimens

Specimen	Top Steel			Bottom Steel			Web Steel *			
	Bars	$A_s f_y$/Bar (kN)	ρ	Bars	$A_s f_y$/Bar (kN)	ρ	No. of Strips	ρ_v	No. of Horiz. Bars	ρ_h
1/1.0N	-	-	-	6-20M	114	0.0095	4	0.0015	-	-
1/1.0S	-	-	-	6-20M	114	0.0095	-	-	-	-
2/1.0N	2-6mm	16.2	0.0003+	6-20M	114	0.0095	4	0.0015	4	0.0006
2/1.0S	2-6mm	16.2	0.0003+	6-20M	114	0.0095	-	-	4	0.0006
3/1.0	4-20M	114	0.0063	3-20M	114	0.0046	4	0.0015	-	-
4/1.0	4-20M	114	0.0063	3-20M	114	0.0046	-	-	4	0.0006
5/1.0	4-20M	121	0.0063	3-20M	121	0.0046	16	0.0060	-	-
6/1.0	4-20M	121	0.0063	3-20M	121	0.0046	-	-	12	0.0018
7/1.0	4-20M	121	0.0063	3-20M	121	0.0046	-	-	-	-
1/1.5N	-	-	-	6-15M	91	0.0112	5	0.0019	-	-
1/1.5S	-	-	-	6-15M	91	0.0112	-	-	-	-
2/1.5N	2-6mm	16.2	0.0003*	6-15M	91	0.0112	5	0.0019	4	0.0011
2/1.5S	2-6mm	16.2	0.0003*	6-15M	91	0.0112	-	-	4	0.0011
3/1.5	6-15M	91	0.0072**	2-10M 4-15M	46 91	0.0096	5	0.0019	-	-
4/1.5	6-15M	91	0.0072**	2-10M 4-15M	46 91	0.0096	-	-	4	0.0011
5/1.5	6-15M	91	0.0072**	2-10M 4-15M	48 91	0.0096	16	0.0060	-	-
6/1.5	6-15M	91	0.0072**	2-10M 4-15M	48 91	0.0096	-	-	12	0.0032
7/1.5	6-15M	91	0.0072**	2-10M 4-15M	46 91	0.0096	-	-	-	-
8/1.5	6-15M	91	0.0072**	2-10M 4-15M	46 91	0.0096	5	0.0019	4	0.0011
1/2.0N	-	-	-	4-15M	91	0.0088	4	0.0014	-	-
1/2.0S	-	-	-	4-15M	91	0.0088	-	-	-	-
2/2.0N	2-6mm	16.2	0.0003+	4-15M	91	0.0088	4	0.0014	4	0.0012
2/2.0S	2-6mm	16.2	0.0003+	4-15M	91	0.0088	-	-	4	0.0012
3/2.0	4-15M 2-10M	91 48	0.0088**	2-10M 4-15M	48 91	0.0119	4	0.0014	-	-
4/2.0	4-15M 2-10M	91 46	0.0088**	2-10M 4-15M	46 91	0.0119	-	-	4	0.0013
5/2.0	4-15M 2-10M	91 48	0.0088**	2-10M 4-15M	48 91	0.0119	16	0.0057	-	-
6/2.0	4-15M 2-10M	91 46	0.0088**	2-10M 4-15M	46 91	0.0019	-	-	12	0.0039
7/2.0	4-15M 2-10M	91 48	0.0088**	2-10M 4-15M	48 91	0.0019	-	-	-	-
5/2.5	4-15M	91	0.0113	4-15M	91	0.0113	16	0.0057	-	-

* All web steel was 6 mm deformed bars with $A_s f_y$ per bar = 16.2 kN. ρ_v and ρ_h based on average d.

** Due to bar cut offs within the interior shear span, only 4-15M were effectively anchored. The P given includes only these bars.

\+ This top steel has been neglected in calculations for simply supported beams.

TABLE 2.2 Geometric Details of Specimens

Specimen	d(mm)			a* (mm)	a/d**
	*** Top steel	Bot.Steel	Average		
1/1.0	-	950	950	750	0.79
2/1.0	980+	950	950	750	0.79
3/1.0	950	975	963	750	0.78
4/1.0	950	975	963	750	0.78
5/1.0	950	975	963	750	0.78
6/1.0	950	975	963	750	0.78
7/1.0	950	975	963	750	0.78
1/1.5	-	535	535	750	1.40
2/1.5	580+	535	535	750	1.40
3/1.5	555	520	538	750	1.40
4/1.5	555	520	538	750	1.40
5/1.5	555	520	538	750	1.40
6/1.5	555	520	538	750	1.40
7/1.5	555	520	538	750	1.40
8/1.5	555	520	538	750	1.40
1/2.0	-	455	455	800	1.76
2/2.0	480+	455	455	800	1.76
3/2.0	455	420	438	800	1.83
4/2.0	455	420	438	800	1.83
5/2.0	455	420	438	800	1.83
6/2.0	455	420	438	800	1.83
7/2.0	455	420	438	800	1.83
5/2.5	355	355	355	800	2.25

* Clear distance between faces of loading and supporting columns.

** Average d used

*** d for effectively anchored bars only. (see footnote to Table 2.2)

\+ This top steel has been neglected in calculations for simply supported beams.

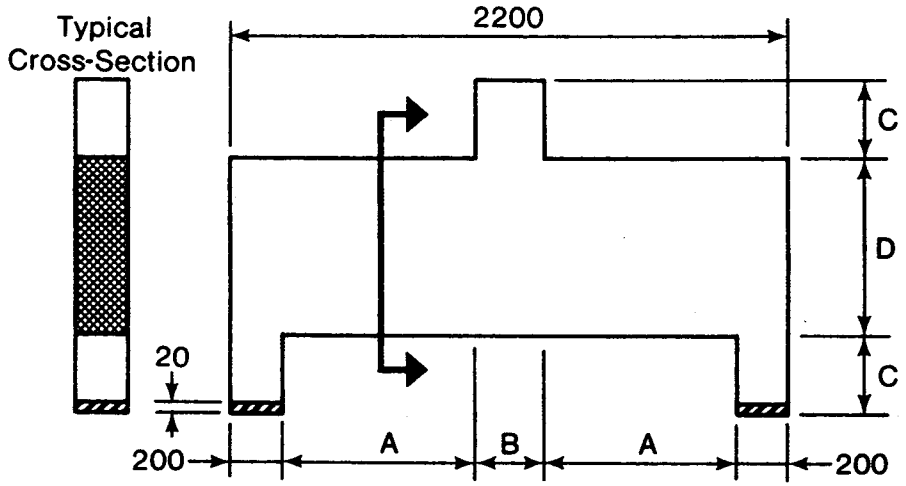

(a) Simple Span Specimens

Series	A	B	C	D
/ 1.0	750	300	450	1000
/ 1.5	750	300	300	600
/ 2.0	800	200	300	500
/ 2.5	800	200	300	400

Note : All Dimensions in mm.

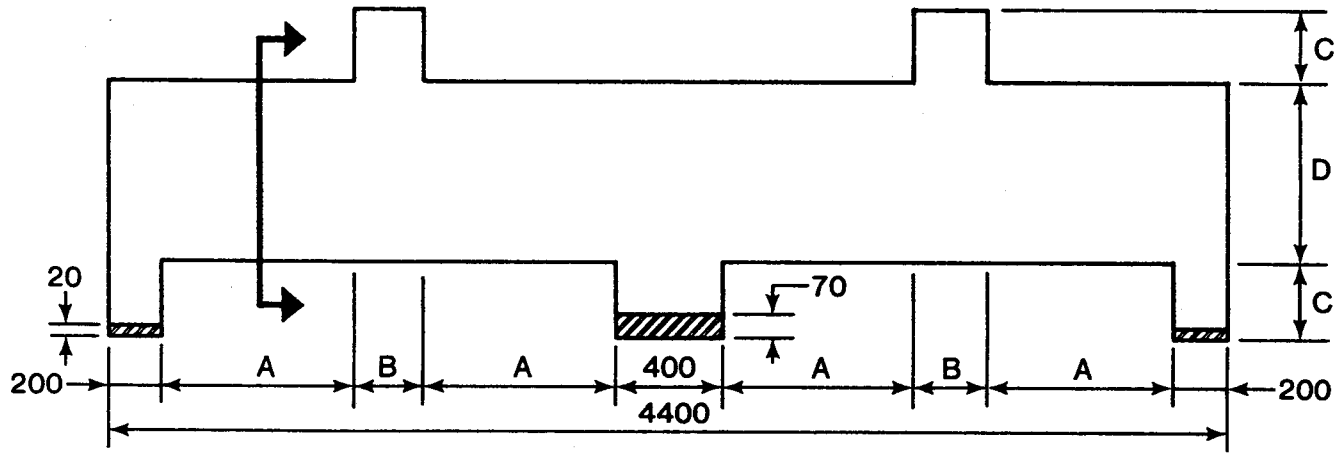

(b) Two Span Specimens

Figure 2.2 Overall Dimensions of Specimens.

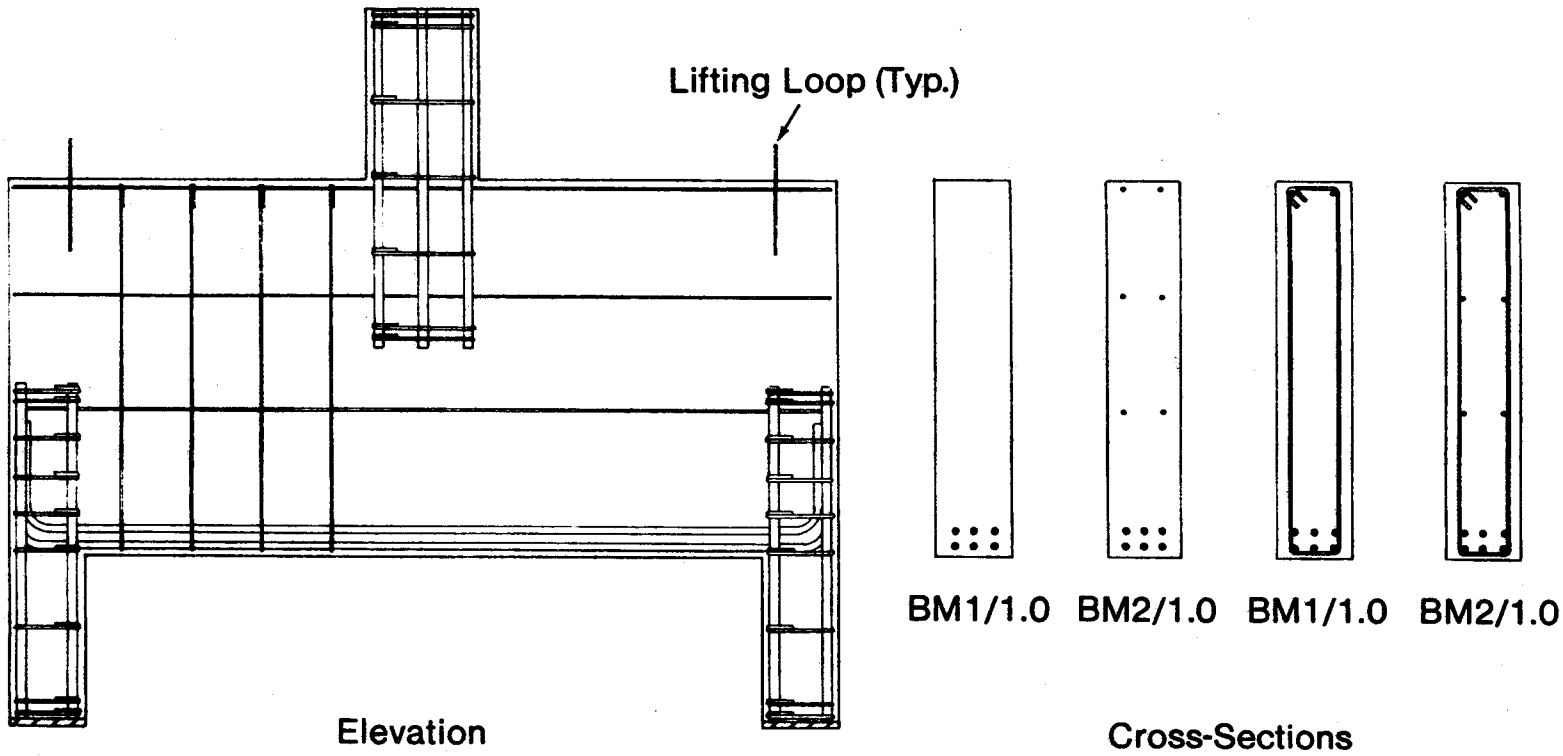

Figure 2.3. Beam 1/1.0 and 2/1.0 Reinforcement Details.

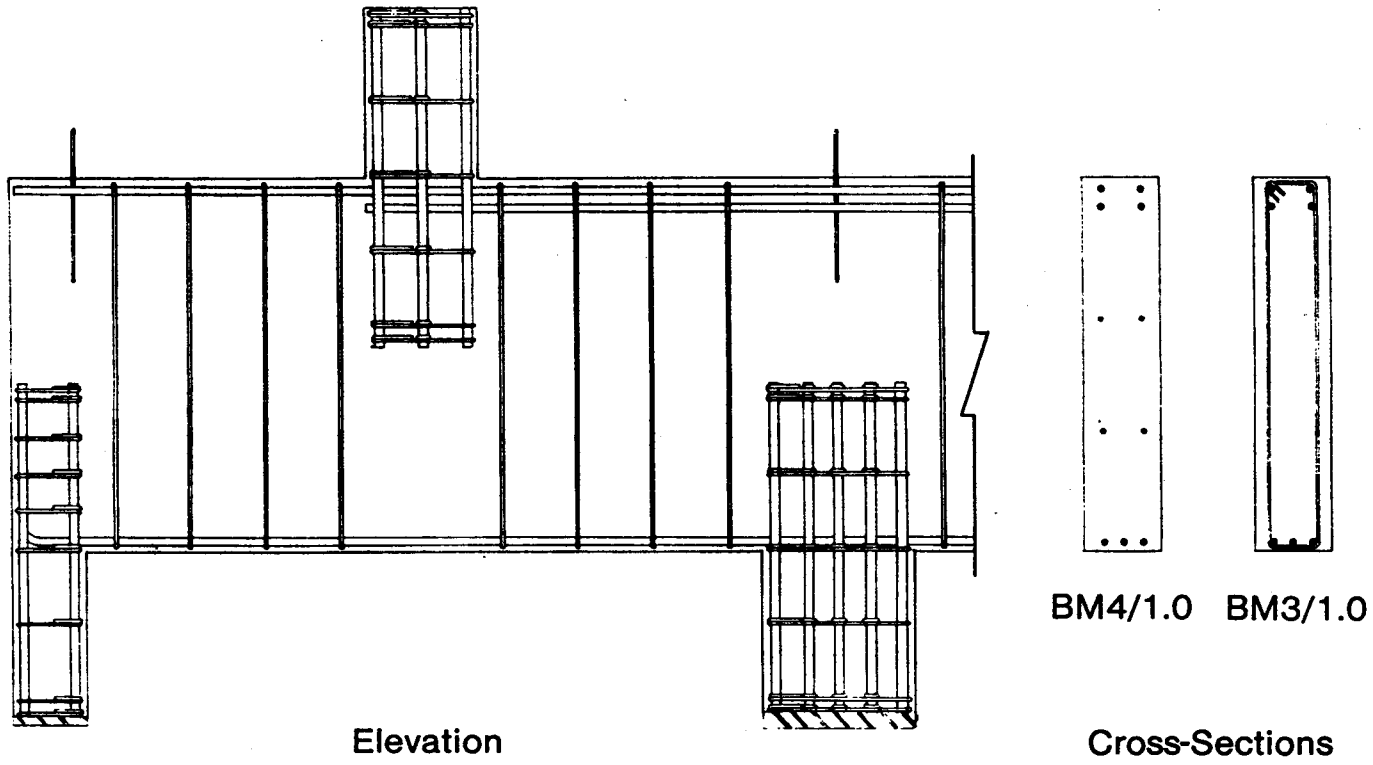

Figure 2.4. Beam 3/1.0 and 4/1.0 Reinforcement Details.

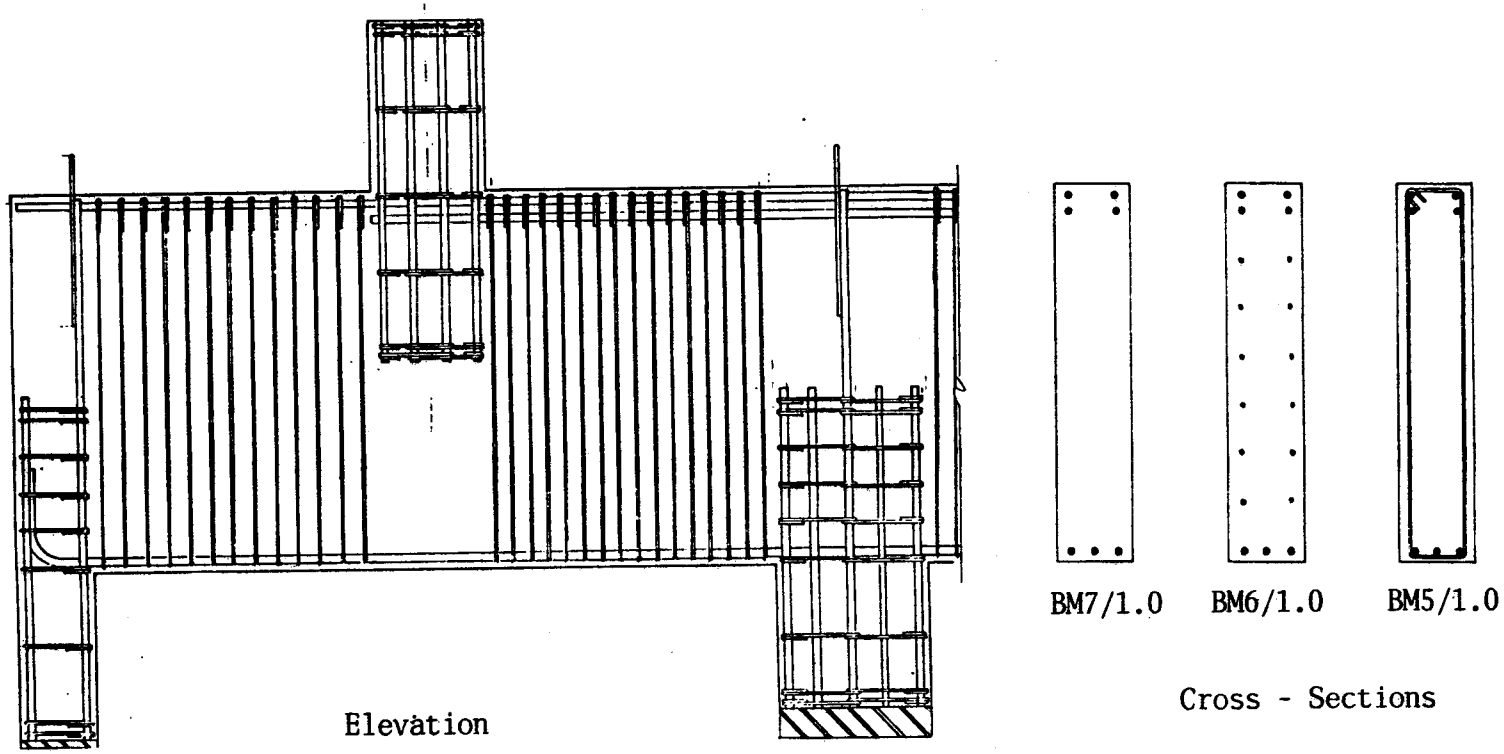

Figure 2.5 Beam 5/1.0, 6/1.0, and 7/1.0 Reinforcement Details

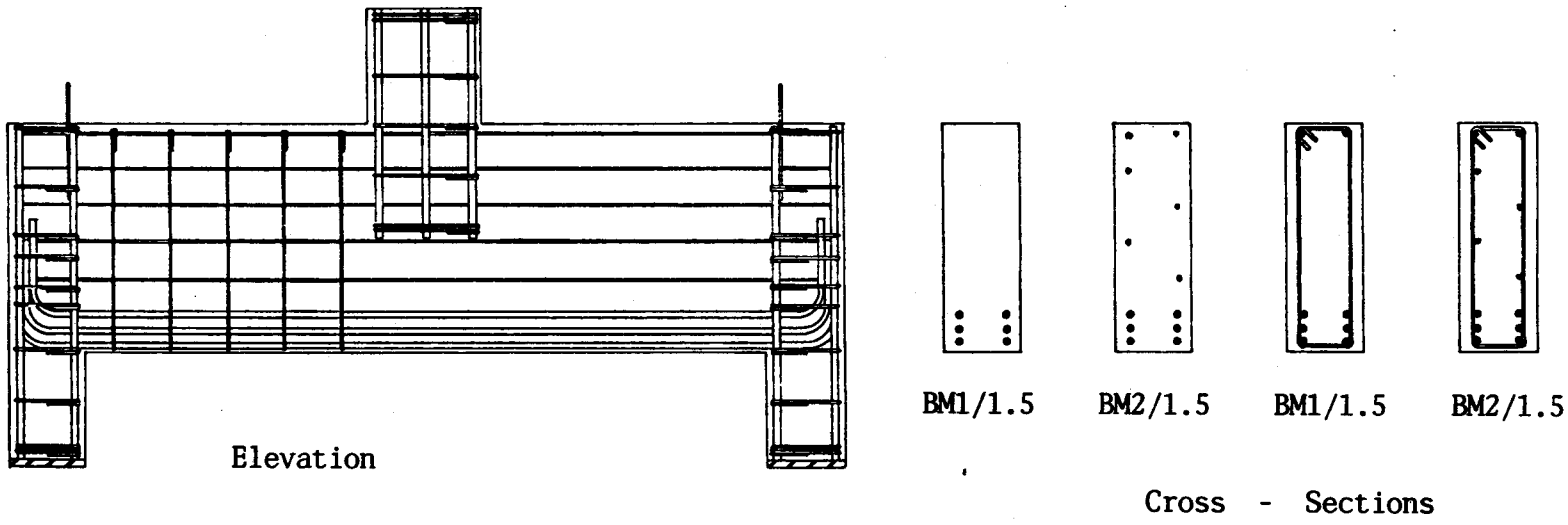

Figure 2.6 Beam 1/1.5 and 2/1.5 Reinforcement Details

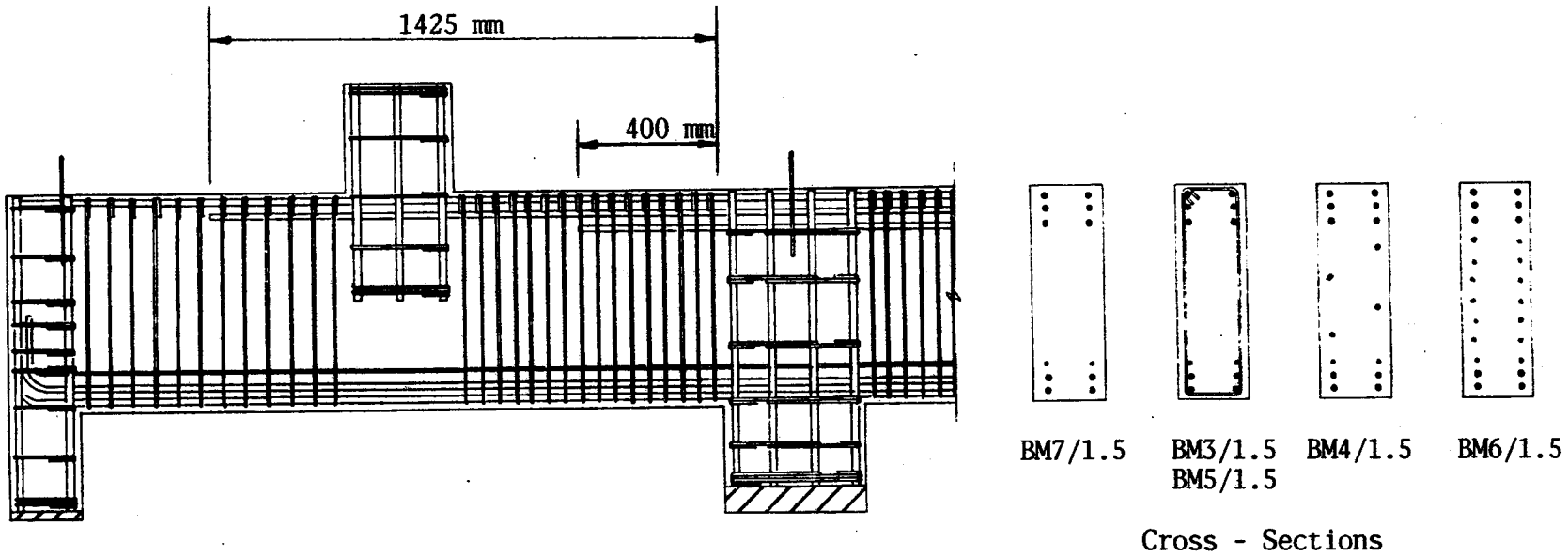

Figure 2.7 Beam 3/1.5, 4/1.5, 5/1.5, 6/1.5, and 7/1.5 Reinforcement Details

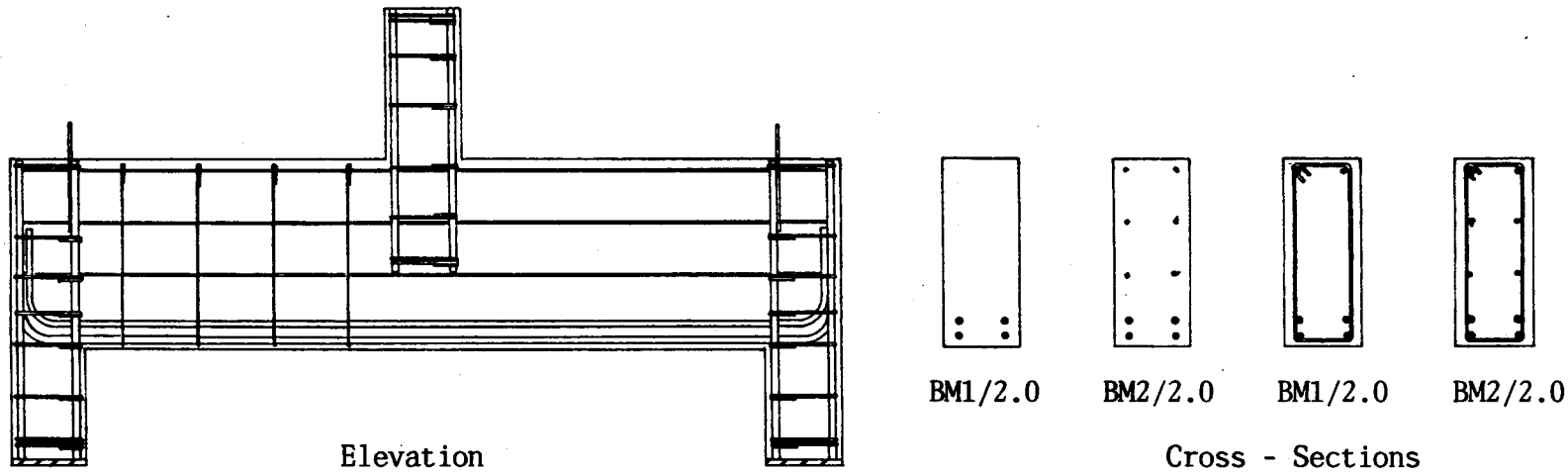

Figure 2.8 Beam 1/2.0 and 2/2.0 Reinforcement Details

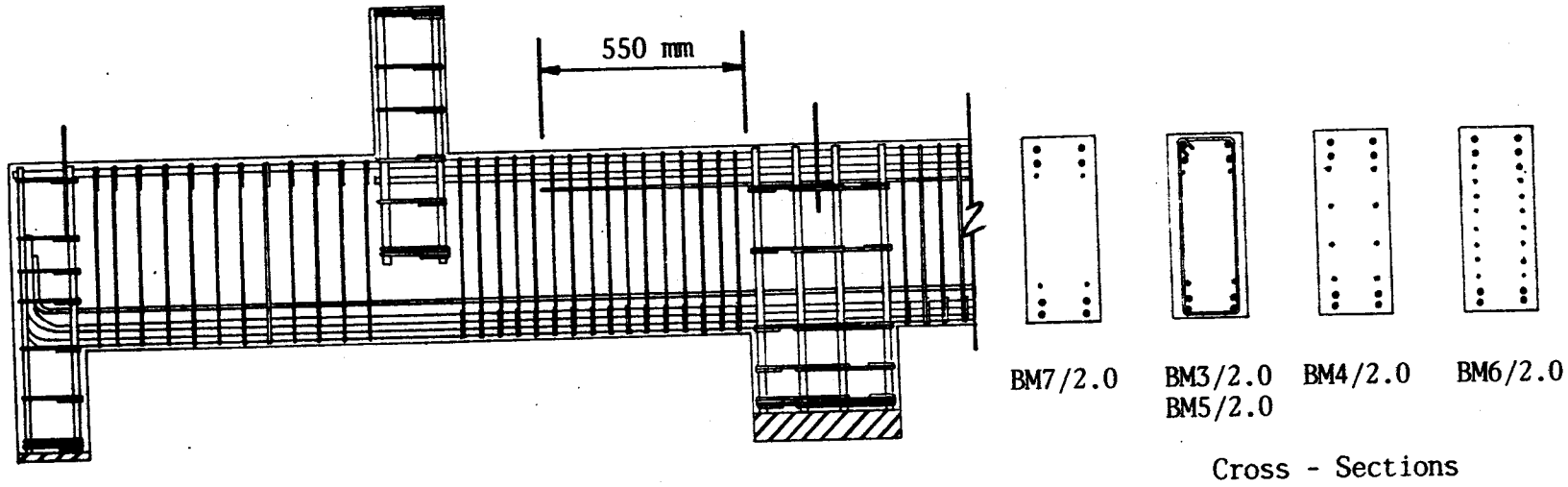

Figure 2.9 Beam 3/2.0, 4/2.0, 5/2.0, 6/2.0, and 7/2.0 Reinforcement Details

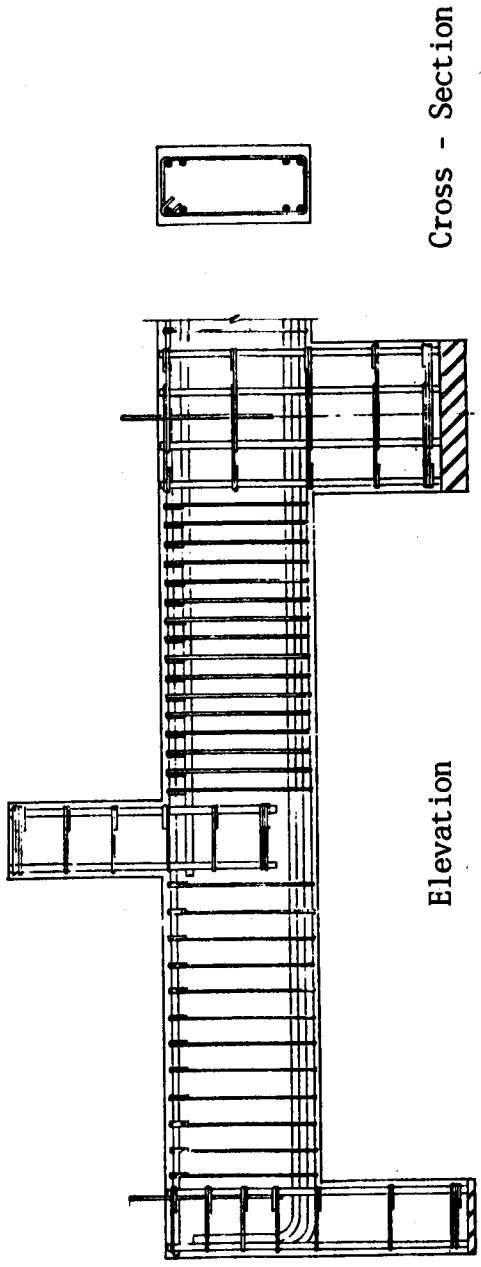

Figure 2.10 Beam 5/2.5 Reinforcement Details

6 mm stirrup support bar. The column bars were saw cut square and tack welded to the steel base plates.

Lifting loops were provided at 200 mm from the end of each beam. The continuous beams were provided with a third lifting loop over the interior supports column except for beams 3/1.0 and 4/1.0 which had extra lifting loops at 400 mm from each face of the interior column. The lifting loops consisted of No. 10M bars or 1/2 inch diameter prestressing strand. Maneuvering the specimens into the loading frame flexed the lifting loops back and forth. The No. 10M bars were abandoned in favour of the prestressing strand because it readily and safely accommodated this flexing. The lifting loops did not appear to influence the behaviour of the beams in any way.

3. Materials and Material Properties

3.1 Reinforcement

3.1.1 Steel Properties

All reinforcement, except the column ties consisted of deformed bars with deformations conforming to ASTM Standard A305. Stirrups and horizontal web reinforcement were made from 6 mm diameter deformed bars obtained from Sweden. No. 10, 15, 20 and 25M bars conforming to CSA Standard G30.12-M-1977 were used for longitudinal and column reinforcement. This steel was obtained locally, and had a specified yield strength of 400 MPa. The actual strengths, based on the nominal bar area ranged from 380 to 480 MPa. The Swedish 6 mm bars had a yield strength of 428 MPa, based on the calculated area given in Table 3.1. The area was calculated from the weight of a 300 mm long piece of bar.

Steel from several different heats was used over the 14 months of fabrication and testing. The strength properties in each batch of delivered reinforcement were determined on at least 2 specimens obtained from different bars. More specimens were tested if the first two tests gave different results. Except for grinding off the deformations in the regions of the bar which fit within the grips of the testing machine, the bars were tested in an undisturbed state. The bars were tested in a Baldwin testing machine in accordance with ASTM Standard A370-65. A "Snap-on" type "Microformer"

TABLE 3.1 Steel Stress-Strain Analysis

Heat	Metric Bar Size	Asfy Measured (kN)	Yield Strain Measured	AsE Measured (kN)	As* Calculated (mm)	E** Calculated (MPa)	fy* Calculated (MPa)	fy** Calculated (MPa)
(1)	(2)	(3)	(4)	(5)	(6)	(7)	(8)	(9)
1	25	216	0.00216	100,000	490	200,000	441	432
2	20	114	0.00185	61,600	302	205,400	377	380
3	20	121	0.00206	58,700	288	195,800	420	403
4	15	91	0.00222	41,000	201	205,000	453	455
5	15	91	0.00227	40,100	196	200,400	463	455
6	10	46	0.00230	20,000	98	200,000	469	460
7	10	48	0.00234	20,500	101	205,100	477	480
8	10	46	0.00232	19,800	97	198,300	473	460
9	6mm	16.2	0.00210	7,700	37.8	273,000	428	573
						Average = 201,300 MPa***		

* Based on an assumed E = 204.000 MPa.

** Based on an assumed As = Norminal Area.

*** Calculated excluding Heat 9.

extensionmeter was used to measure strains up to about 1%. Larger strains were measured using dividers over an 8 inch gage length. The yield point was obtained graphically from the "Snap-on" extensionmeter and Baldwin testing machine. The load-strain plots are given in Figs. 3.1 and 3.2. The results are expressed in terms of force-strain curves because the force in the bar is used in the analysis of test results and it was the quantity measured.

The plot of load vs. strain has a slope equal to AsE, the axial stiffness of the bar. One can assume a value for either As or E, and calculate a compatible value for the other parameter. For comparison purposes, two analyses were done, one assuming E=204,000 MPa (29600 ksi) and one assuming As as the nominal area. The resulting data are summarized in Table 3.1.

Throughout this work, all steel strains have been converted to stresses using a Young's Modulus of 204,000 MPa, until the experimental strains reached the yield strains given in column 4 of Table 3.1. The bar forces were determined using the calculated areas given in column 6 of Table 3.1. Strain hardening was neglected. Nominal bar areas were used in the calculation of geometric reinforcement ratios.

3.1.2 Assembly of Reinforcement

The reinforcing cages were assembled so that the main bars were always within 2 mm of their specified positions,

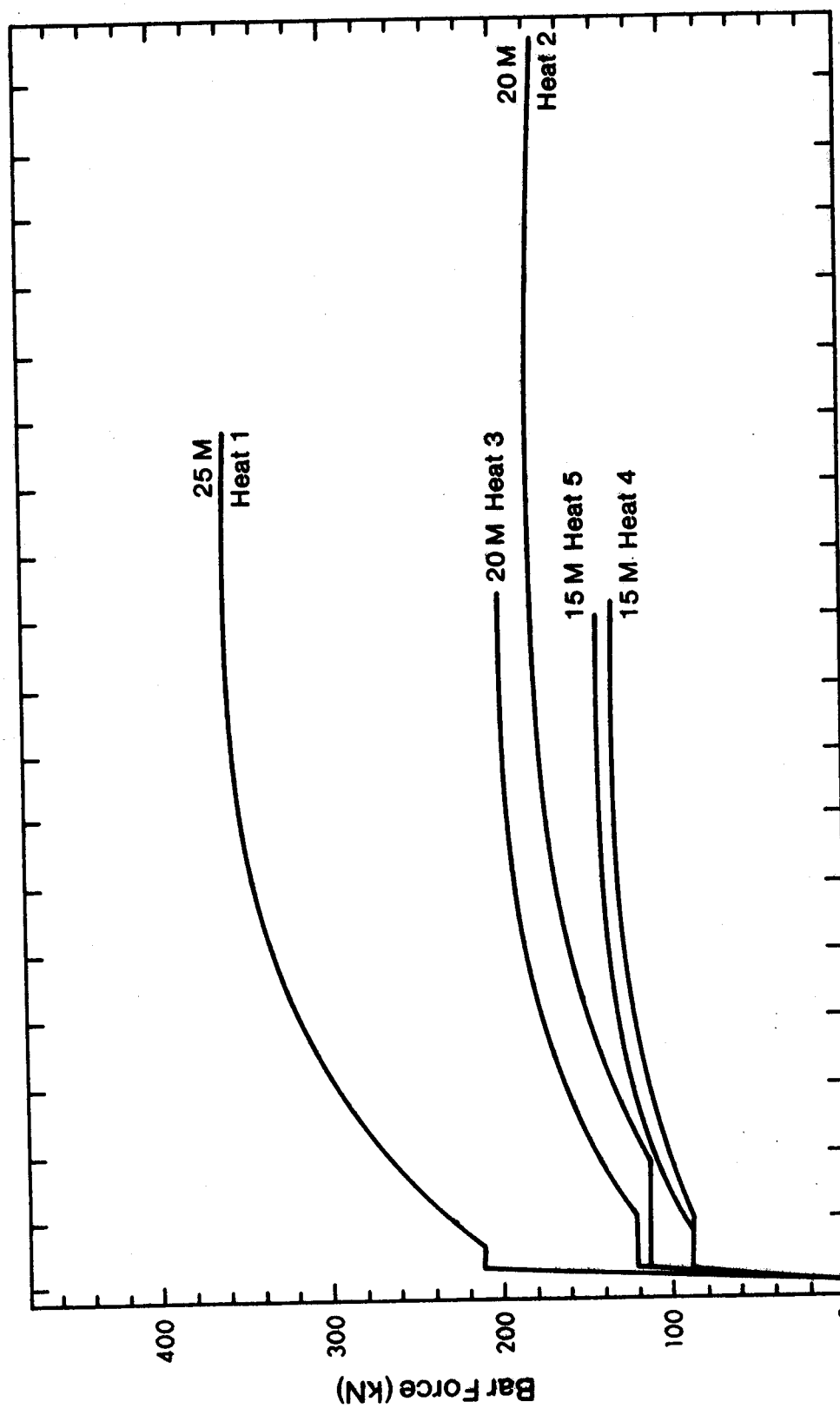

Figure 3.1 Steel Force-Strain Curves 15 M, 20 M and 25 M Bars.

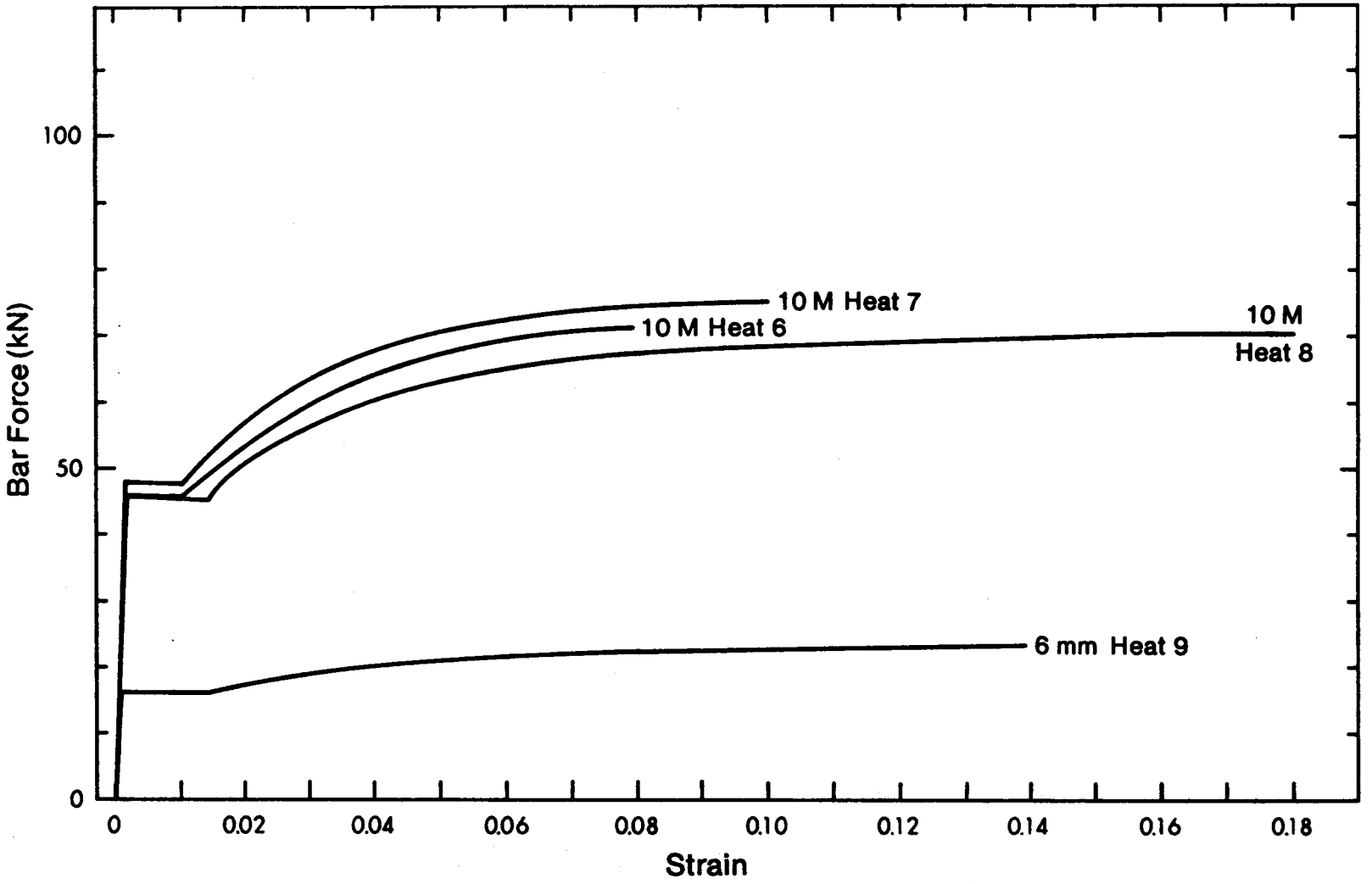

Figure 3.2 Steel Force-Strain Curves 10 M and 6 mm Bars.

while stirrups were within 10 mm of their specified location along the beam. All other dimensions were generally within 2 mm.

The column bars were tack welded to the column base plates. This greatly improved the ease and accuracy of fabrication. No other welding was permitted. All other bars were secured in position with 18 gage black tie wire.

After fabrication of the cage proper, 6.3 mm diameter steel "pins" or "studs" for holding future gage points, were brazed to the bars along which strain measurements were to be made. Preliminary tests indicated that attaching the studs to the reinforcement with tack welds greatly affected the stress-strain characteristics for the reinforcement. Figure 3.3 compares tensile force-strain curves for the 10 M reinforcement for specimens with and without a series of studs attached. The behavior of the bar with studs brazed to it was very similar to the behavior of the virgin bar, while the properties of the bar were strongly affected by welding. Hence, all strain gage studs were brazed to the bars and the heat input during brazing was kept to an absolute minimum. Care was required to prevent heating the reinforcement above its transition temperature. On the otherhand, if insufficient heat was used, the joint had a low strength. A failure rate of 2 or 3 studs per 1000 was observed.

The lateral force due to concrete pushing against the studs, as may happen during bond slip, was prevented by

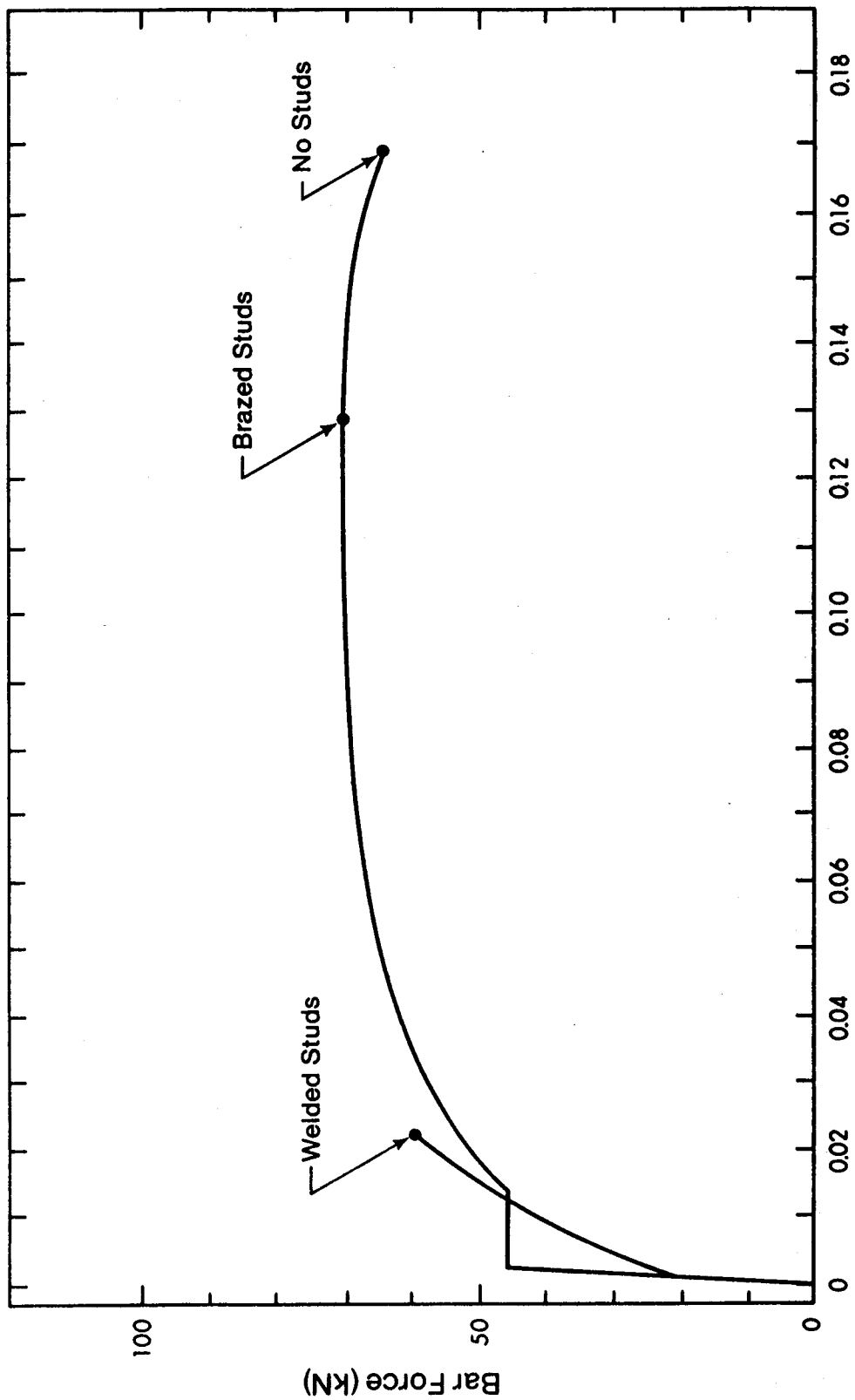

Figure 3.3 Welding and Brazing Effects on 10 M Bars.

providing a 3.2 mm clearance between the pins and the concrete. After the pins were brazed onto the bars, "Plasticine" was applied around the base of the pin, covering the brazing. A film of "Vaseline" petroleum jelly was applied to the pin, then 12.7 mm OD, 6.3 mm ID rubber air hose was slipped over the pin and trimmed flush with the end of the pin. A final film of petroleum jelly was applied to the outside of the rubber hose. When the beams were removed from the forms the rubber hoses were pulled or picked out with pliers leaving a 3.2 mm clear space around the pin. A few steel studs were brazed onto the cages in strategic locations so that they would bear against the formwork to automatically provide proper cover.

3.2 Concrete

3.2.1 Ingredients and Mix Proportions

All of the concrete used in the tests was produced in the laboratory. The concrete mix was designed to provide a 28 day cylinder strength of about 30 MPa. Normal weight river washed sands and gravels were used for aggregate, with a maximum aggregate size of 10 mm. Normal Type 10 portland cement was used. The slump was approximately 100 mm. All of the ingredients were batched by weight, and mixed in a vertical axis drum mixer with water added until the desired workability was reached. The typical batch size was approximately 0.2 cubic meters with up to 5 batches to a

specimen. Owing to variations in the supply of aggregates and cement over a period of 14 months, the inevitable delay in the testing of individual specimens and the variable curing conditions in the laboratory, there was considerable scatter in the values of concrete strength at the time of testing.

The aggregates were obtained locally and had a grain size distribution as shown in Fig. 3.4. The moisture content of the aggregates tended to vary. This necessitated constant adjustment of the amount of water added to the mix, to obtain the desired workability. The maximum aggregate size and slump were chosen in order to obtain sound concrete even in the regions of maximum steel congestion.

The proportions of ingredients and other relevant data for a typical batch of concrete are given in Table 3.2.

The concrete was placed in the formwork immediately after mixing. The production and placing rate was approximately four batches per hour. Each batch was placed symmetrically within the beam, half of each batch into each shear span. This was done to make the two shear spans as nearly identical as possible.

Compaction was accomplished with a common immersion type internal vibrator. The beams were cast in a vertical position and when excess water had evaporated from the surface a trowel was used to give the top a smooth finish. Plastic settlement cracks were observed in some beams over top of, and parallel to the top reinforcement. Final

TABLE 3.2 Mix Design for 8 Cubic Foot Batch

ITEM	WEIGHT (LBS)
Water	102
Cement	190
Fines	475
Coarse	375

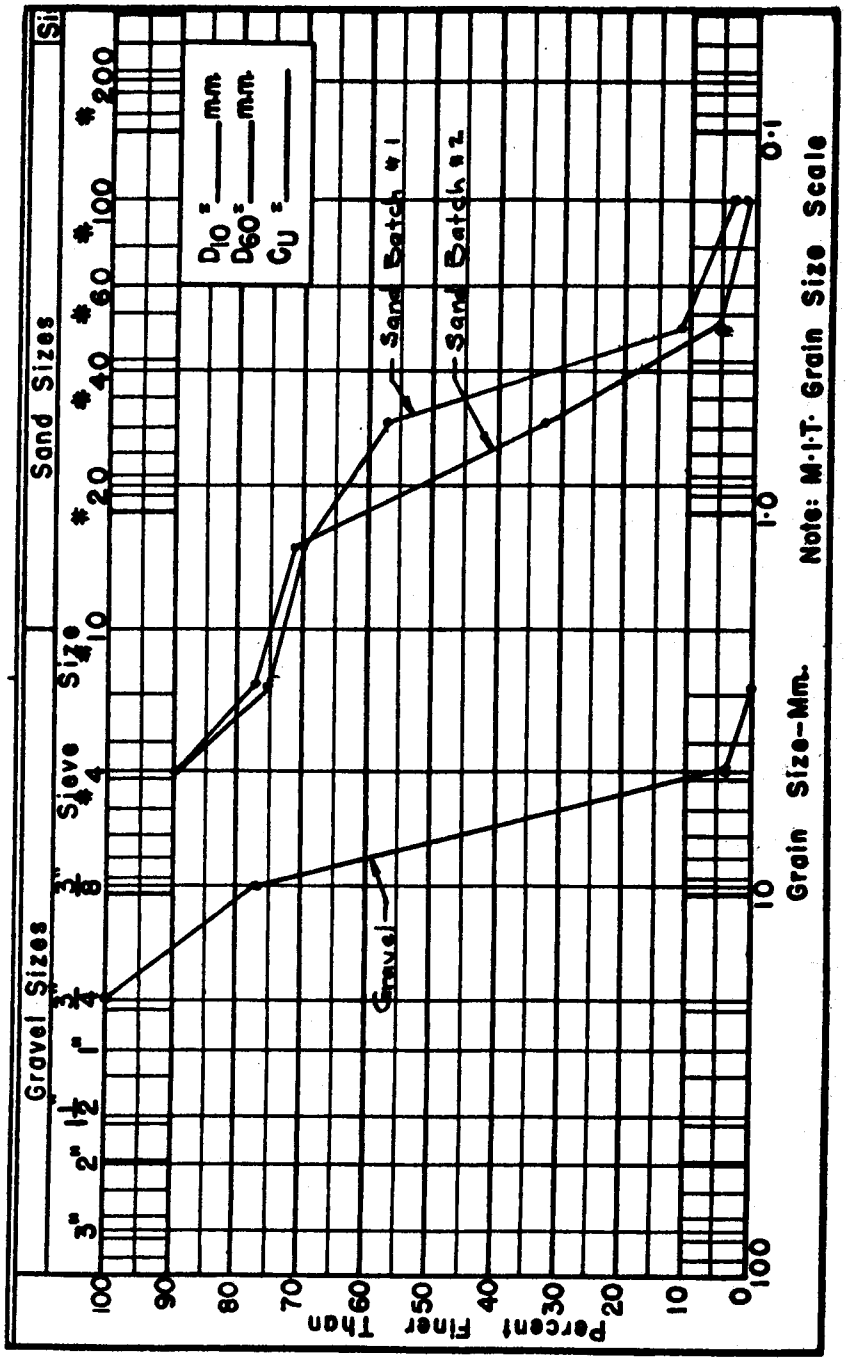

Figure 3.4. Aggregate Grain Size Analysis.

trowelling usually removed these cracks. In some, but not all cases, longitudinal splitting over the top bars developed along these plastic settlement cracks.

Three 6 x 12 inch cylinders were cast from each concrete batch using wax coated cardboard molds. These were hand compacted in three equal lifts with 25 rod strokes per lift.

The beam specimens and cylinders were moist cured with wet burlap under polyethelene sheeting for a minimum of 7 days, and usually until 2 or 3 days before testing. The forms were loosened 24 hours after casting. At an age of 3 days the beams were lifted from the forms and the cylinders were stripped. The cylinders were stored adjacent to the beams to ensure similar curing conditions.

3.2.2 Concrete Strength Properties

The standard concrete cylinders were tested during or after the main test. Of the three cylinders per batch, one was used for a split cylinder tesile test in accordance with ASTM Standard C496. The remaining two cylinders were tested in compression in accordance with ASTM Standard C39. One cylinder for each beam was used to determine the modulus of elasticity in accordance with ASTM Standard¬ . Plots of the stress-strain data indicated a linear response up to at least 50% of f'c. The concrete properties are summarized in Table 3.3.

TABLE 3.3 Concrete Properties

Beam	f'c (MPa)	COV* of f'c	fsp (MPa)	Ec (GPa)	Age (Days)	$E_c(f'_c)^{-0.5}$	$f_{sp}(f'_c)^{-0.5}$	$f_{sp}(f'_c)^{-0.7}$
1/1.0	26.1	-	2.28	20.0	72	3915	0.446	0.232
2/1.0	26.8	-	2.65	23.4	106	4520	0.512	0.265
3/1.0	28.9	0.10	2.48	20.8	128	3869	0.461	0.235
4/1.0	28.5	0.03	2.86	-	127	4017	0.536	0.274
5/1.0	36.9	0.04	3.10	24.4	20	4017	0.510	0.248
6/1.0	35.8	0.04	2.97	21.2	20	3543	0.496	0.243
7/1.0	34.5	0.06	2.99	21.6	20	3677	0.510	0.251
1/1.5	42.4	0.04	3.27	21.1	72	3241	0.502	0.237
2/1.5	42.4	0.04	3.27	21.1	72	3240	0.502	0.237
3/1.5	14.5	0.06	-	-	-	-	-	-
4/1.5	32.5	0.04	-	-	-	-	-	-
5/1.5	39.6	0.06	2.98	23.6	66	3750	0.474	0.227
6/1.5	45.0	0.02	3.19	24.6	73	3667	0.476	0.222
7/1.5	30.4	0.06	-	-	-	-	-	-
8/1.5	37.2	0.04	-	-	-	-	-	-
1/2.0	43.2	0.04	3.09	24.8	39	3773	0.470	0.221
2/2.0	43.2	0.04	3.09	24.8	39	3773	0.470	0.221
3/2.0	42.5	0.04	2.34	22.9	58	3513	0.359	0.170
4/2.0	38.3	0.04	2.44	22.4	55	3620	0.394	0.190
5/2.0	41.1	0.03	2.86	22.5	62	3510	0.446	0.212
6/2.0	37.4	0.04	2.41	21.6	30	3532	0.394	0.191
7/2.0	46.8	0.03	2.64	24.0	66	3508	0.386	0.179
5/2.5	34.0	0.05	2.46	20.4	21	3499	0.422	0.204
					Mean	3694	0.461	0.224
					COV	0.08	0.11	0.12

* Coefficient of Variation of the batches making up one beam.

The tensile strength of the concrete could be represented by: fsp = 0.461 x f'c with a coefficient of variation of 0.11. Alternatively the form of equation proposed by Lew and Carino could be used: fsp = 0.224 x $f'c^{0.7}$ with a coefficient of variation of 0.12.

The modulus of elasticity of the concrete could be represented by E = 3694 x$\sqrt{f'c}$ with a coefficient of variation of 0.08.

4. Instrumentation

4.1 Overview

The specimens were heavily instrumented to obtain as much information as possible about the behavior of the beams at each stage of loading. All loads and reactions were determined with load cells. The steel and concrete strains were measured using Demec Gages (demountable meachanical extensometers). Displacements were measured with standard dial gages and LVDT's. During the first 8 tests, all of the data was monitored and recorded by hand because the data acquisition computer was not functional. During the testing of the last 15 specimens, loads, reactions and midspan deflections were recorded automatically using a computer.

4.2 Loads and Reactions

All loads and reactions were measured with load cells. This enabled shear force and bending moment diagrams to be drawn at every load step. This is particularly important in the continuous beams which were one degree statically indeterminate. The loads and end reactions were measured using Durham Instruments FTC-A100 - 400k load cells with a range of 0 to 1780 kN and an accuracy of +- 1kN. The interior reactions were measured using a Durham Instruments FTC-A100 - 600k load cell with a range of 0 to 2670 kN and an accuracy of +- 1.5 kN. An overall check of statics in the vertical direction indicated that the sum of the

reactions was usually within 1% of the sum of the applied loads, and was never out by more than 2% (See Table 6.2).

The values of the measured loads and reactions were adjusted so that they satisfied statics, in much the same way as a surveying traverse is adjusted to eliminate the error of closure. First it was assumed that the jack load cells were just as accurate as the support load cells, thus half of the error in the summation of vertical loads was assigned to the jack load cells, and half to the support load cells. Adjustments to the jack loads were made in proportion to the relative magnitude of the jack loads. The correction applied to the interior support was proportional to the relative magnitude of the interior reaction to the sum of the support reactions. The end support reactions were determined by summing moments about each end. The resulting adjusted loads and reactions satisfy statics, i.e. the sum of the vertical forces equals zero, and the sum of the moments about any point equals zero.

All reported loads and reactions unless otherwise noted are adjusted values. All bending and shear forces were determined from the adjusted loads and reactions.

In order to determine if lateral loads were being transmitted through the jack load cells, bonded resistance gages were attached to what would have been the maximum extreme fibres in tension and compression on the base portion of the load cells. These strain gages indicated that both faces of the load cells were experiencing similar

strains and thus no appreciable lateral loads were transmitted through the jacks and load cells.

4.3 Steel Strains

The steel strains were measured using a Demec gage. This is a demountable mechanical gage with gage points to measure the change in distance between targets attached to the specimen. A standard gage length of 5 inches was used. The targets were attached with sealing wax to 6.3 mm diameter steel pins which, in turn, were brazed to the reinforcing bars, as described in section 3.1.2. The readings were made visually from a dial on the Demec gage. The least count on the gage represented 15.3 microstrain. The repeatability of readings was very much dependent upon the instrument man, and was improved with practice. The initial readings were generally taken as the average of 3 readings which agreed within 3 dial divisions (45 microstrain) while subsequent readings were taken as the average of 2 readings which agreed within 3 dial divisions. If the readings did not agree within these limits, additional readings were taken. The multiple readings were essential in identifying and eliminating erroneous readings such as might occur when the points of the Demec gage were not properly seated in the holes of the targets. Undetected, erroneous readings can lead to extremely large errors in strain. The general result is that the measured strains can be considered to be within +- 30 microstrains

with 90% confidence. An error of 30 microstrains corresponds to an error in steel stress of 6 MPa or roughly 1.3% of the yield strength.

4.4 Concrete Strains

The concrete strains were measured using a 2 inch gage length Demec gage in all tests except beam 1/1.0 in which the 5 inch Demec gage previously described in section 4.3 was used. The least count for the 2 inch Demec gage represented 25 microstrain. The initial readings were generally taken as the average of 3 readings which agreed within 3 dial divisions (75 microstrains) while subsequent readings were taken as the average of 2 readings which agreed within 3 dial divisions. As with the steel strain readings, if the agreement between readings was worse than these limits, additional readings were taken. The general result is that the strains measured with the 2 inch Demec gage can be considered to be within +- 50 microstrains with 90% confidence. The cracking and crushing strains of concrete are in the order of 200 microstrains and 2000 microstrains, respectively.

Readings were taken on targets attached to the surface of the concrete with sealing wax. The Demec targets were laid out in various patterns. The pattern finally chosen, and used for 21 tests consisted of eight targets arranged in a 2 inch diameter circle giving readings on vertical, horizontal and two 45 degree gage lines. The rosette

provides strain measurements in 4 different directions hence 4 sets of principal strains can be determined, and averaged giving a good estimate for the state of strain in the area of the rosette. This rosette has the advantage of still being able to provide principal strains when a Demec target falls off or a crack passes through one arm of the rosette. Both events were not infrequent.

The actual number and location of the rosettes used, depended upon the a/d ratio and whether the beams were simple span or continuous. The typical layouts used are shown in Fig. 4.1.

The steel strains were measured on the west face of the beam and concrete strains on the east face. Throughout this report the crack patterns and steel strains are shown as seen on the west face, the concrete strains are shown as seen looking through the beam from the west face. This is done in an attempt to illustrate the relationship between concrete and steel strains and the crack patterns. The Demec patterns in Fig. 4.1 are shown as they would be seen looking through the beam from the west face.

4.5 Displacements

The midspan deflections of each span were measured with mechanical dial gages and/or LVDT's. The dial gages had a least count of 0.001 inches. The LVDT's were Hewlette Packard model 7DCDT-1000, and had a full scale output of 4.8 volts DC with a full scale displacement range of +- 25 mm.

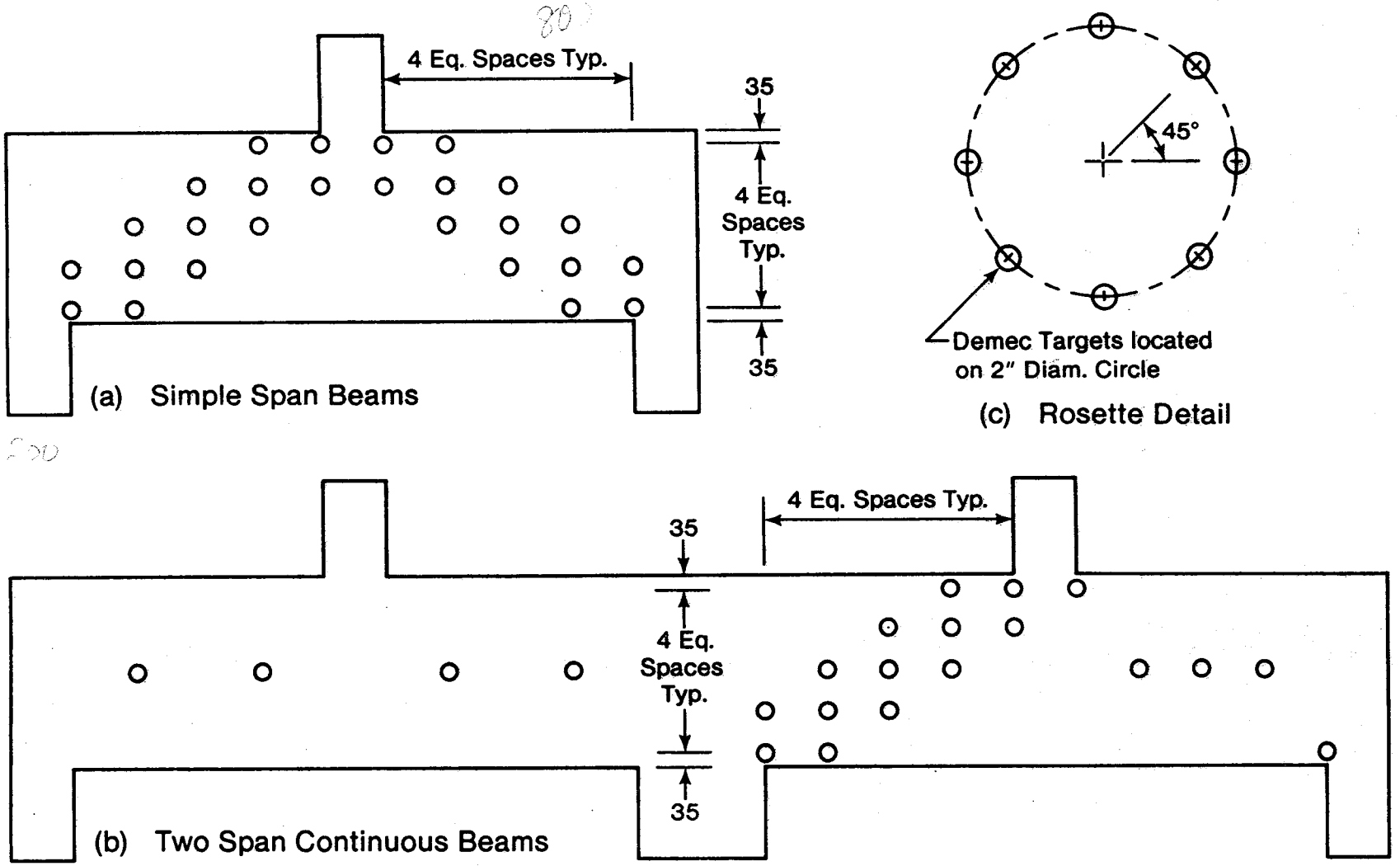

Figure 4.1 Typical Concrete Strain Gage Layout.
(Seen looking through the beam from the West Face).

The maximum nonlinearity was +- 0.5% of full scale.

For the continuous beams, the settlement of each of the supports was measured with mechanical dial gages which had a least count of 0.0001 inches. Measurements were taken from an independent reference frame to the steel base plates at the lower end of the support column stubs. The gages were located on the east face of the beam at the support centre-lines.

The horizontal displacements of the north and south ends of the beam were measured with mechanical dial gages which had a least count of 0.0001 inches. These measurements were taken in order to determine if the overall beam was travelling in a north or south direction indicating imminent stability failure in a horizontal (north-south) direction. Horizontal hydraulic rams were provided at each end of the beam which could bring the average horizontal (north-south) displacement back to zero. These rams were never needed during testing, but were maintained as a safety precaution.

4.6 Crack Observations

Before any loads were applied at the beginning of the test, and after each increment in load, the cracks were marked and photographed. The concrete surface was left unpainted permitting easy crack observation. The cracks were observed with the naked eye, supplemented when necessary with a 3X illuminated hand lense and were marked

with a felt pen.

5. Testing

5.1 Test Set-Up

The test specimens were tested in the loading frame shown in Fig. 5.1. The hydraulic rams used for loading the specimens were pressurized with an "air on oil" system which maintained constant load provided that the rams did not travel too quickly. The result of this was that test was a load controlled test until the specimen reached peak strength. After peak strength, the test was a displacement rate controlled test and was governed by the rate at which the pump could pump oil into the rams. The use of this loading system ensured that the load was kept constant while strain readings were taken, and allowed the descending portion of the load deflection curves to be obtained in most cases.

5.2 Testing Procedure

The loads were applied in increments. After the load was incremented, the specimen was left for one to two minutes for the deflections and cracking to stabilize. A set of displacement readings were the first data taken. After this, steel and concrete strains were measured. Each gage was read at least twice, with several minutes between readings. The cracks were then marked and photographed. A final set of displacement readings was taken before increasing the load to the next increment. This process

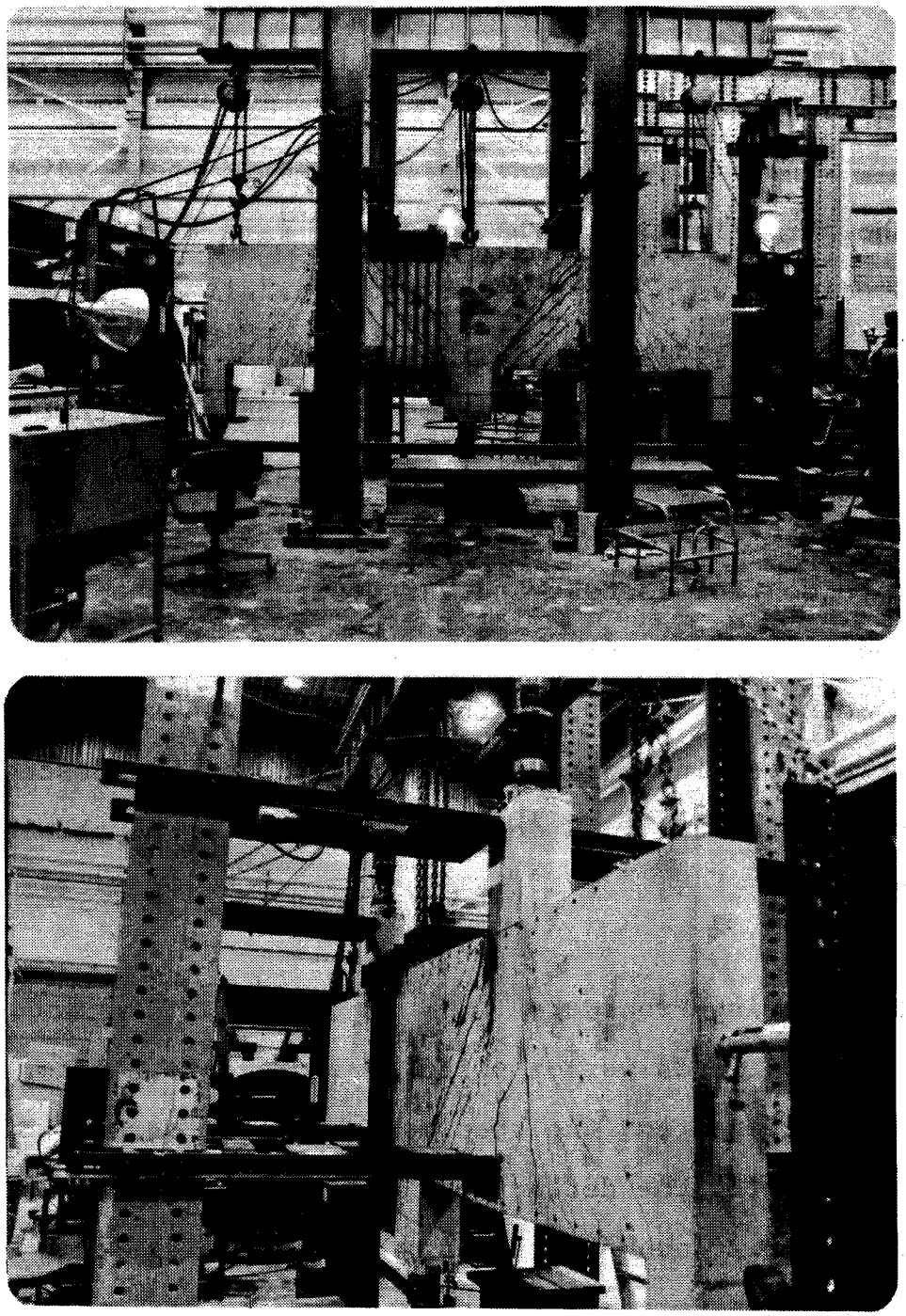

Figure 5.1 Loading Frame and Test Set-up
(Beam 5/1.0 is shown in the testing frame)

required approximately one hour during which the load was kept constant. The creep which occurred during these periods was clearly evident on the load-deflection curves which were plotted as the test progressed.

The size of the load increments was chosen to give approximately seven load increments to failure. This resulted in a test duration of 7 to 9 hours and permitted a monotonic loading to failure of a specimen in one day. If it appeared that the specimen would not fail during this first day, the test was stopped, and the beam was unloaded with load and displacement readings taken as the load was released slowly. The next day, the beam was reloaded to the previous maximum load with load and displacement readings taken as the load was increased slowly. Strain readings were taken again at this load level, and compared to the previous days measurements. The test was then continued in the normal manner until failure. After failure, the cracks were marked and photographed in detail.

Each beam was tested to failure twice. After the first shear span failed, it was reinforced with external stirrups consisting of a yoke above and below the beam with twelve 3/4 inch diameter tie rods acting as stirrups, running from one yoke to the other (see Fig. 5.1). The top yoke was set in a bed of plaster to take up any uneveness in the top surface of the beam. When the plaster had set, the bottom yoke was put in place and the tie rods were tightened as much as possible with an airpowered wrench. This process

closed the failure crack and required tightening each rod several times to take up the slack as the crack closed. Plaster was then placed between the column stubs and the end face of each yoke, so that horizontal force could be transmitted directly from the yokes to the column stubs. The support reactions of the continuous beams were then replastered to allow for any movement due to the reinforcing procedure. The beams were then retested.

The retesting of the specimen proceeded in a manner similar to the virgin test. Load and displacement readings were taken as the beam was slowly loaded to the level at which the last complete set of strain measurements was taken. This was the first load increment in the retest. Strain and displacement readings were taken, and cracks were marked and photographed. The test then proceeded in the usual manner.

5.3 Support Settlement

The continuous deep beams were susceptible to differential support movements. In the tests, this took the form of "settlement" of the interior support relative to the exterior support, which increased the positive bending moments at midspan, and reduced the negative bending moment. The formation of positive flexural cracks before the negative flexural cracks was a manifestation of this problem.

The interior support settlements were due to elastic shortening of the support load cell, delaminated floor topping, and improper seating and plastering of bearing plates above and below the load cell. The floor topping was delaminated in the region of the interior support. The gap between the topping and the structural floor proper, was approximately 0.1 mm, and took about 100 kN of jack load to close. This source of differential deflection was reduced by prestressing the topping to the structural floor, and casting a 790 x 790 x 155 mm thick reinforced concrete pedestal over this region to bridge over any remaining hollow spots. Displacement measurements indicated that this was a successful remedy. Beams 3/1.0, 4/1.0, and 7/1.5 were tested before the pedestal was cast. The elastic shortening of the interior load cell could not be avoided. The interior load cell had a capacity of 1.5 times that of the exterior load cells, but it was required to carry a load at least 2 times that of the exterior load cells, hence it shortened more than the exterior load cells. Replacing the interior load cell with one of larger capacity would have reduced the support settlement somewhat, but a suitable load cell was not available. Improper seating and plastering of the bearing plates was extremely variable. Through trial and error it was found that this error was greatly reduced if all three bases were plastered at the same time. This was done by covering the cap plates of the support load cells with fluid plaster, and slowly lowering the specimen

onto the supports. The thickness of the plaster was kept less than 3 mm by inserting steel shim plates into the plaster when necessary. Plaster was applied above and below the shim plates to eliminate the effects of curvature in the plates. Due to the confinement of the steel plates, thin layers of plaster exhibited greater strength and stiffness than thicker layers. Plaster of Paris was abandoned in favour of Hydrocal 105 for the stronger test specimens. Hydrocal 105 is a full hydrate plaster and attains a compressive strength of approximately 30 MPa in 24 hours. The need to reinforce the plaster was by no means trivial since the actual bearing stresses in the plaster reached 80 MPa in at least one instance. This detail was responsible for about 1/3 of the differential settlement. Differential elastic shortening of the load cells accounted for most of the remainder.

The support settelements did not appear to effect the experimental results because:

1. While the beam was relatively uncracked, the actual distribution of the reactions was very similar to the elastic distribution of the reactions for a beam with uncracked EI and shear deformations.
2. The flexural reinforcement was proportioned on the basis of the elastic distribution of moments without support settlement. Thus, when extensive plasticity developed, the distribution of support reactions was similar to that predicted by elastic

theory without support settlement.

3. The differential support settlement was small and ranged between L/1875 and L/13100, which is much better than one could expect in a real structure.

6. Test Results

6.1 Presentation of Results

This chapter will present the test results for all of the specimens. Discussion of the results will follow in a discertation by the senior author. Most of the data has been reduced to graphical form for ease of interpretation.

All of the beams were tested spanning in a north-south direction. The figures illustrating the beams always have the north end of the beam shown as the left end regardless of whether the east face (concrete strains) or west face (steel strains) are being shown.

6.2 Failure Loads

The measured loads and reactions at failure (peak values) are given in Table 6.1. The second set of readings for each beam correspond to the retest. An asterisk in the north and south support reaction columns indicates the end of the beam in which failure occurred for that line of data. The measured loads and reactions did not satisfy statics exactly. The values given in Table 6.2 have been adjusted by the processes outlined in section 4.2 so that the values given satisfy statics.

Finally, the ultimate shear in the shear span at the time of its failure is given in Table 6.3.

TABLE 6.1 Experimental Loads and Reactions

Beam Mark	Type of Web Reinforcement	R1	P1	R2	P2	R3
		N. Support Reaction (kN)	N. Jack Load (kN)	Int. Support Reaction (kN)	S. Jack Load (kN)	S. Support Reaction (kN)
1/1.0	Min. Vert. None	604* 700	1200 1400			603 694*
2.1.0	Min. Horz. Min. Vert. + Min. Horiz.	750 750*	1500 1500			750* 750
3/1.0	Min. Vert. Min. Vert.	395* 393	1100 1180	1380 1536	1086 1154	396 388*
4/1.0	Min. Horiz. Min. Horiz.	410 372*	1093 1001	1326 1225	1083 984	418* 369
5/1.0	Max. Vert. Max. Vert.	408* 306	1294 966	1734 1486	1277 1340	404 491*
6/1.0	Max. Horiz. Max. Horiz.	454 470*	1111 1084	1277 1186	1087 1034	450* 461
7/1.0	None None	282 389*	714 1107	840 1370	700 1077	282* 398
1/1.5	None Min. Vert.	306 356*	606 707			300* 354
2/1.5	Min. Horiz. Min. Vert. + Min. Horiz.	227 347*	452 697			225* 348
3/1.5	Min. Vert. Min. Vert.	153 178*	405 472	483 569	401 467	156* 178
4/1.5	Min. Horiz. Min. Horiz.	115* 133	327 377	409 463	324 372	116 137*
5/1.5	Max. Vert. Max. Vert.	290* 317	863 894	1120 1131	852 885	286 308*
6/1.5	Max. Horiz. Max. Horiz.	146 148*	407 410	515 513	399 406	144* 149
7/1.5	None None	131 215*	362 572	444 689	359 569	139* 220
8/1.5	Min. Vert. + Min. Horiz. Min. Vert. + Min. Horiz.	197 212*	546 606	679 757	540 599	198* 214
1/2.0	None Min. Vert.	179 198*	353 400			176* 199
2/2.0	Min. Horiz. Min. Vert. + Min. Horiz.	369 407*	369 407			185* 204
3/2.0	Min. Vert. Min. Vert.	163* 164	428 451	519 554	425 444	159 162*
4/2.0	Min. Horiz. Min. Horiz.	101* 124	303 376	388 485	299 372	103 126*
5/2.0	Max. Vert. Max. Vert.	218* 234	684 709	891 913	668 699	216 238*
6/2.0	Max. Horiz. Max. Horiz.	110 97*	302 238	371 277	299 228	110* 93
7/2.0	None None	106 80*	298 233	372 298	293 228	106* 80
5/2.5	Max. Vert. Max. Vert.	152* -	492 -	649 -	484 -	152 -

*Indicates end of beam in which failure occurred.

TABLE 6.2 Balanced Loads and Reactions

Beam Mark	Type of Web Reinforcement	R1	P1	R2	P2	R3	e/D (%)
		N. Support Reaction (kN)	N. Jack Load (kN)	Int. Support Reaction (kN)	S. Jack Load (kN)	S. Support Reaction (kN)	
1/1.0	Min. Vert.	602*	1204			602	1
	None	699	1397			699*	0
2/1.0	Min. Horiz.	750	1500			750*	0
	Min Vert. + Min. Horiz.	750*	1500			750	0
3/1.0	Min. Vert.	400*	1085	1385	1082	393	-1
	Min. Vert.	400	1176	1540	1150	386*	-1
4/1.0	Min. Horiz.	420	1087	1330	1078	415*	-1
	Min. Horiz.	378	996	1229	979	369	-1
5/1.0	Max. Vert.	413	1288	1740	1271	405	-1
	Max. Vert.	304	961	1491	1333	499*	-1
6/1.0	Max. Horiz.	461	1107	1280	1083	448*	-1
	Max. Horiz.	479*	1084	1186	1034	453	0
7/1.0	None	287	711	842	698	280*	-1
	None	405*	1100	1377	1070	389	-1
1 1.5	None	303	606			303*	[illegible]
	Min. Vert.	354*	709			354	0
2/1.5	Min. Horiz.	226	452			226*	0
	Min. Vert. + Min. Horiz.	348	696			348	0
3/1.5	Min. Horiz.	158	401	485	398	156*	-2
	Min. Vert.	181*	468	572	464	179	-1
4/1.5	Min. Horiz.	118*	324	411	321	116	-2
	Min. Horiz.	138	373	467	368	136*	-2
5/1.5	Max. Vert.	293*	858	1126	847	287	-1
	Max. Vert.	318	888	1136	879	313*	-1
6/1.5	Max. Horiz.	147	407	515	399	143*	0
	Max. Horiz.	150*	408	514	405	148	-1
7/1.5	None	137	360	445	357	135*	-1
	None	220*	568	693	565	219	-1
8/1.5	Min. Vert. + Min. Horiz.	201	543	681	537	198*	-1
	Min. Vert. + Min. Horiz.	218*	600	762	594	214	-2
1/2.0	None	177	354			177*	1
	Min. Vert.	199*	399			199	-1
2/2.0	Min. Horiz.	185	369			185*	0
	Min. Vert. + Min. Horiz.	204*	407			204	0
3/2.0	Min. Vert.	164*	425	521	422	162	-1
	Min. Vert.	167	447	557	440	163*	-2
4/2.0	Min. Horiz.	105*	300	390	297	103	-2
	Min. Horiz.	128	373	488	369	126*	-2
5/2.0	Max. Vert.	224*	677	899	661	216	-2
	Max. Vert.	242	703	918	693	237*	-2
6/2.0	Max. Horiz.	113	299	372	297	111*	-2
	Max. Horiz.	97*	238	277	228	92	0
7/2.0	None	108	296	374	291	106*	-1
	None	82	232	299	227	79	-1
5/2.5	Max. Vert.	156*	486	656	478	152	-2
	Max. Vert.	-	-	-	-	-	-

*indicates end of beam in which failure occurred.

TABLE 6.3 Ultimate Shear Strengths

Beam Mark	Type of Web Reinforcement	V_u (kN)	v_u (MPa)	f'_c (MPa)	$v_u(f'_c)^{-0.5}$ (SI)	$v_u(f'_c)^{-1}$
1/1.0	Min. Vert. None	602 699	3.17 3.68	26.1 26.1	0.62 0.72	0.121 0.141
2/1.0	Min. Horiz. Min. Vert. + Min. Horiz.	750 750	3.95 3.95	26.8 26.8	0.76 0.76	0.147 0.147
3/1.0	Min. Vert. Min. Vert.	685 764	3.61 4.02	28.9 28.9	0.67 0.75	0.125 0.139
4/1.0	Min. Horiz. Min. Horiz.	663 618	3.49 3.25	28.5 28.5	0.65 0.61	0.122 0.114
5/1.0	Max. Vert. Max. Vert.	875 834	4.61 4.39	36.9 36.9	0.76 0.72	0.125 0.119
6/1.0	Max. Horiz. Max. Horiz.	635 605	3.34 3.18	35.8 35.8	0.56 0.53	0.093 0.089
7/1.0	None None	418 695	2.20 3.66	34.5 34.5	0.37 0.62	0.064 0.106
1/1.5	None Min. Vert.	303 354	2.86 3.34	42.4 42.4	0.44 0.51	0.067 0.079
2/1.5	Min. Horiz. Min. Vert. + Min. Horiz.	226 348	2.13 3.28	42.4 42.4	0.33 0.50	0.050 0.077
3.15	Min. Vert. Min. Vert.	242 287	2.30 2.73	14.5 14.5	0.61 0.72	0.159 0.188
4/1.5	Min. Horiz. Min. Horiz.	206 232	1.96 2.21	32.5 32.5	0.34 0.39	0.060 0.068
5/1.5	Max. Vert. Max. Vert.	565 566	5.38 5.39	39.6 39.6	0.86 0.86	0.136 0.136
6/1.5	Max. Horiz. Max. Horiz.	256 258	2.44 2.46	45.0 45.0	0.36 0.37	0.054 0.055
7/1.5	None None	222 348	2.11 3.31	30.4 30.4	0.38 0.60	0.069 0.109
8/1.5	Min. Vert. + Min. Horiz. Min. Vert. + Min. Horiz.	339 382	3.23 3.64	37.2 37.2	0.53 0.60	0.087 0.098
1/2.0	None Min. Vert.	177 199	1.30 2.21	43.2 43.2	0.20 0.34	0.030 0.051
2/2.0	Min. Horiz. Min. Vert. + Min. Horiz.	185 204	2.06 2.27	43.2 43.2	0.31 0.34	0.048 0.053
3/2.0	Min. Vert. Min. Vert.	261 277	2.97 3.15	42.5 42.5	0.45 0.48	0.070 0.074
4/2.0	Min. Horiz. Min. Horiz.	195 243	2.22 2.76	38.3 38.3	0.36 0.45	0.058 0.072
5/2.0	Max. Vert. Max. Vert.	453 456	5.15 5.18	41.1 41.1	0.80 0.81	0.125 0.126
6/2.0	Max. Horiz. Max. Horiz.	186 141	2.11 1.60	37.4 37.4	0.35 0.26	0.056 0.43
7/2.0	None None	185 150	2.10 1.70	46.8 46.8	0.31 0.25	0.045 0.036
5/2.5	Max. Vert. Max. Vert.	330 -	4.65 -	34.0 -	0.80 -	0.137 -

6.3 Deflections and Support Settlements

The observed midspan deflections are presented in Figs. 6.1 to 6.8. For the continuous beams, the jack load and midspan deflection are given for the span which actually failed in shear during the particular test in question. Part of the measured deflection was due to settlement of the support reactions. The midspan deflection due to support settlements being the average of the interior support settlement and exterior support settlement. The range in midspan deflection due to support settlements is plotted on each of the load-deflection diagrams. The true midspan deflection can be obtained by subtracting the deflection due to support settlement from the total deflection shown. From the diagrams, it can be seen that this correction is small. The curves for the beams tested by Ong (3/1.5, 4/1.5, 7/1.5 and 8/1.5) already have support settlement effects deducted from them.

6.4 Mode of Data Presentation

The remaining data is presented beam by beam. Each set of data begins with a description of observations made during the test, drawing attention to any special behavior. This is followed by a sketch of the crack patterns as seen from the west face of the beam. The crack pattern on the west face is presented as is, while the crack pattern on the east face has been reversed so that the left end of the sketch is always north. In the crack drawings, shaded areas

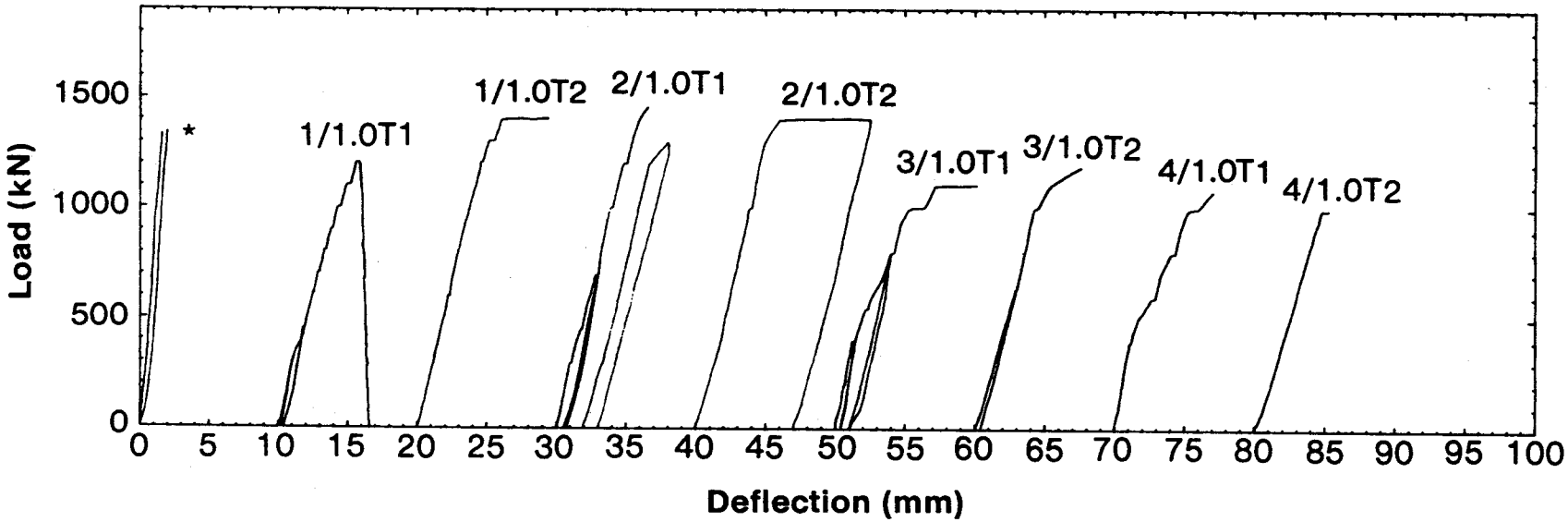

*Range of midspan deflection due to suport settlement

Figure 6.1. Beam 1/1.0, 2/1.0, 3/1.0, and 4/1.0 Load Deflection Curves

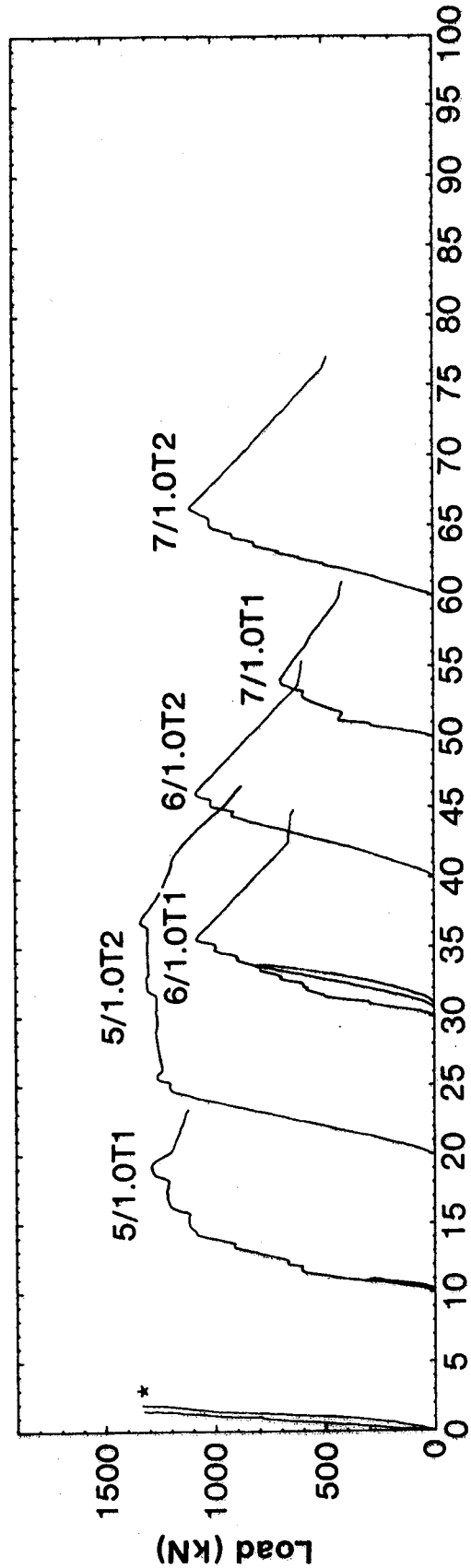

*Range of midspan deflection due to support settlement

Figure 6.2. Beam 5/1.0, 6/1.0, and 7/1.0 Load Deflection Curves

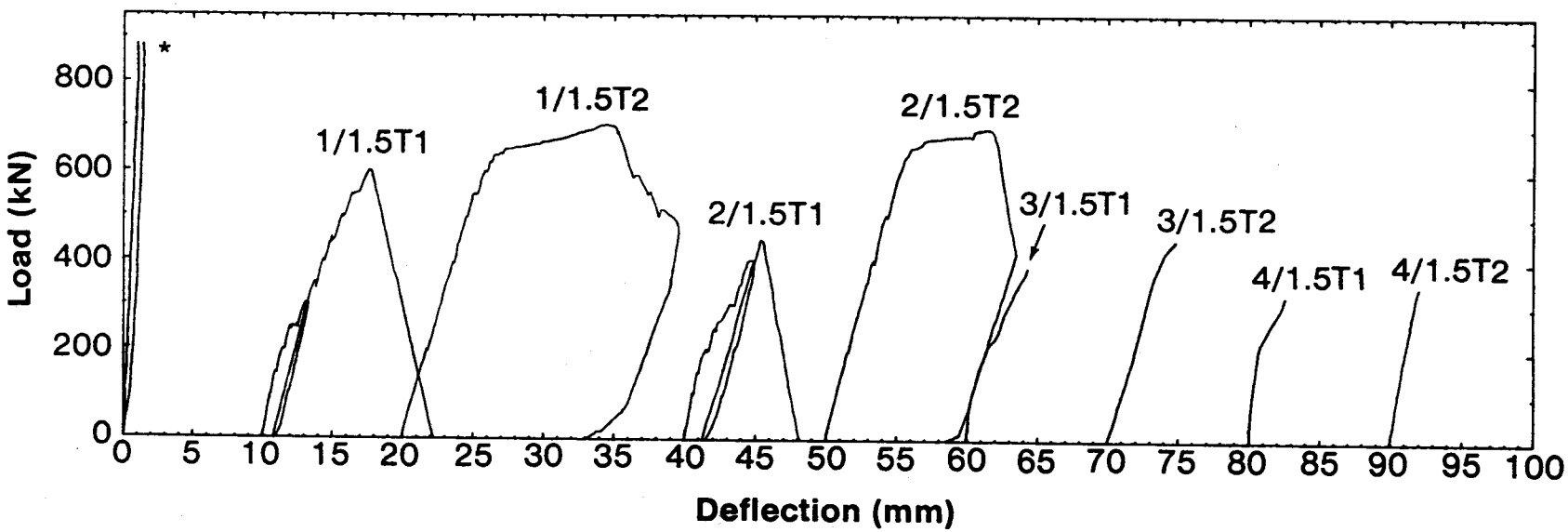

*Range of midspan deflection due to support settlement

Figure 6.3. Beam 1/1.5, 2/1.5, 3/1.5, and 4/1.5 Load-Deflection Curves

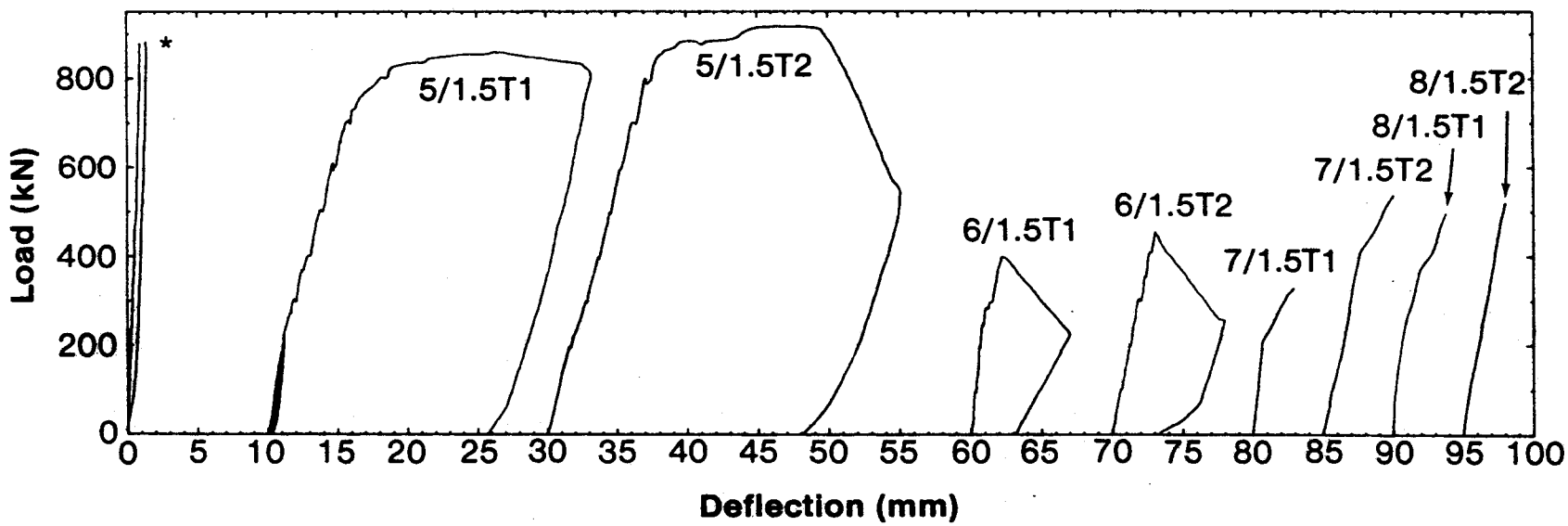

*Range of midspan deflection due to support settlement

Figure 6.4. Beam 5/1.5, 6/1.5, 7/1.5, and 8/1.5 Load-Deflection Curves

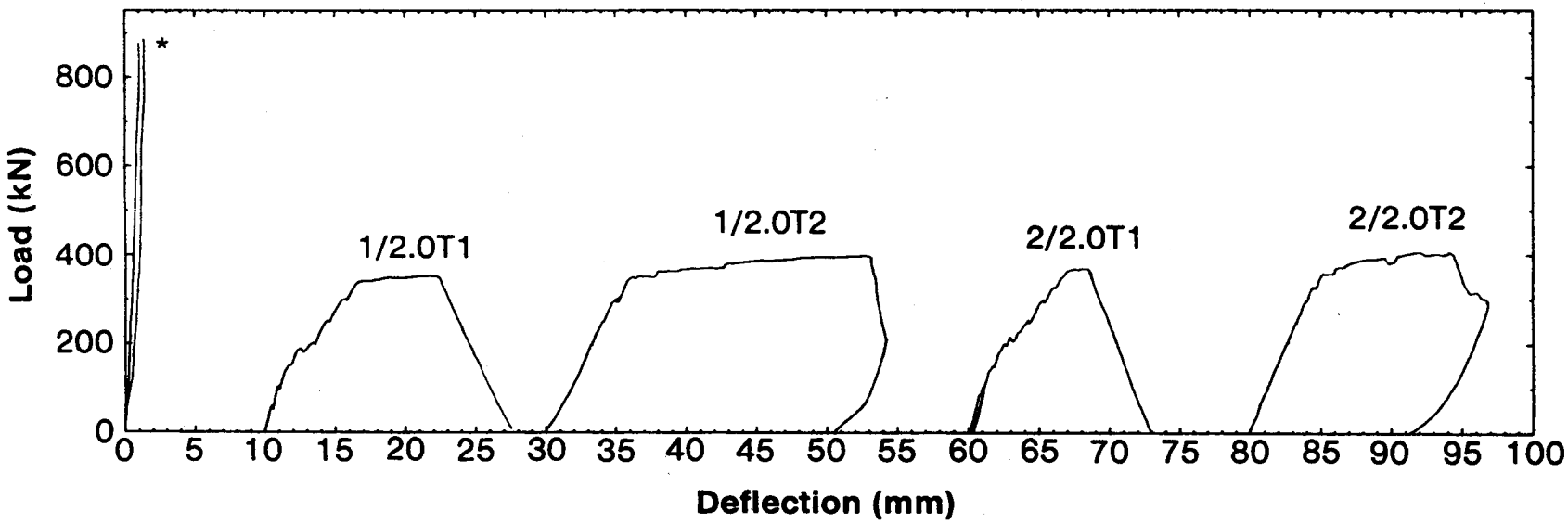

*Range of midspan deflection due to support settlement

Figure 6.5. Beam 1/2.0 and 2/2.0 Load-Deflection Curves

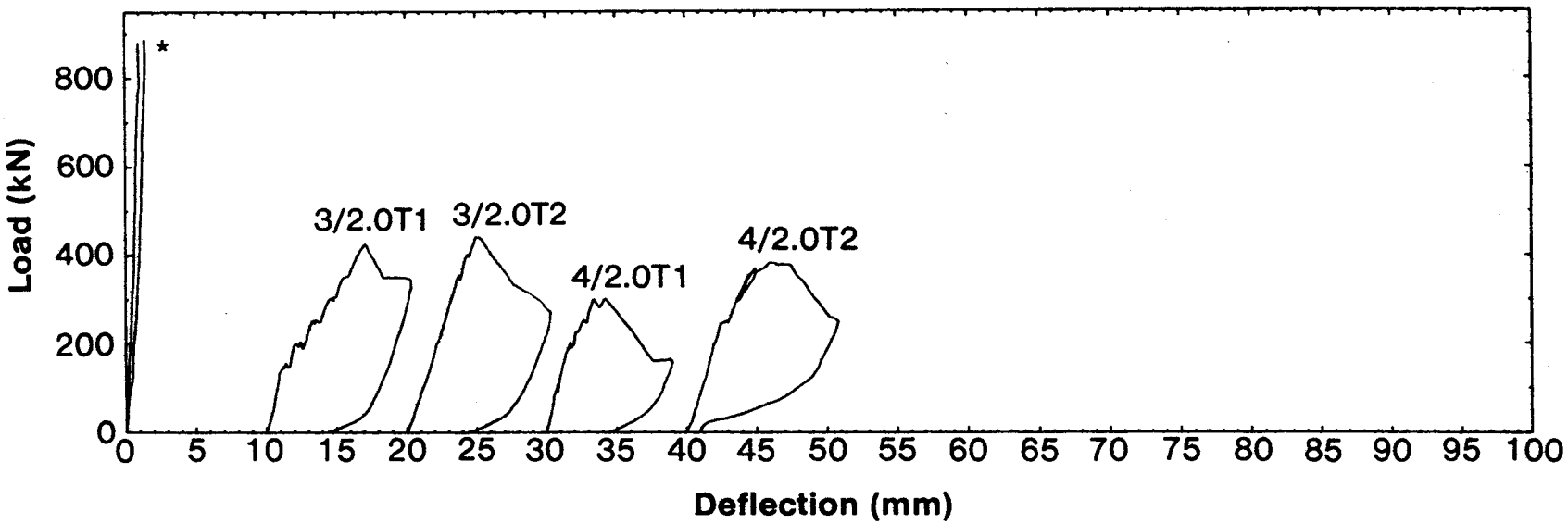

*Range of midspan deflection due to support settlement

Figure 6.6. Beam 3/2.0 and 4/2.0 Load-Deflection Curves

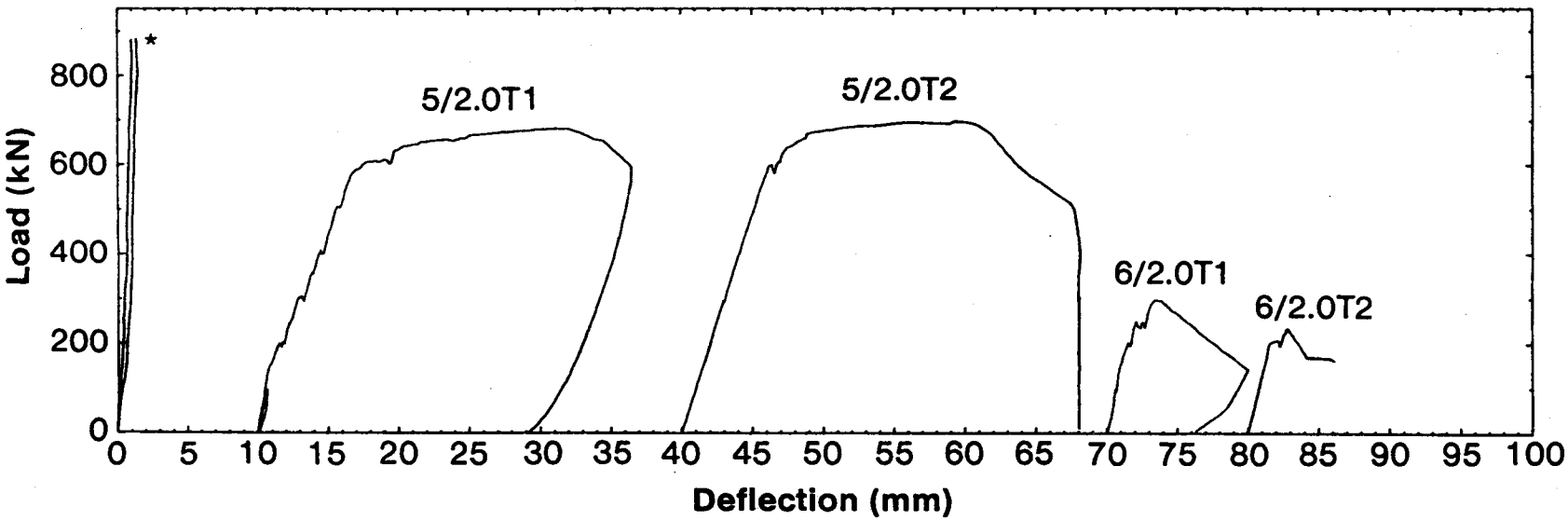

*Range of midspan deflection due to support settlement

Figure 6.7. Beam 5/2.0 and 6/2.0 Load-Deflection Curves

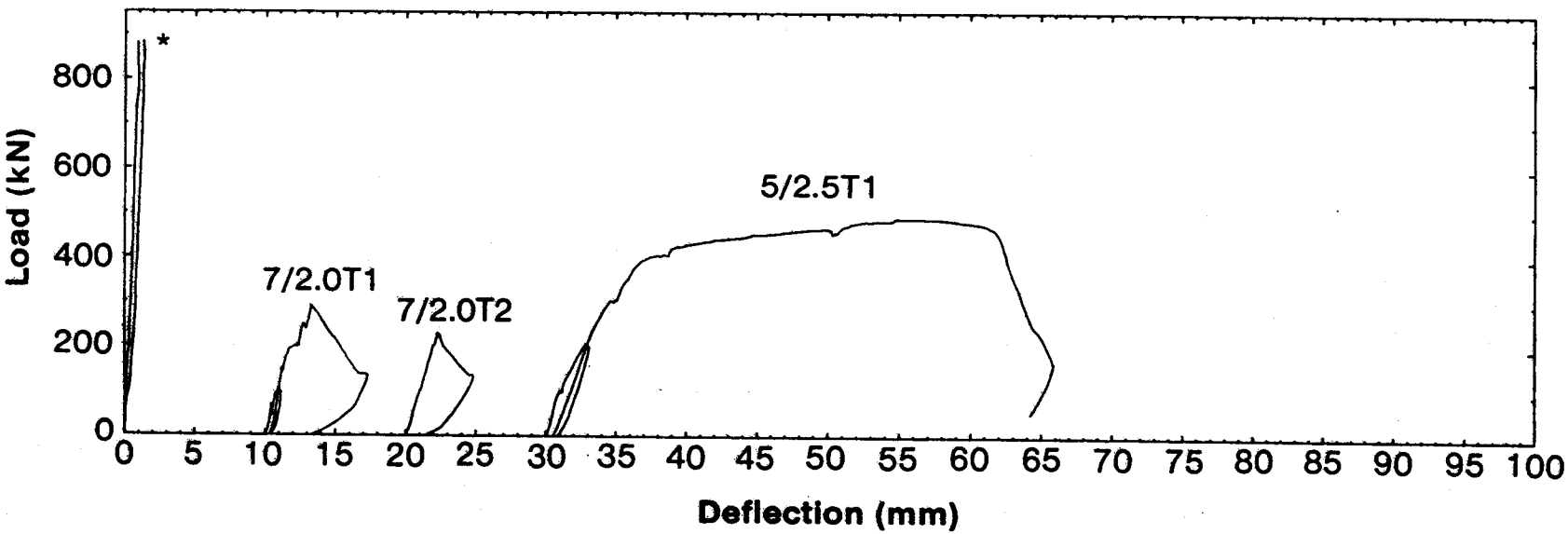

*Range of midspan deflection due to support settlement

Figure 6.8. Beam 7/2.0 and 5/2.5 Load-Deflection Curves

represent areas that crushed at failure. The crack drawings are followed by a plot of the concrete compression strains as obtained from the rosette data. Only the maximum compression strains are plotted for clarity. Two figures are used to present the steel strain data. The first is an elevation of the beam showing the location of the reinforcement and Demec targets superimposed on the crack patterns as seen from the west side of the beam. Directly below this, the main steel strains are plotted as a function of position along the bars. A second plot relates the strain in selected gage locations (which were identified in the first plot) to the applied jack load. In this figure, solid lines are used for main steel, broken lines for web steel.

The data is described in some detail for the first few beams, and in much less detail for the rest.

6.5 Beam 1/1.0

This beam had light stirrups in the north end and no stirrups in the south end. Inclined cracking occurred very suddenly at a load of about 350 kN. Cracks formed almost instantaneously in the two shear spans and appeared to be very severe even though the load was only about 25% of the eventual ultimate load.

The failure in the virgin test occurred, after the beam had resisted the failure load for a period of about 20 minutes. The failure was preceded by a slight cracking

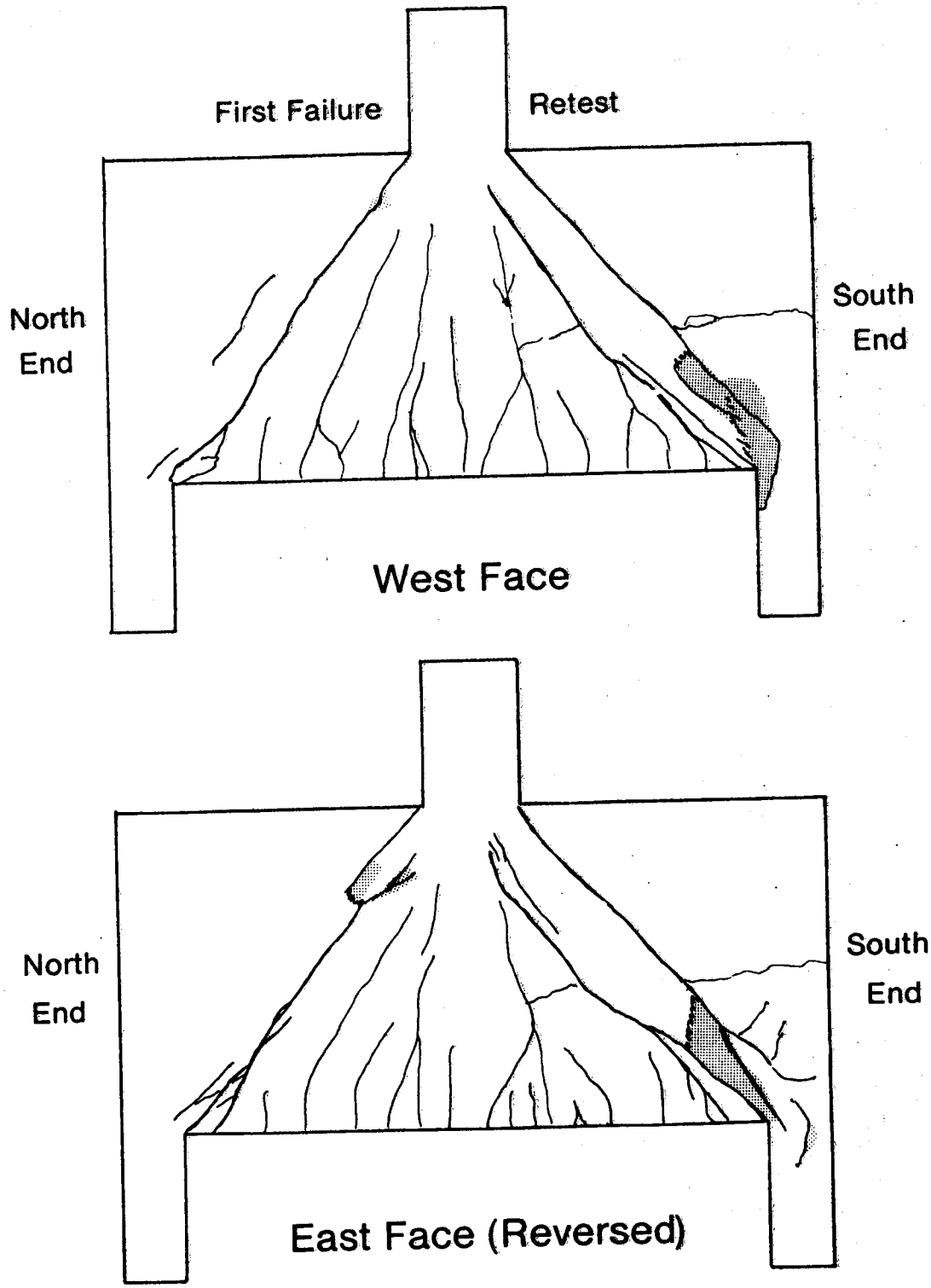

Figure 6.9. Beam 1/1.0 Crack Patterns

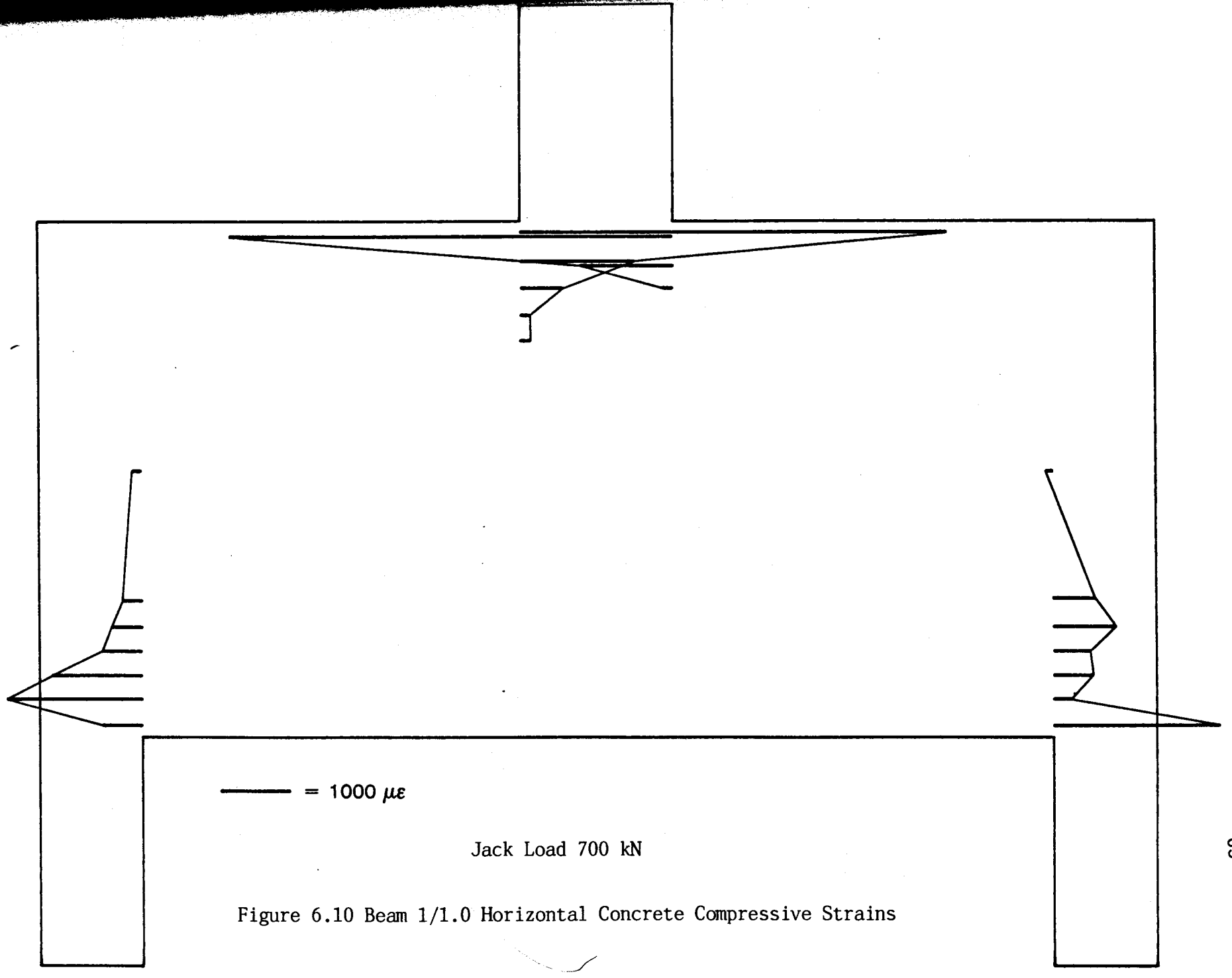

Figure 6.10 Beam 1/1.0 Horizontal Concrete Compressive Strains

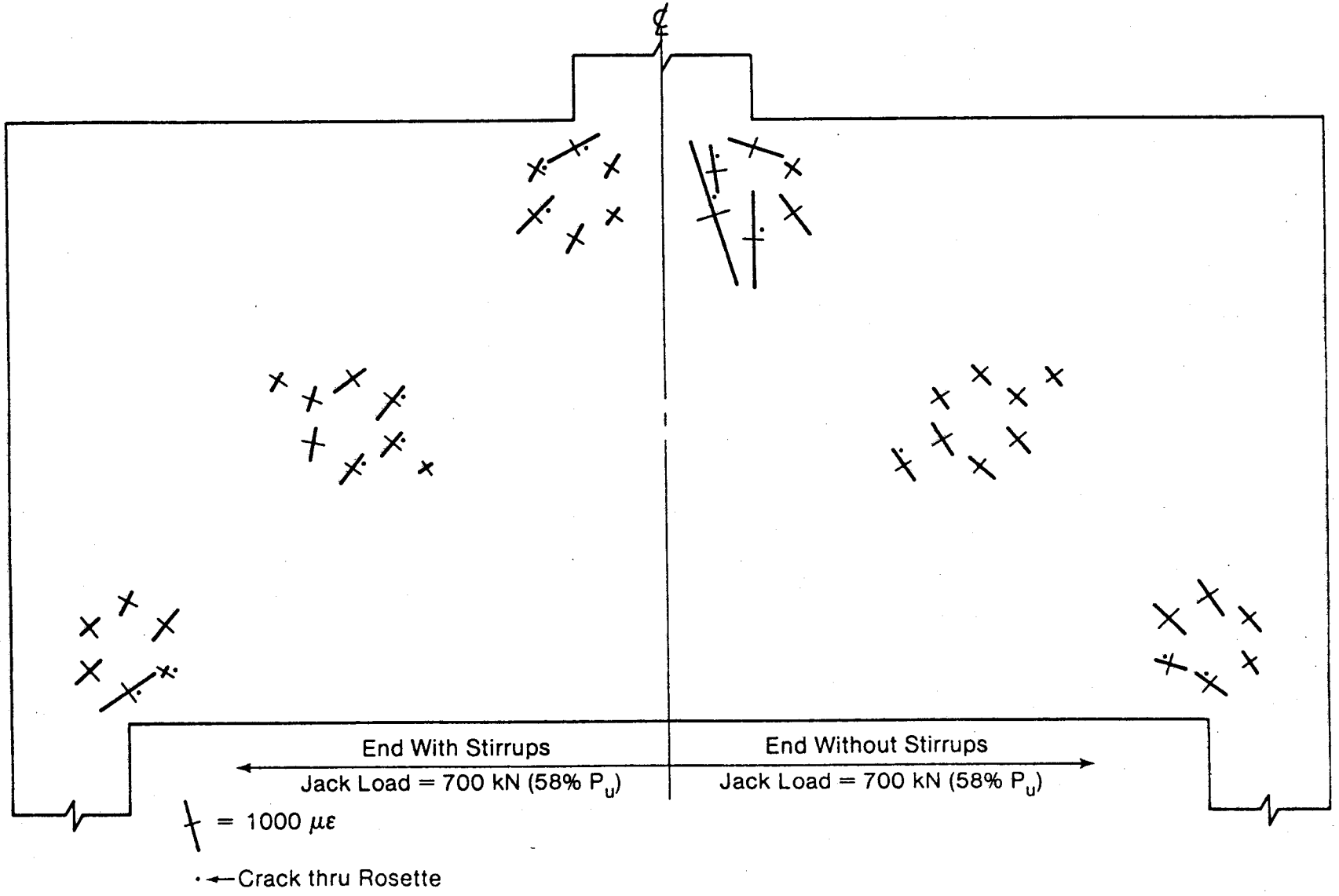

Figure 6.11 Beam 1/1.0 Concrete Compressive Strains

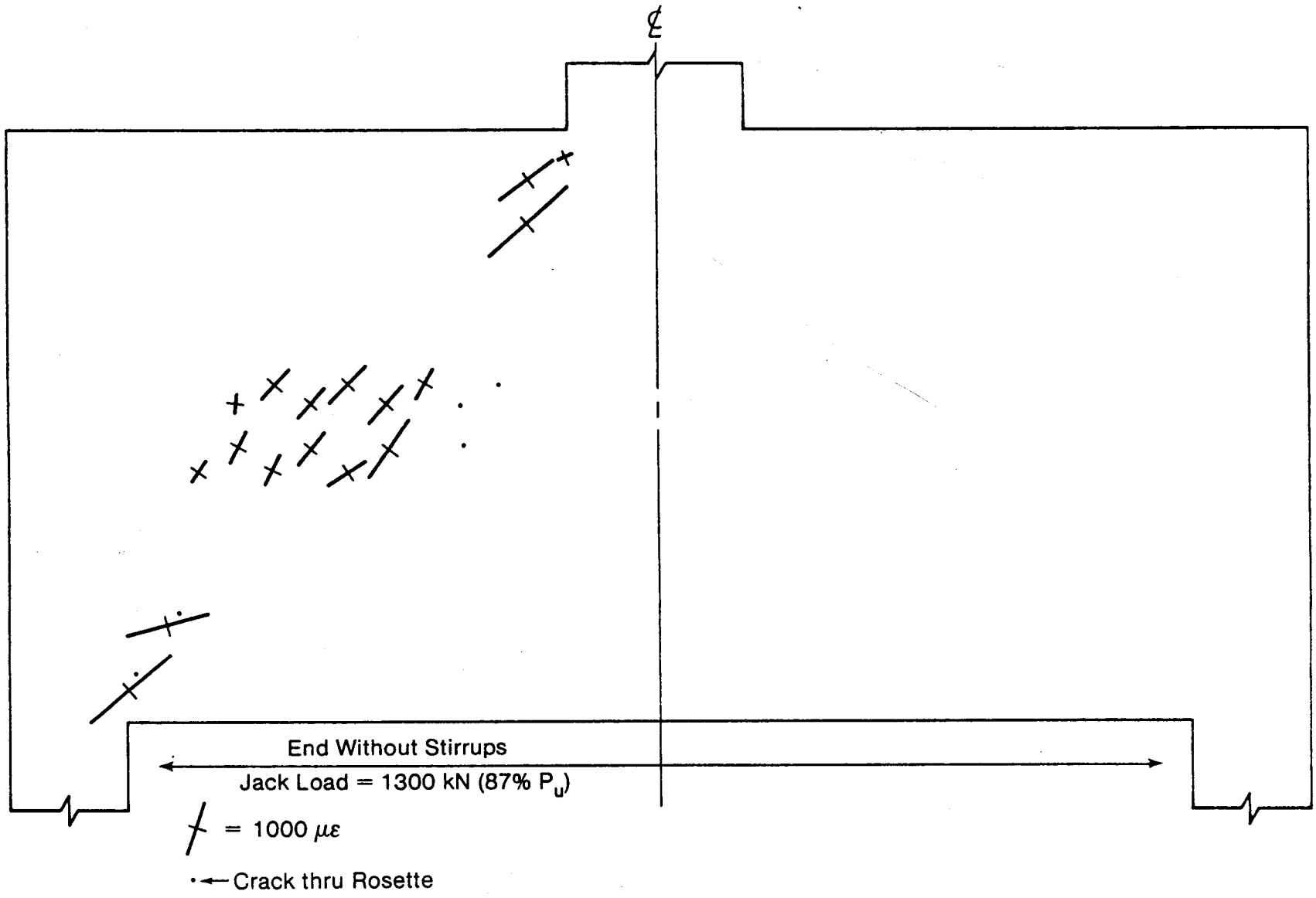

Figure 6.12 Beam 1/1.0 Retest Concrete Compressive Strains

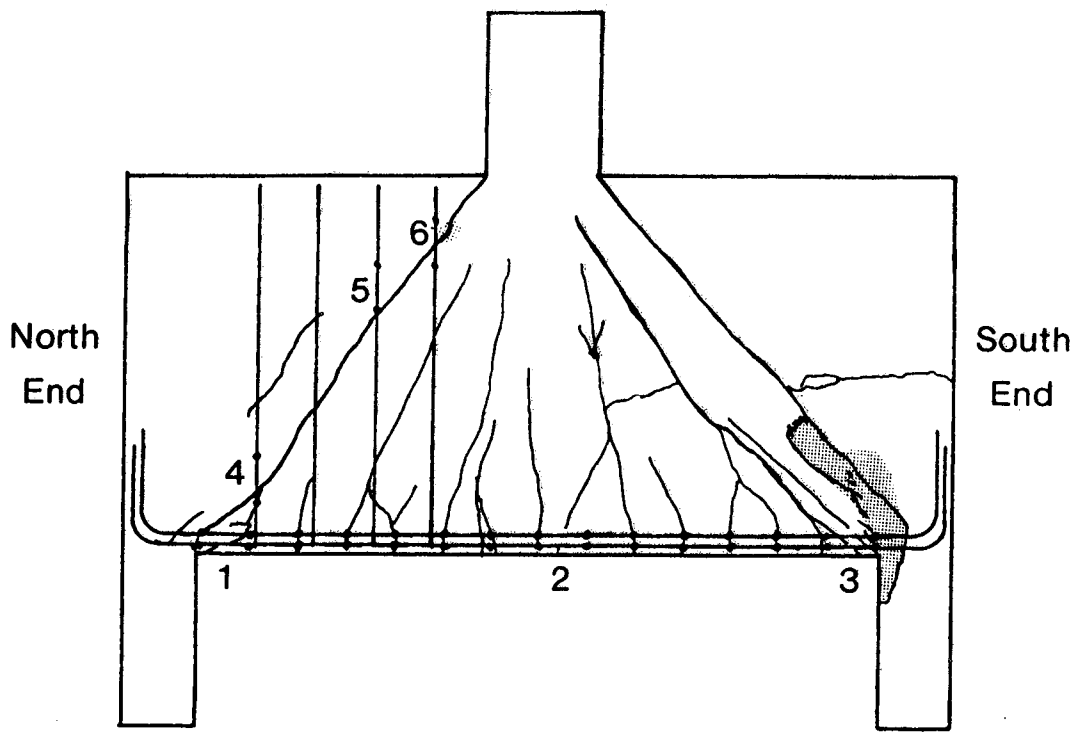

Gage Locations

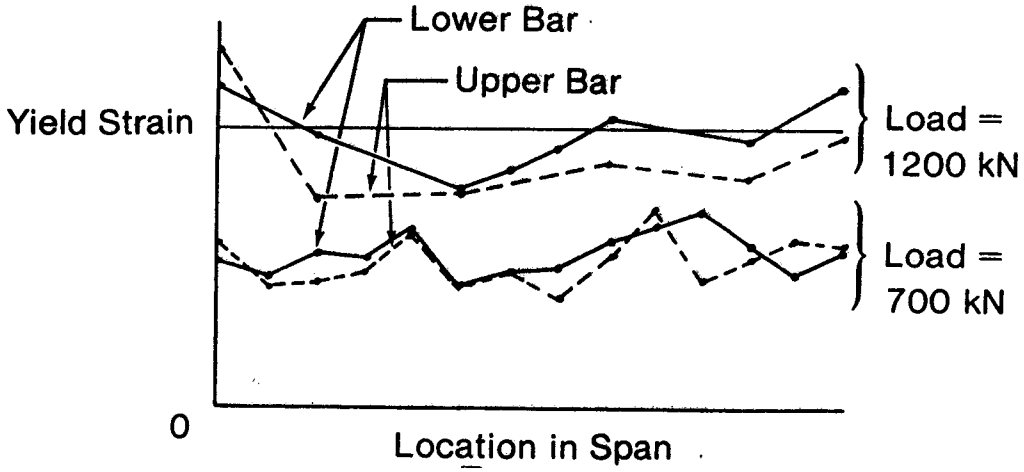

Main Steel Strains

(Strain Scale: 1mm = 50 Micro-Strain)

Figure 6.13 Beam 1/.1.0 Steel Strains.

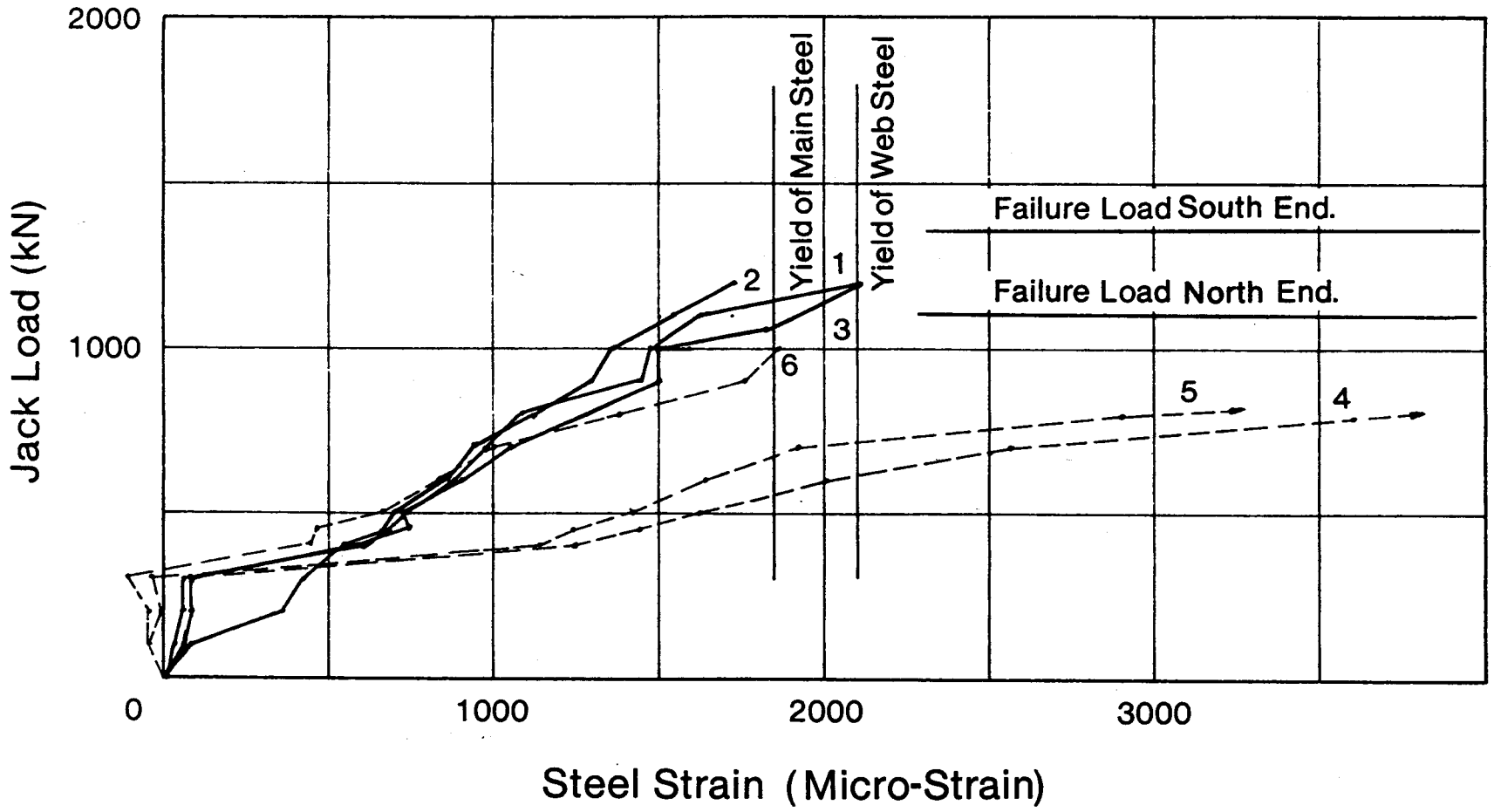

Figure 6.14 Beam 1/1.0 Load vs. Steel Strain

sound and about 5 seconds of warning. The load deflection curve in Fig. 6.1 (for 1/1.0T1) shows how brittle the failure was. It should be noted that the shear span with stirrups failed rather than the shear span without web reinforcement.

During the retest, the unreinforced south shear span deflected plasticly (with extensive yielding of the main reinforcement) to failure at constant load with a large crushed region near the south support. The unreinforced shear span failed a little more violently than the shear span with stirrups, but both displayed sudden explosive final failures. The inclined cracks were 2 to 3 mm in width before failure of the south shear span. The inclined cracks opened about 3 to 4 times as much as they slipped. The crack pattern as well as the concrete strains indicated that fairly well defined compression struts formed within the concrete. The stirrups and main flexural reinforcement had yielded before failure occurred. The distribution of tension in the main longitudinal bars was almost constant at failure. The beam behaved like a truss with two inclined compression members and a tension tie. It appeared that the concrete compression struts had the strength to equilibrate the yield force in the reinforcement, but could not tolerate the deformation required in the joints of the truss when the tension chord yielded and elongated.

6.6 Beam 2/1.0

This beam had light horizontal web reinforcement in both shear spans plus light vertical web reinforcement in the north shear span.

The crack pattern clearly illustrates the formation of compression struts. A pair of inclined cracks outlined each strut. The interior inclined cracks occurred in the north and south shear spans at loads of 500 and 400 kN respectively. The exterior inclined cracks occurred when the maximum load was reached. This was accompanied with some loss in strength and stiffness. The beam was unloaded and cracks etc. were marked and photographed. It was then reloaded slowly. At about 90% of the previous maximum load the specimen deformed plastically with the deformations growing at constant loads (See Beam 2/1.0T1 Fig. 6.1). The south strut finally crushed at the south support. The retest of the north span which had stirrups exhibited significantly more ductility (Beam 2/1.0T2 Fig. 6.1) but it too finally failed with crushing at one end of the concrete strut.

In both shear spans there was a crushing and sliding failure with a series of fine parallel cracks where the "dead" triangular corners above the inclined cracks connected to the loading column.

Again the longitudinal reinforcement and vertical stirrups yielded before failure while the horizontal stirrups had relatively small strains.

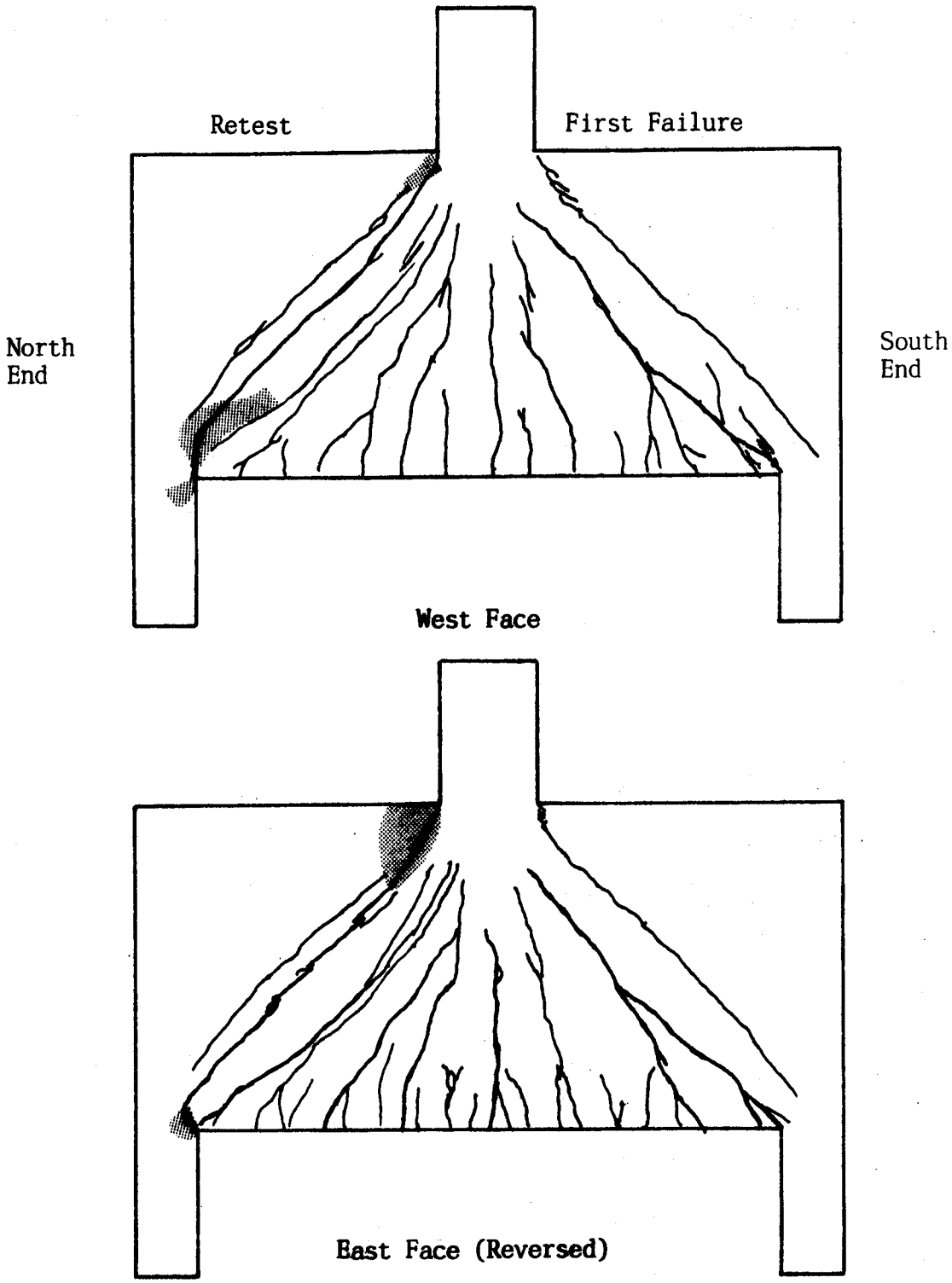

Figure 6.15 Beam 2/1.0 Crack Patterns

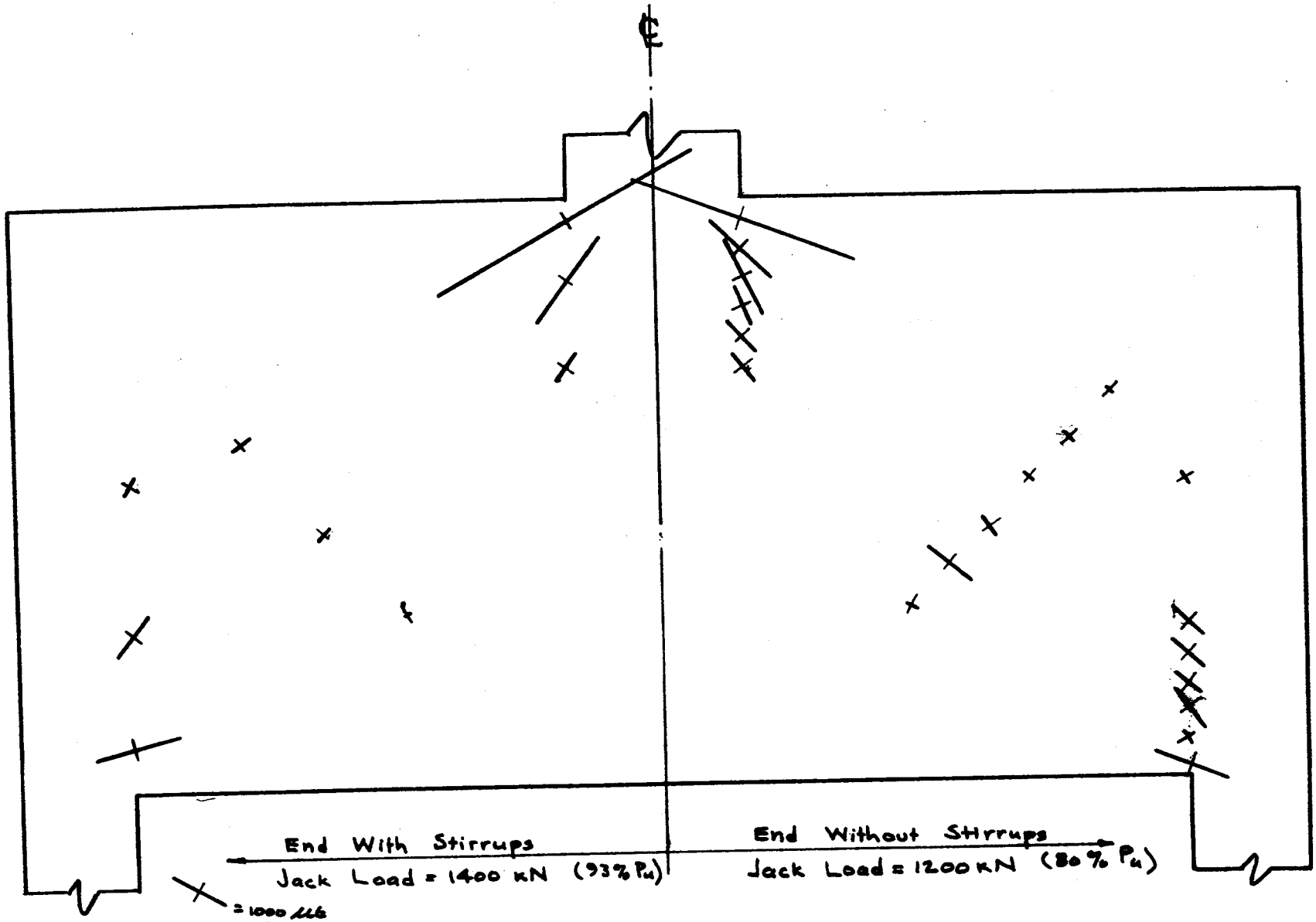

Figure 6.16 Beam 2/1.0 Concrete Compressive Strains

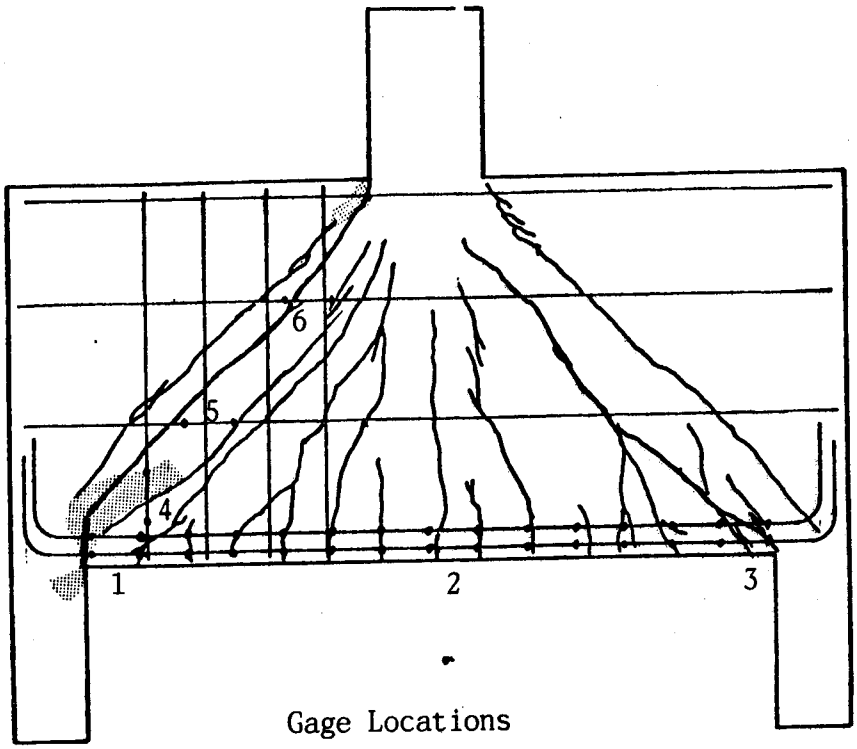

Gage Locations

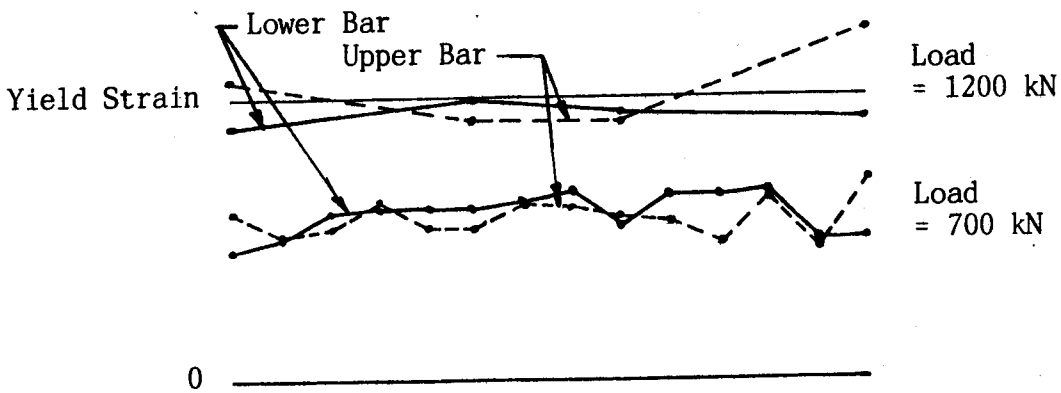

Main Steel Strains

(Strain Scale: 1mm = 50 Microstrain)

Figure 6.17 Beam 2/1.0 Steel Strains

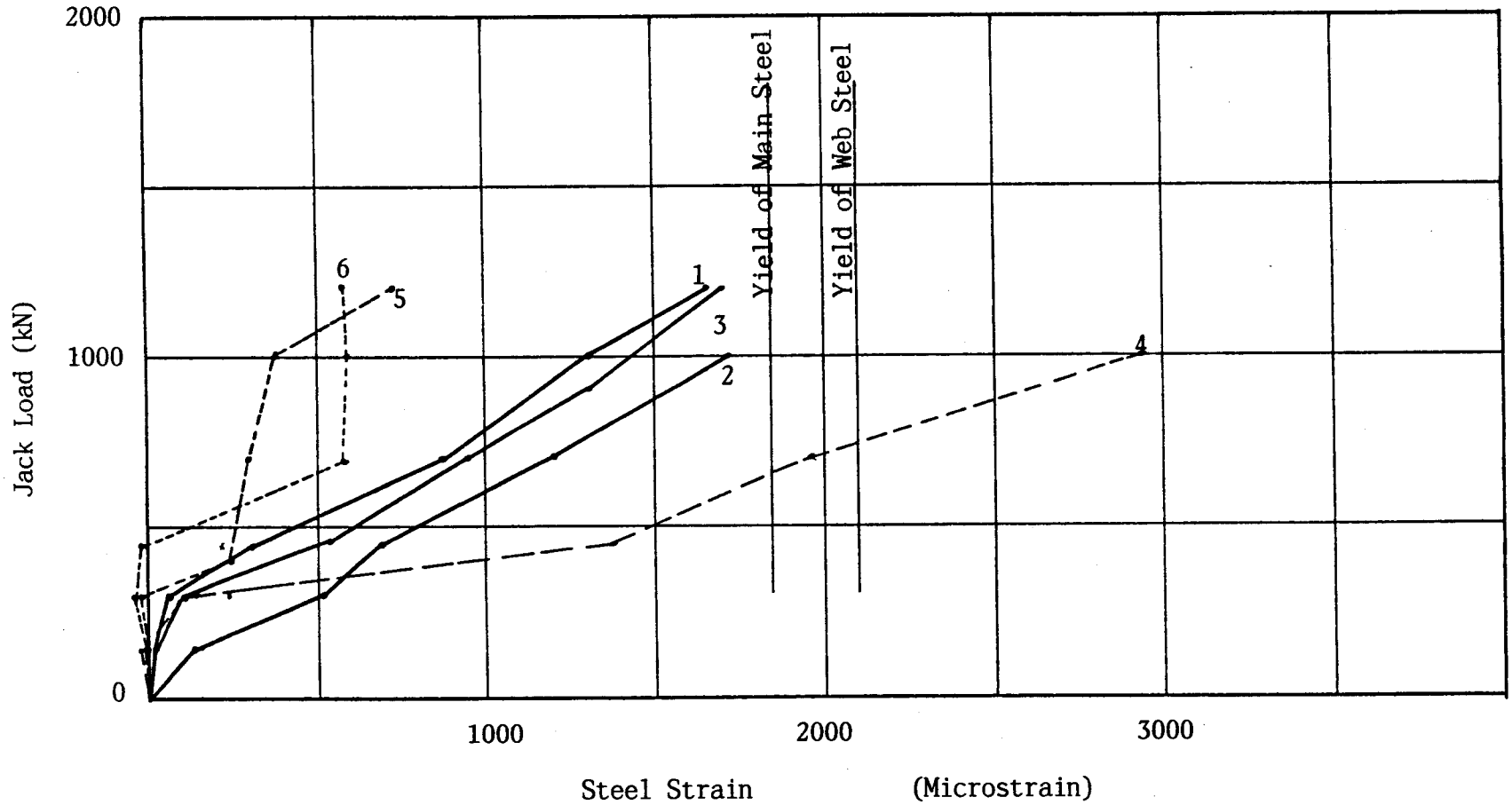

Figure 6.18 Beam 2/1.0 Load vs. Steel Strain

6.7 Beam 3/1.0

Beam 3/1.0 was a continuous beam with light stirrups in all four shear spans.

Positive flexural cracks first occurred at a load of 200 kN while negative flexural cracks did not develop until a load of 400 kN. The first inclined cracks formed at a load of 635 kN. The test was moderately ductile as shown in Fig. 6.1 (Beam 3/1.0T1) in that there was yielding of the main reinforcement. Final failure occurred when the concrete strut in the north interior shear span failed. The inclined crack in this shear span opened vertically. This resulted in separation at the top end of the crack, and a shear compression failure at the bottom of the strut. The failure load was 1084 kN.

During the retest, the south interior shear span failed with crushing and splitting of the compression strut it self. Several parallel cracks were visable in the upper end of the strut. These were very similar to vertical cracks which occur in some concrete cylinder tests.

The strains in the lower longitudinal reinforcement were practically constant over the entire length of the beam and indicated yielding prior to failure. The top bars were in tension throughout the length of the two interior shear spans but did not yield. The stirrups in the south interior shear span yielded at about 70% of the ultimate load.

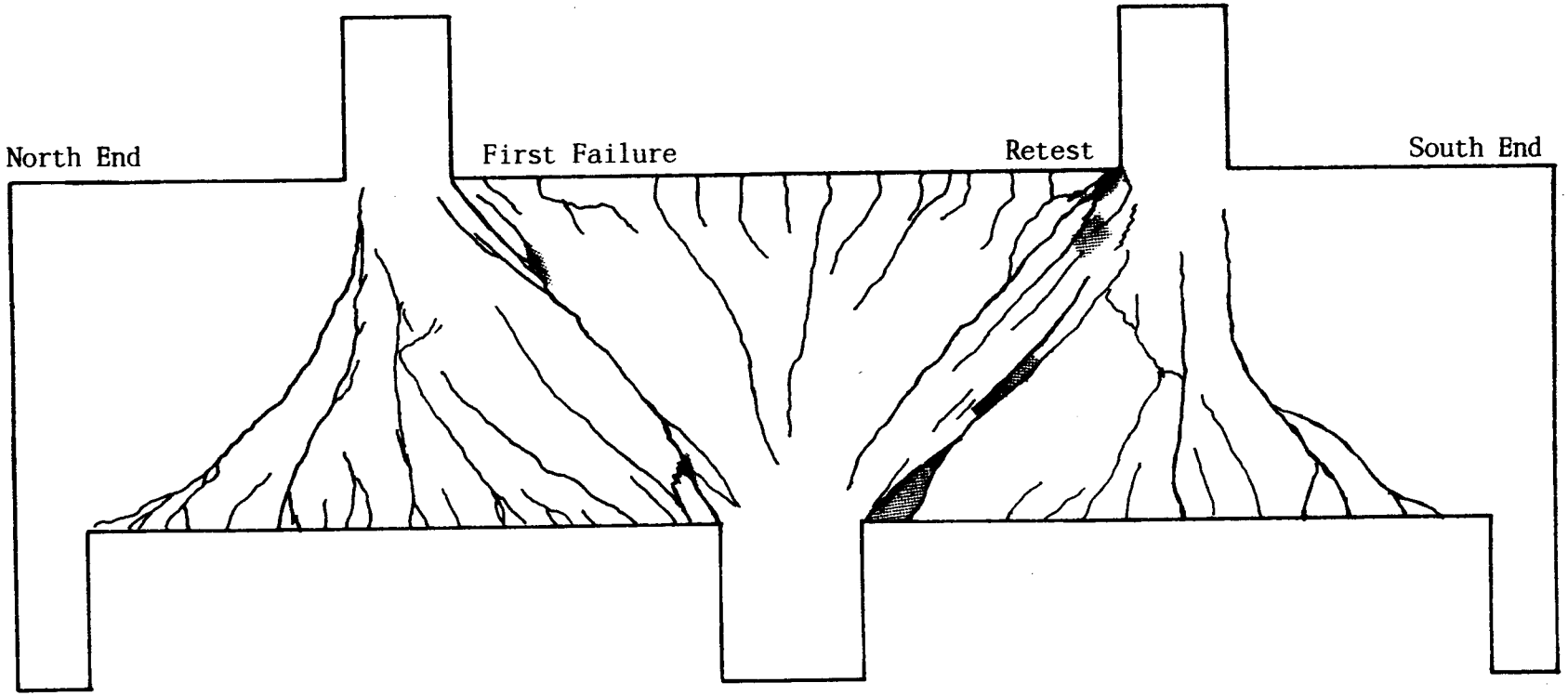

Figure 6.19 Beam 3/1.0 Crack Pattern - West Face

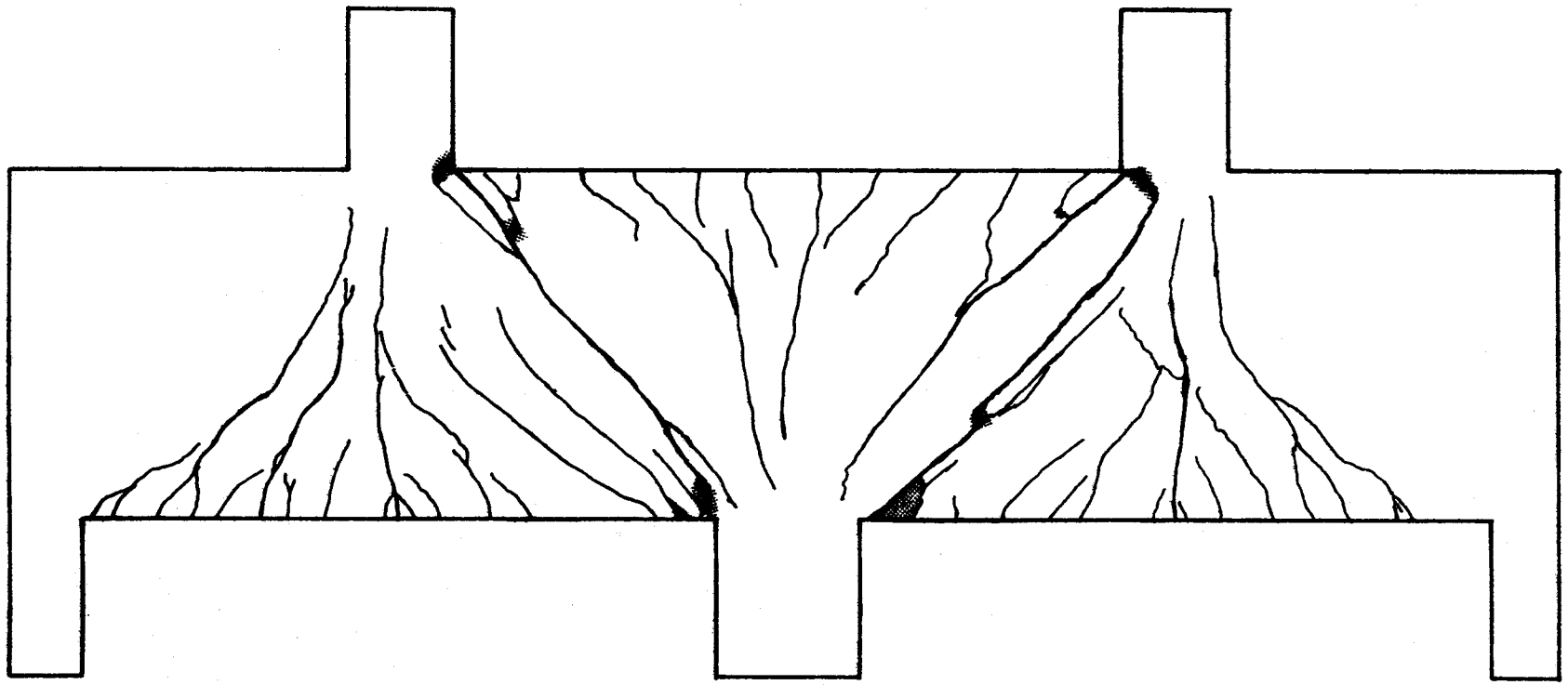

Figure 6.20 Beam 3/1.0 Crack Pattern - East Face (Reversed)

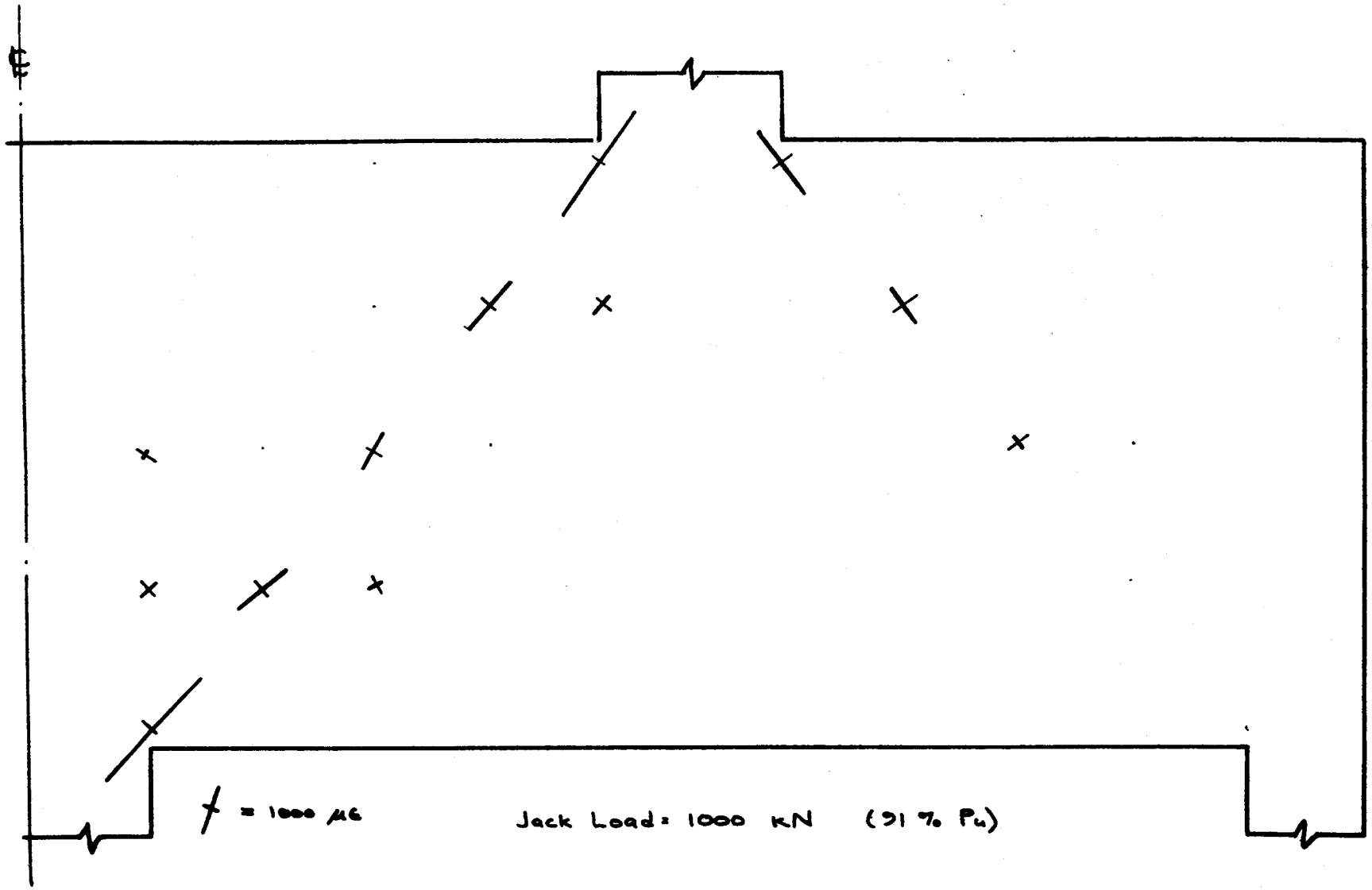

Figure 6.21 Beam 3/1.0 Concrete Compressive Strains

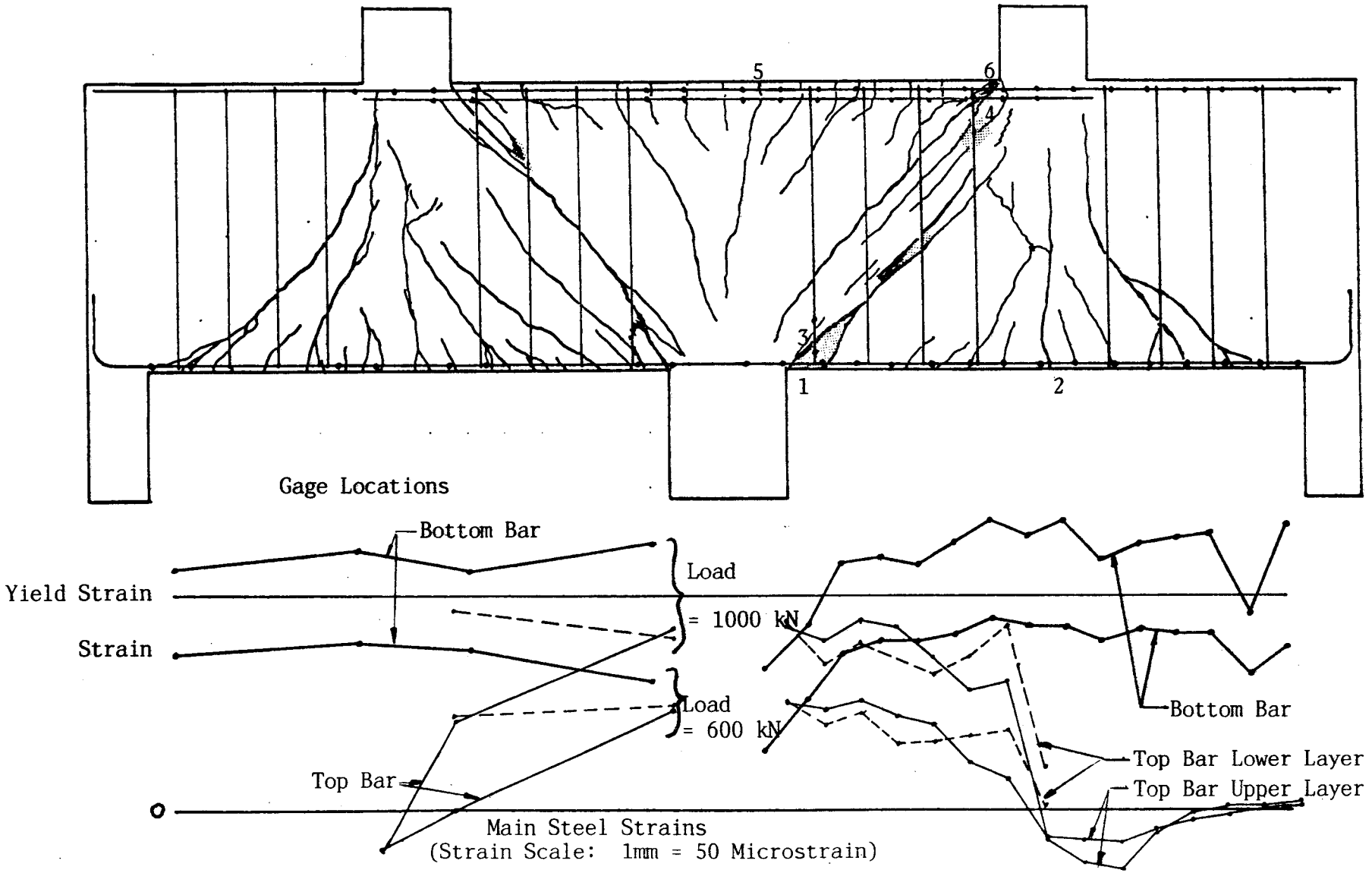

Figure 6.22 Beam 3/1.0 Steel Strains

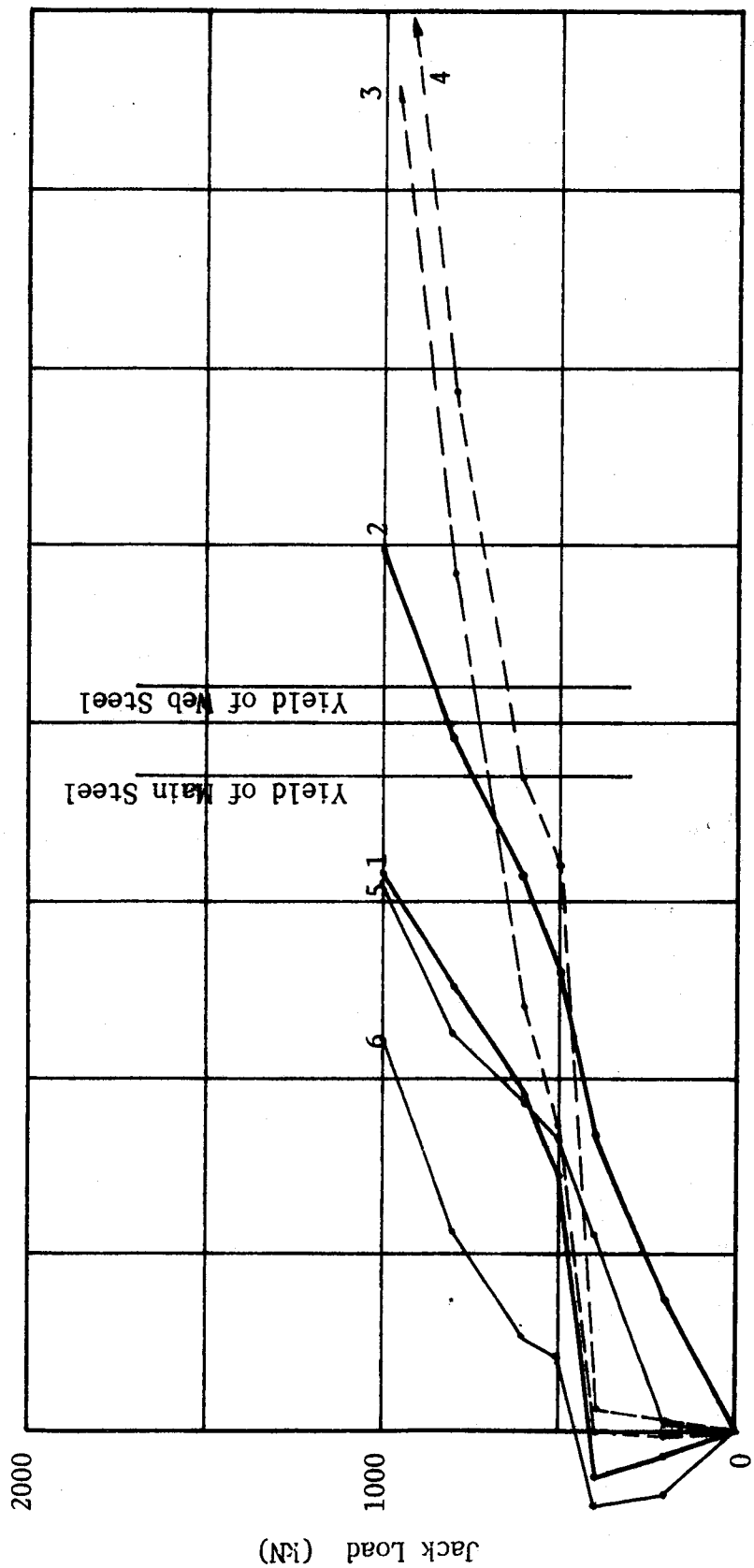

Figure 6.23 Beam 3/1.0 Load vs. Steel Strain

6.8 Beam 4/1.0

This two span continuous beam had light horizontal web reinforcement throughout both spans. Inclined cracks produced rather wide and very well defined compression struts in the interior shear spans. There was yielding of the bottom steel well before failure. Failure in both interior shear spans was due to crushing at the top end of each compression strut. This appeared to be precipated by "joint rotations" when the top steel yielded.

6.9 Beam 5/1.0

This two span beam had heavy stirrup reinforcement throughout. Inspite of the large number of stirrups present, inclined cracking occurred with loud "thuds" in the north and south interior shear spans at 676 and 600 kN, respectively. The compression struts tended to be less well defined than in the other tests. There was clearly a "fan" of flexural cracks under each point load and over the interior support. The compression struts formed between these fans. The north strut failed by shear compression at the top of the strut, accompanied by a vertical opening of the inclined crack defining the bottom of the strut. The south strut was pulled apart and had several large cracks which opened vertically. All of the stirrups were yielded, tending to pull the strut apart. There was finally a shear compression failure through the top end of the strut.

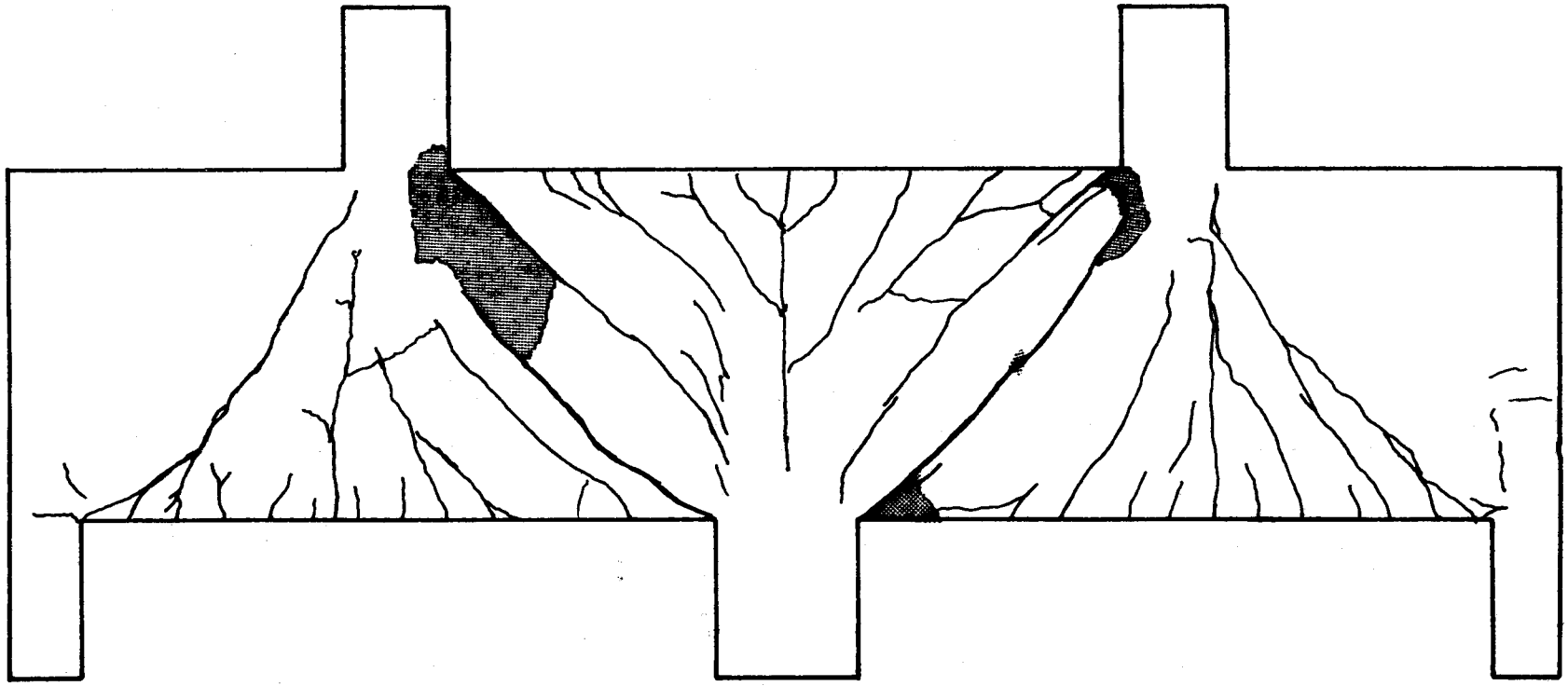

Figure 6.24 Beam 4/1.0 Crack Pattern - West Face

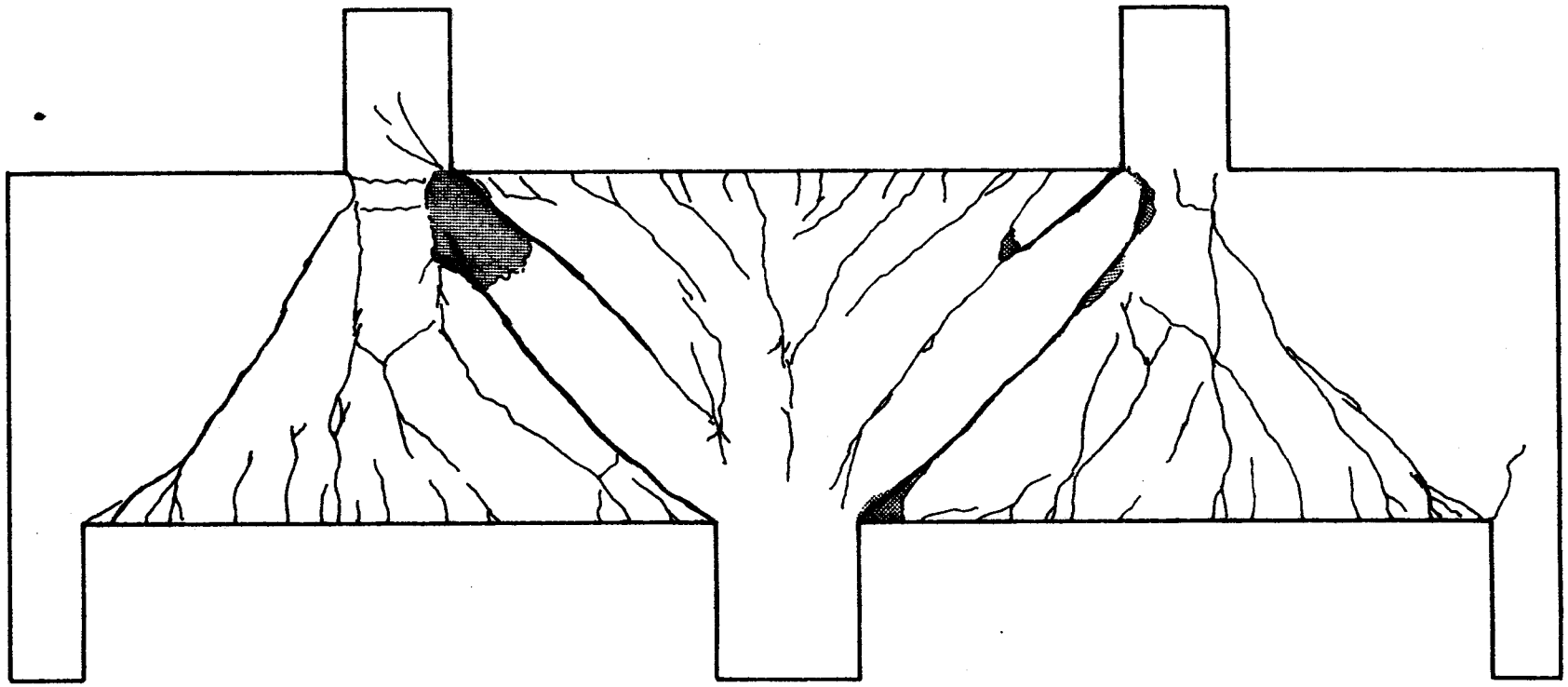

Figure 6.25 Beam 4/1.0 Crack Pattern - East Face (Reversed)

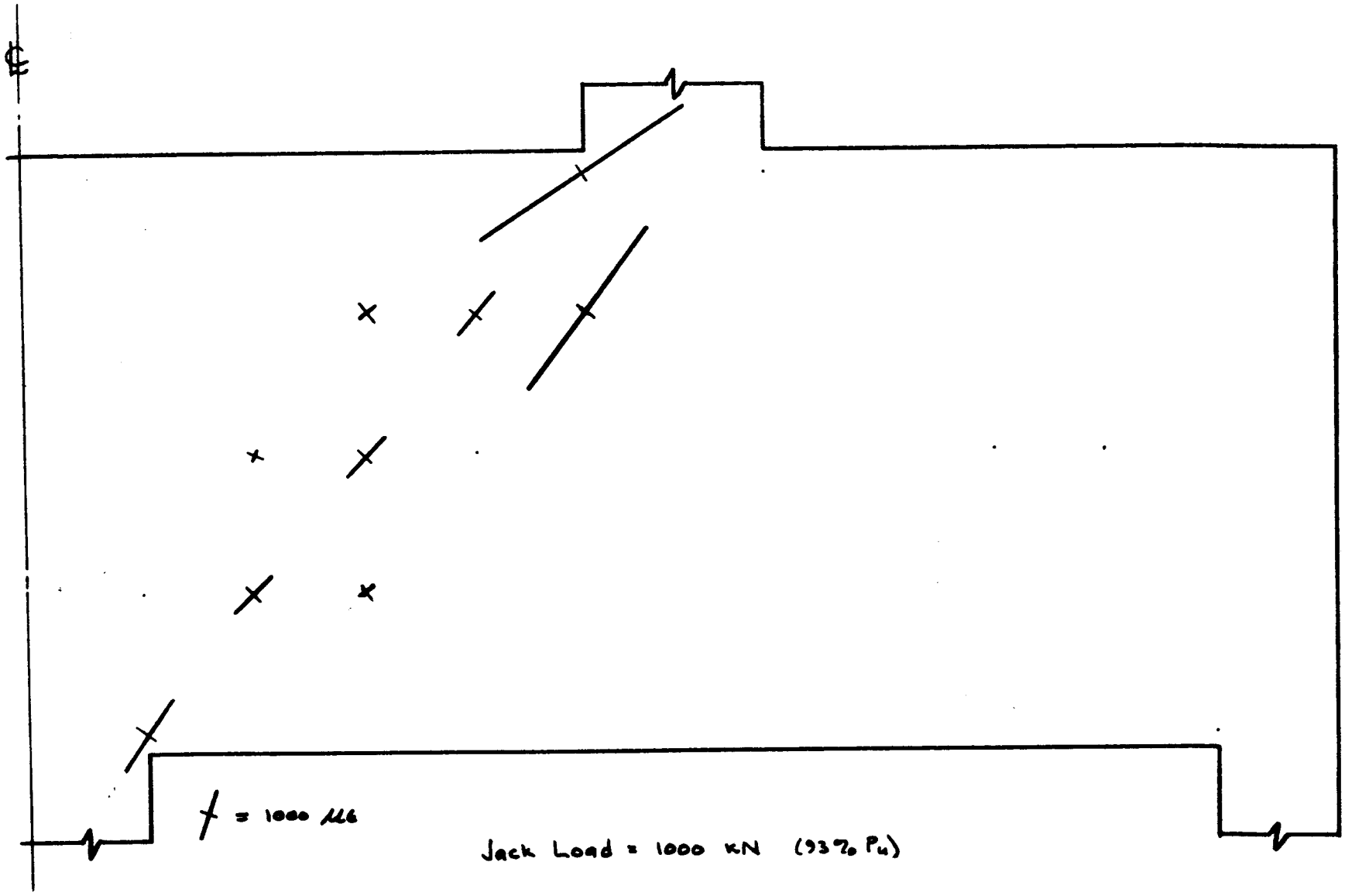

Figure 6.26 Beam 4/1.0 Concrete Compressive Strains

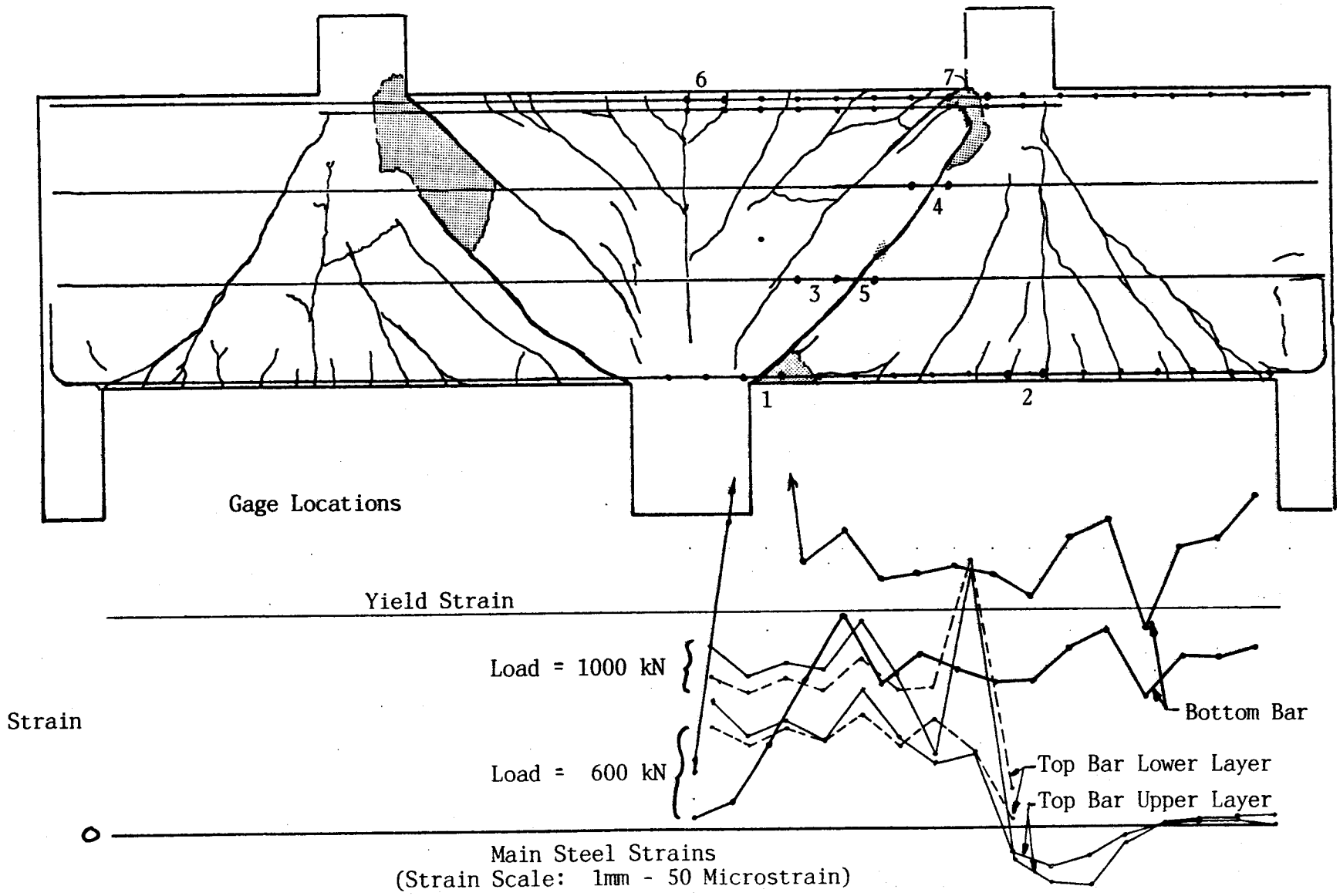

Figure 6.27 Beam 4/1.0 Steel Strains

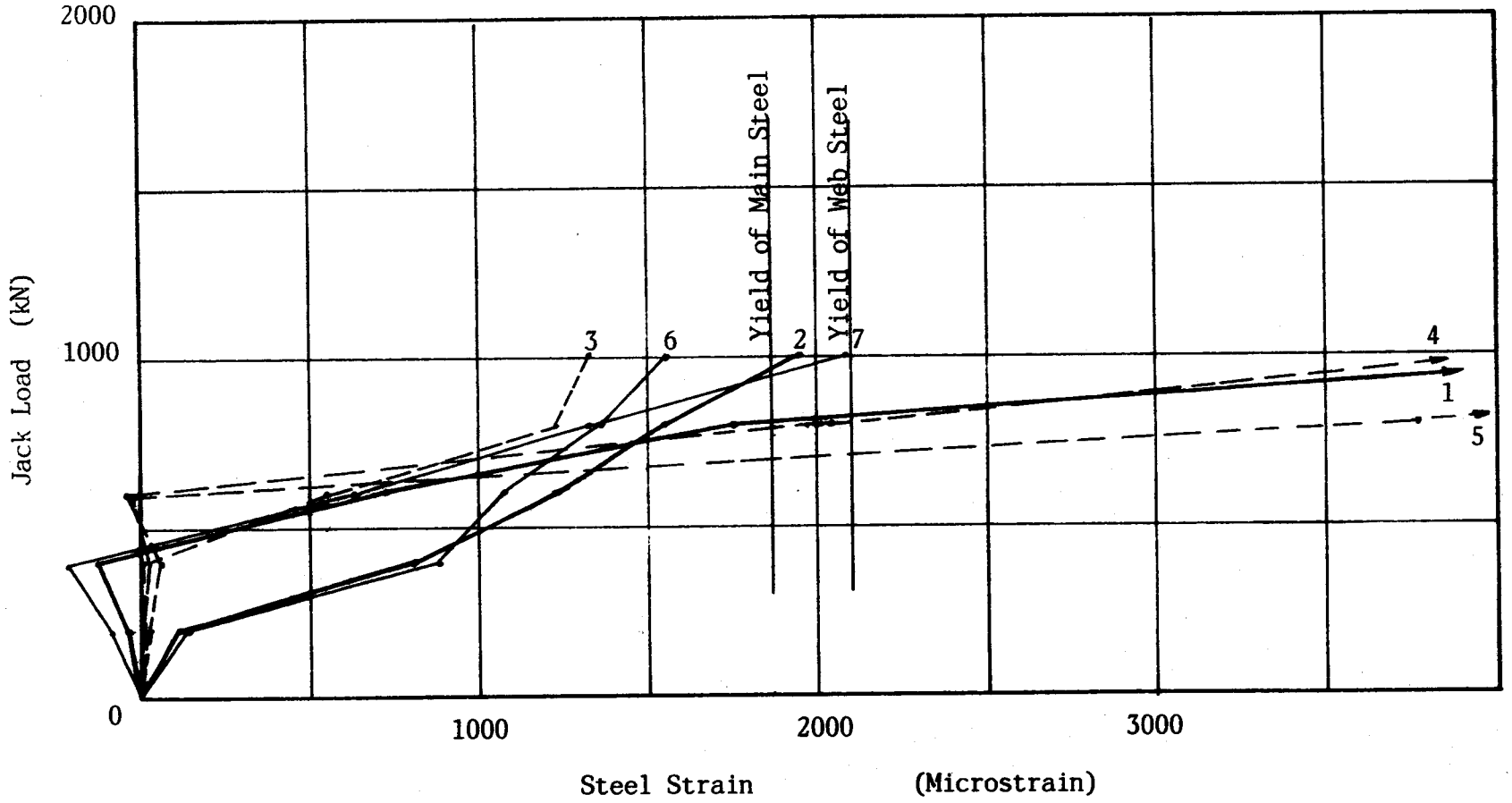

Figure 6.28 Beam 4/1.0 Load vs. Steel Strain

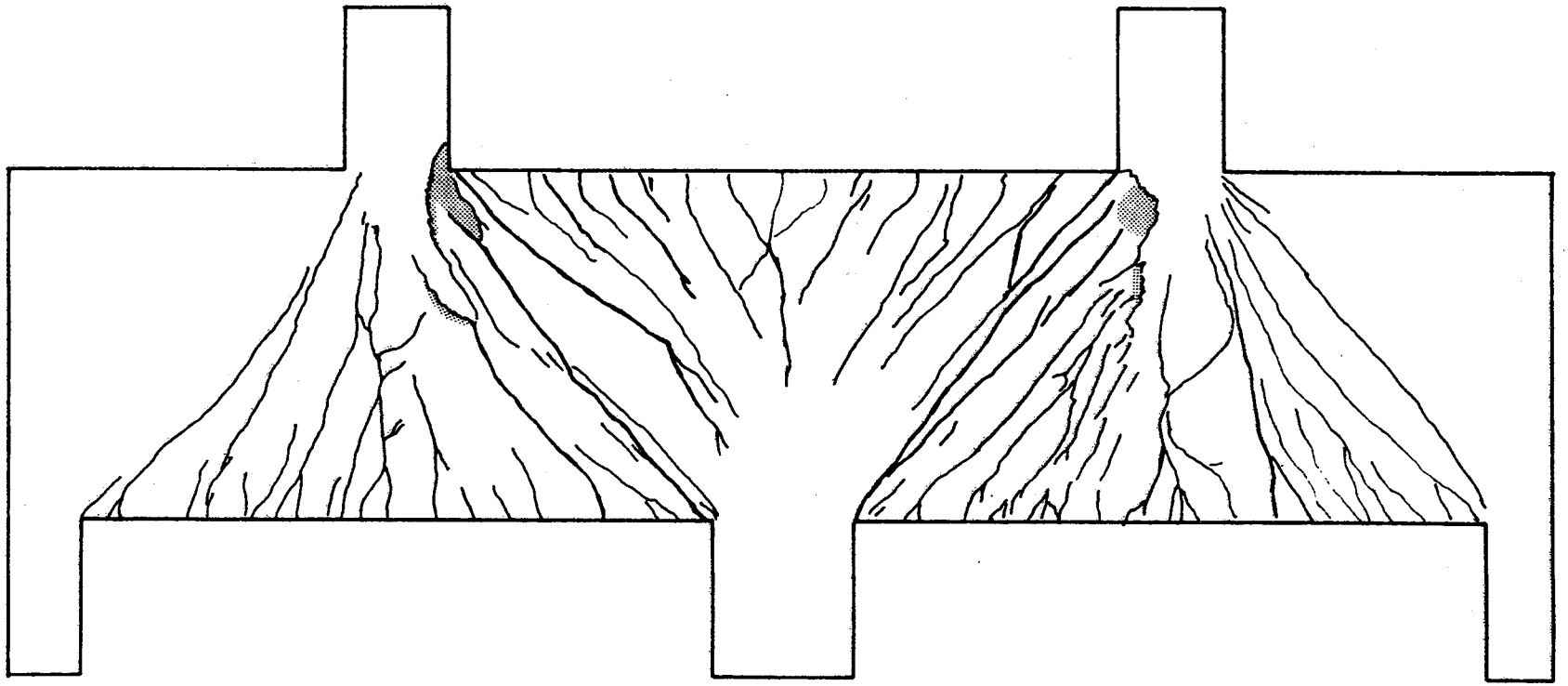

Figure 6.29. Beam 5/1.0 Crack Pattern – West Face

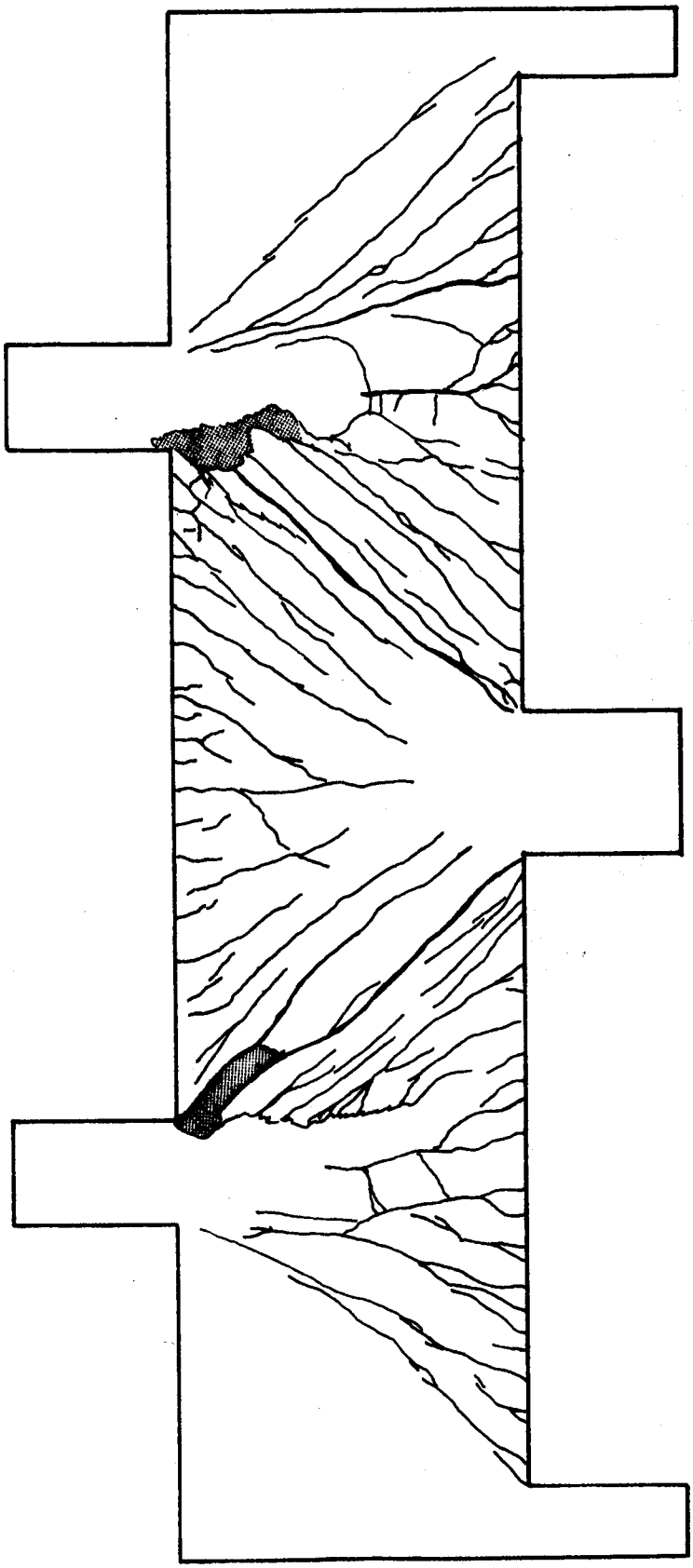

Figure 6.30 Beam 5/1.0 Crack Pattern - East Face (Reversed)

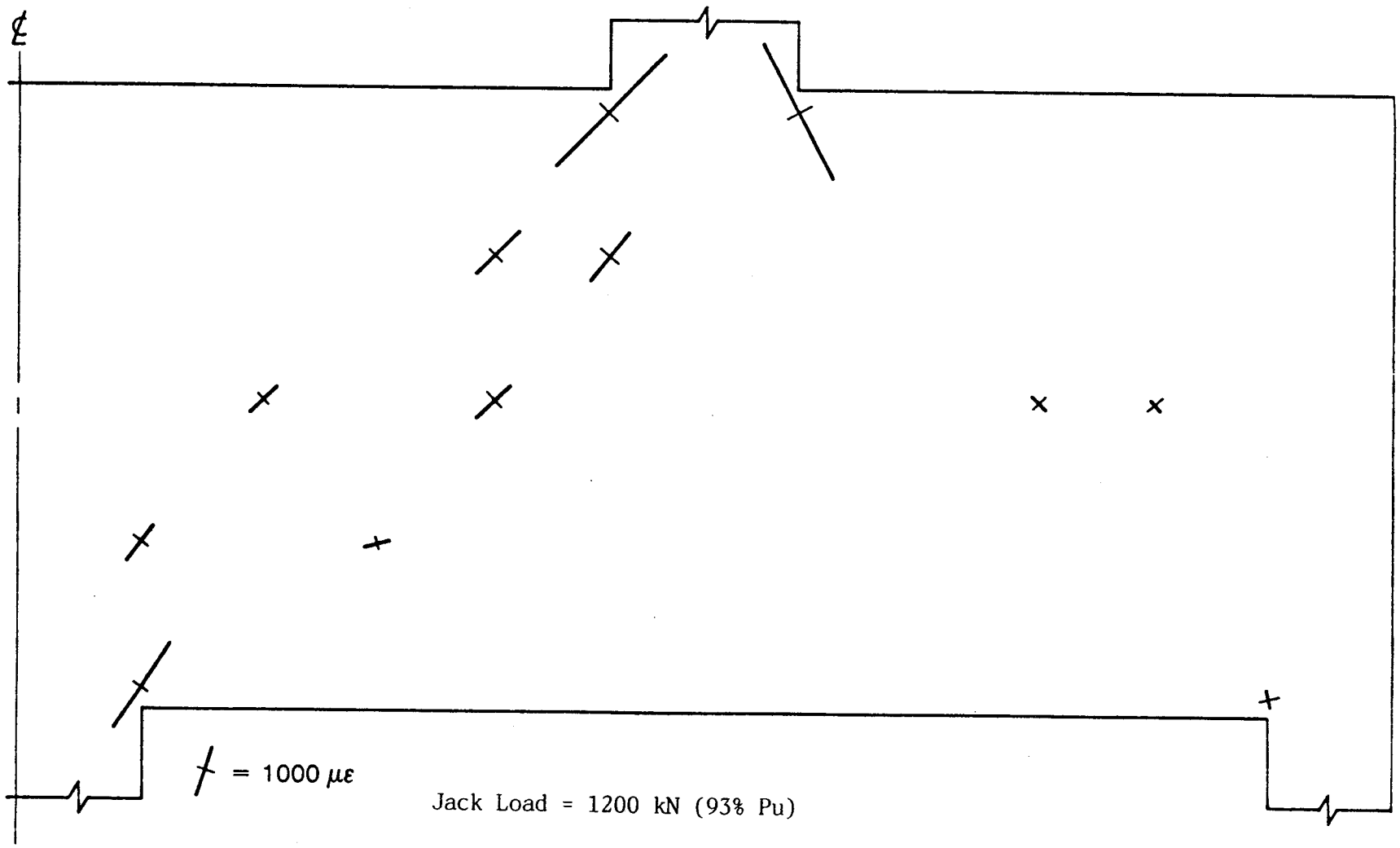

Figure 6.31 Beam 5/1.0 Concrete Compressive Strains

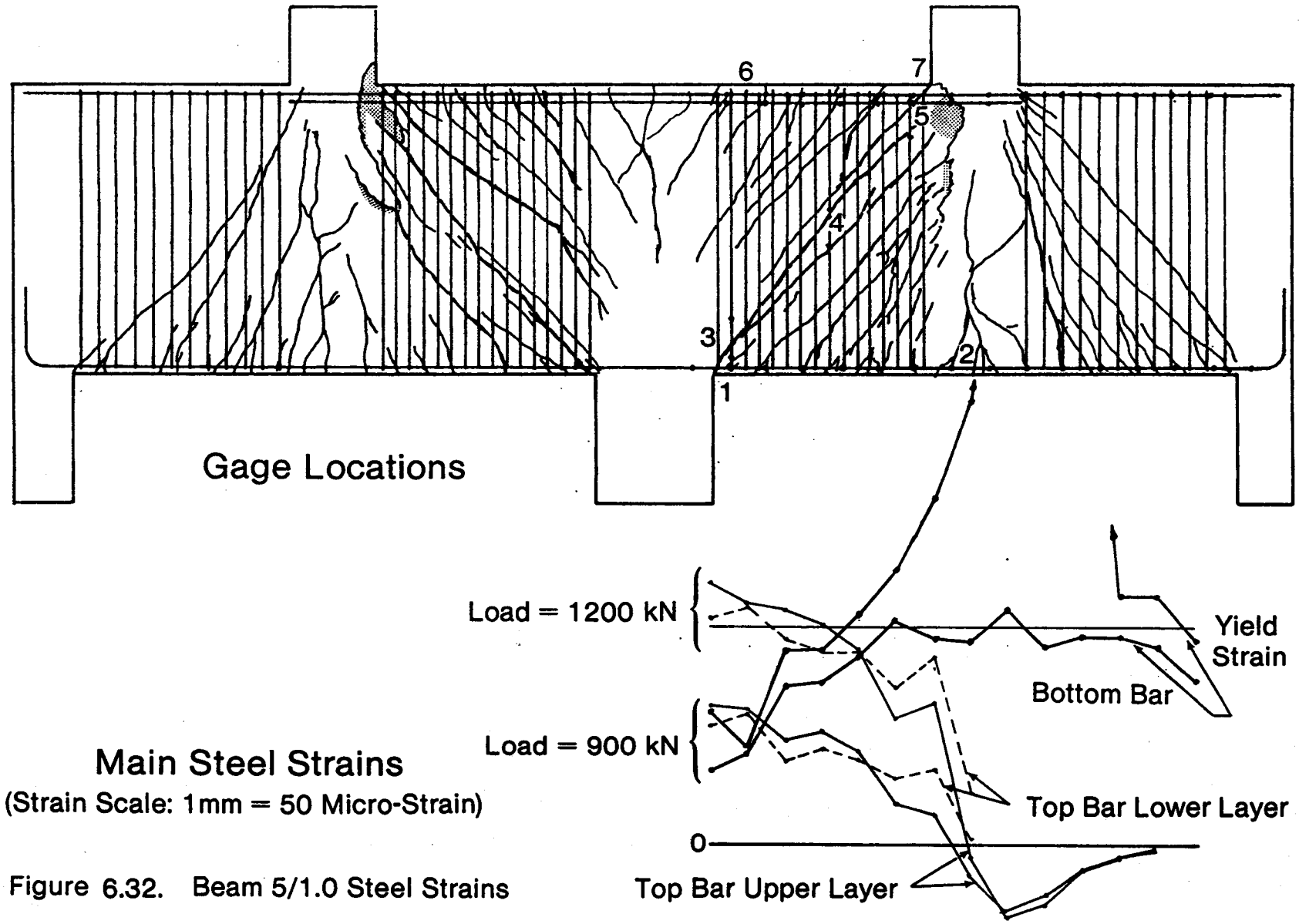

Figure 6.32. Beam 5/1.0 Steel Strains

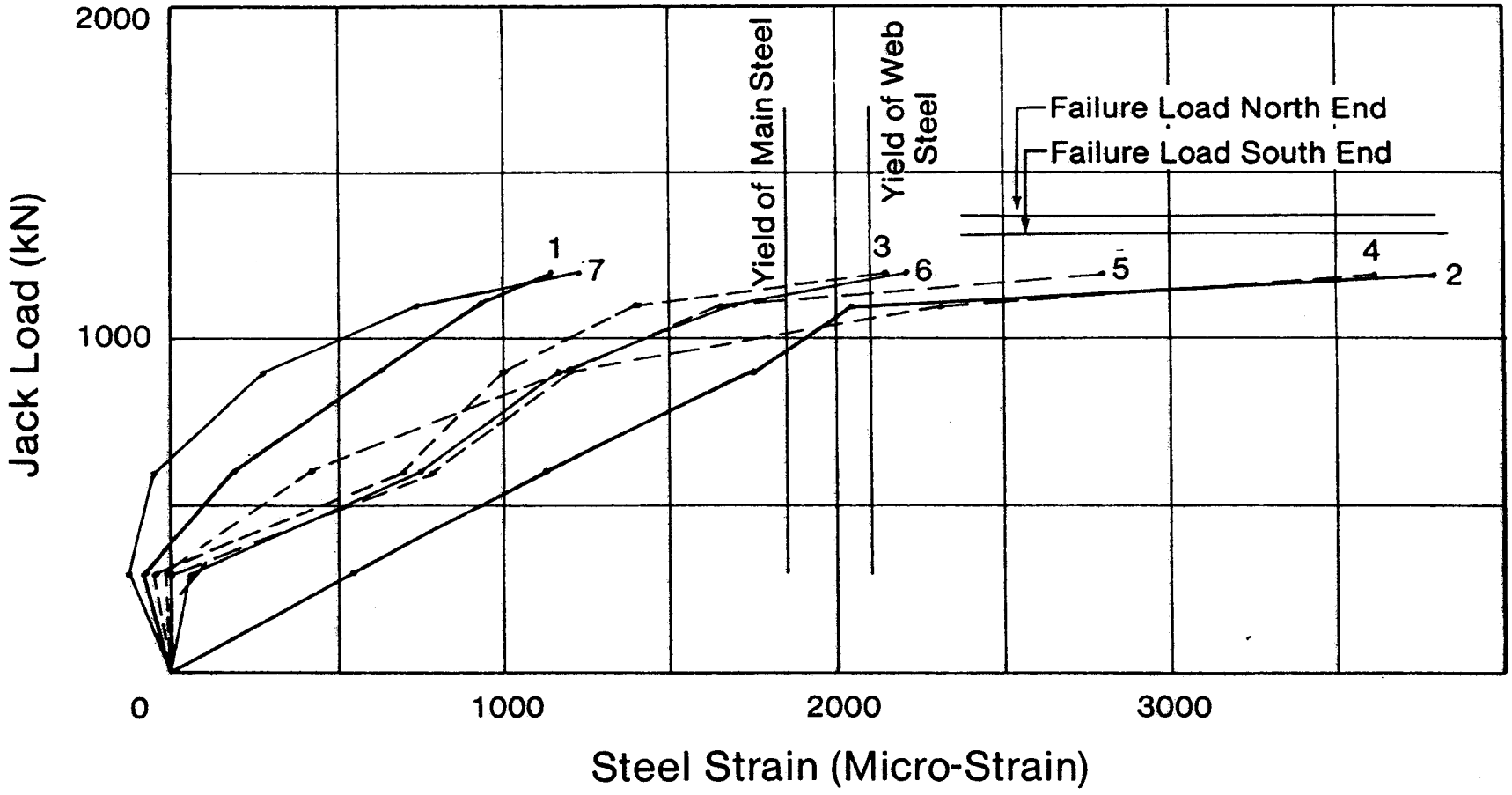

Figure 6.33. Beam 5/1.0 Load vs. Steel Strain

Although the longitudinal steel was stressed in tension over the entire length of the interior shear spans, the decrease in stress near the ends was more marked than in Beam 3/1.0.

The failures were ductile, as shown in Fig. 6.2.

6.10 Beam 6/1.0

This two span continuous beam had a high ratio of horizontal web reinforcement throughout both shear spans.

This beam suffered some damage during handling when one of three lifting chains broke. There was some minor damage to the north support bearing plate which was repaired. More serious however, were vertical cracks on either side of the interior support, starting at the soffet, and running upward to approximately mid-depth. These were hairline cracks with a width of about 0.001 in., and can be seen in the crack patterns. This beam behaved like the other beams at inclined cracking. The failure of the north strut was due to shear compression failure at the top of the strut accompanied by vertical opening of the lower inclined crack. The behaviour of the south interior shear span appeared to be influenced by the handling damage. The failure was a large vertical separation (+- 15 mm) along the inclined crack with vertical shearing along the lower 350 mm of the pre-existing handling crack surface. Inspite of the difference in failure mechanisms in the shear span, the failure loads were almost identical. In both instances,

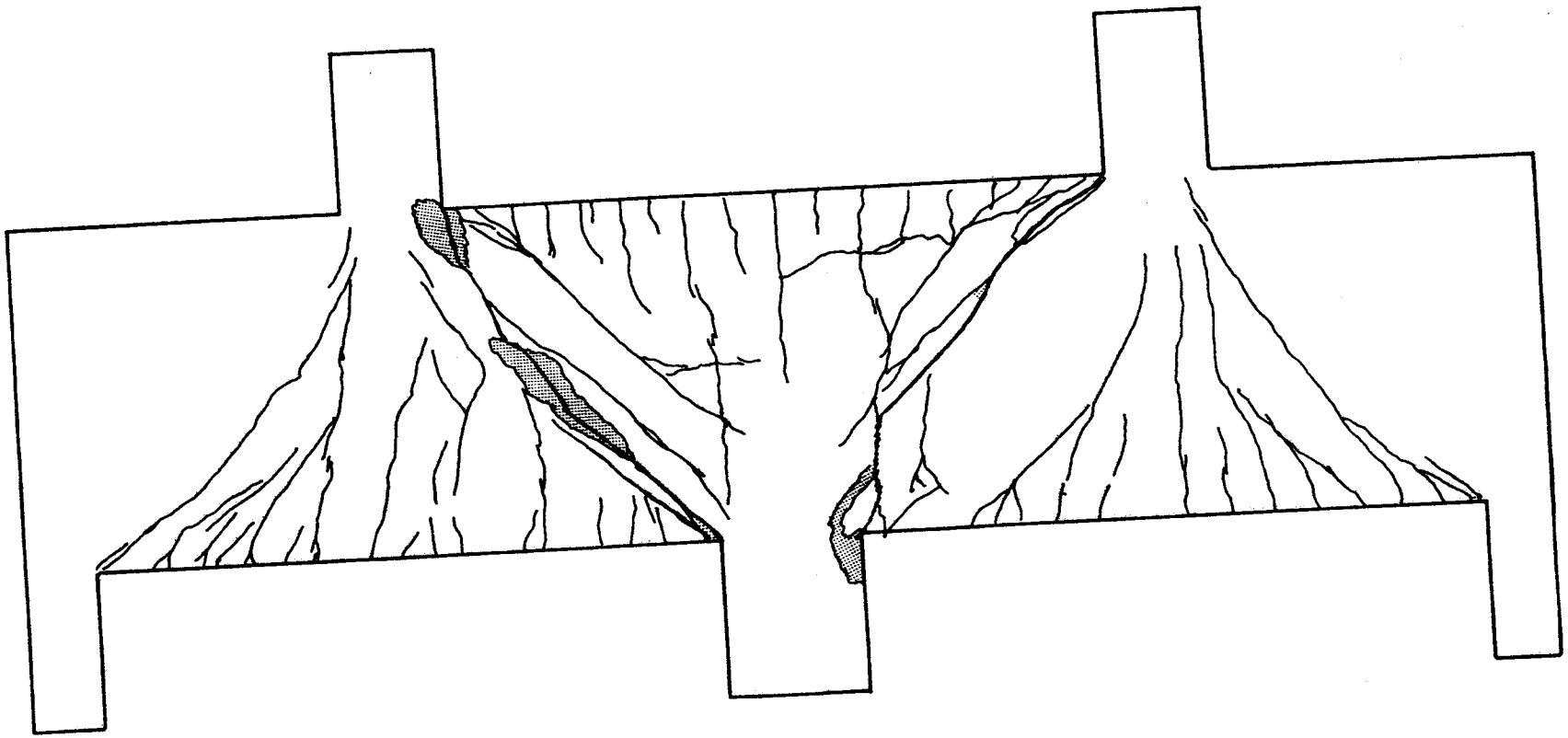

Figure 6.34. Beam 6/1.0 Crack Pattern – West Face

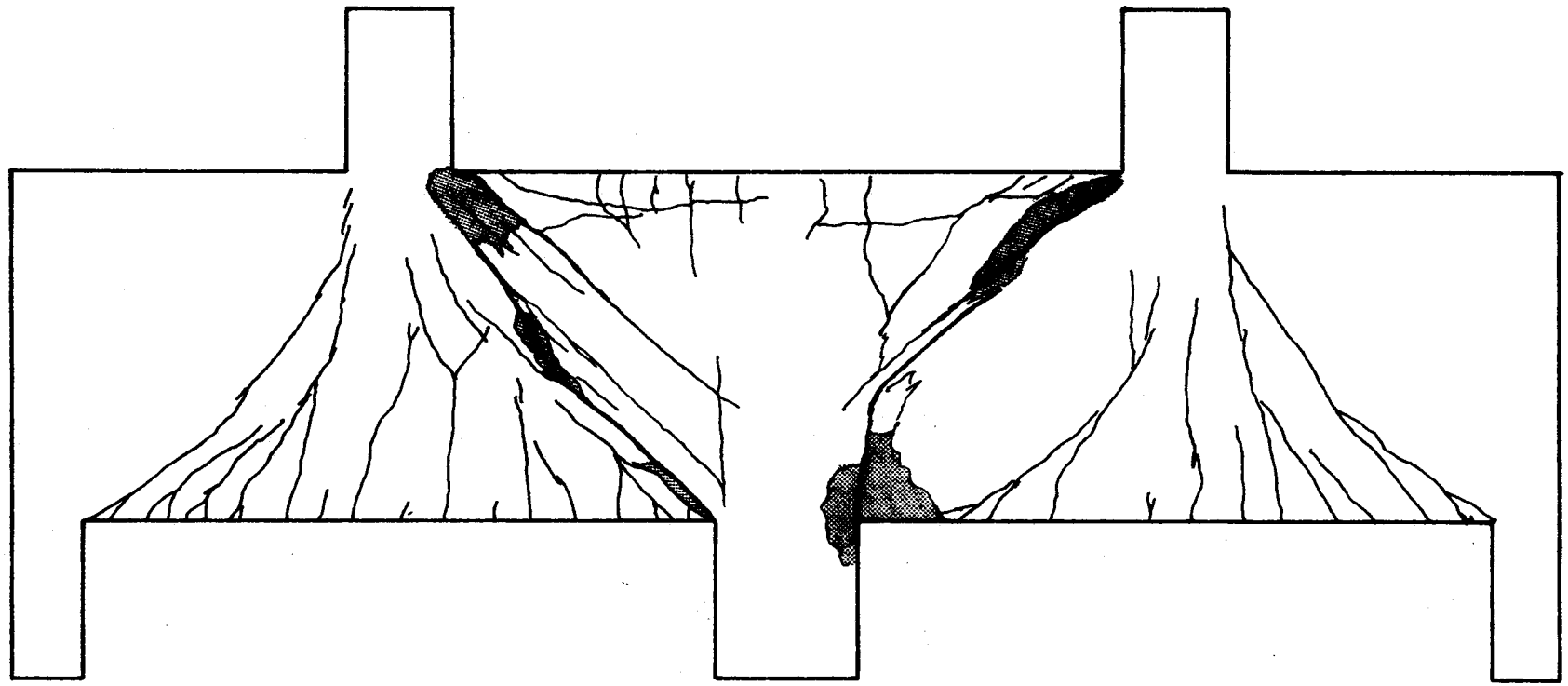

Figure 6.35 Beam 6/1.0 Crack Pattern - East Face (Reversed)

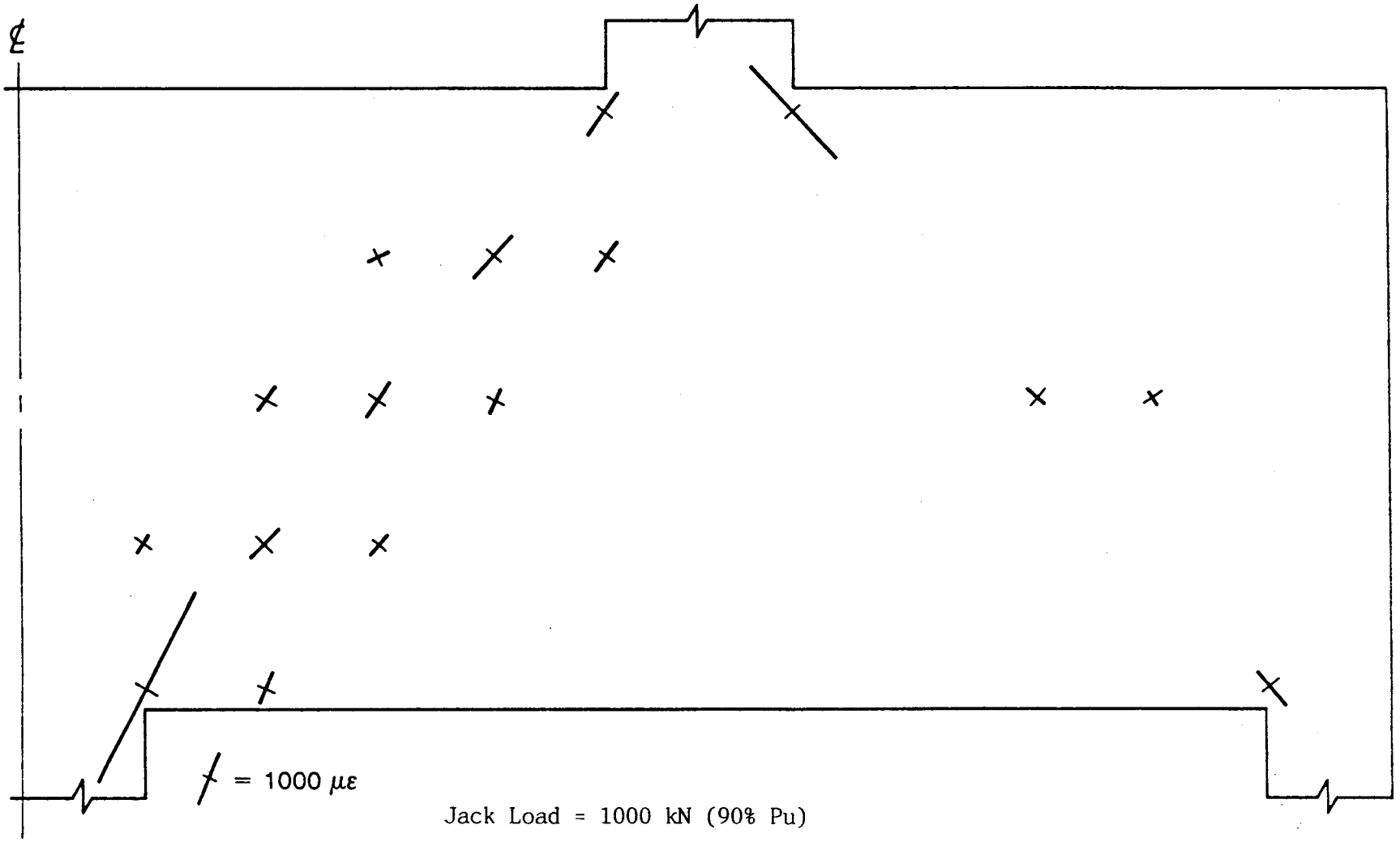

Figure 6.36 Beam 6/1.0 Concrete Compressive Strains

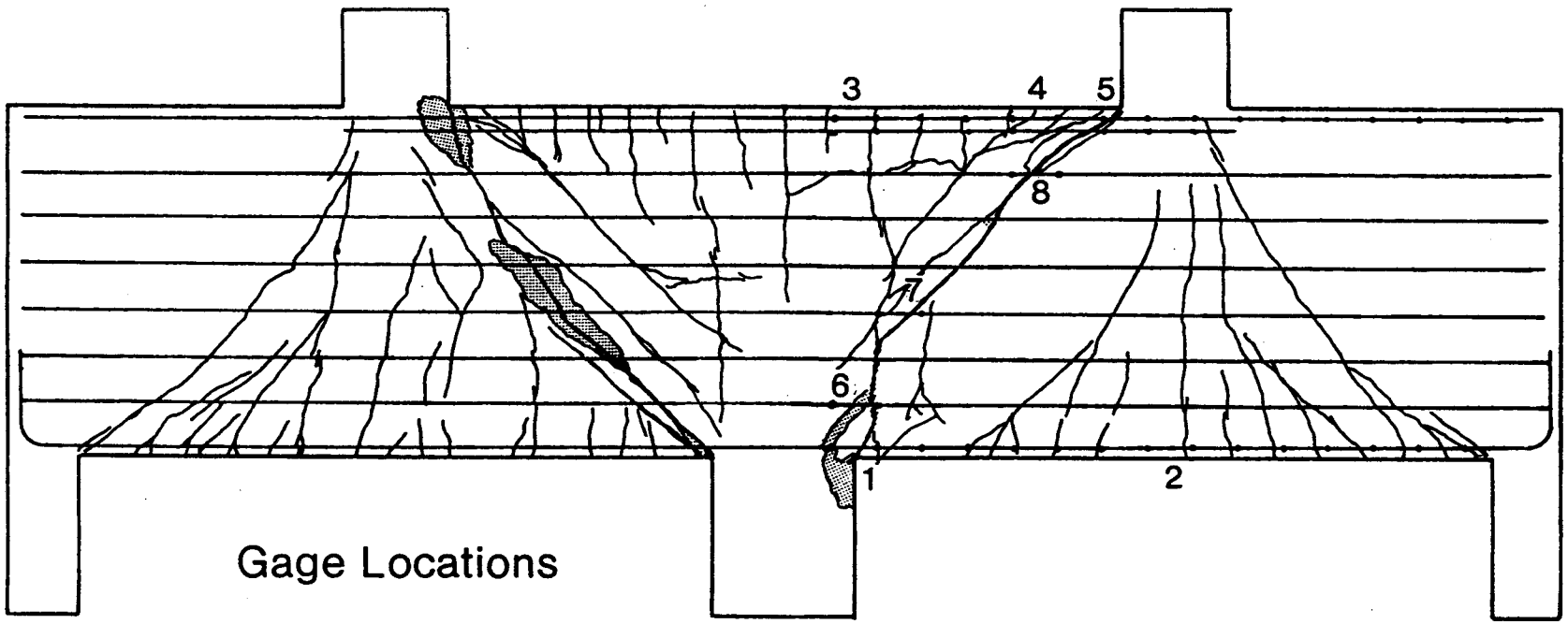

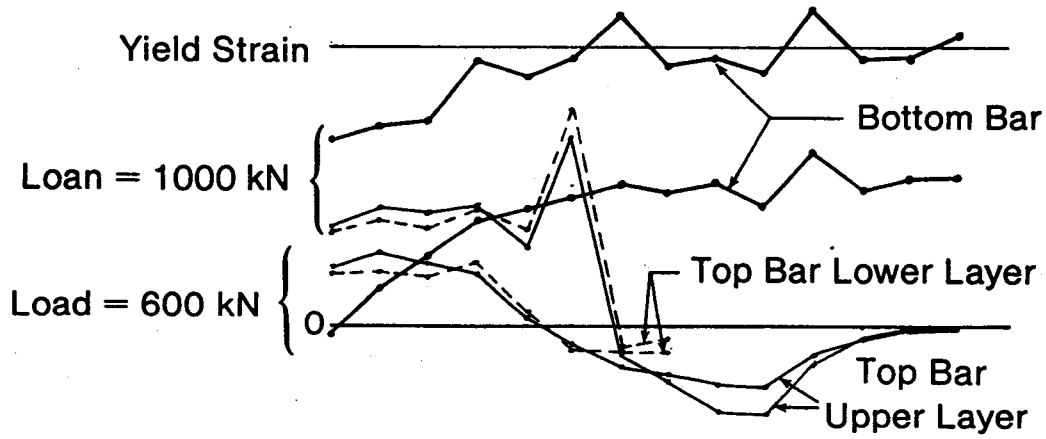

Main Steel Strains

(Strain Scale: 1mm = 50 Micro-Strain)

Figure 6.37 Beam 6/1.0 Steel Strains

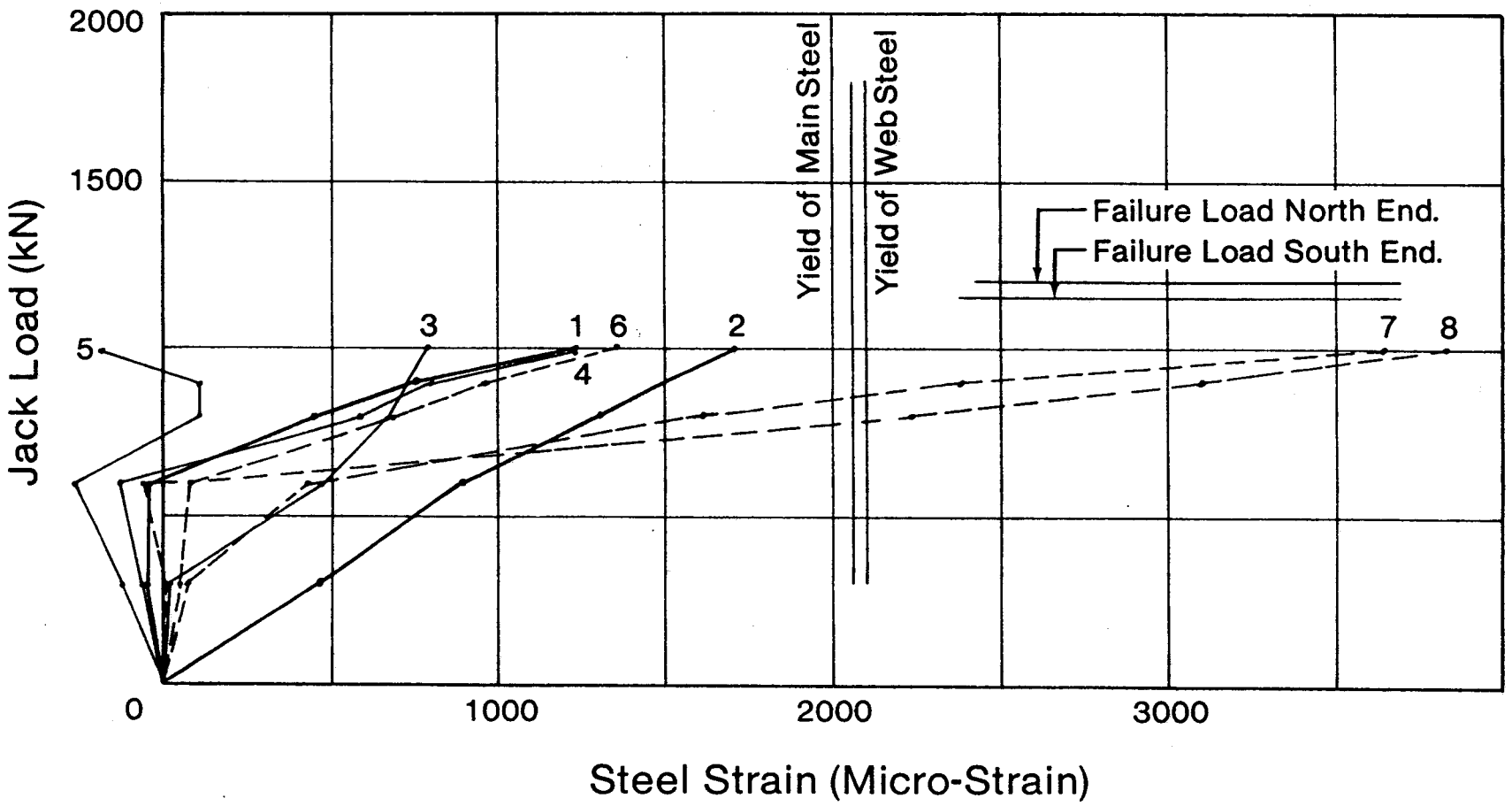

Figure 6.38. Beam 6/1.0 Load vs. Steel Strain

there was considerable cracking but the failure behaviour could not be described as ductile (See Fig. 6.2).

6.11 Beam 7/1.0

This two span continuous beam did not have any web reinforcement. The behaviour of this beam was not very symmetrical. In the first test the south interior shear span developed a very straight inclined crack at 440 kN, while the north interior shear span did not develop an inclined crack at all. The south interior shear span failed suddenly at 714 kN with a shear compression failure at the top of the strut and vertical opening of the inclined crack. In the retest, the north interior shear span experienced considerable dowel cracking at the interior support before failure. Failure of this shear span at a load of 1107 kN, 55% greater than the south interior shear span, was due to crushing of the compression strut between two partially developed inclined cracks. The large difference in failure loads was apparently due to the critical nature of the inclined crack in the south interior shear span. This beam also lacked web reinforcement and hence had to rely on the tensile strength of the concrete which is quite variable. The steel strain measurements indicated that the steel strain did not vary in accordance with the bending moment diagram, but rather in accordance with a truss model, with the strains being constant along each tension member.

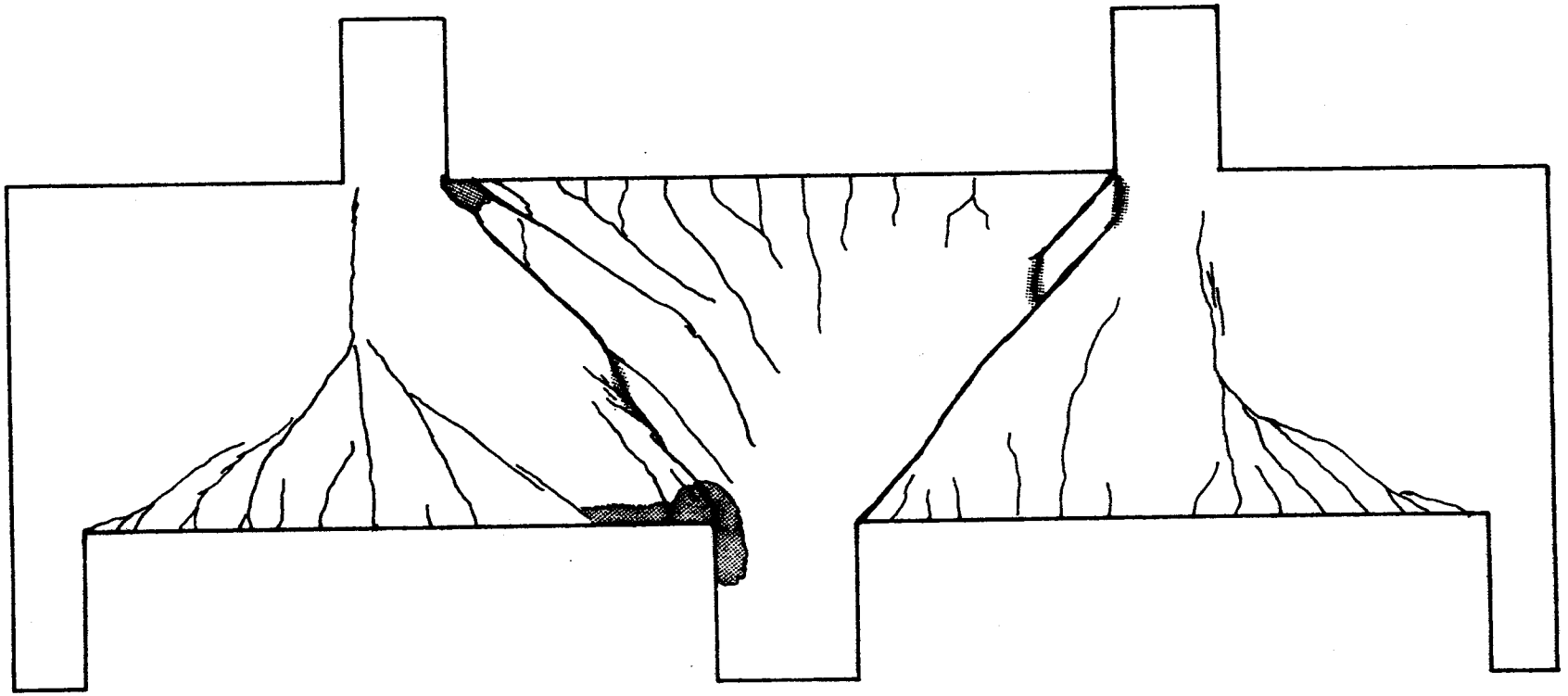

Figure 6.39 Beam 7/1.0 Crack Pattern - West Face

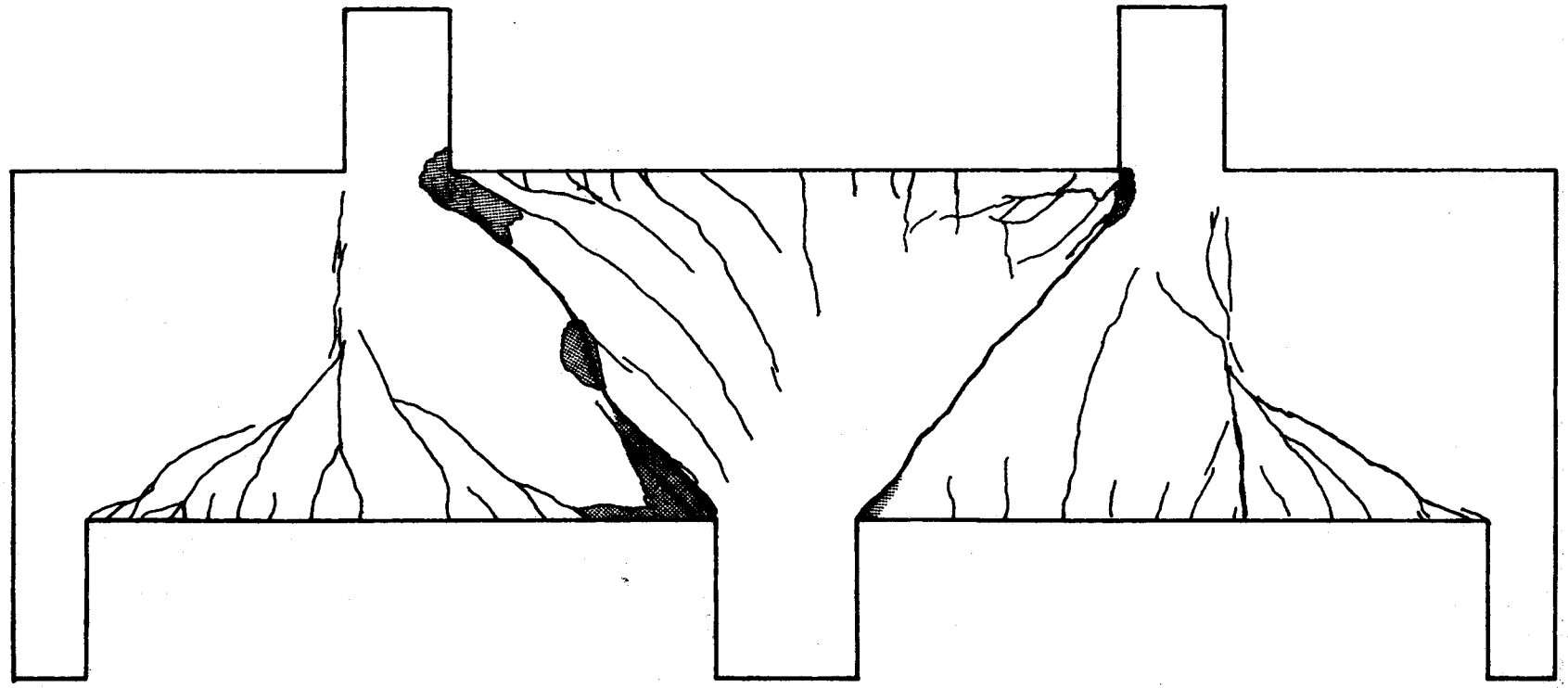

Figure 6.40 Beam 7/1.0 Crack Pattern - East Face (Reversed)

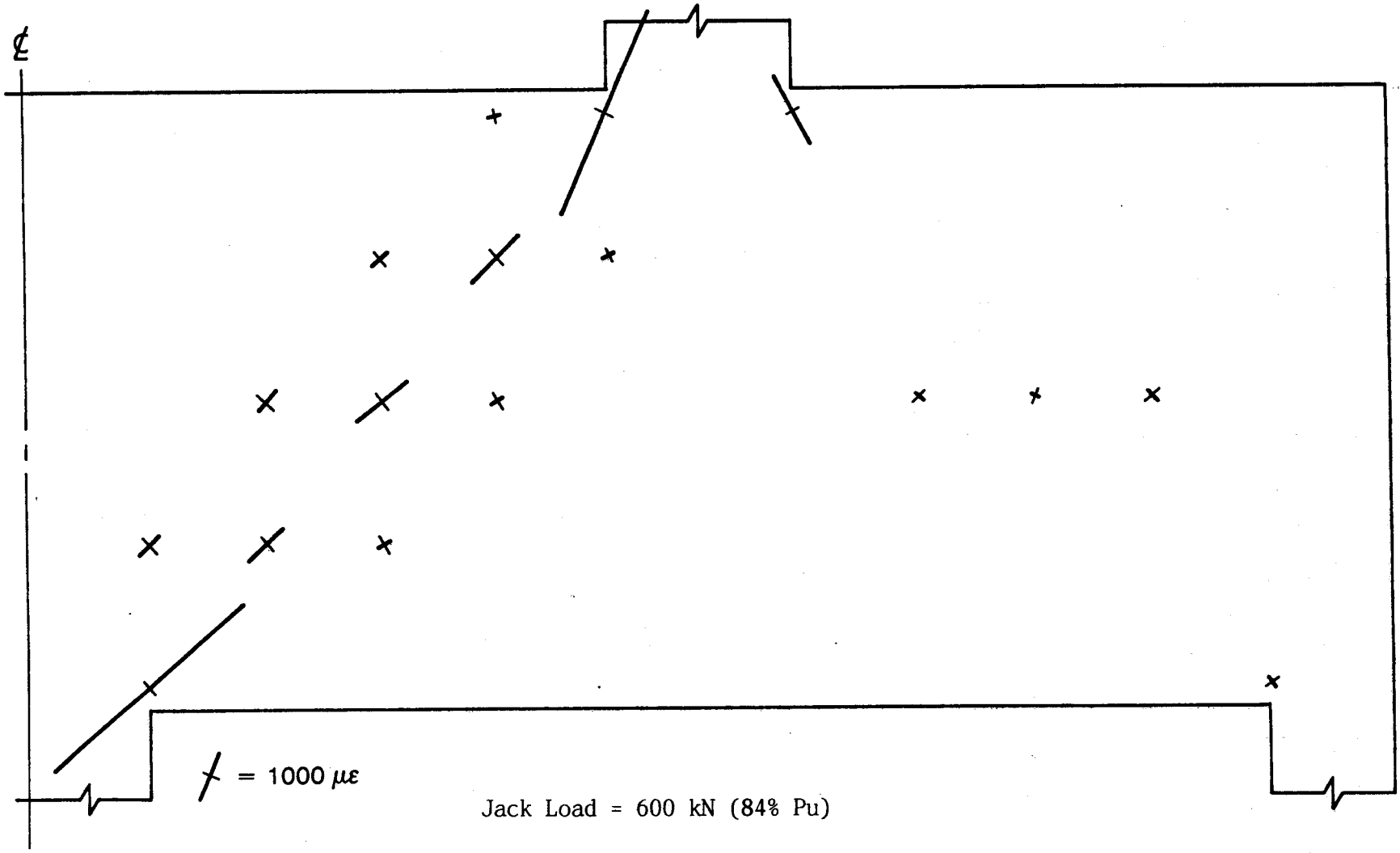

Figure 6.41 Beam 7/1.0 Concerete Compressive Strains

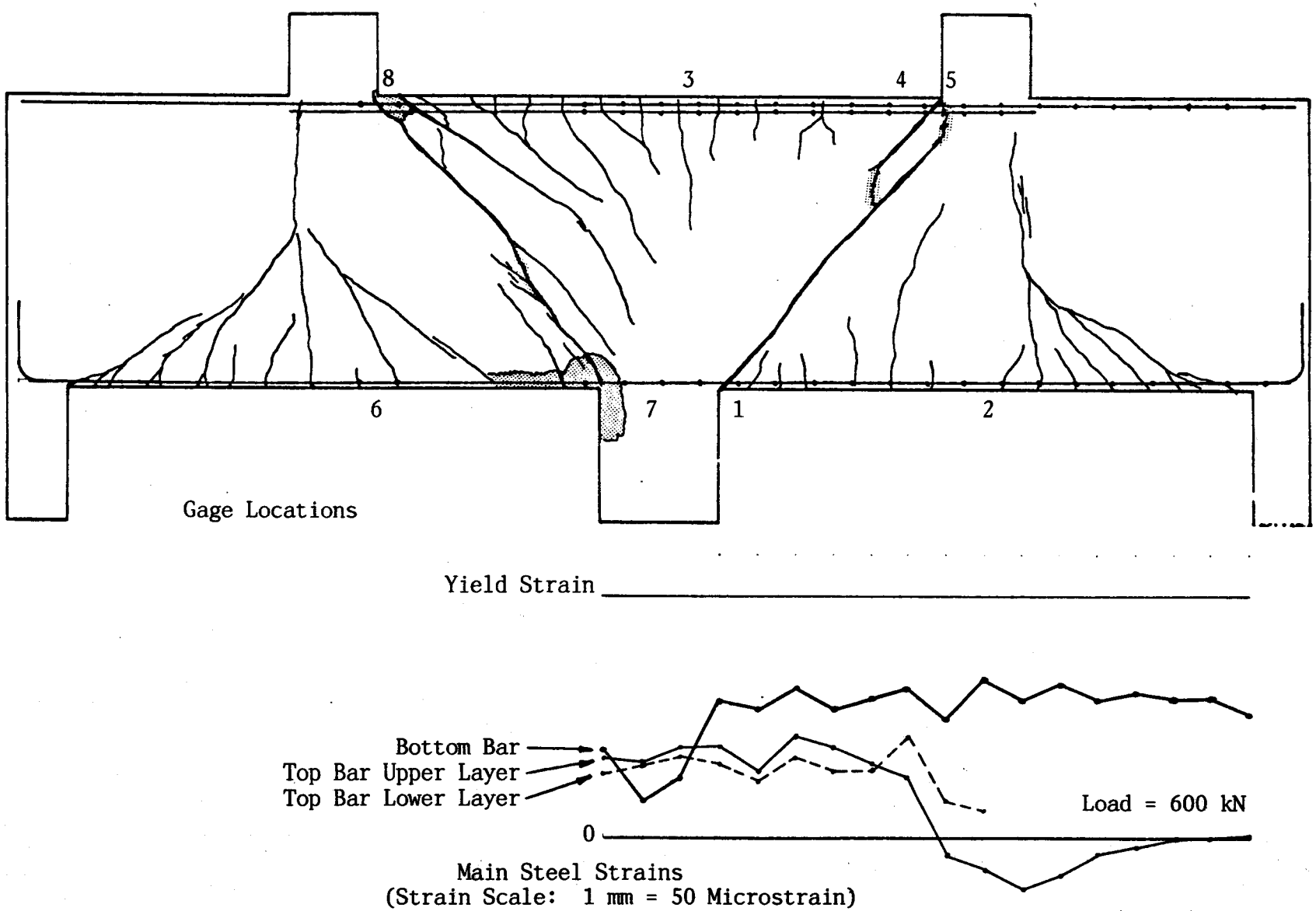

Figure 6.42 Beam 7/1.0 Steel Strains

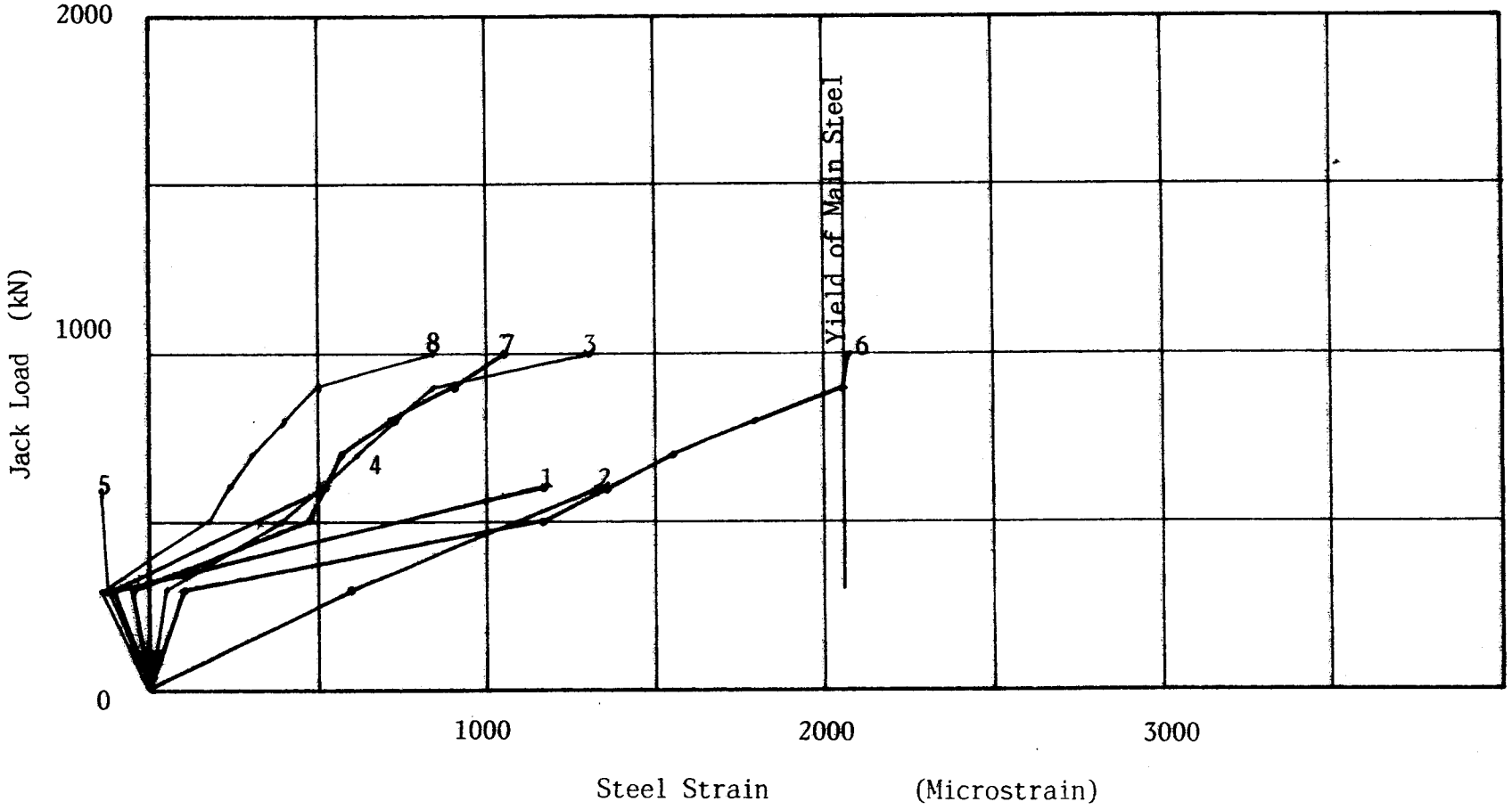

Figure 6.43 Beam 7/1.0 Load vs. Steel Strain

6.12 Beam 1/1.5

This simple span beam had no stirrups in the south end and minimum stirrups in the north end. The south end failed at a load of 606 kN. Following splinting, the north end was reloaded and failed at 709 kN. Both shear spans developed inclined cracks at about 240 kN. The inclined cracks extended from the soffet about 300 mm from the face of the support columns to about 50 mm below the top of the beam at the face of the loading column. As the load was increased a considerable amount of dowel cracking developed at the south support. The cracks moved progessively outward as the bars were pushed down. The bottom bars were kinked with a "flexural span" of about 300 mm. The resulting deformations finally produced a compression-shear failure at the top of the compression strut.

The north shear span, being reinforced with stirrups behaved quite differently. The stirrups prevented a peeling back of the dowels. In doing so, the stirrups were stressed in tension and seemed to pull the concrete apart creating cracks similar to the dowel splitting cracks but somewhat longer and narrower.

At a load of 500 kN, the inclined crack widths at midheight of the beam in the north and south shear spans were 0.5 mm and 2 mm respectively. The north shear span exhibited a relatively ductile load-deflection curve (Fig. 6.3) with final failure being caused by crushing at the top of the compression strut. Both sides of the

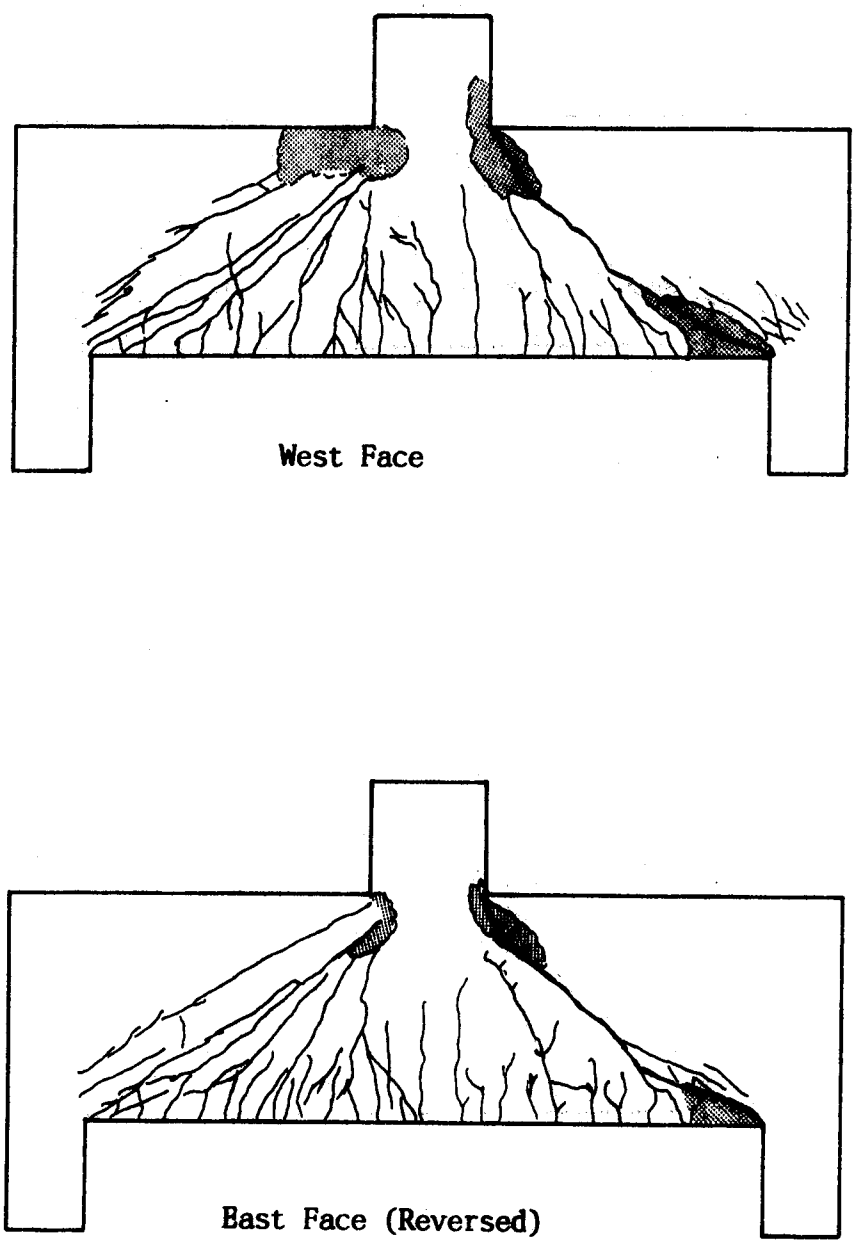

Figure 6.44 Beam 1/1.5 Crack patterns

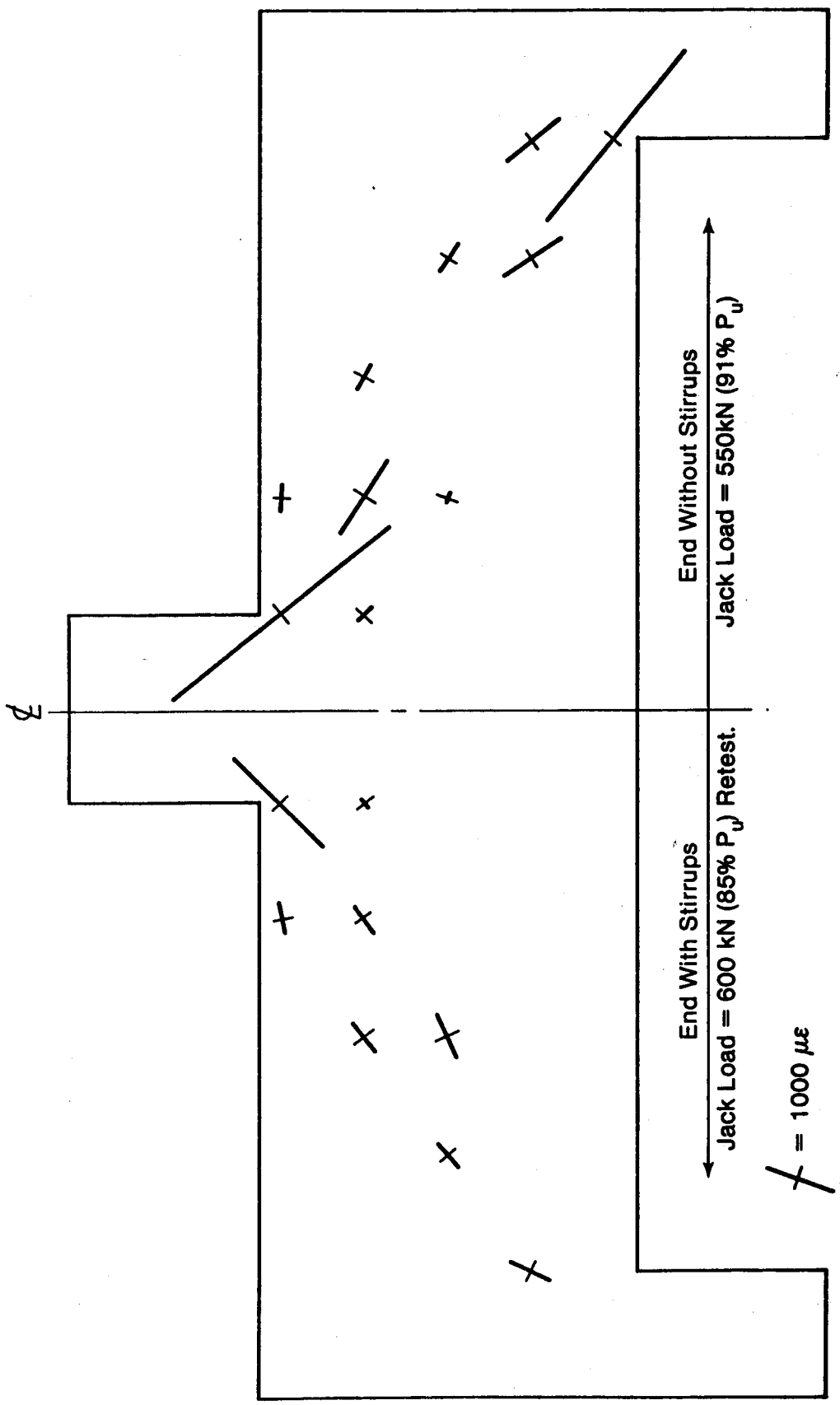

Beam 6.45 Beam 1/1.5 Concrete Compressive Strains

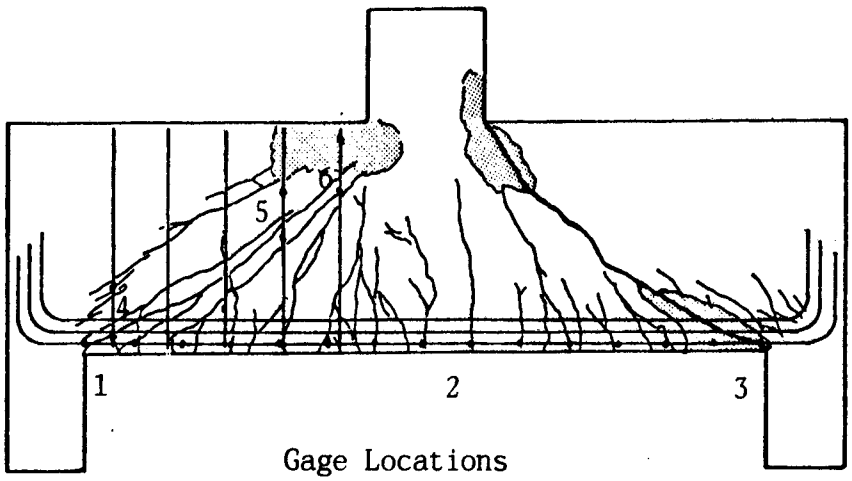

Gage Locations

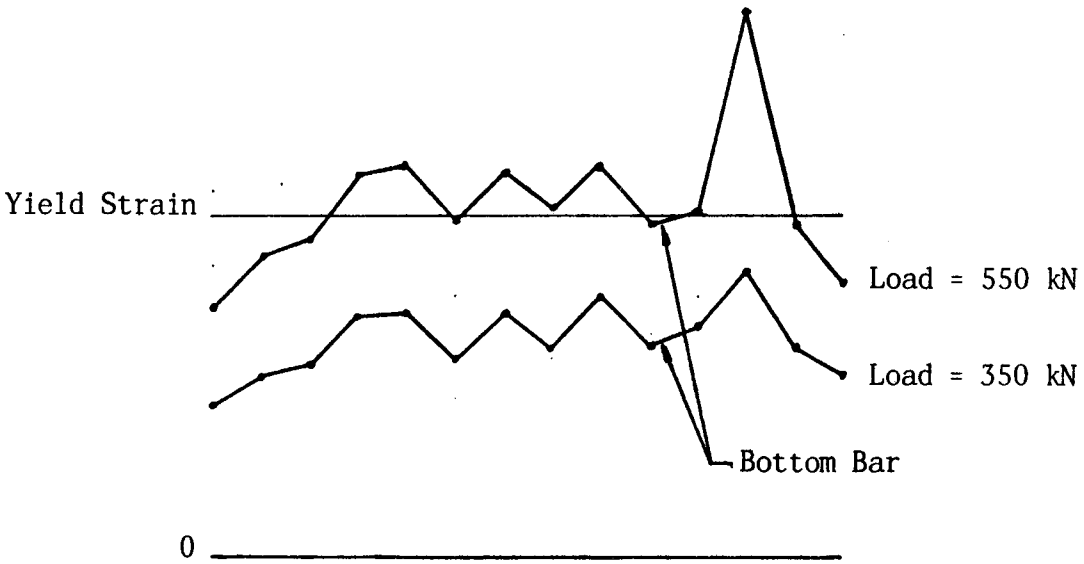

Main Steel Strains

(Strain Scale: 1 mm = 50 Microstrain)

Figure 6.46 Beam 1/1.5 Steel Strains

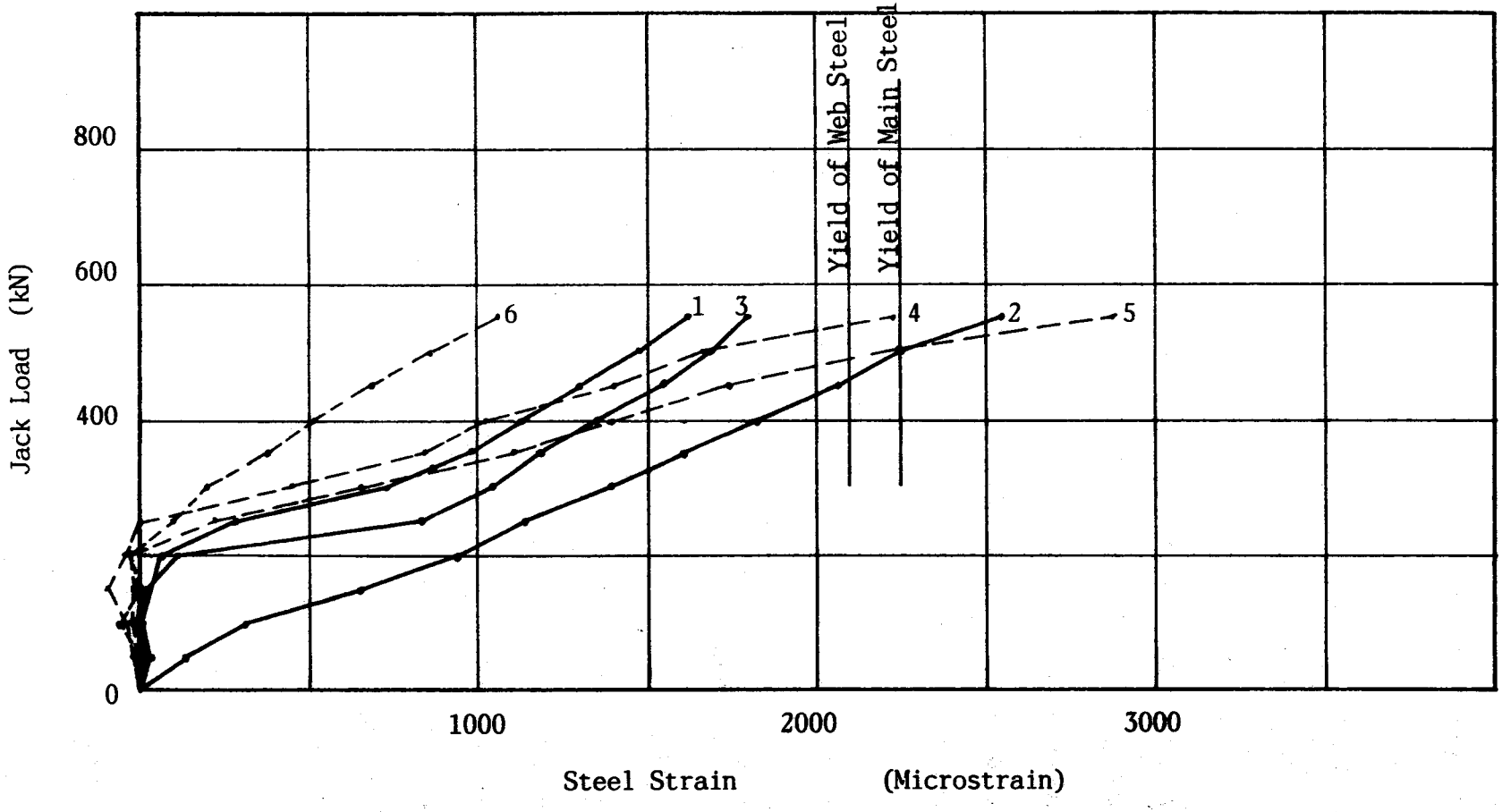

Figure 6.47 Beam 1/1.5 Load vs. Steel Strain

compression strut in the north shear span were defined by cracks while only the lower side of the south compression strut was defined by a crack.

6.13 Beam 2/1.5

This simple span beam had light horizontal reinforcement in both shear spans plus light vertical web reinforcement in the north shear span. Both shear spans developed inclined cracks at about 275 kN. In the south shear span, the inclined crack extended from 33 mm below the face of the loading column to 50 mm above the face of the support column, and was reasonably straight. The inclined crack in the north shear span extended from 100 mm below the face of the loading column to the soffet of the beam about 300 mm from the face of the support column, and was slightly "s" curved. At a load of 300 kN the inclined crack widths at midheight of the beam were about 0.2 mm and 0.6 mm respectively. The south strut failed violently with a compression-shear failure at a load of 452 kN. In the retest the north strut failed with a nonviolent controlled crushing of the upper end of the strut. There were parallel splitting type cracks at the top of the strut before failure.

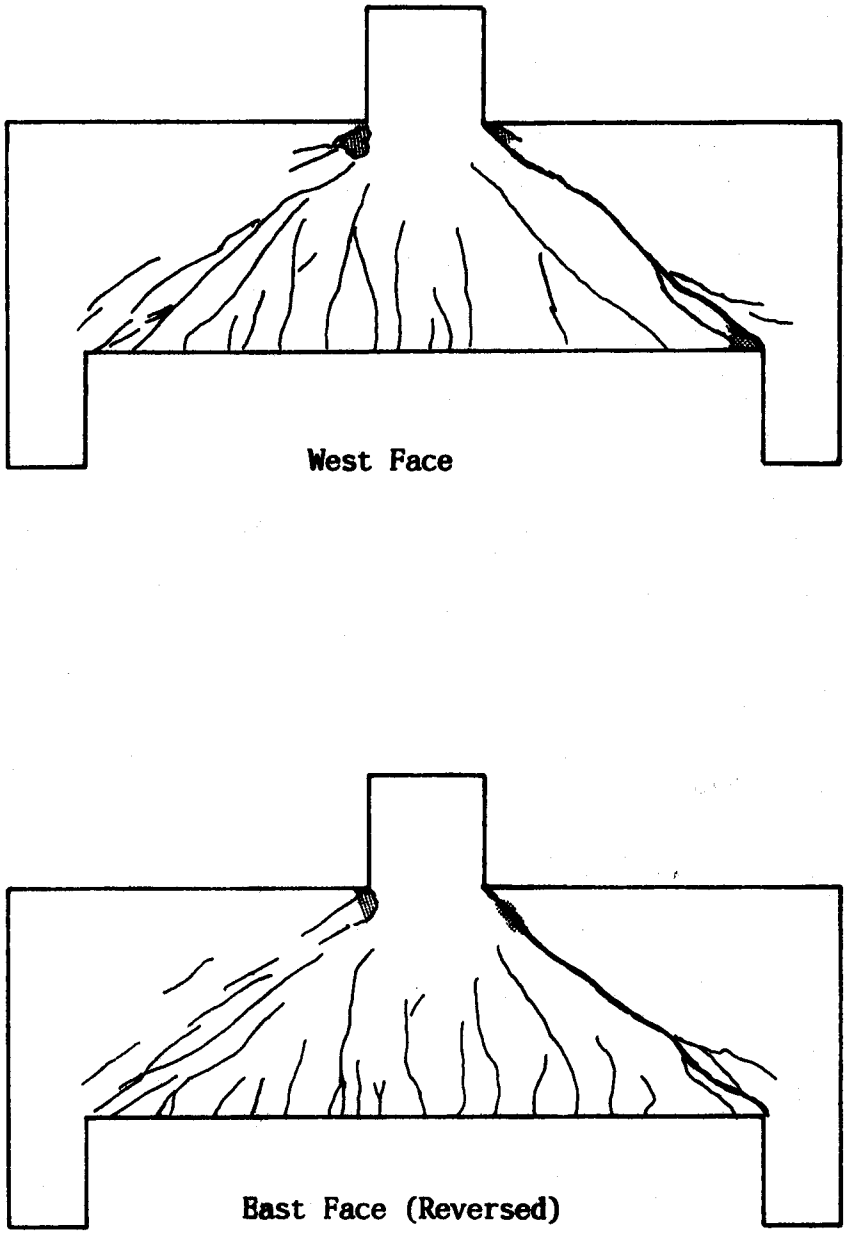

Figure 6.48 Beam 2/1.5 Crack Patterns

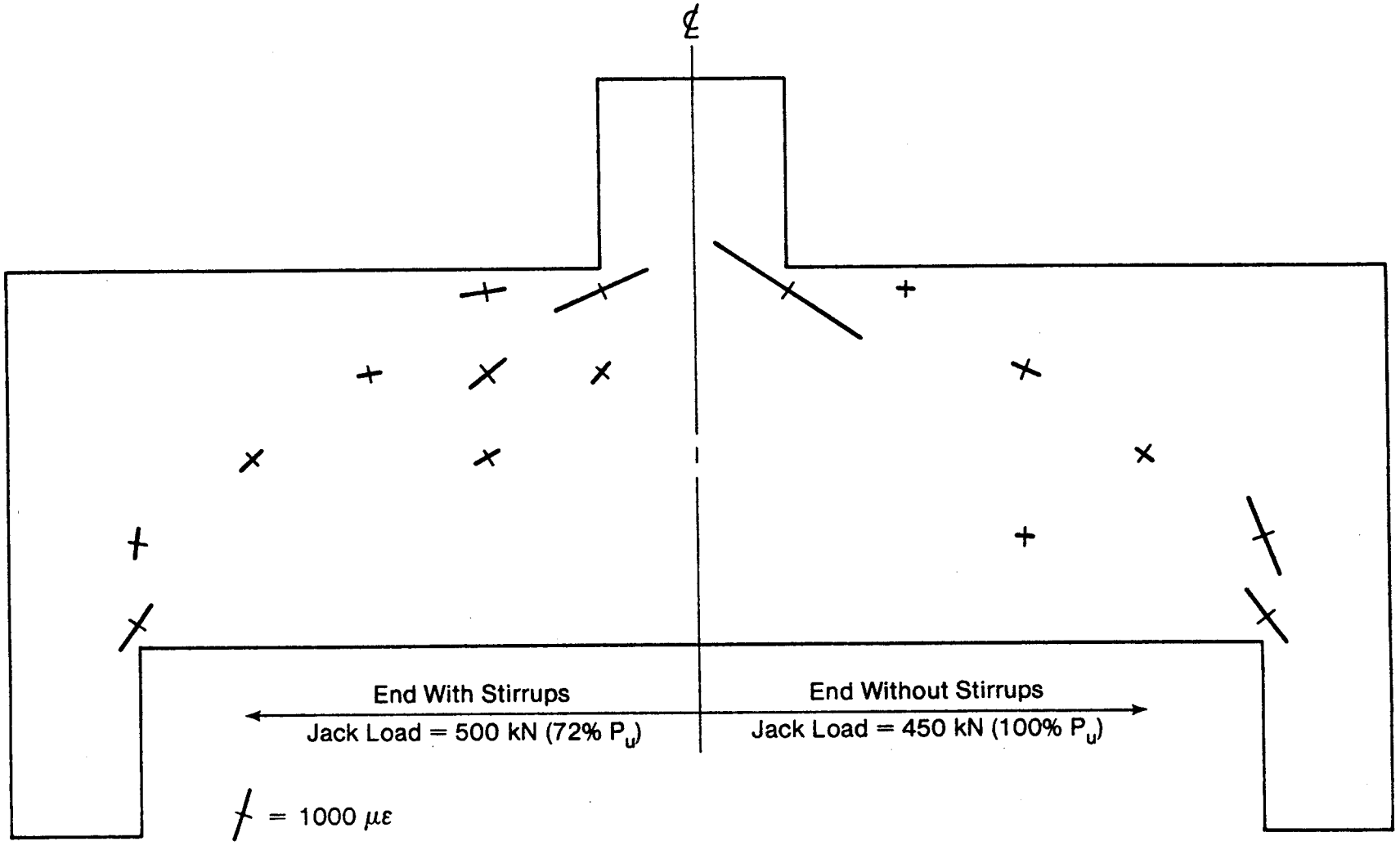

Figure 6.49 Beam 2/1.5 Concrete Compressive Strains

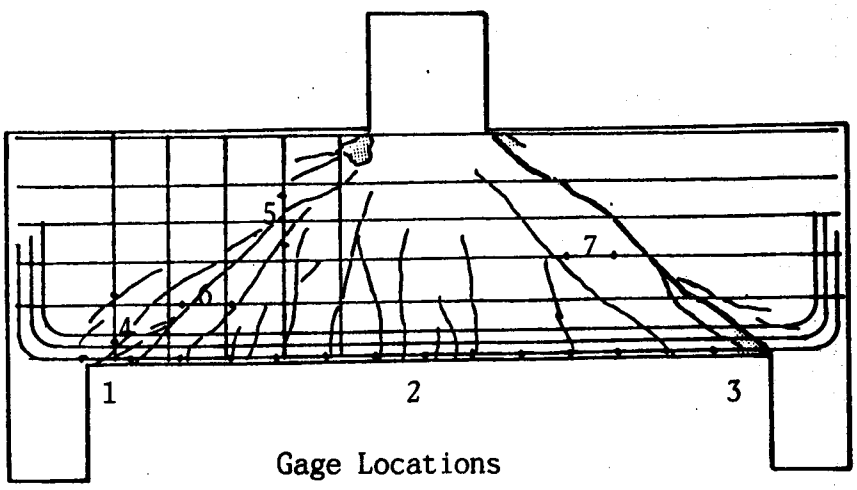

Gage Locations

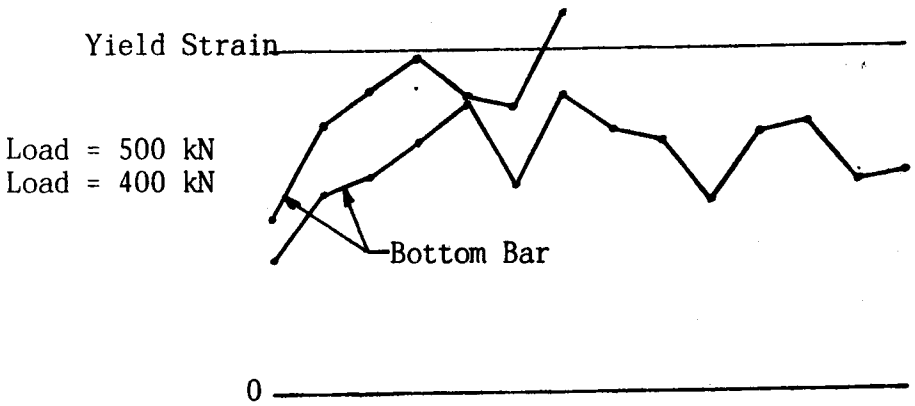

Main Steel Strains
(Strain Scale: 1 mm = 50 Microstrain)

Figure 6.50 Beam 2/1.5 Steel Strains

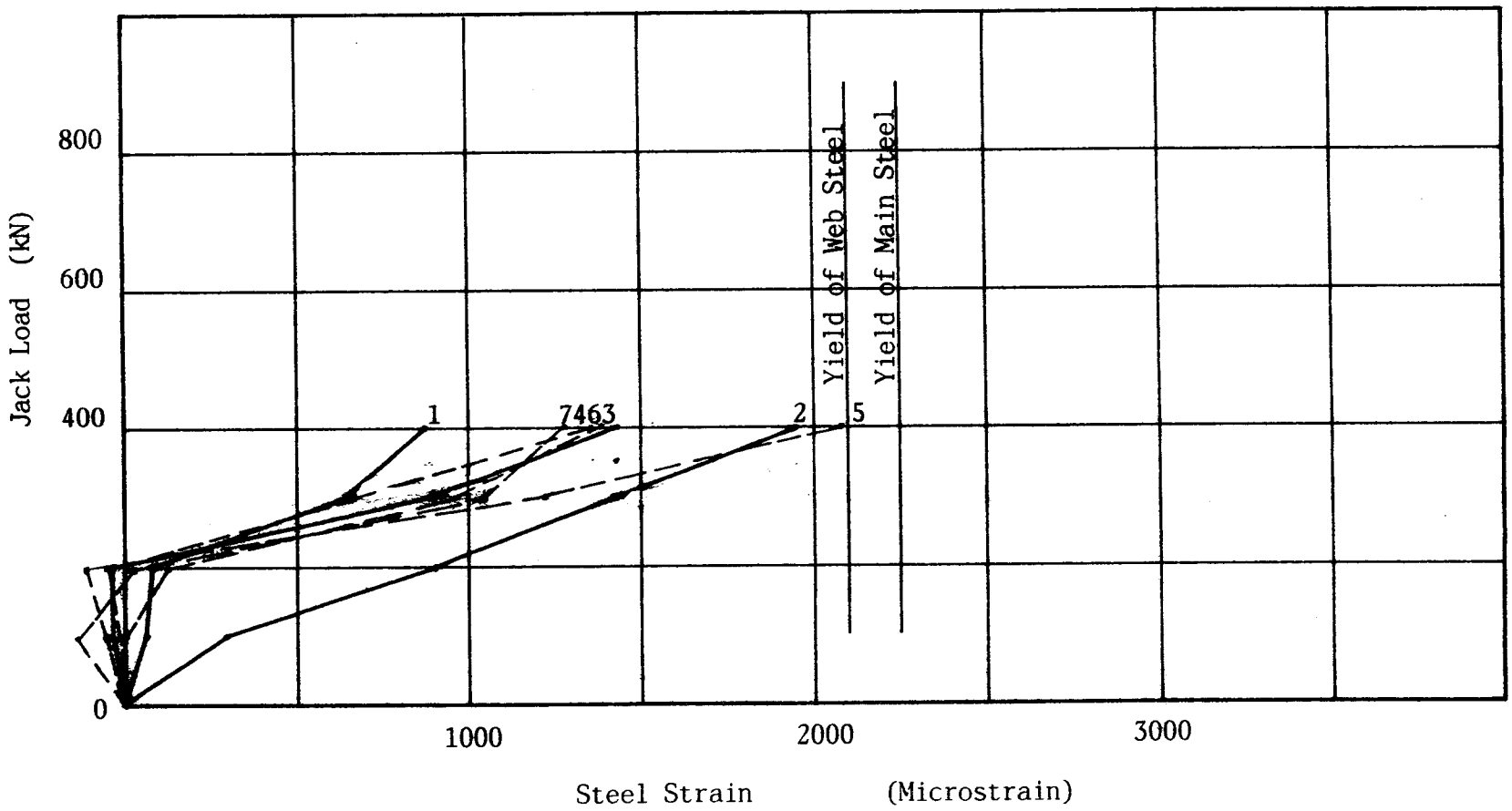

Figure 6.51 Beam 2/1.5 Load vs. Steel Strain

6.14 Beam 3/1.5

This beam was fabricated and tested by Ong (1982).It was reported by him as beam No. 2. Detailed beam by beam observations are not available.

6.15 Beam 4/1.5

This beam was fabricated and tested by Ong (1982). It was reported by him as beam No. 3. Detailed beam by beam observations are not available.

6.16 Beam 5/1.5

This two span continuous beam had 16 - 6 mm closed stirrups in each interior shear span, thus it represents the case of maximum stirrups. The inclined cracking was less well defined than in the other specimens. Inclined cracks in both interior shear spans developed at a jack load of about 275 kN. The crack formation was rather silent and occurred over a period of a few seconds. The first inclined cracks were sloped at about 52 degrees from the horizontal and were thus steeper than in the other beams. Cracks continued to develop, forming fans over the interior support and under each point load. Failure occurred in the north interior shear span with rapidly increasing deflections, but no marked loss in load. An inclined crack running from the face of the interior support to the face of the loading column opened vertically about 6 mm and closed horizontally about 1.5 mm. The displacements were relatively uniform

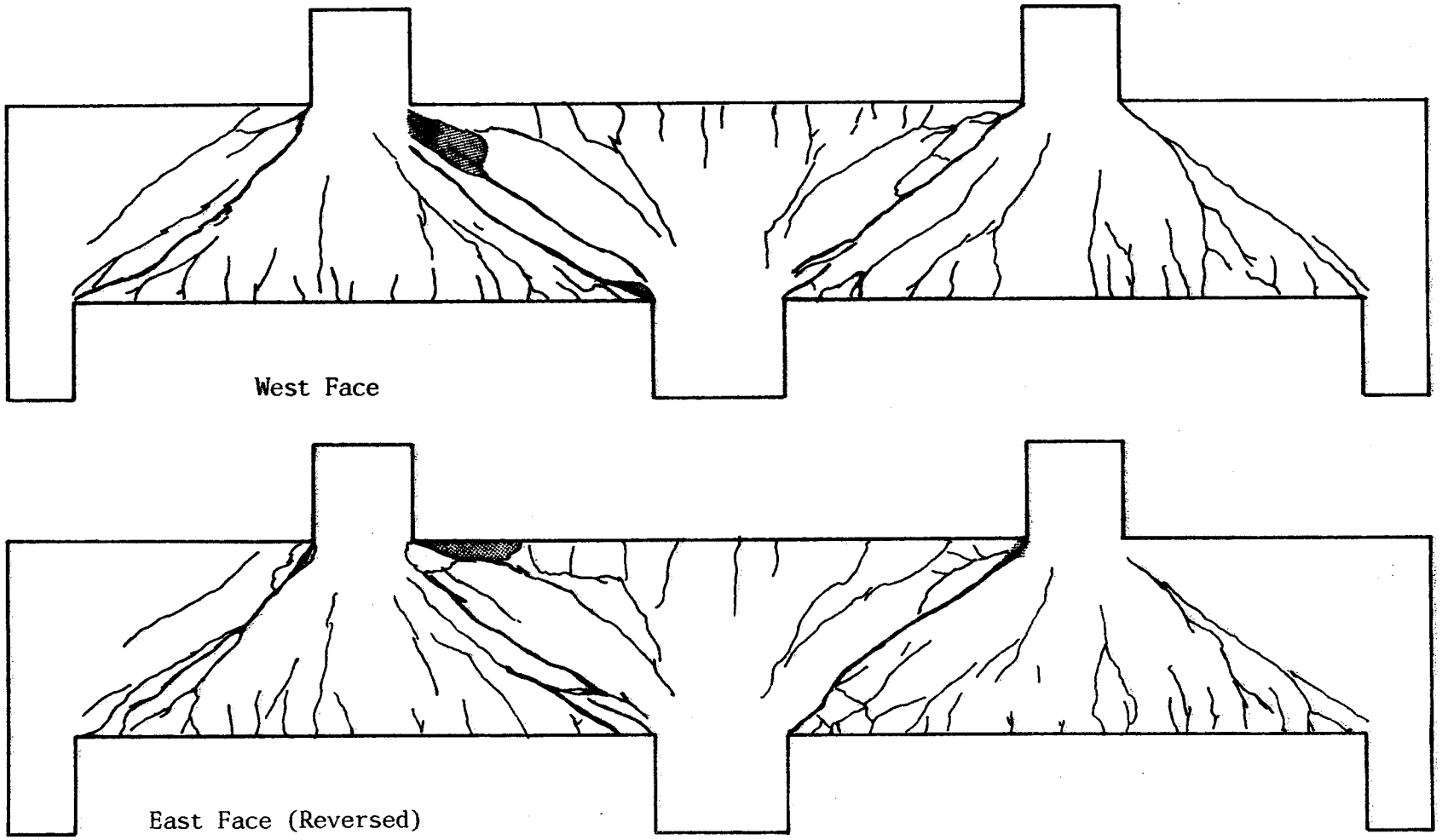

Figure 6.52 Beam 3/1.5 Crack Patterns

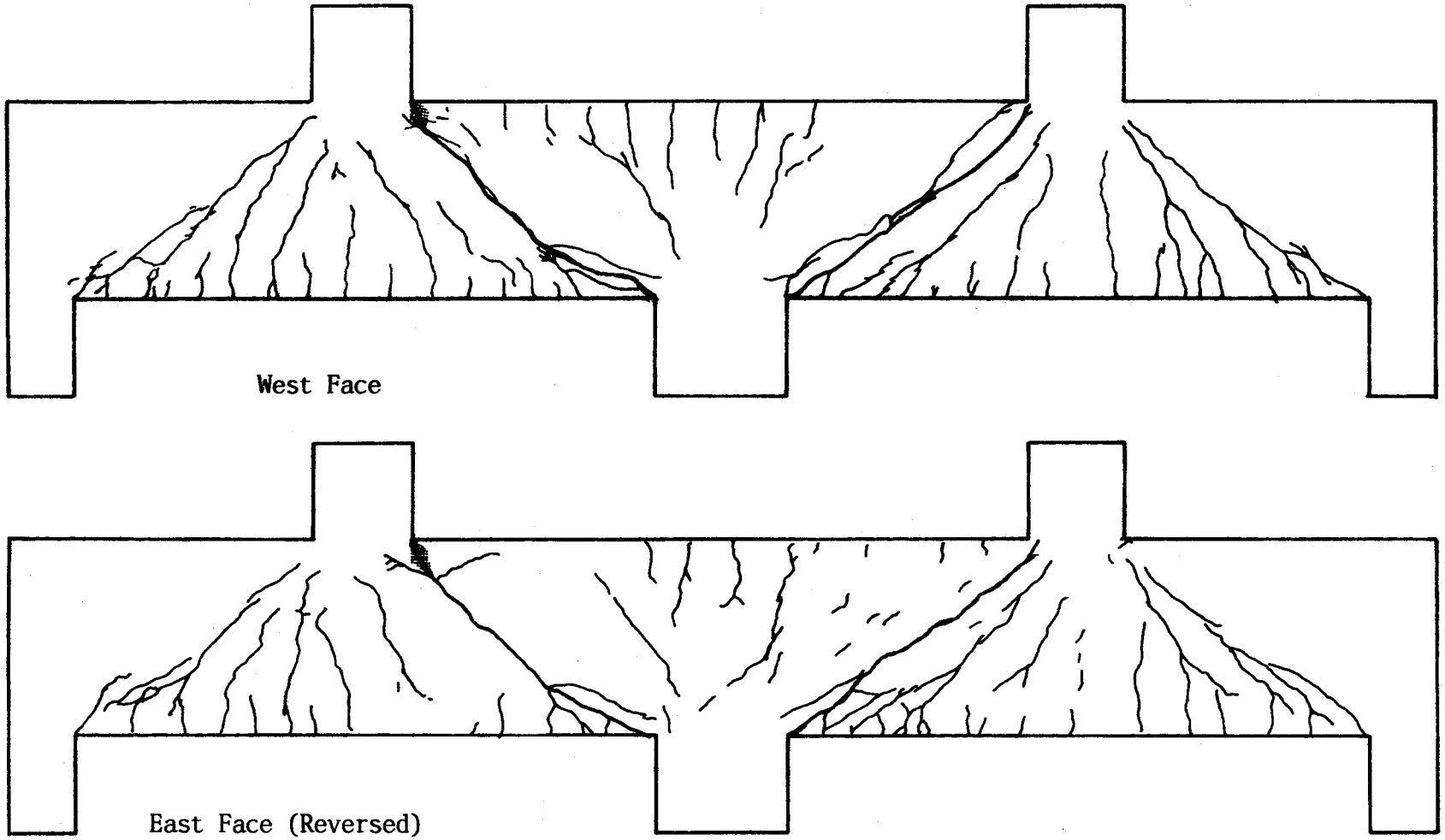

Figure 6.53 Beam 4/1.5 Crack Patterns

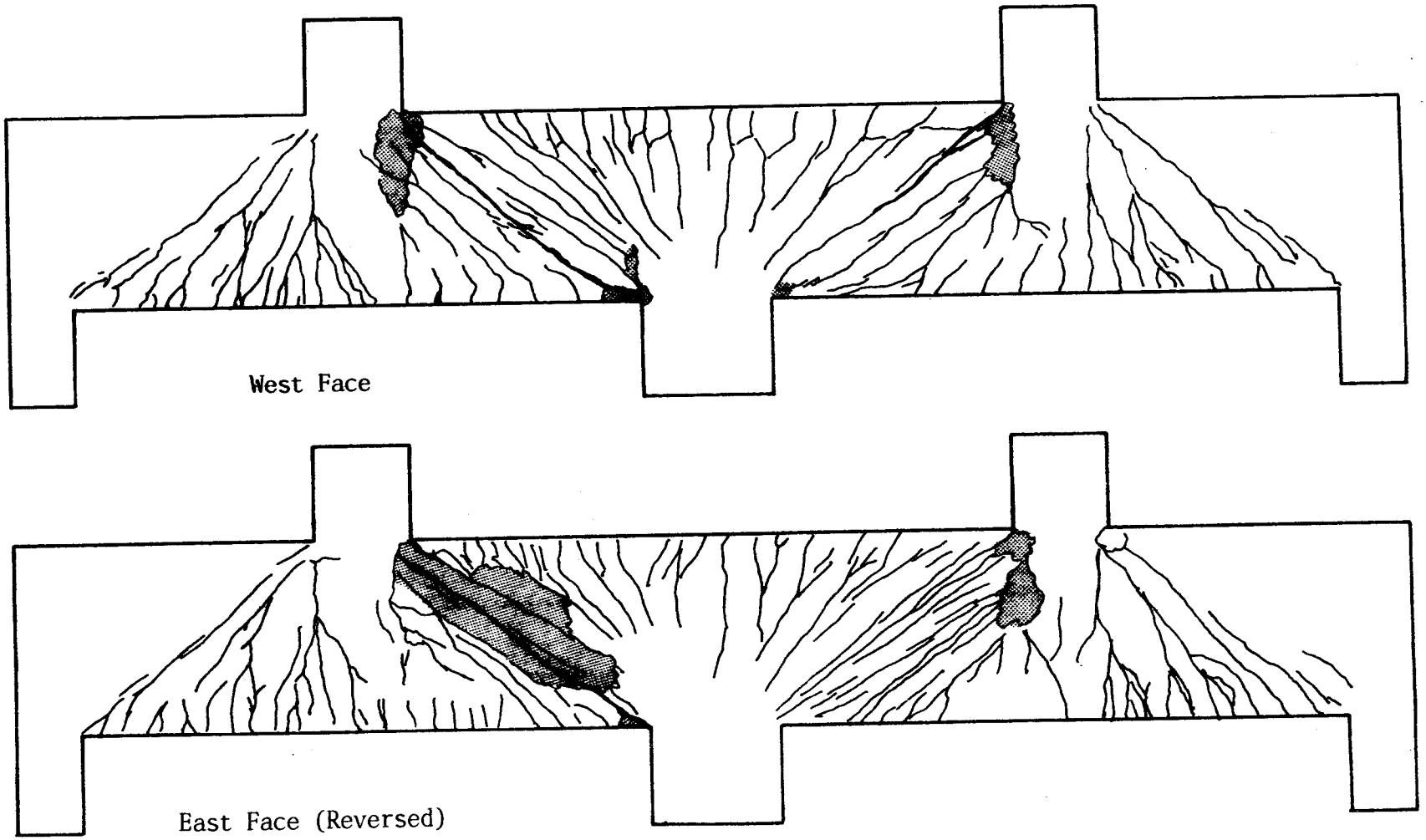

Figure 6.54 Beam 5/1.5 Crack Patterns

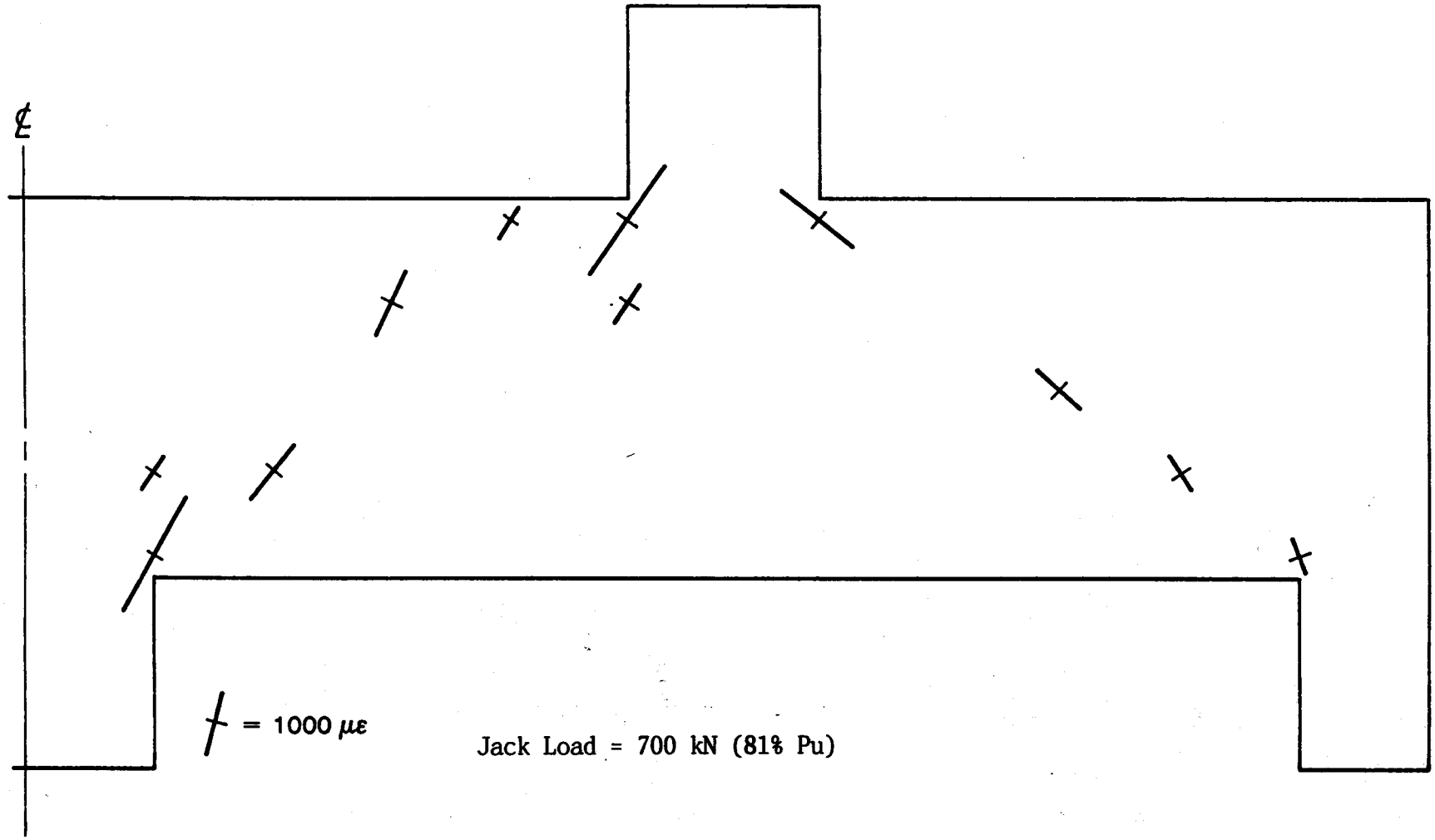

Figure 6.55 Beam 5/1.5 Concrete Compressive Strains

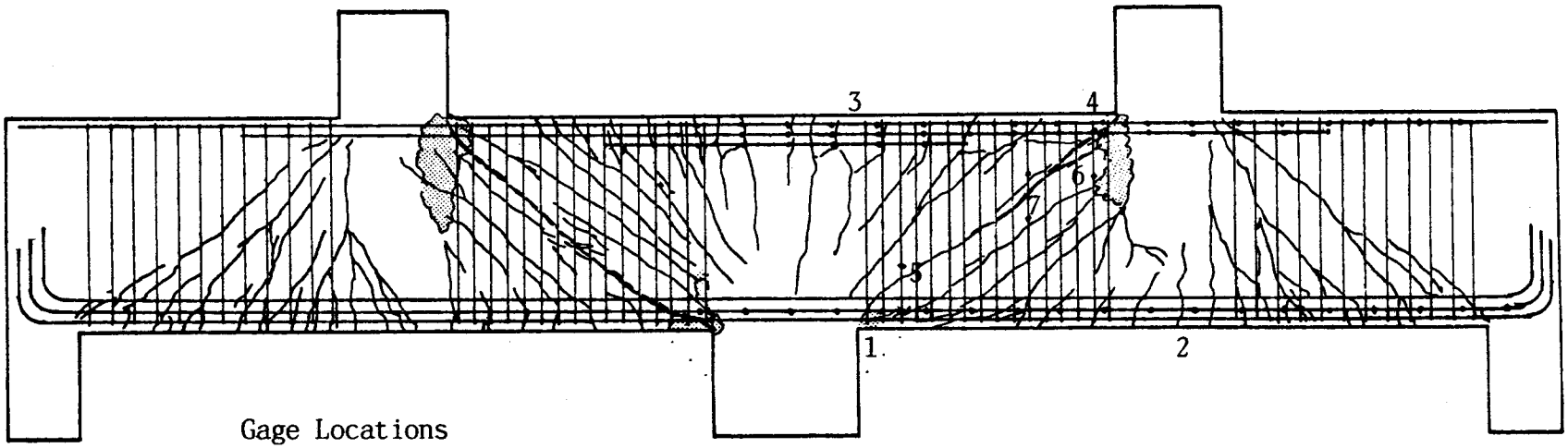

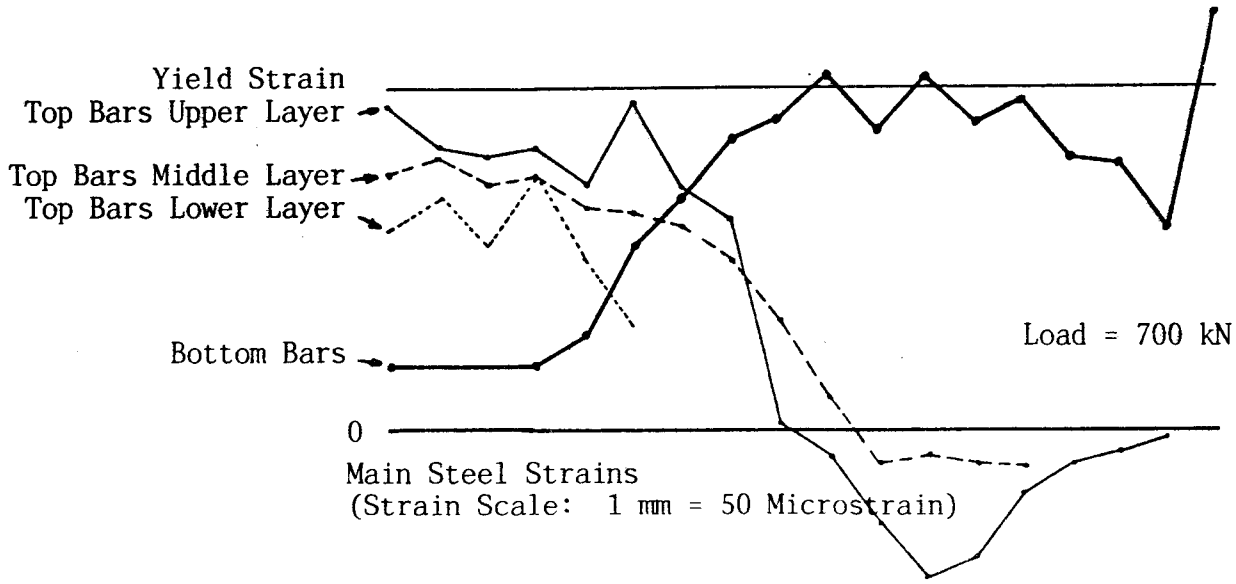

Figure 6.56 Beam 5/1.5 Steel Strains

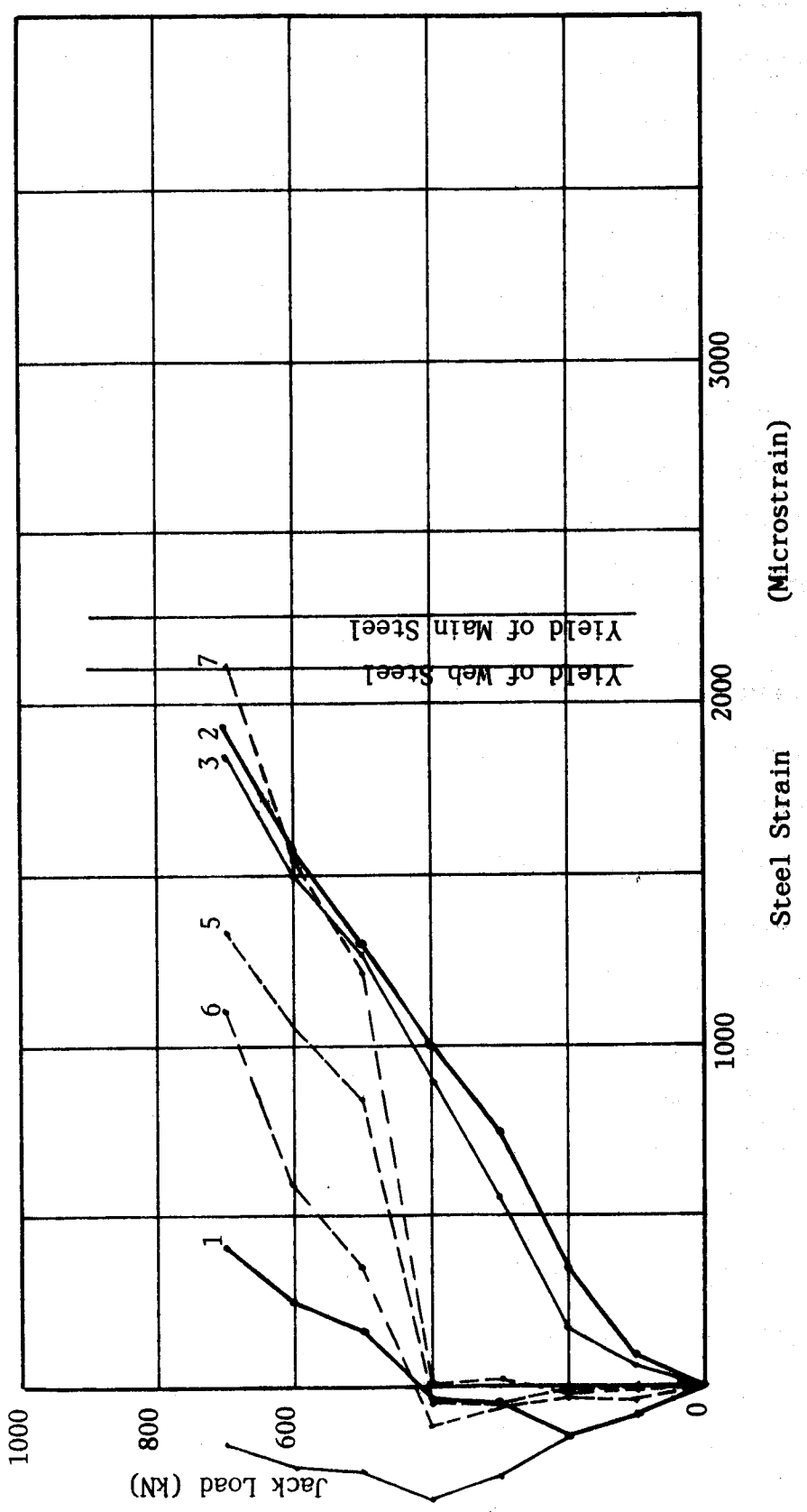

Figure 6.57 Beam 5/1.5 Load vs. Steel Strain

over the entire crack. Bar kinking type of dowel action developed at each end of this major crack as the deformation increased. Much of the concrete cover spalled or split off along the plane of the stirrup centre-lines. The concrete cover remained attached to the beam at the top and bottom, but buckled away from the beam at mid-height.

The failure zone was reinforced, and the beam was reloaded until failure of the south interior shear span. Again, deformations increased rapidly without loss of load, until about 20 mm of deflection, at which point there was crushing of the concrete at the face of the south loading column over the top half of the beam depth. This resulted in a loss of load capacity and is responsible for the descending portion of the load deflection curve in Fig. 6.4. The major crack running from the face of the loading column to the face of the interior support column was much wider at the top than the bottom, indicating a rotational type of mechanism, with the rotation taking place about the intersection of the beam soffet and the face of the interior support.

The steel strains reduced more rapidly near the supports than in the other beams of the 1.5 series. This and the concrete compressive strains acting across the upper boundary of the beam indicated that fan action was occurring.

6.17 Beam 6/1.5

This two span continuous beam contained 12 - 6 mm horizontal bars as web reinforcement, and represents the case of maximum horizontal web reinforcement. Inclined cracks occurred in the north and south interior shear spans at 250 kN and 280 kN respectively. These cracks formed suddenly with an audible "thud". They had a width of about 0.1 mm with the north crack being slightly wider and flatter than the south inclined crack. Failure occurred in the south interior shear span with the very sudden and loud formation of a diagonal interior crack running from the face of the interior support to the face of the loading column. The failure load was 403 kN.

The specimen was reinforced, and reloaded until failure occurred in the north interior shear span. Again failure occurred with the very sudden and very loud formation of a diagonal tension crack running "corner to corner". The diagonal tension cracks both had a vertical opening of about 6 mm and a horizontal closing of about 1.5 mm. The steel strain data indicates that none of the reinforcement was anywhere near yield. The failure load was 406 kN.

6.18 Beam 7/1.5

This beam was fabricated and tested by Ong (1982). It was reported by him as beam No. 1. Detailed beam by beam observations are not available.

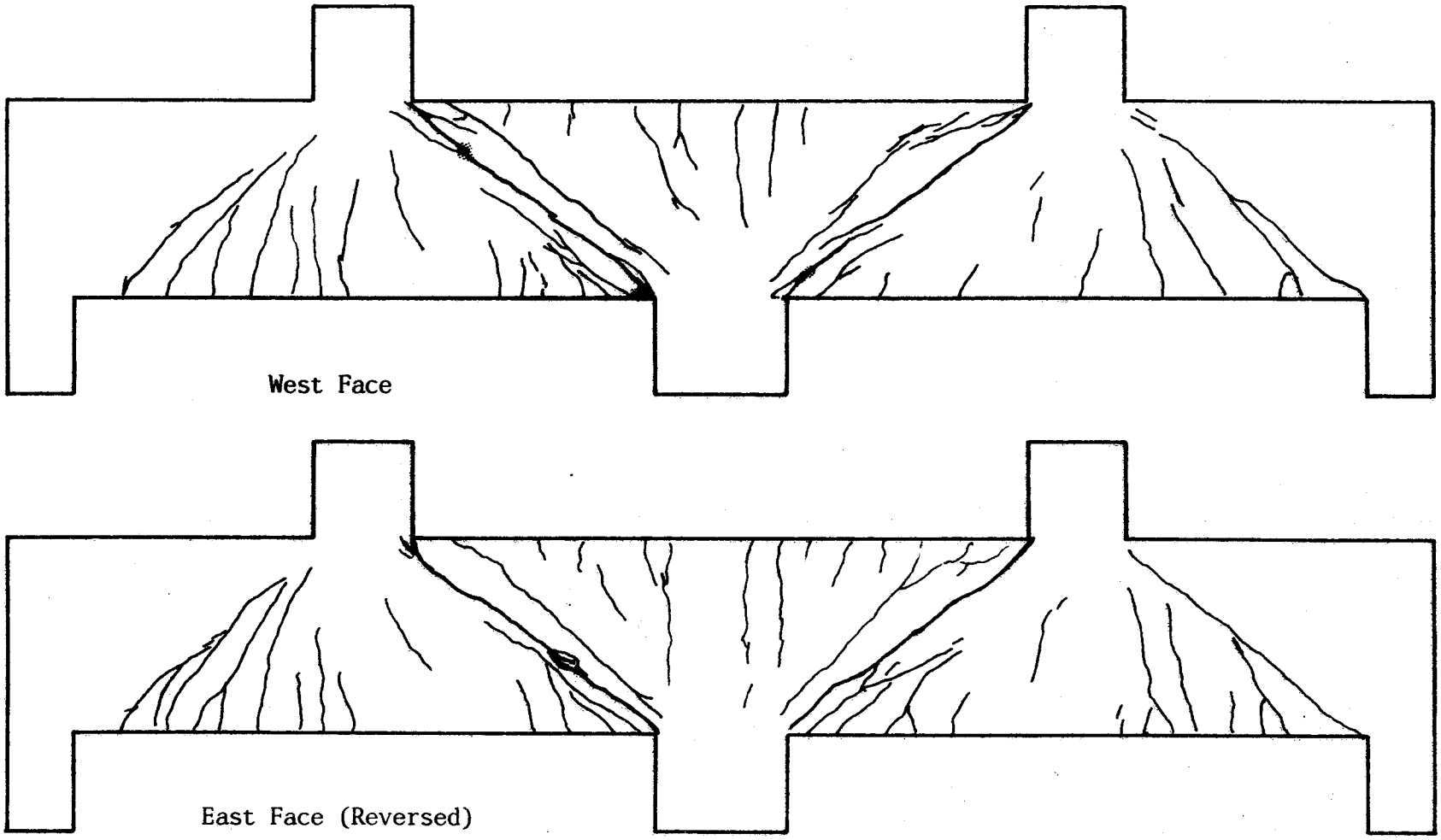

Figure 6.58 Beam 6/1.5 Crack Patterns

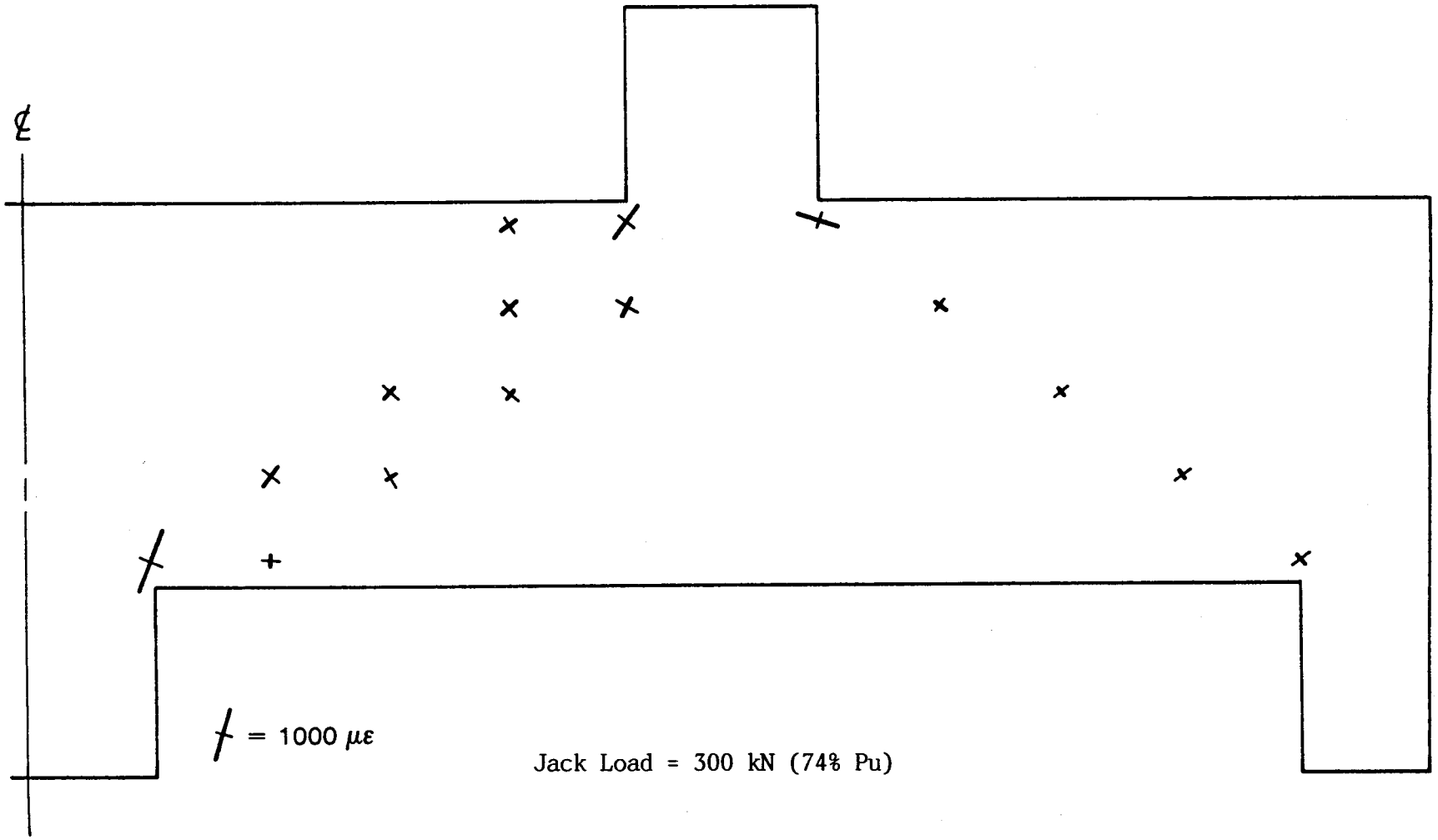

Figure 6.59 Beam 6/1.5 Concrete Compressive Strains

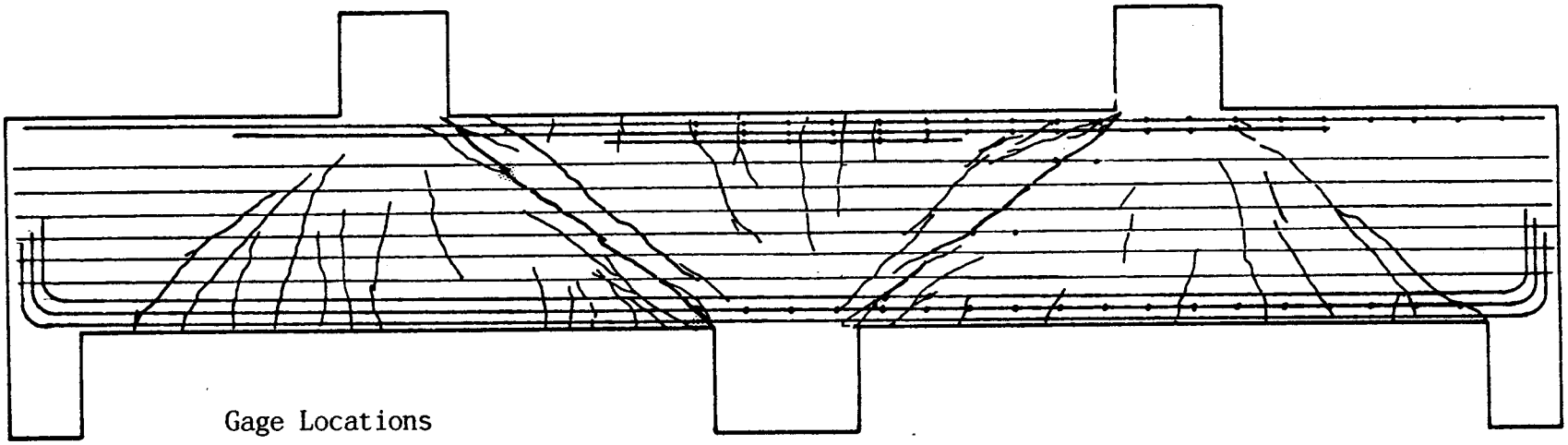

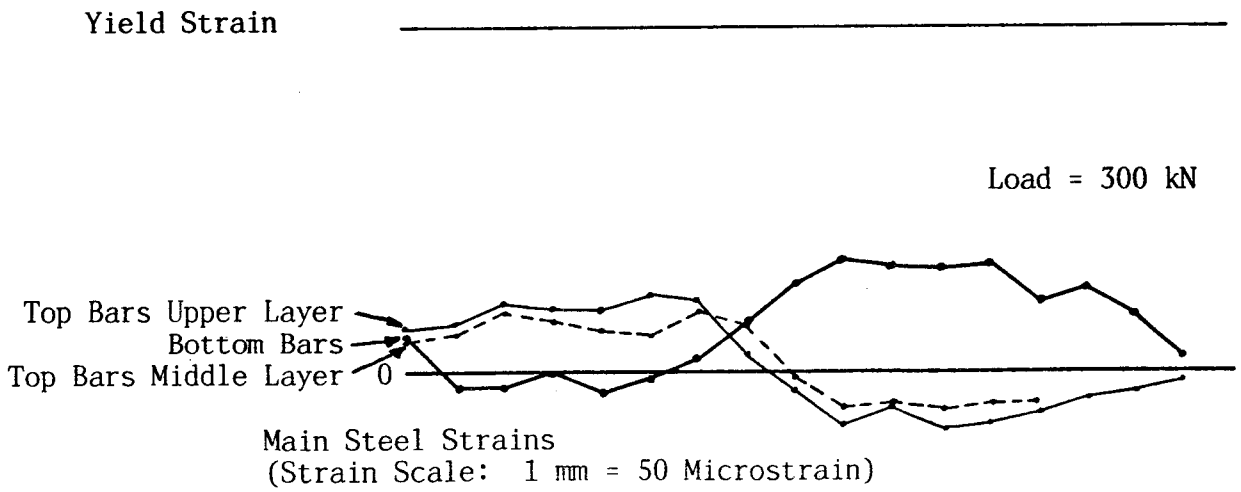

Figure 6.60 Beam 6/1.5 Steel Strains

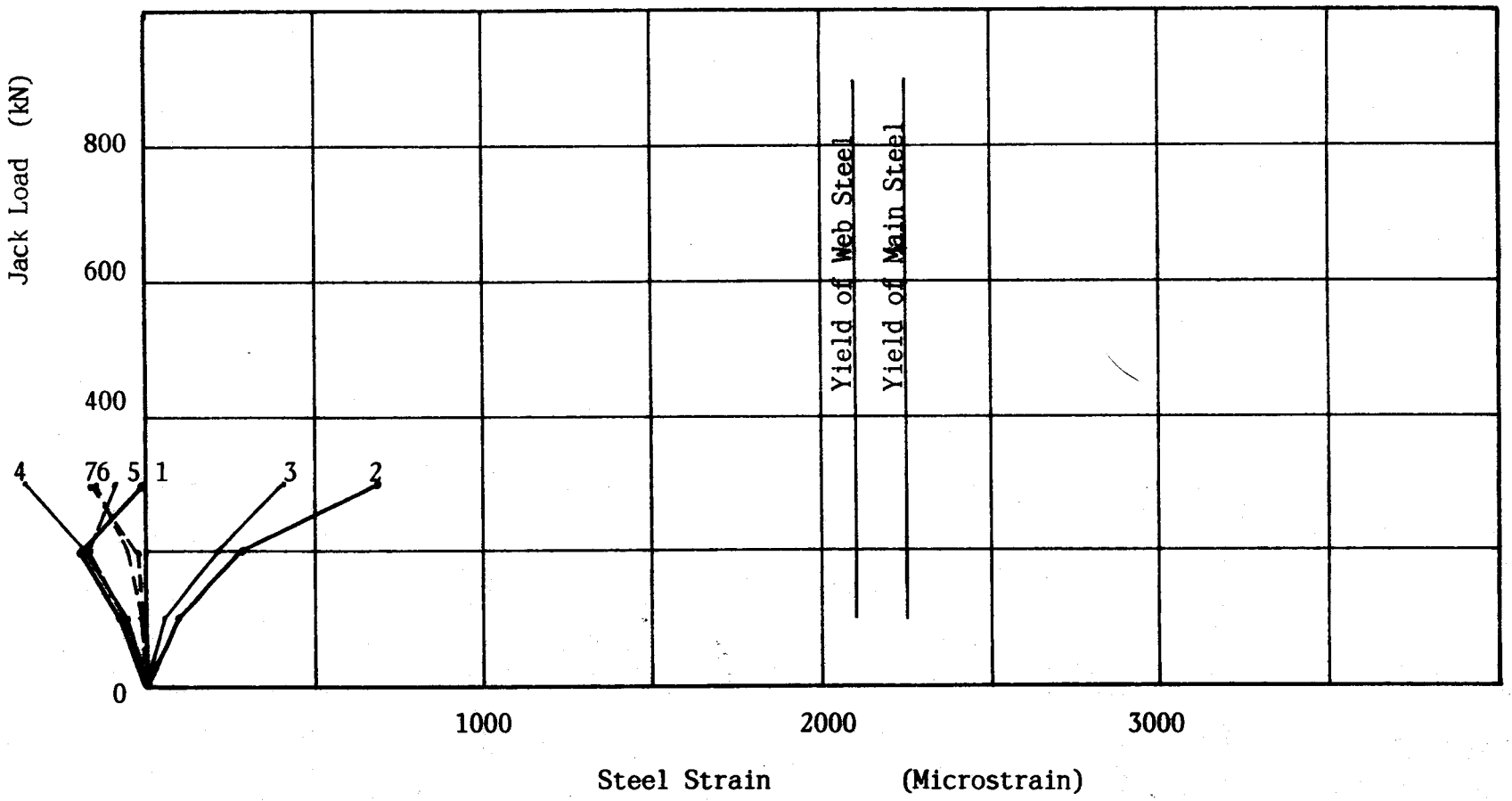

Figure 6.61 Beam 6/1.5 Load Vs. Steel Strain

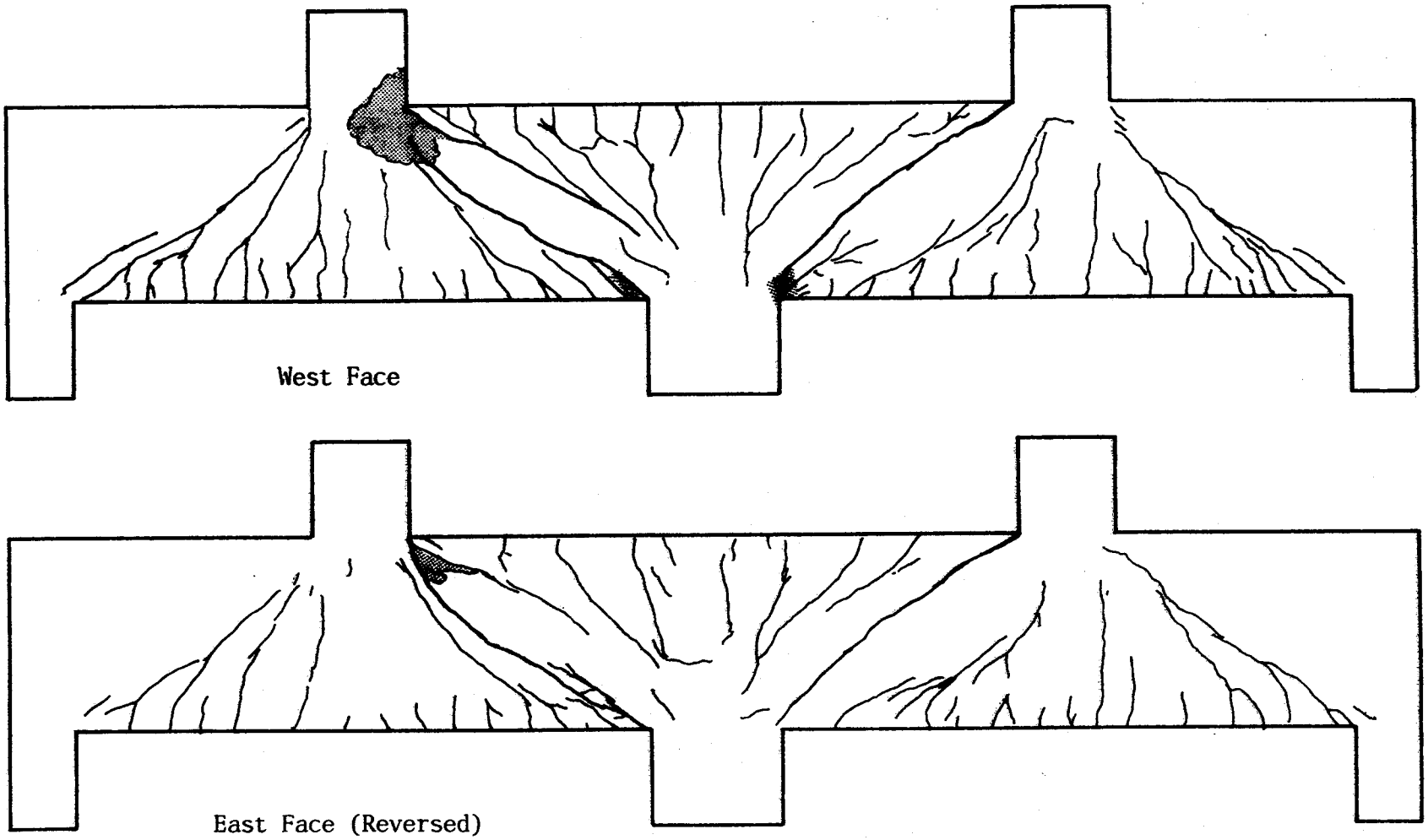

Figure 6.62 Beam 7/1.5 Crack Patterns

6.19 Beam 8/1.5

This beam was fabricated and tested by Ong (1982). It was reported by him as beam No. 4. Detailed beam by beam observations are not available.

6.20 Beam 1/2.0

This was a simply supported beam with approximately minimum stirrups in the north shear span and no web reinforcement in the south shear span. Inclined cracking developed in the south shear span at a load of about 190 kN. The crack started from a point along the soffet about 200 mm from the face of the support column, and ran to a point about 50 mm below the top of the beam at the face of the loading column. The inclined crack in the north shear span developed slowly making it difficult to determine the inclined cracking load. As the load increased, considerable dowel kinking or bending developed at the south support. This was accompanied with a rotational opening of the inclined crack with rotation taking place about the top end of the inclined crack. The 50 mm of concrete above the head of the inclined crack exhibited fine parallel cracks before finally failing in shear-compression. The load deflection curve shown in Fig. 6.8 indicates a remarkable amount of ductility for a member without web reinforcement. This was probably due to the significant amount of dowel action which developed, this in turn was enhanced by the use of two layers of bottom bars.

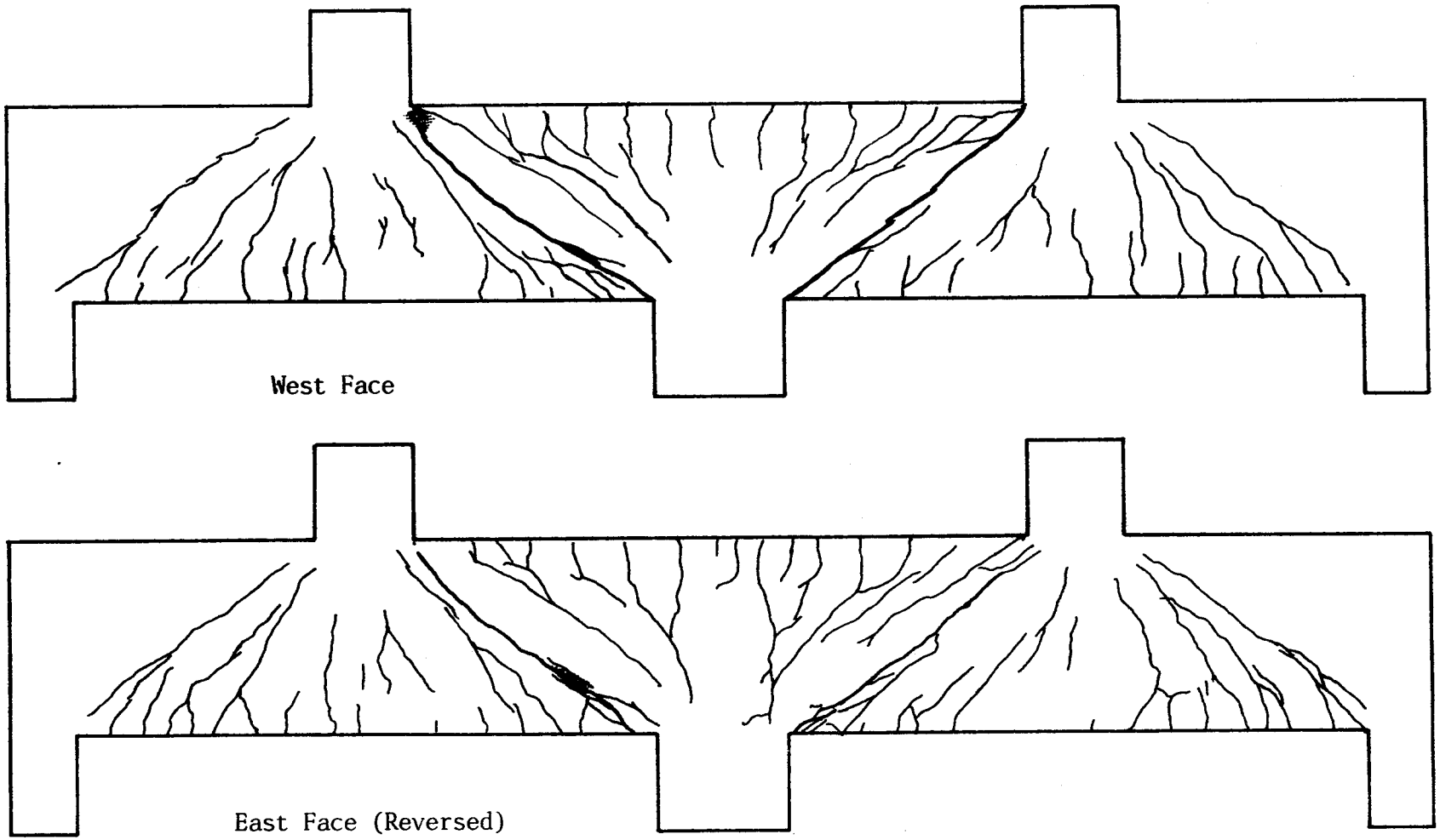

Figure 6.63 Beam 8/1.5 Crack Patterns

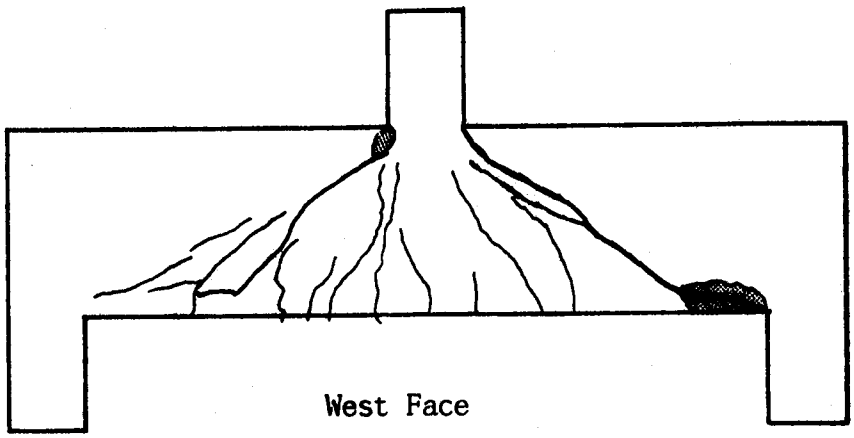

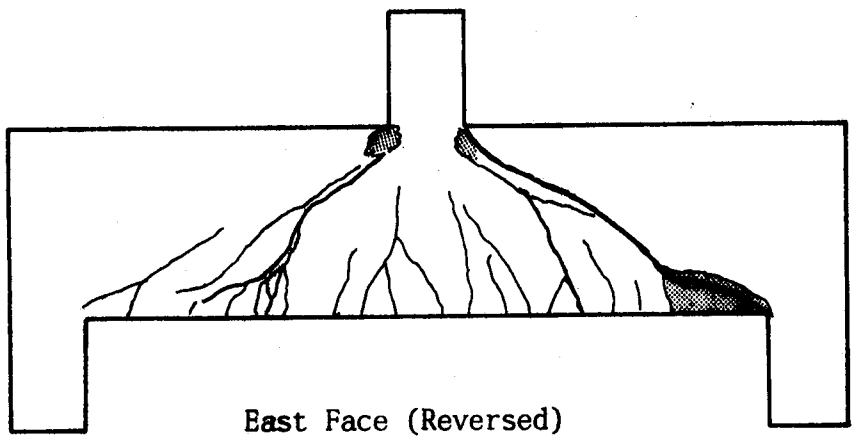

Figure 6.64 Beam 1/2.0 Crack patterns

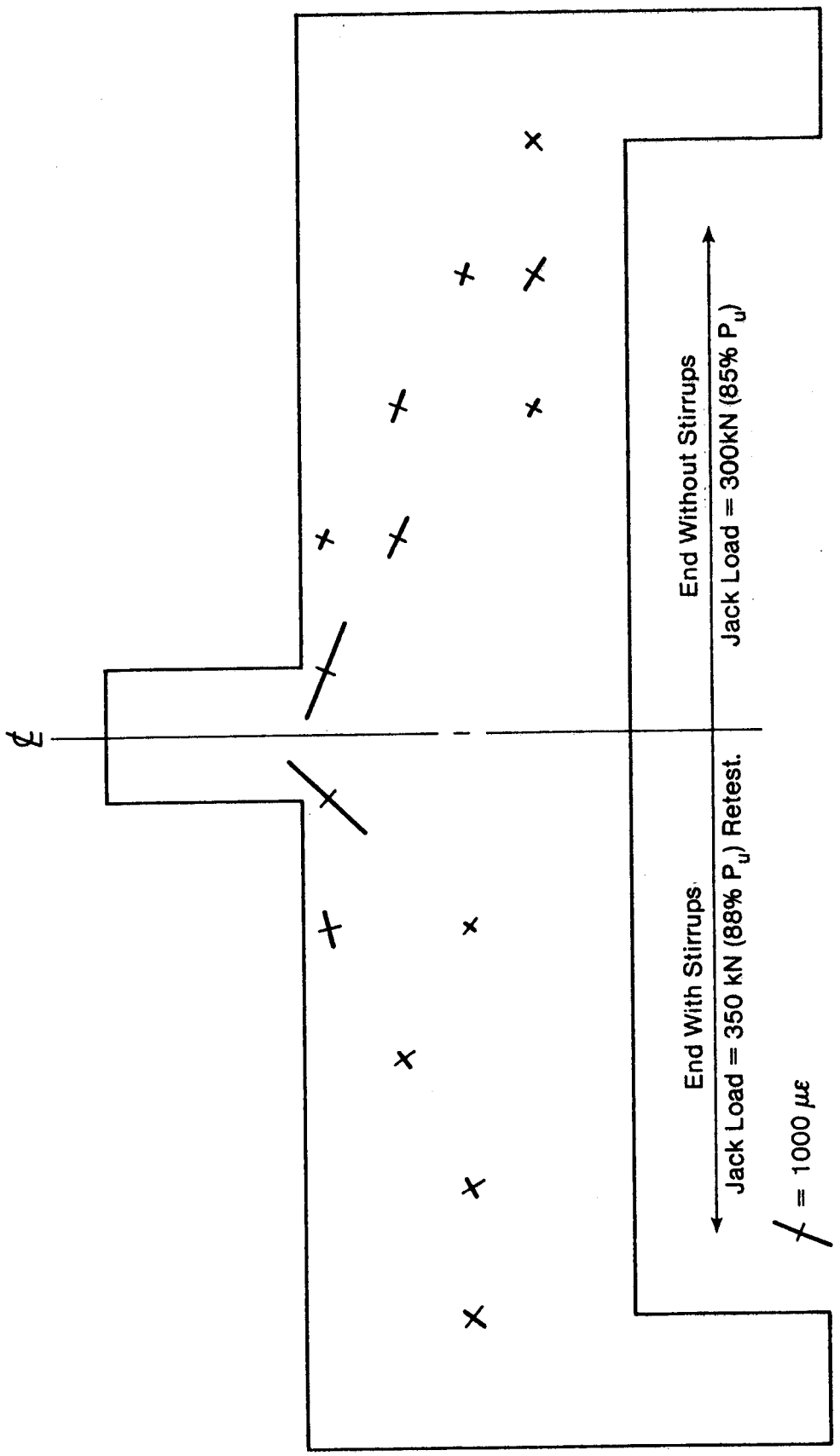

Figure 6.65 Beam 1/2.0 Concrete Compressive Strains

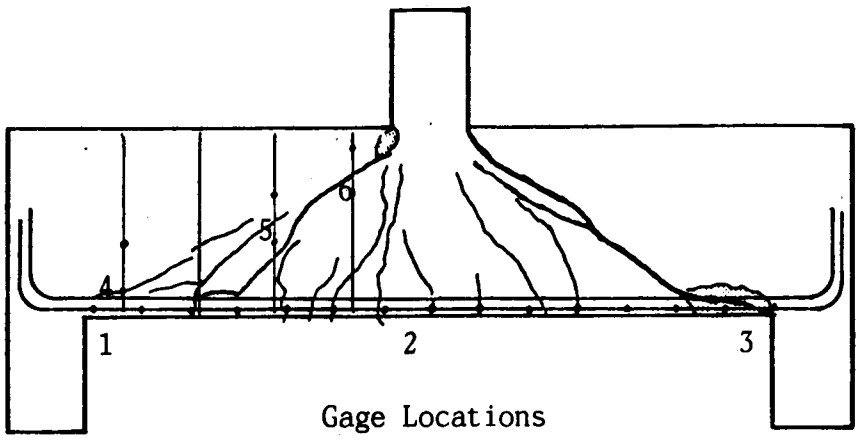

Gage Locations

0

Main Steel Strains
(Strain Scale: 1 mm = 50 Microstrain)

Figure 6.66 Beam 1/2.0 Steel Strains

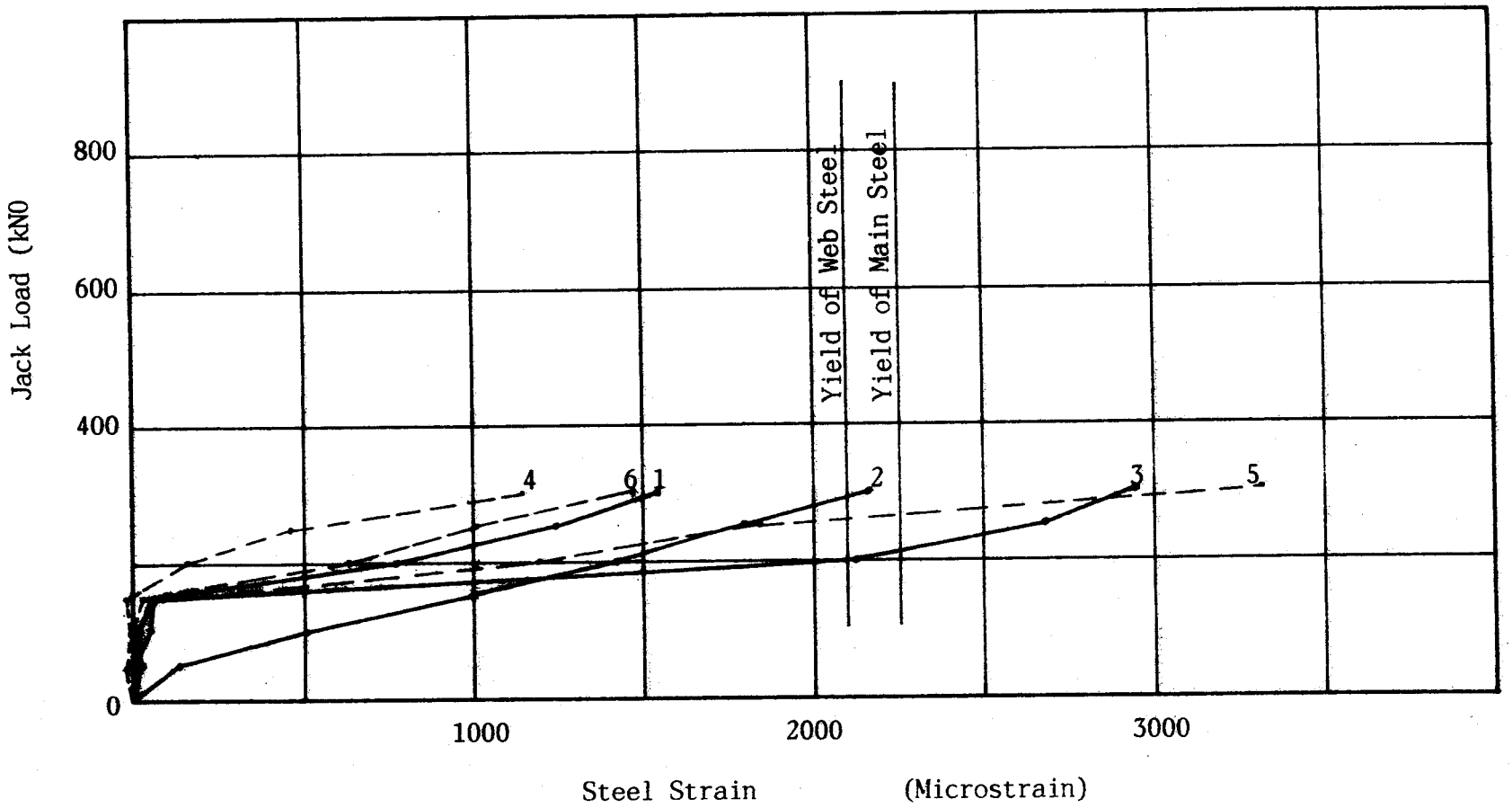

Figure 6.67 Beam 1/2.0 Load vs. Steel Strain

The failure zone was reinforced, and the beam was reloaded. At 350 kN it appeared that the flexural crack directly below the north face of the loading column would produce failure since it had a width of about 2 mm, and the deflections had increased rapidly. The critical crack which produced failure was the major sloped crack which intersected the soffet about 400 mm from the face of the support column. After considerable deformation, a shear compression failure occurred at the top of this sloped crack. The crack opened vertically about 6 mm and closed horizontally about 1.5 mm over most of its length. There was some dowel kinking at the bottom of this crack. The horizontal cracks associated with this behavior were controlled, but not eliminated by the stirrups.

6.21 Beam 2/2.0

This simple span beam had minimum horizontal web reinforcement in the south end with minimum vertical and minimum horizontal web reinforcement in the north end. The inclined cracking loads for the north and south shear spans were 240 kN and 215 kN respectively. The behavior of this beam was virtually identical to the south end of beam 1/2.0, the end without web reinforcement, but with slightly less deflection before failure. The crack types and failure mechanisms were very similar. It appeared that the horizontal web reinforcement made no practical difference.

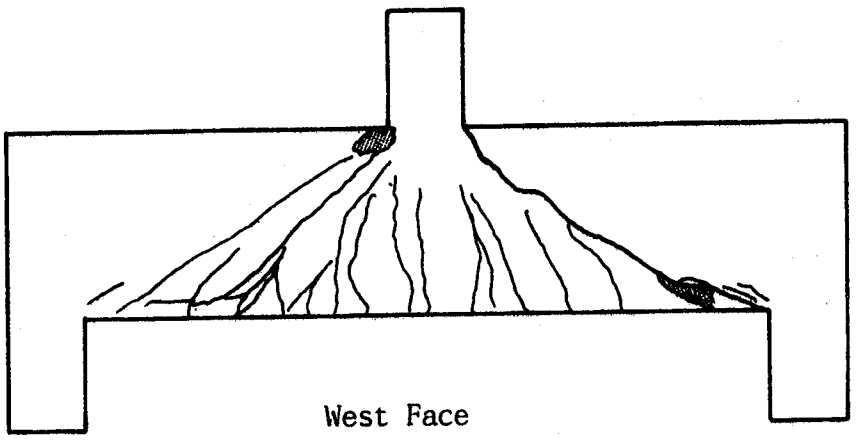

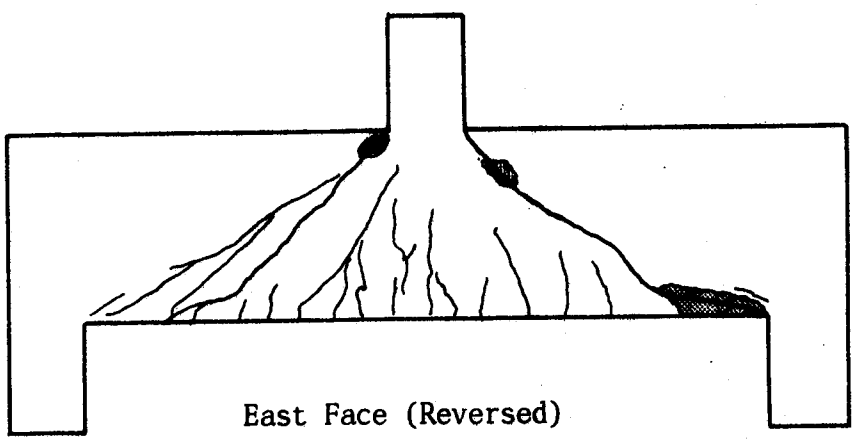

Figure 6.68 Beam 2/2.0 Crack Patterns

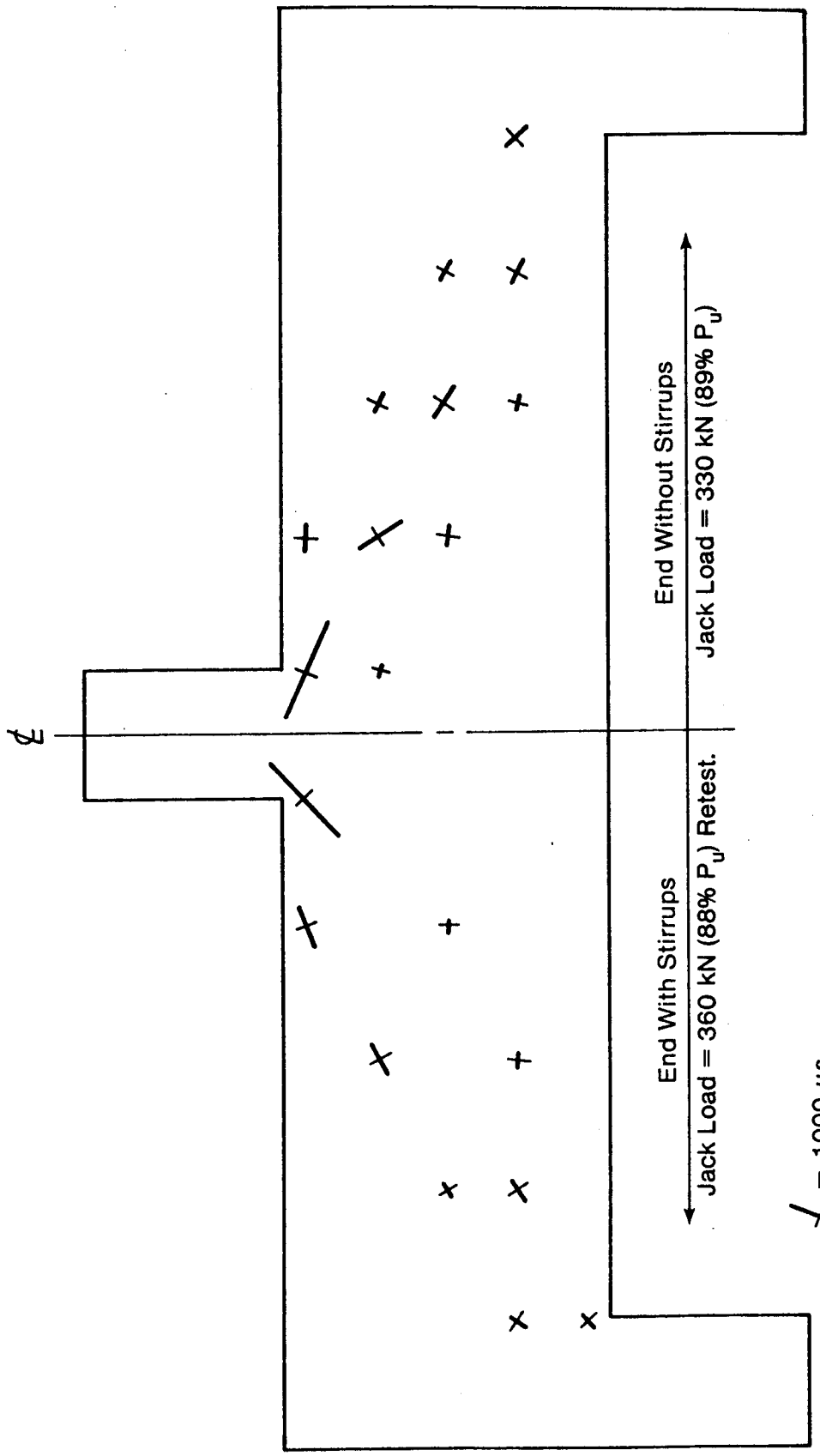

Figure 6.69 Beam 2/2.0 Concrete Compressive Strains

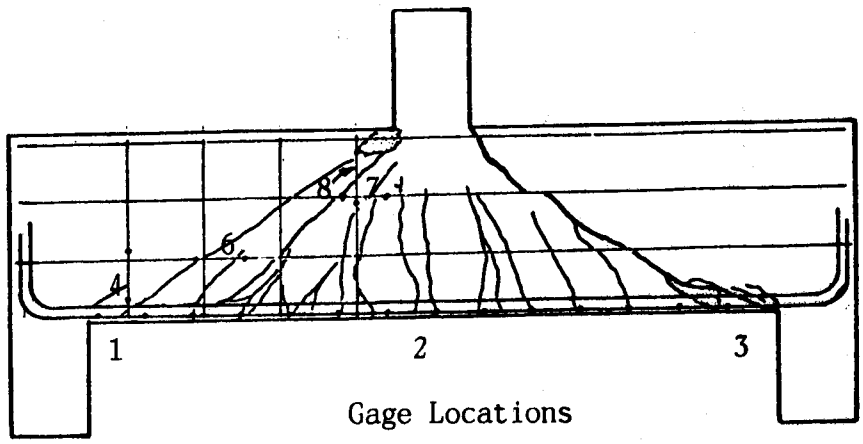

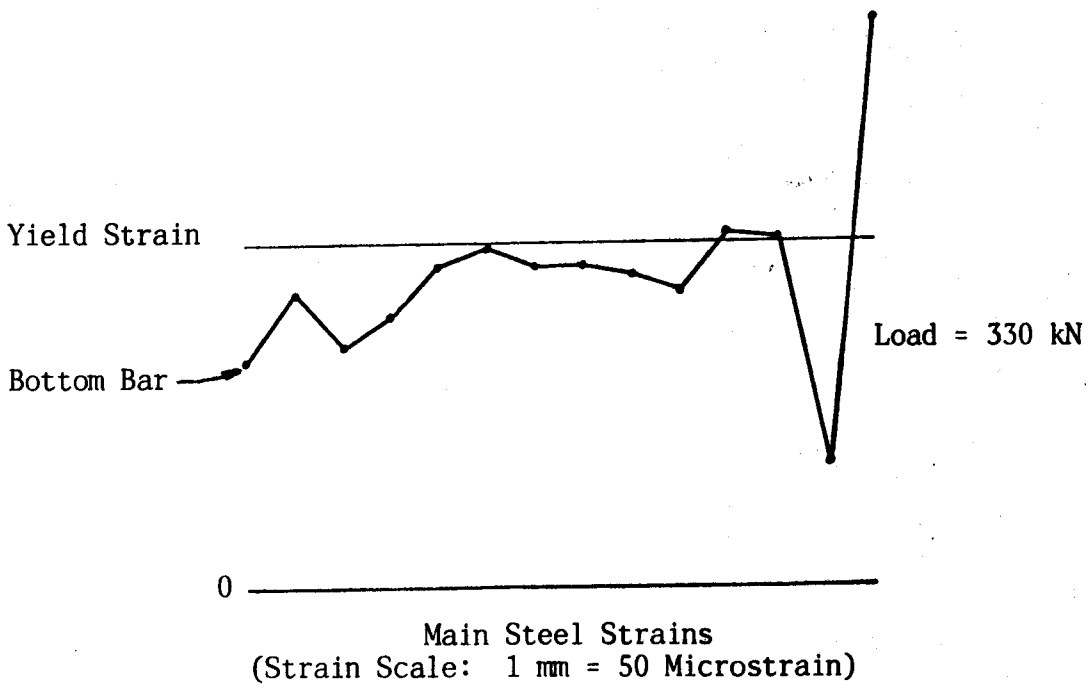

Figure 6.70 Beam 2/2.0 Steel Strains

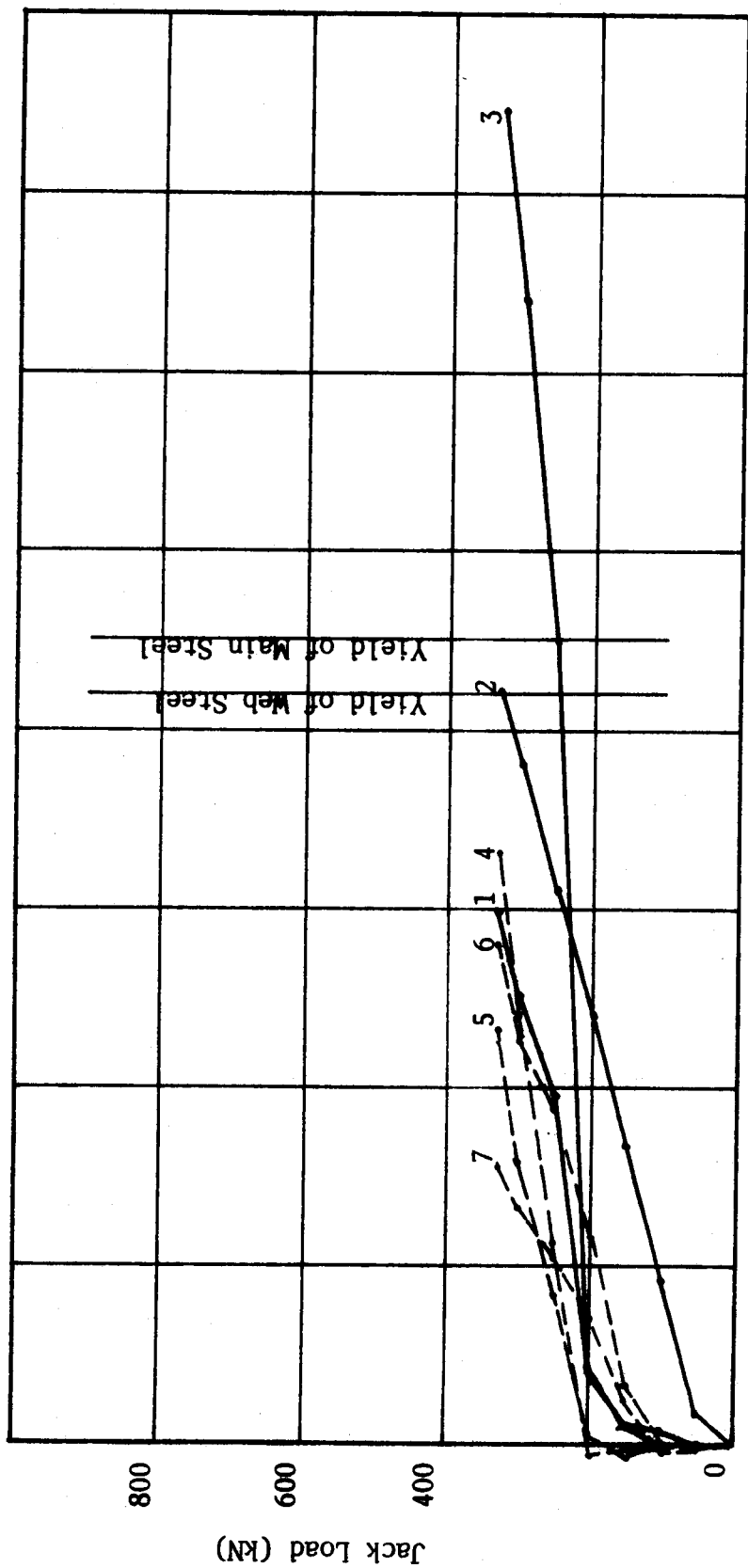

Figure 6.71 Beam 2/2.0 Load vs. Steel Strains

6.22 Beam 3/2.0

This two span beam contained minimum stirrups throughout. This beam did not have a well defined inclined cracking load. The diagonal cracking was progressive but the final fatal crack was sudden. This crack caused the failure in the north interior shear span but it was a "quiet" failure due to vertical opening of the crack. When the beam was reinforced and reloaded, failure in the south interior shear span resulted from an inclined crack running down from the face of the loading column at about 45 degrees and flattening out at the bottom steel. Again, the predominant movement was vertical opening of the crack. This beam did not have a flat ductile yield plateau on the load deflection curve.

6.23 Beam 4/2.0

This two span beam had minimum horizontal web reinforcement throughout. Inclined cracking occurred in the south interior shear span at a load of 200 kN. This was followed by a major inclined crack in the north exterior shear span at a load of 300 kN. A loud sudden diagonal tension failure running "corner to corner" occurred in the north interior shear span at a load of 303 kN. Some load shedding from the exterior to interior north shear spans seems to have occurred.

On retesting the beam, the south exterior shear span developed major inclined cracks at a load of 250 kN. At

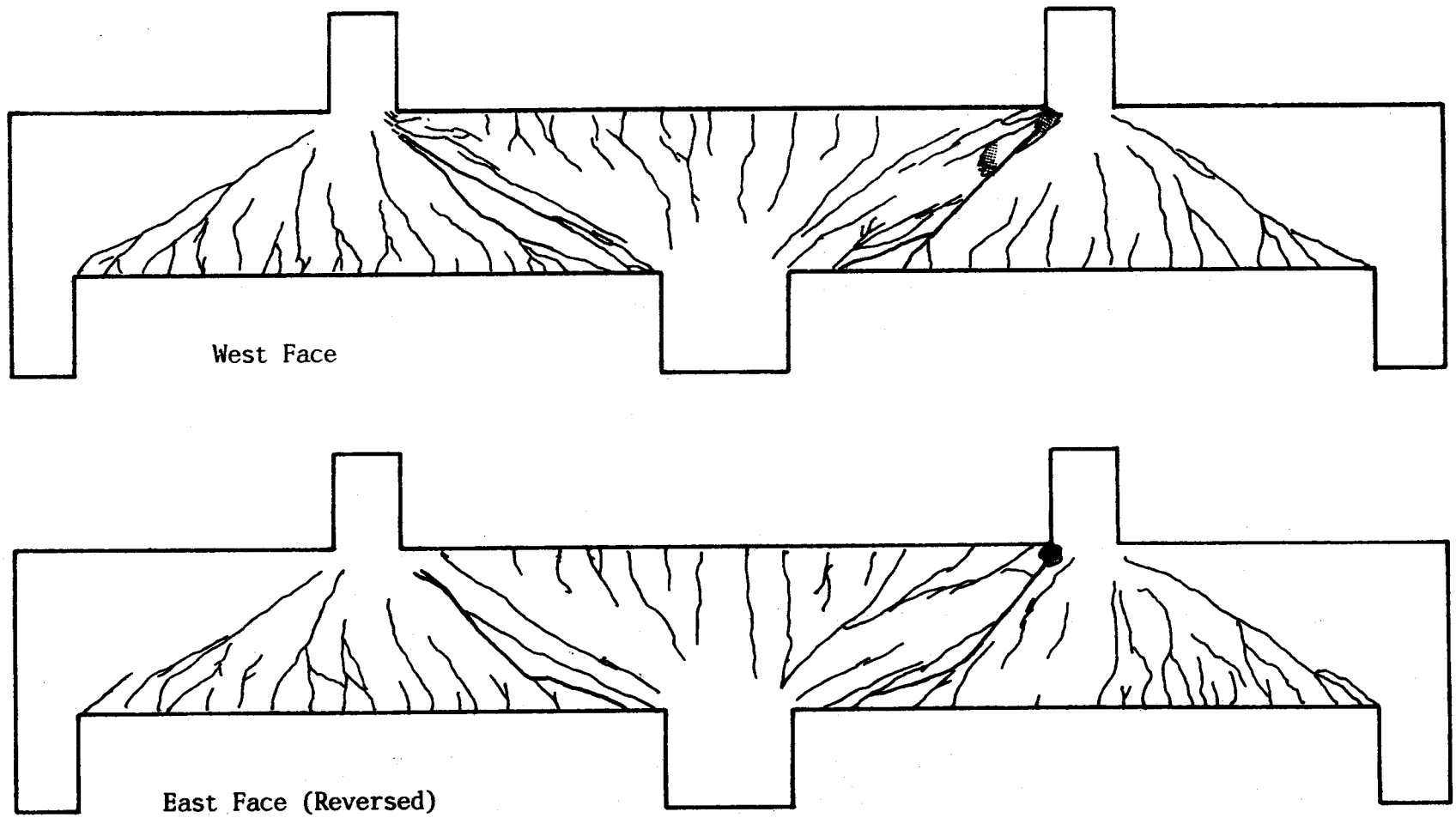

Figure 6.72 Beam 3/2.0 Crack Patterns

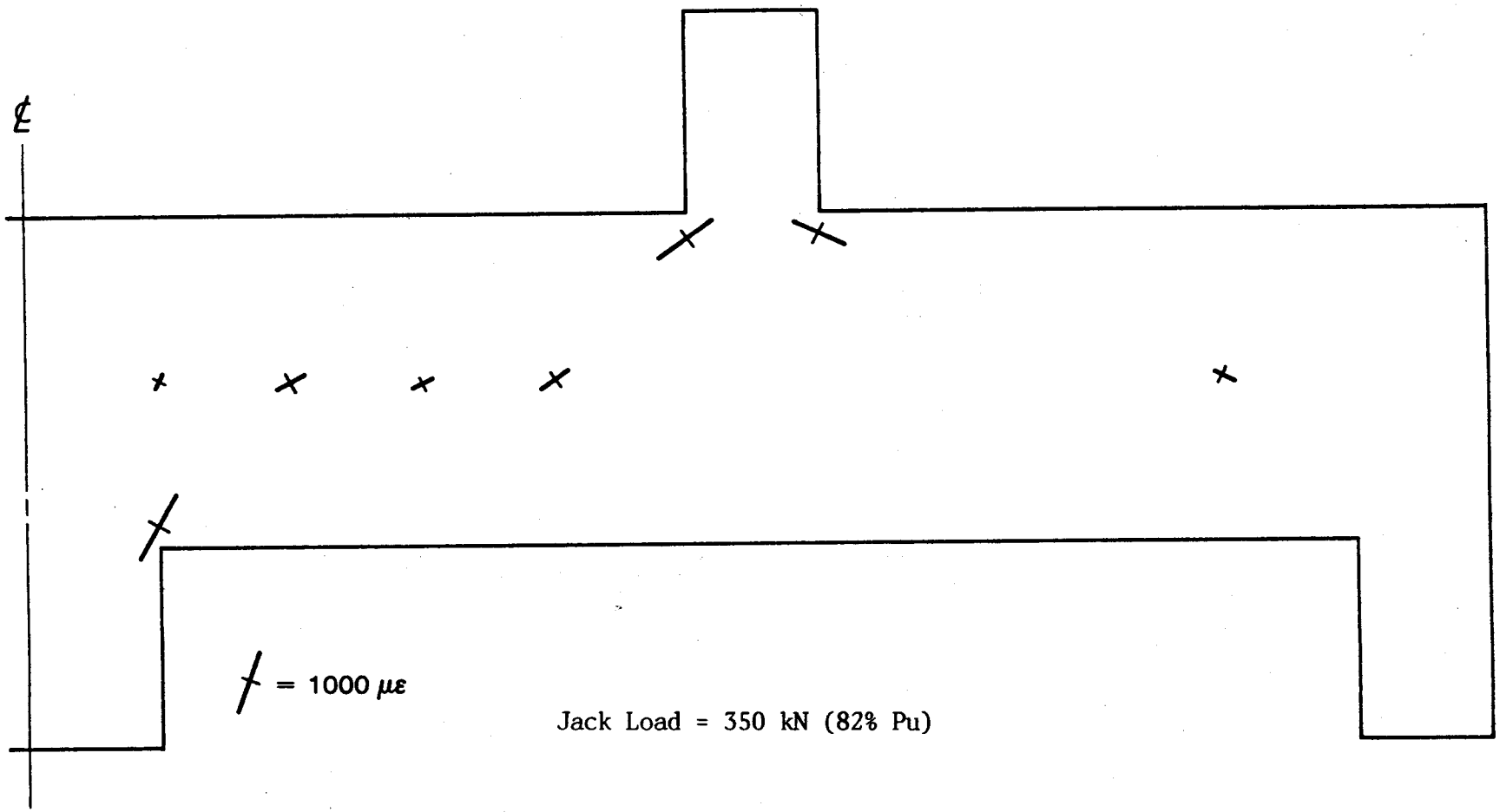

Figure 6.73 Beam 3/2.0 Concrete Compressive Strains

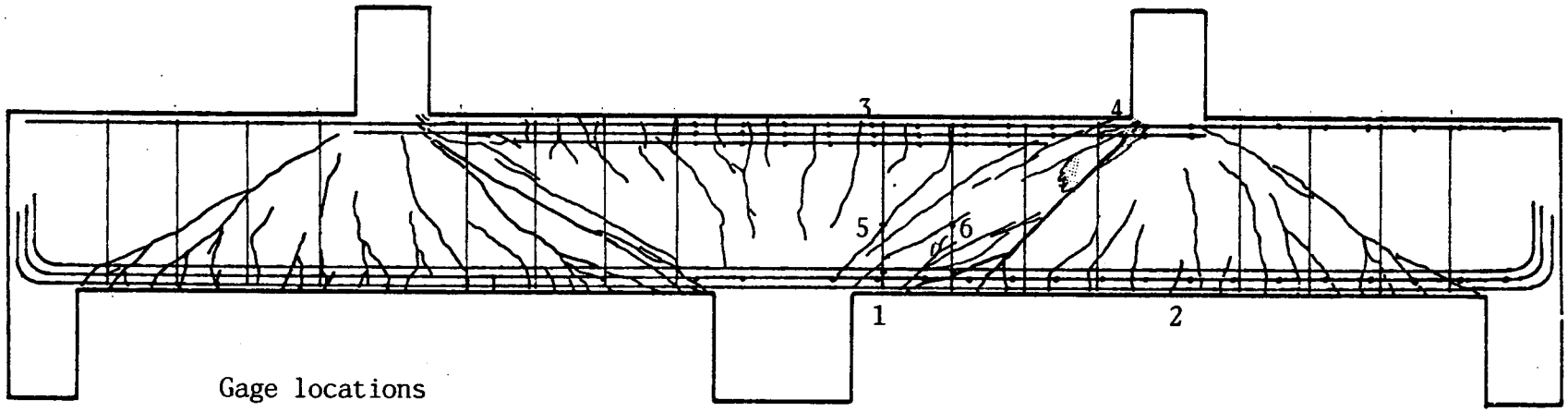

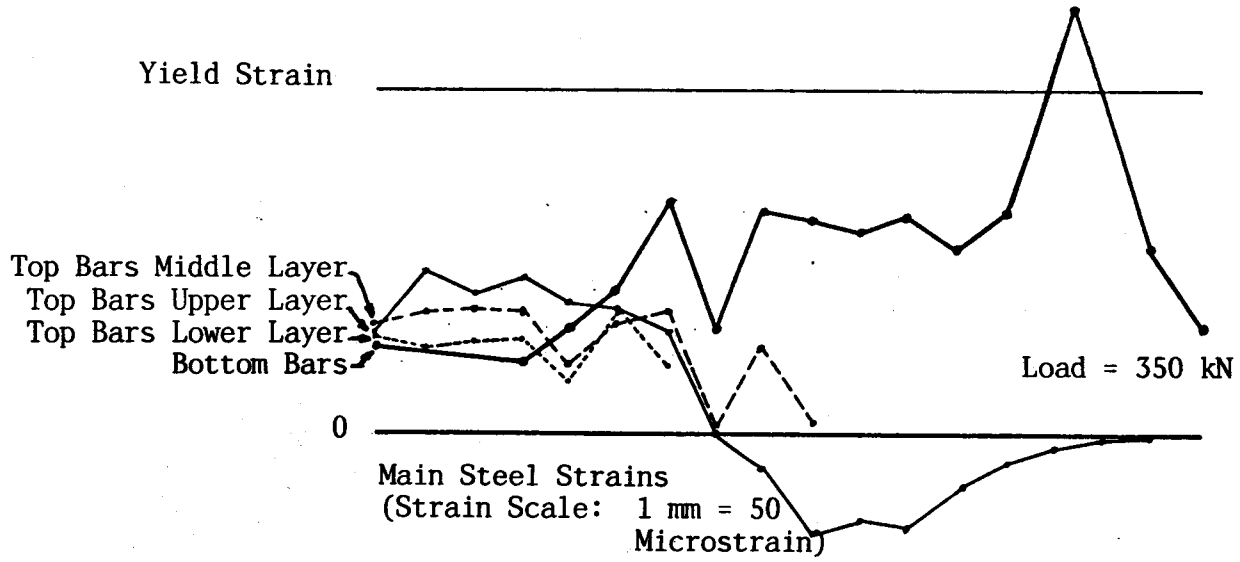

Figure 6.74 Beam 3/2.0 Steel Strains

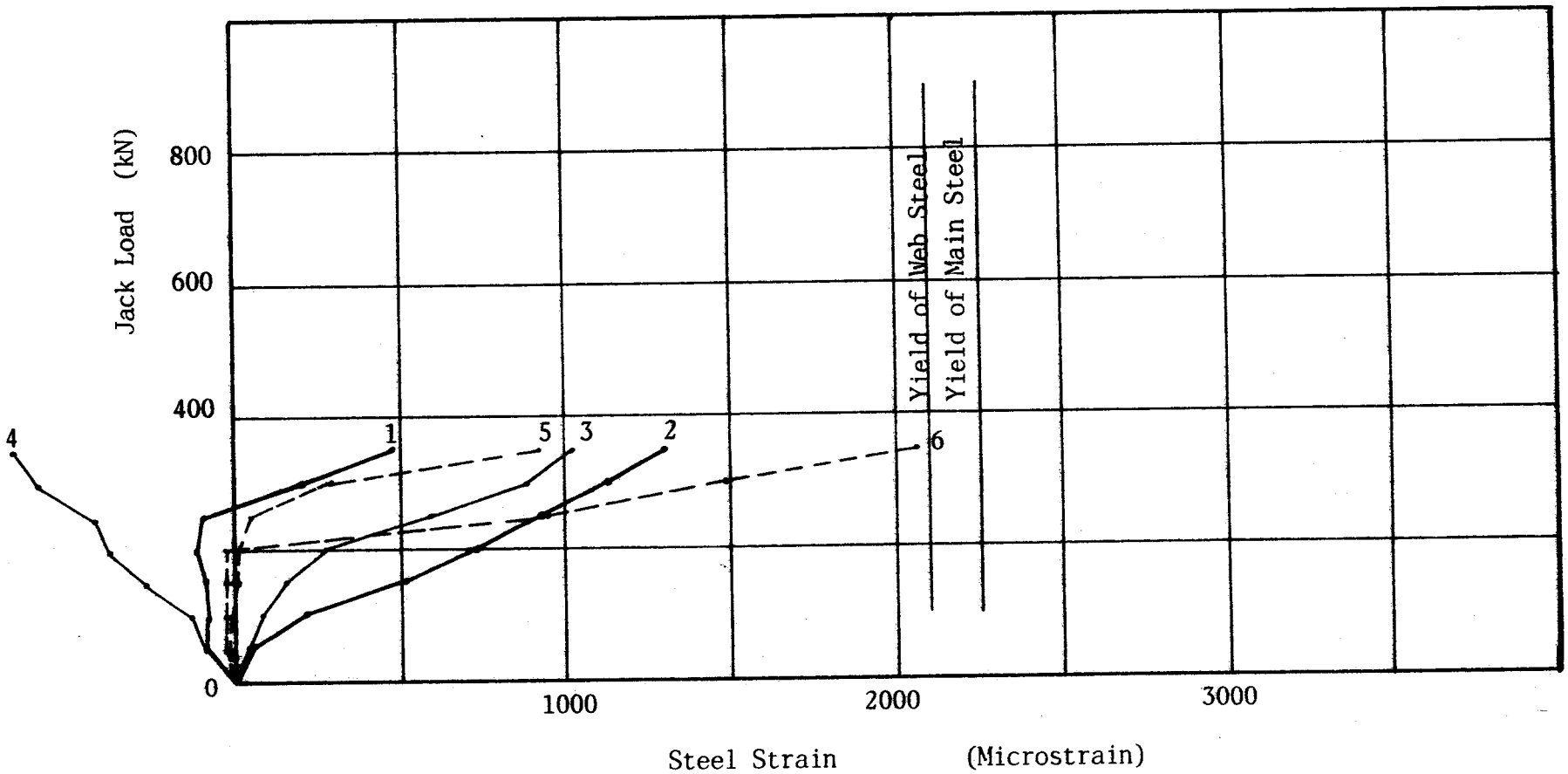

Figure 6.75 Beam 3/2.0 Load vs. Steel Strain

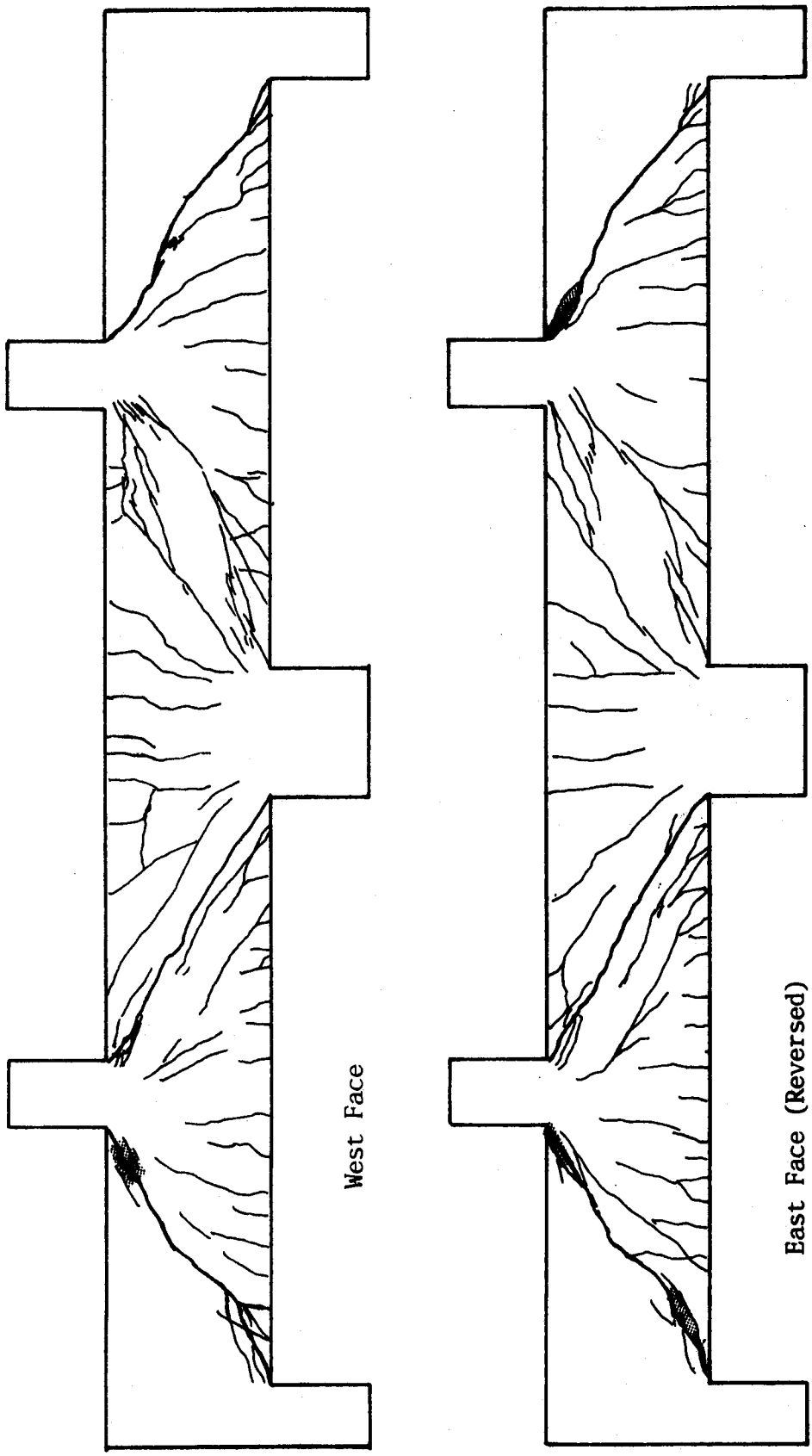

Figure 6.76 Beam 4/2.0 Crack Patterns

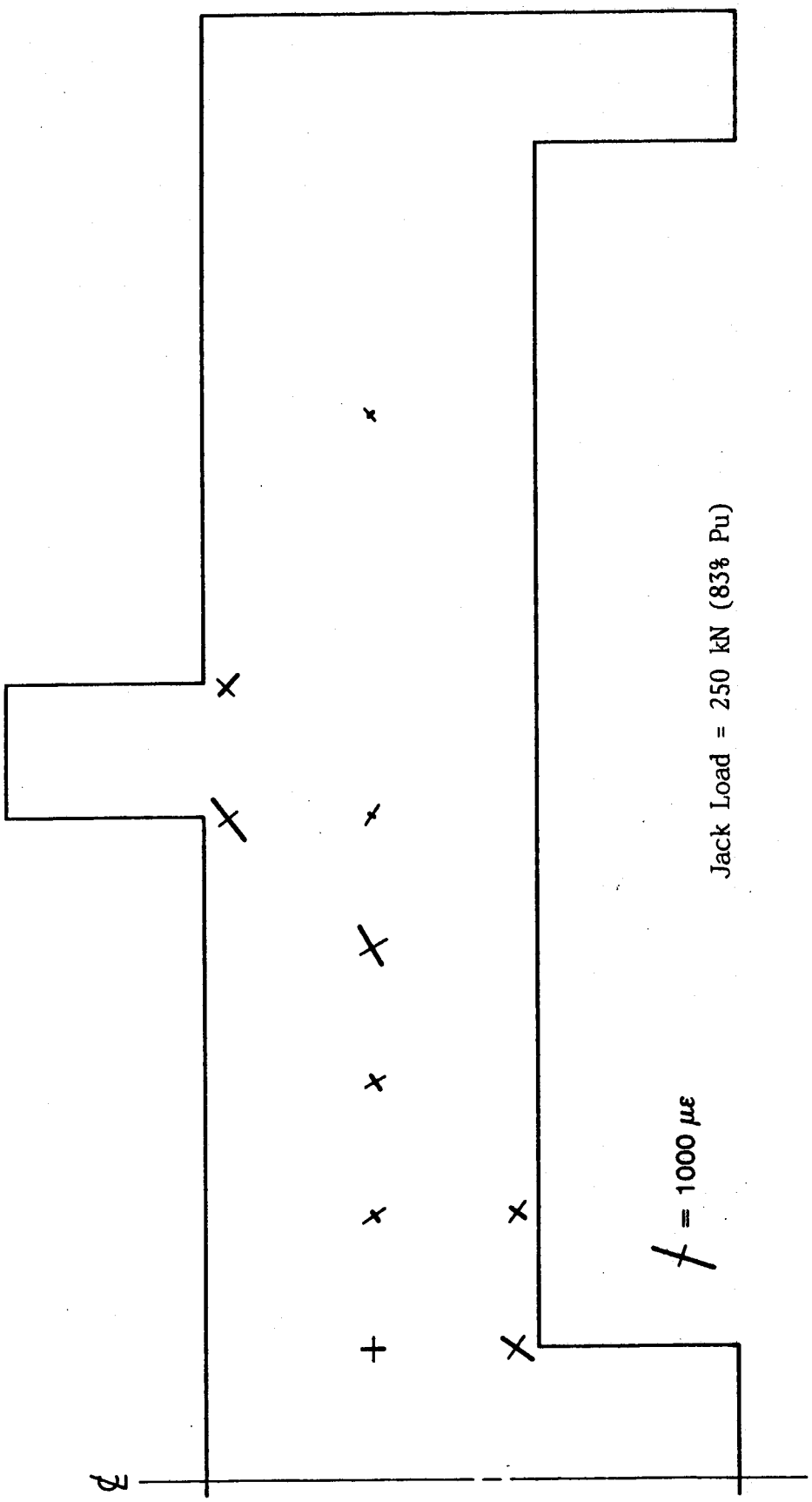

Figure 6.77 Beam 4/2.0 Concrete Compressive Strains

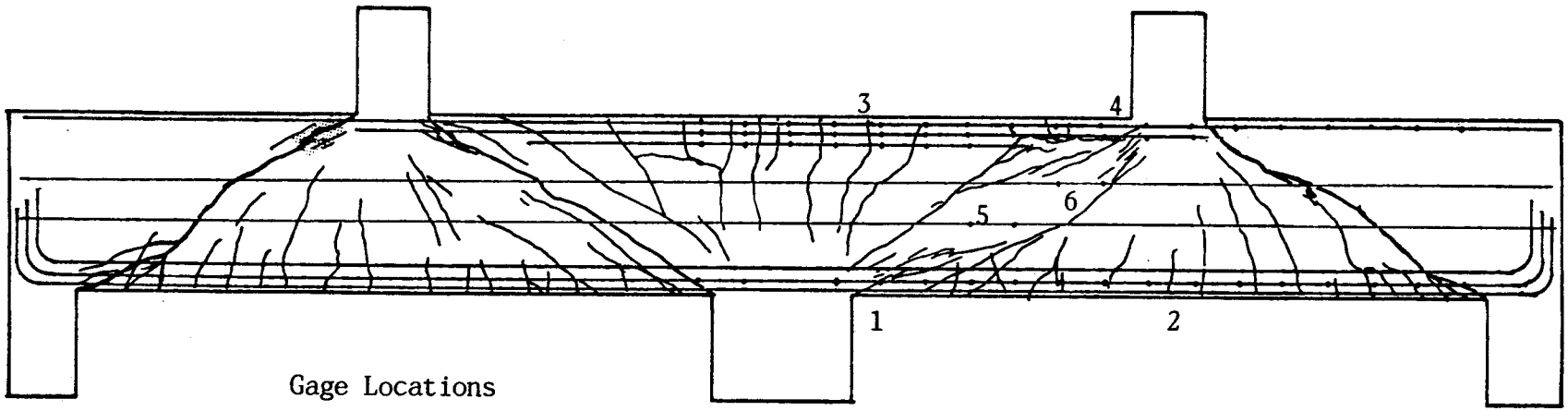

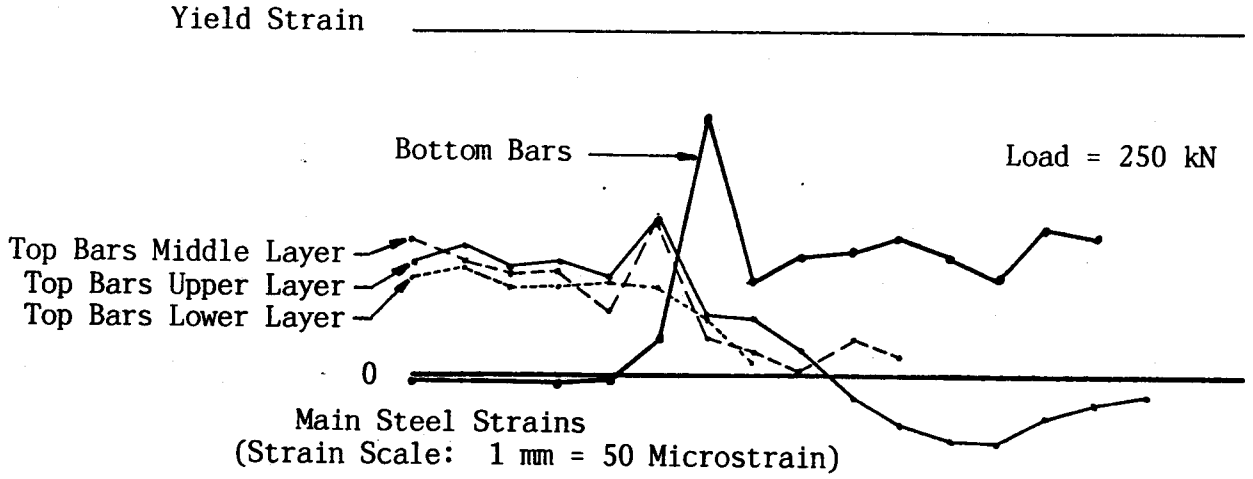

Figure 6.78 Beam 4/20 Steel Strains

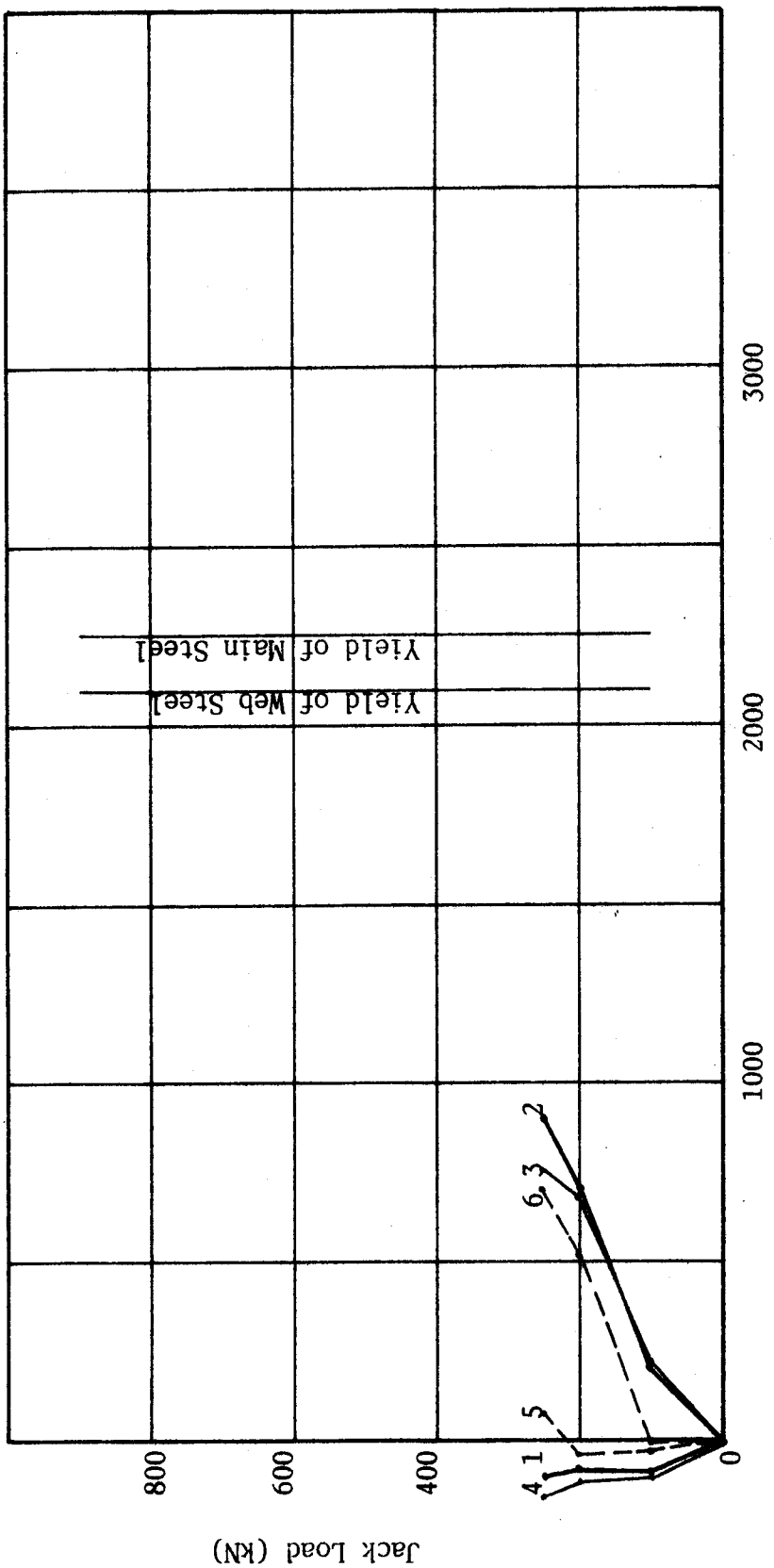

Figure 6.79 Beam 4/2.0 Load vs. Steel Strain

about 376 kN the north exterior shear span failed with a shear compression failure at the top of the inclined crack while the crack opened vertically. The pressure valve to the north jack was closed, thus maintaining load in the north jack, while the south jack load was increased. Horizontal cracking indicated that the top and bottom bars were acting as dowels, and were being peeled back in the south interior shear span. Failure of this span appeared imminent when there was a sudden shear compression failure in the south exterior shear span.

6.24 Beam 5/2.0

This two span beam had maximum stirrup reinforcement throughout. Inclined cracking of the south interior shear span occurred at a load of 370 kN. Inclined cracking in the north interior shear span occurred at a slighly higher but less distinct load. Extensive cracking in the form of "fans" above the interior support, and below each load developed before a very ductile failure in the north interior shear span. There was slow destructon of the concrete at the top of the inclined crack. Similar behavior was exhibited by the south shear span upon reloading. As with beam 5/1.5, the side cover delaminated along the plane of the stirrups.

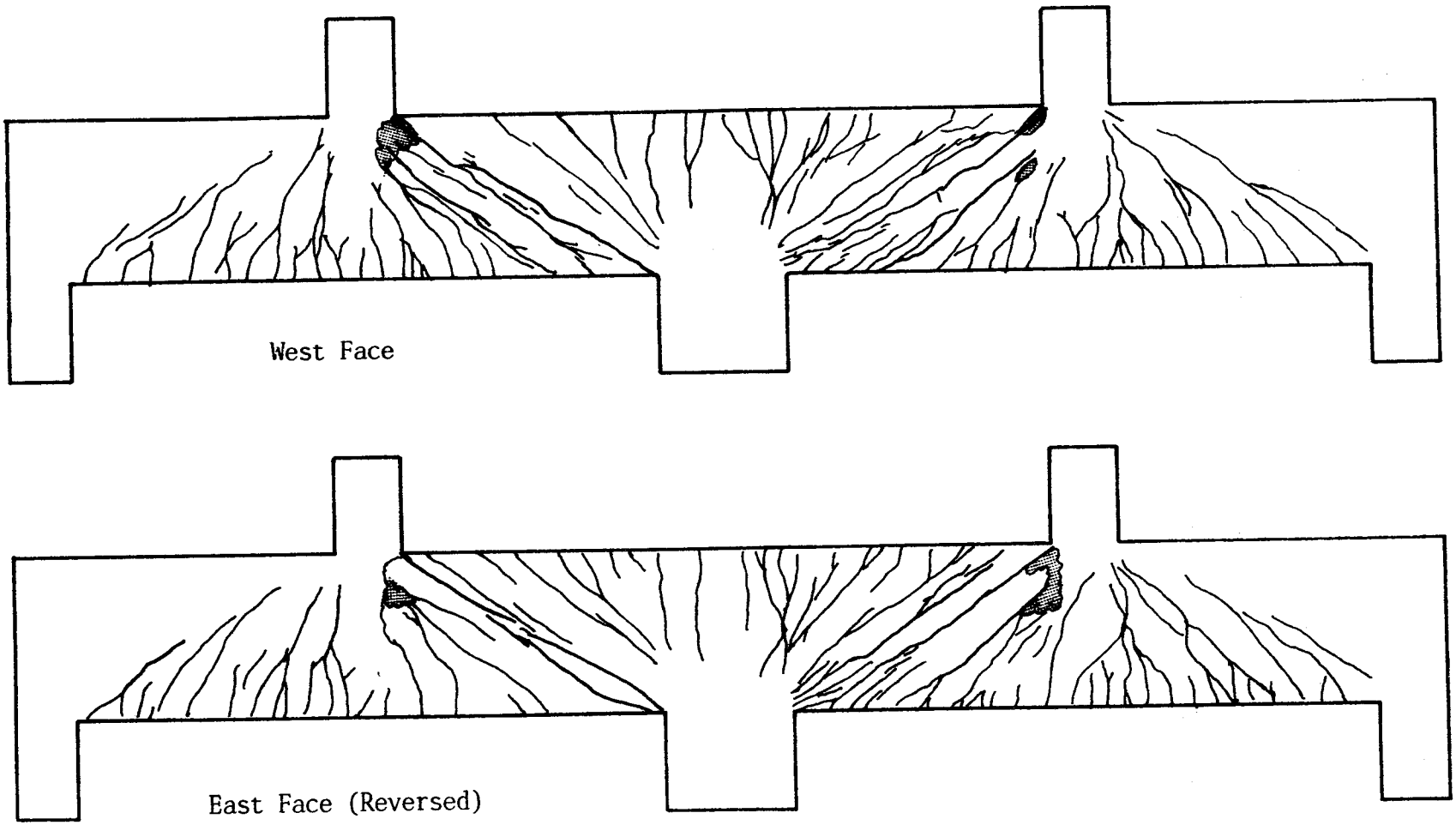

Firue 6.80 Beam 5/2.0 Crack Patterns

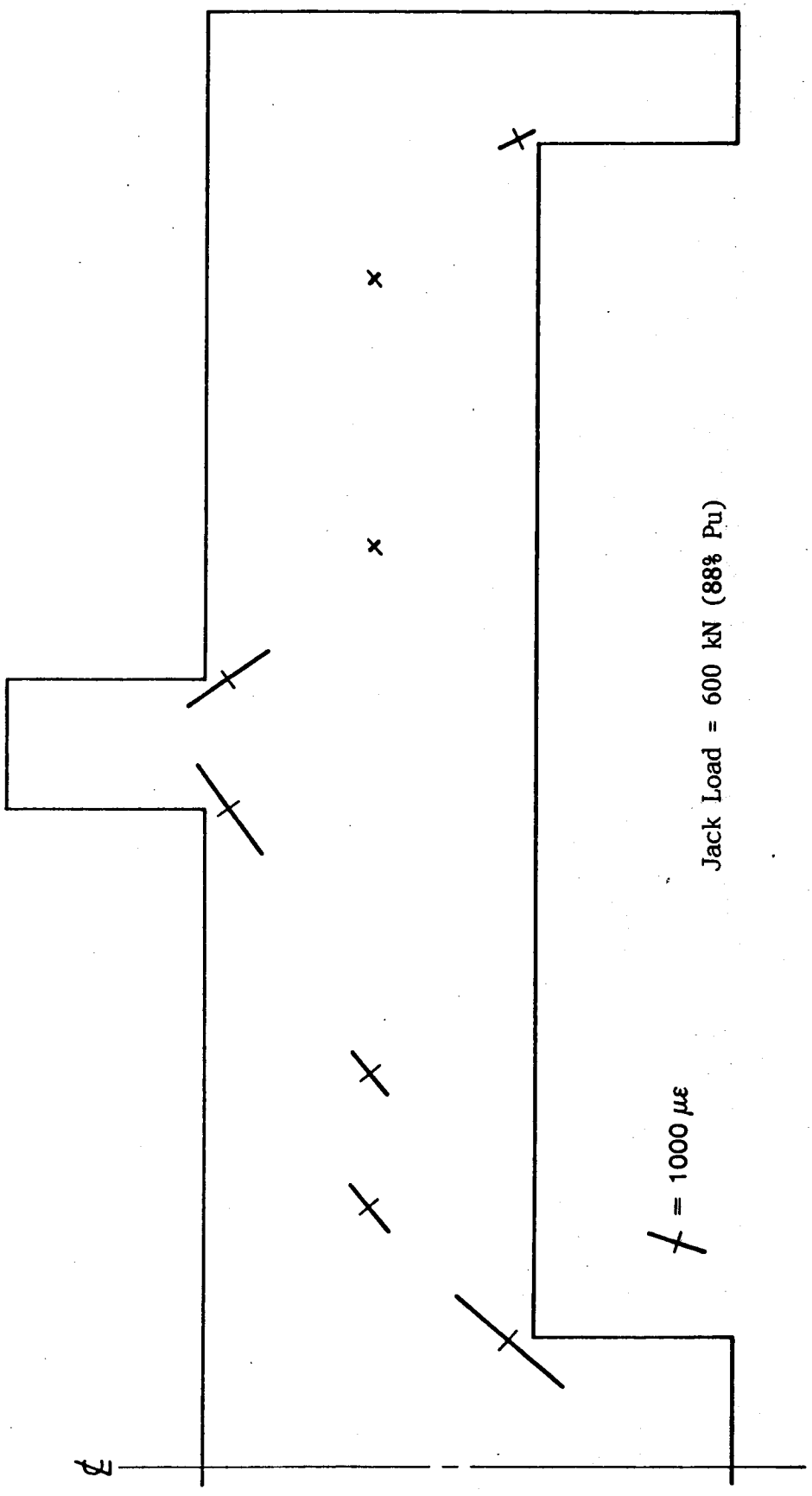

Figure 6.81 Beam 5/2.0 Concrete Compressive Strains

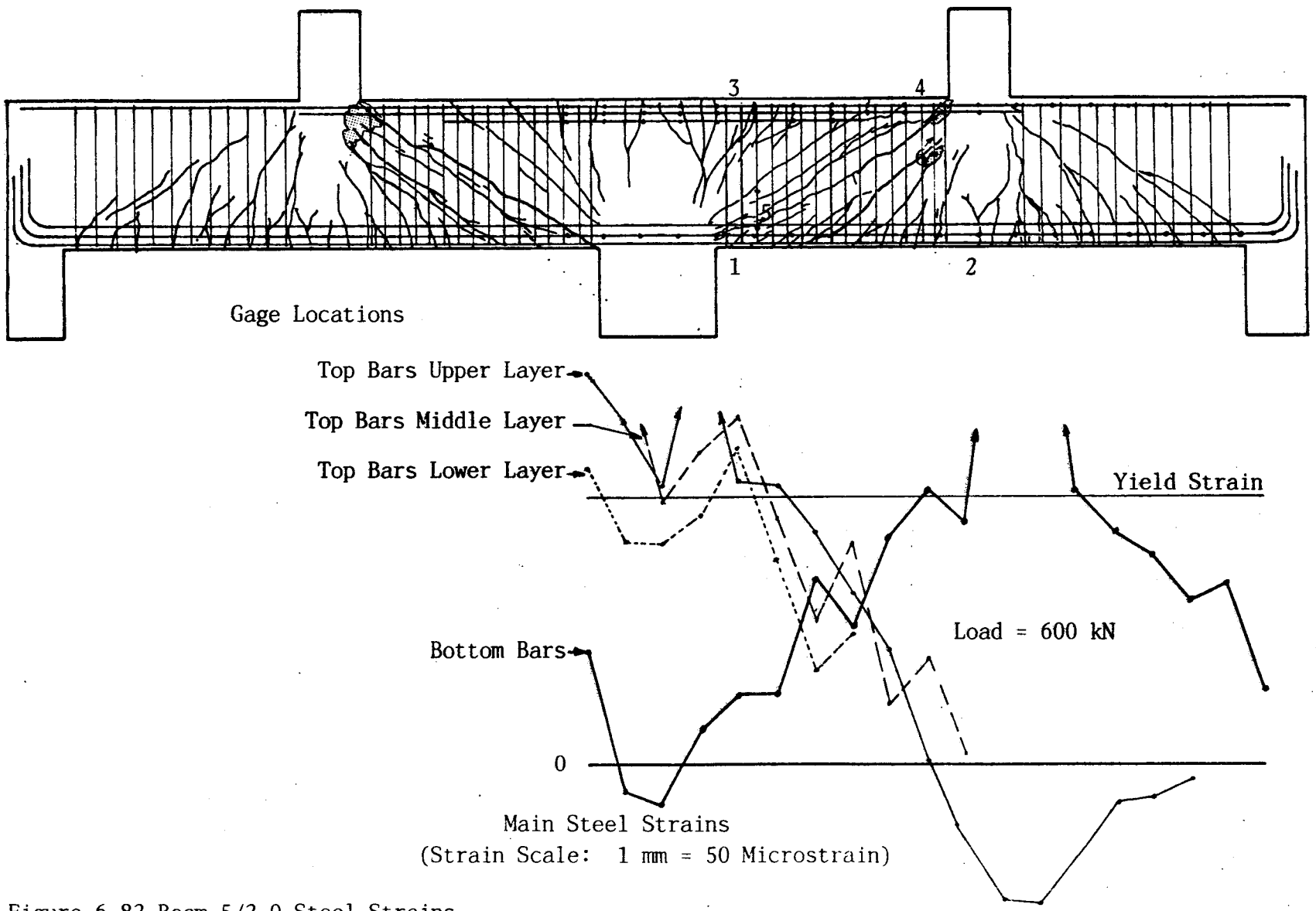

Figure 6.82 Beam 5/2.0 Steel Strains

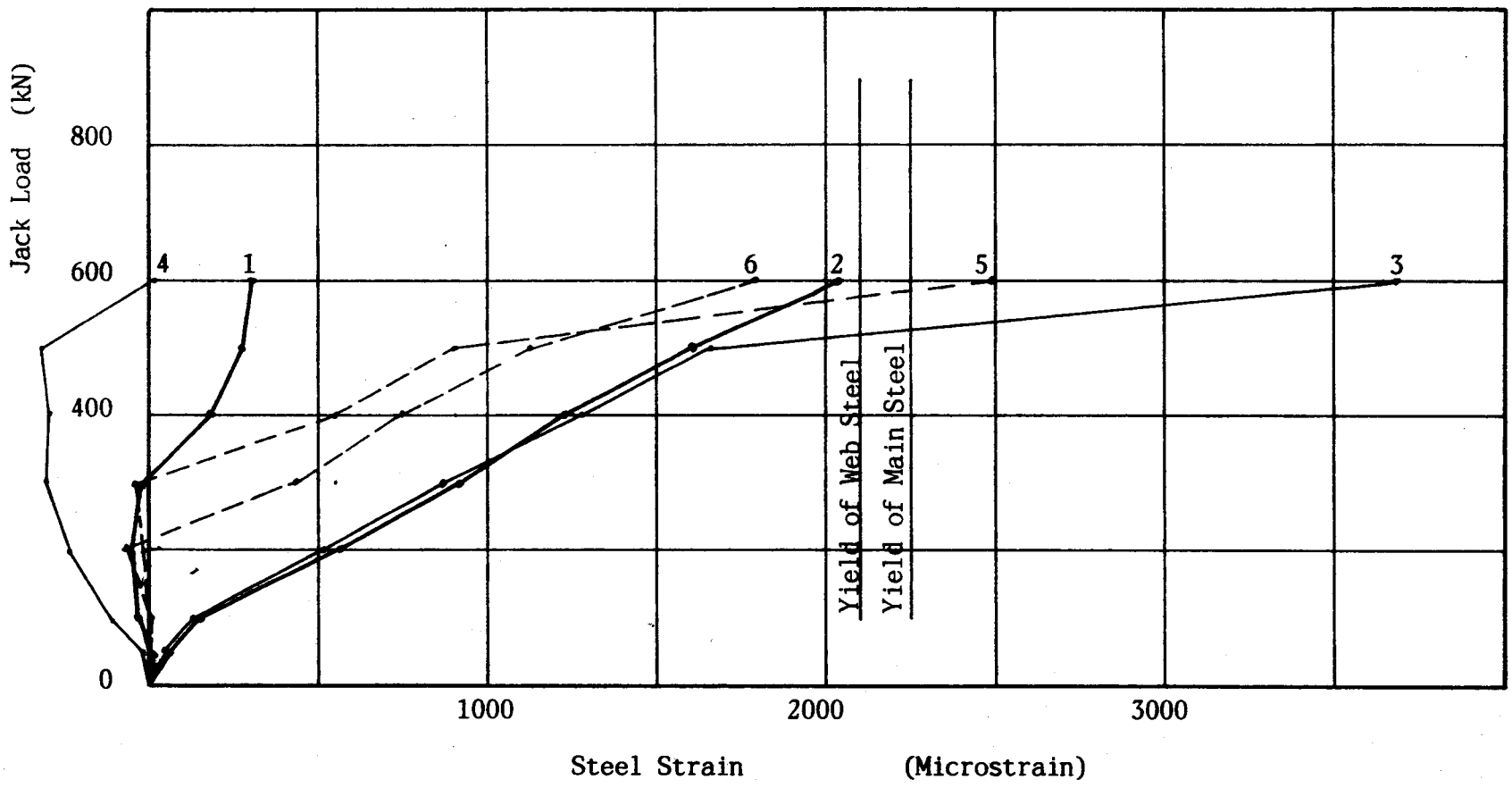

Figure 6.83 Beam 5/2.0 Load vs. Steel Strain

6.25 Beam 6/2.0

This two span beam had maximum horizontal web reinforcement throughout. First inclined cracking occurred in the south interior shear span at a load of 250 kN. The crack extended from about 50 mm below the face of the loading column downward at a slope of about 45 degrees, until it flattened out along the bottom reinforcement. At this load, a similar but steeper crack at 60 degrees from the horizontal developed in the north interior shear span. Dowel splitting developed at the bottom end of both of these inclined cracks. Failure occurred quietly in the south interior span by vertical opening of the major inclined crack with sliding through the concrete at the top of this crack. In the retest, a major corner to corner inclined crack developed in the north interior shear span. Quiet failure of this shear span followed shortly. In this beam, the inclined cracks tended to branch or divide into 2 or 3 smaller cracks at about the middle of the shear span. These smaller cracks would coalesce into a single major crack above and below this region. The 2 or 3 smaller cracks coalesced or sheared through as a vertical opening mechanism developed at failure.

For reasons which are not clear, this beam had more positive flexural cracks in the exterior shear spans than the other specimens.

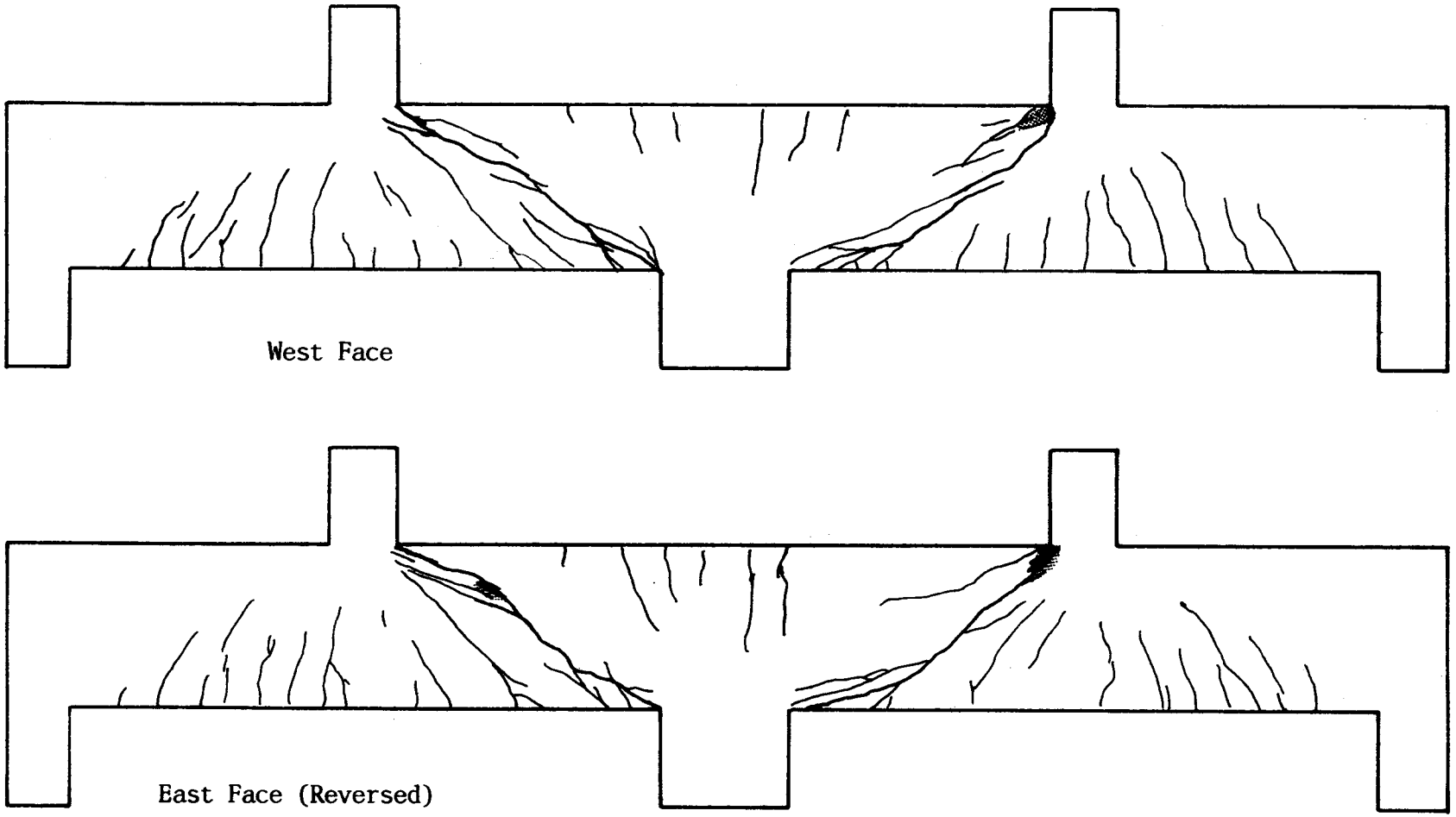

Figure 6.84 Beam 6/2.0 Crack Patterns

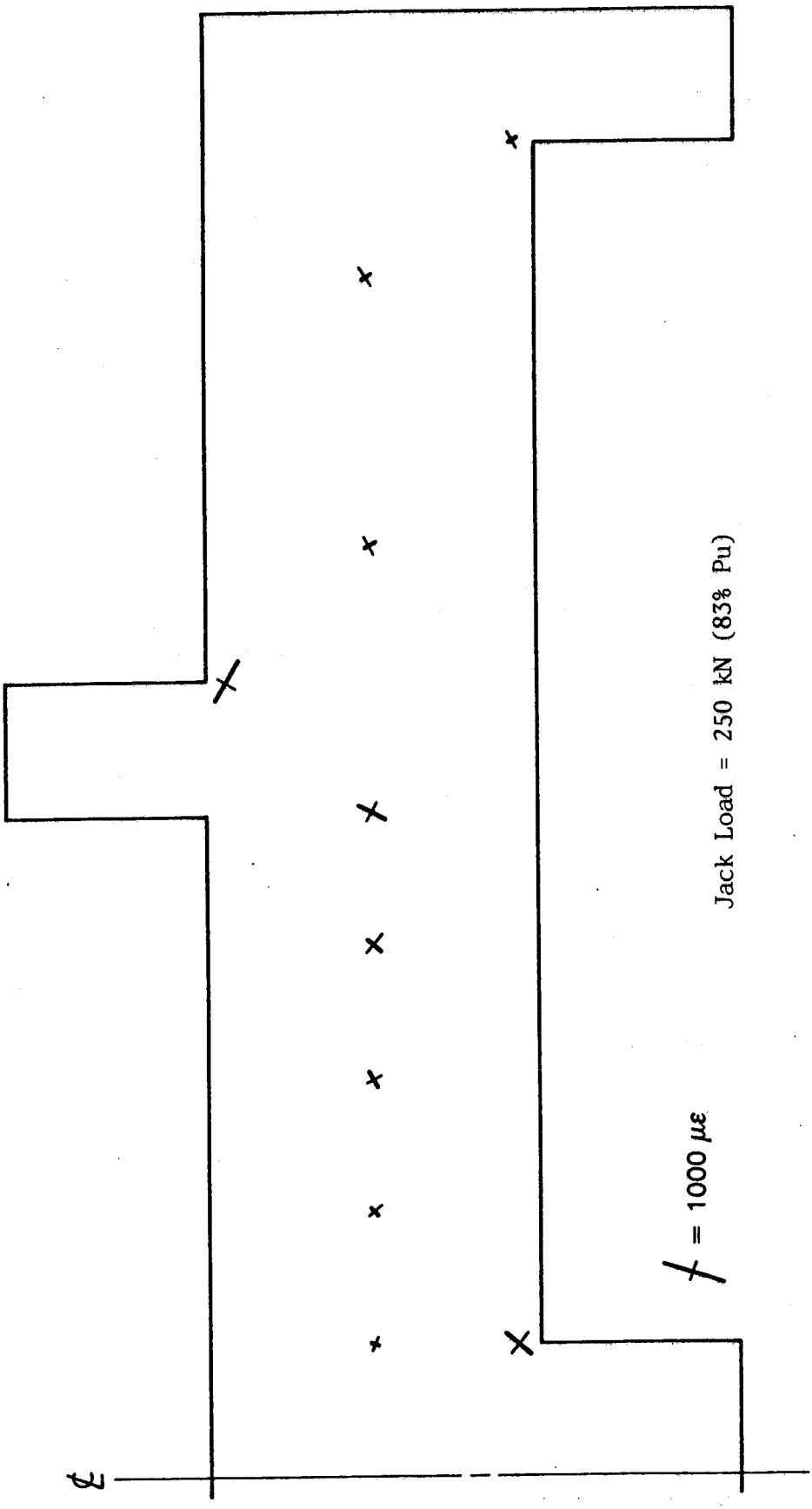

Figure 6.85 Beam 6/2.0 Concrete Compressive Strains

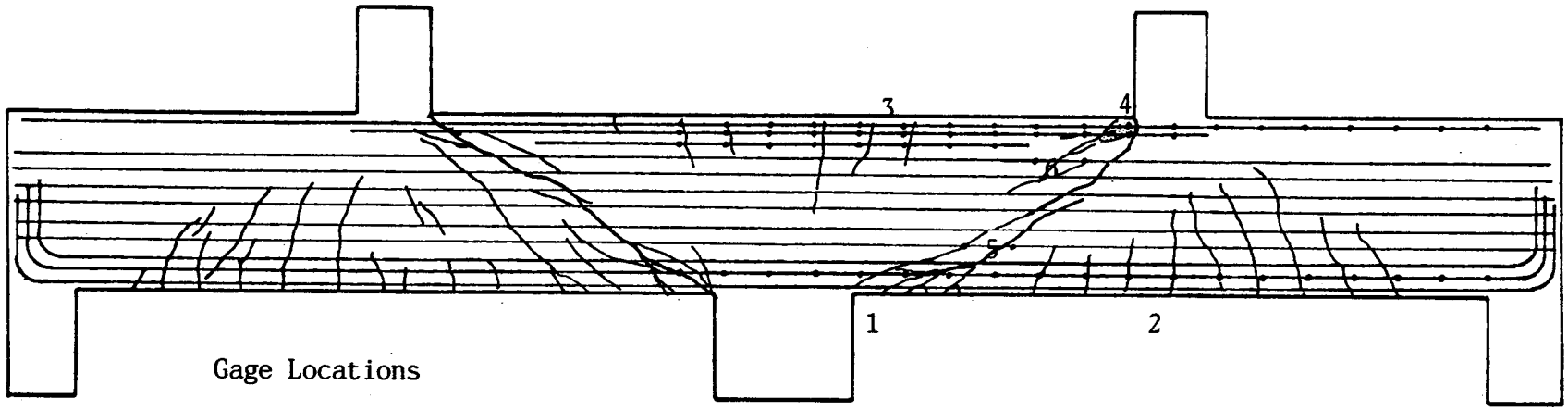

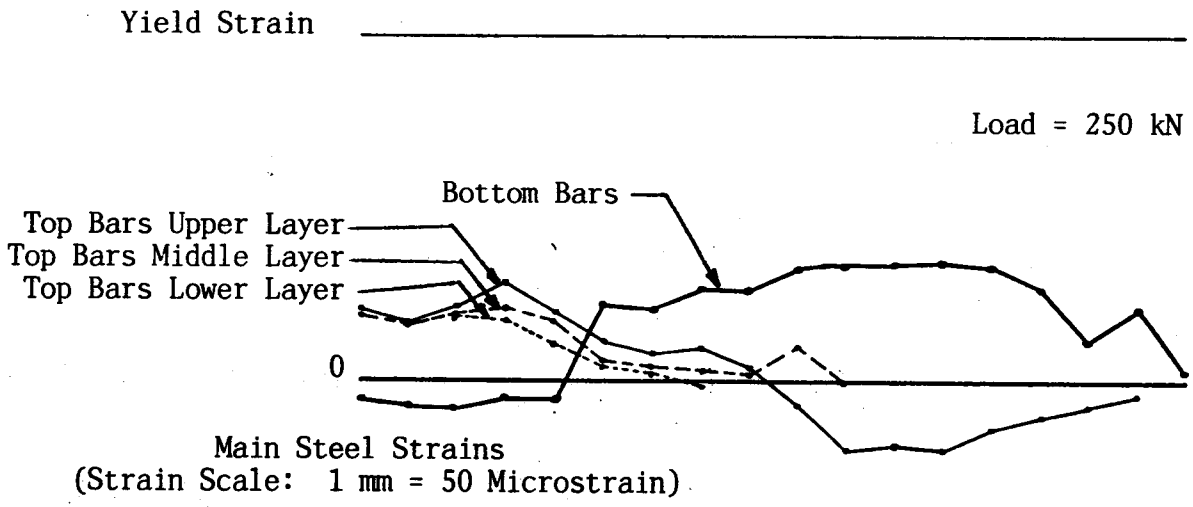

Figure 6.86 Beam 6/2.0 Steel Strains

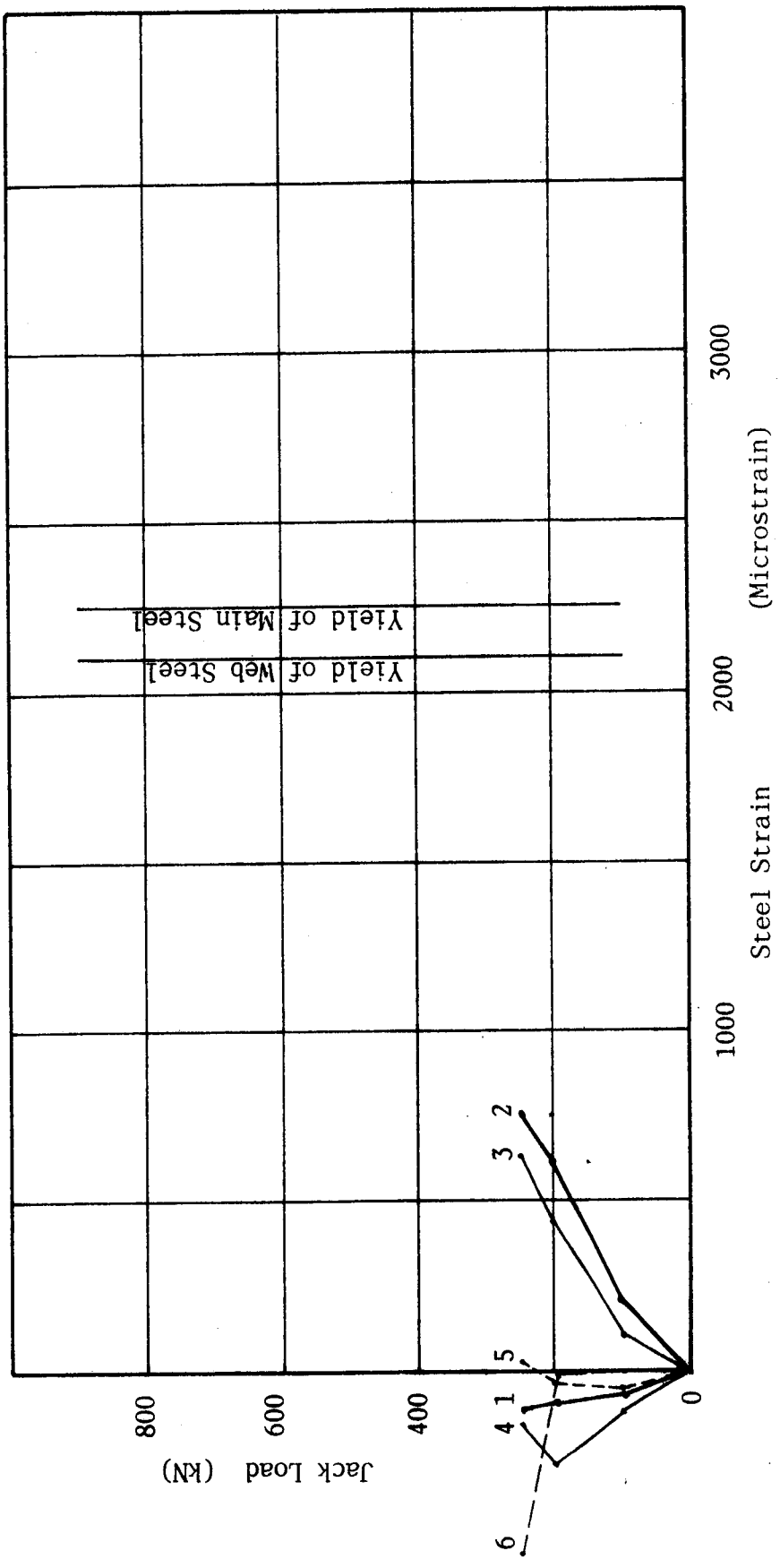

Figure 6.87 Beam 6/2.0 Load vs. Steel Strain

6.26 Beam 7/2.0

This two span beam did not have any web reinforcement. Some flexural shear cracks developed in the north exterior shear span and it appeared that these would produce a failure, since all other cracks were flexural and were very small. However, at 298 kN, the south interior shear span failed with the very sudden and loud formation of a diagonal tension crack running corner to corner. This crack was quite straight with a slight deviation as it crossed the top bars. The crack opened about 6 mm vertically, and closed horizontally perhaps 1.5 mm. The retest produced a similar failure crack in the north interior shear span.

6.27 Beam 5/2.5

This two span beam had maximum stirrups throughout. Inclined cracks developed in both interior shear spans about 350 kN. They formed very quietly and were narrow. Extensive crack fans developed over the interior support and under each load. The behavior was very ductile with a positive moment hinge forming at the south face of the south loading column. The north interior shear span failed in a very ductile manner with the "fingers" of the fan over the central supporting column separating from each other by rotating about their lower ends. This rotation produced destruction of the concrete in the region of the centre of rotation. Because of the extensive yielding in the south span, the specimen was not retested, so no shear failure was

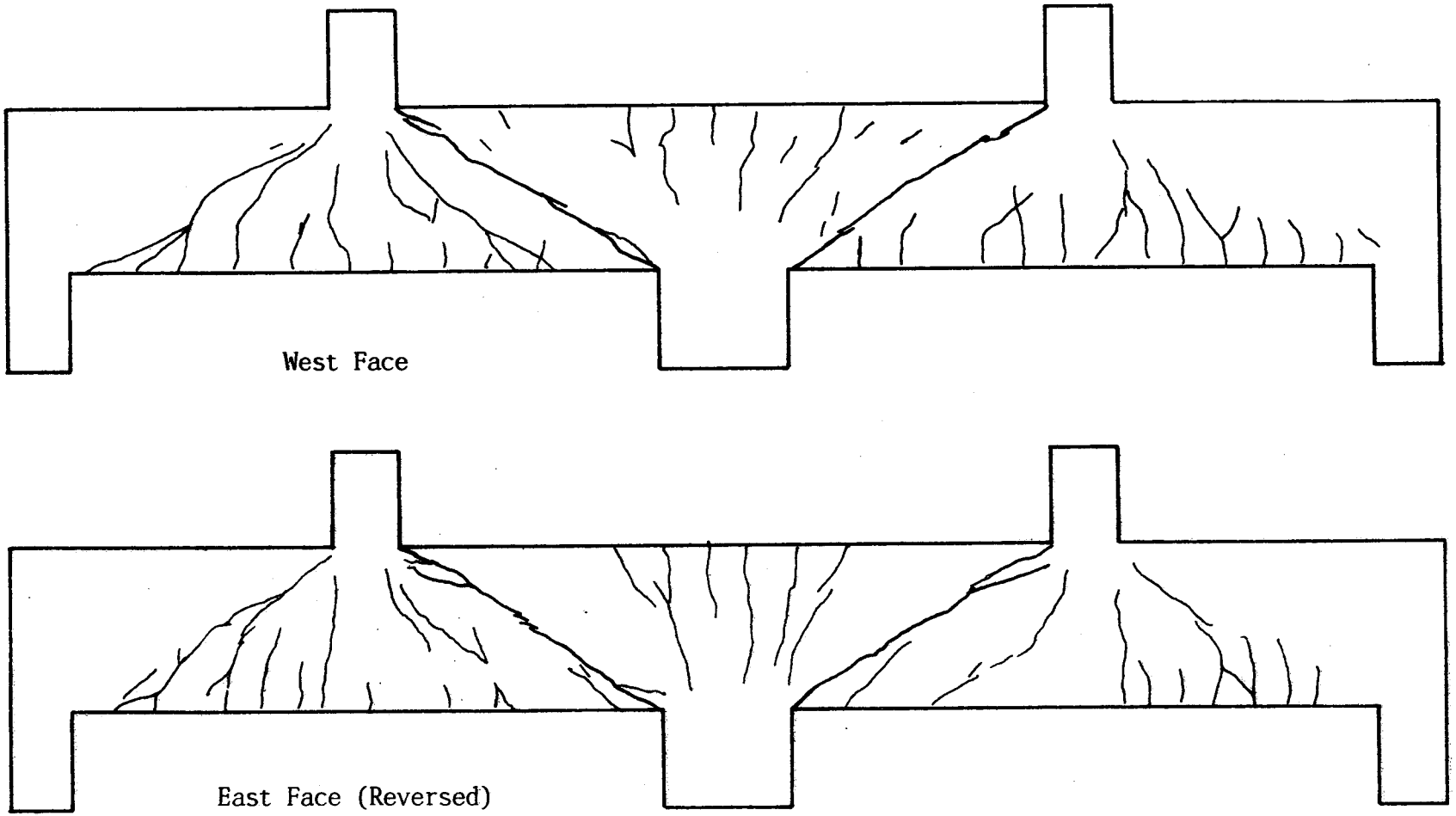

Figure 6.88 Beam 7/2.0 Crack Patterns

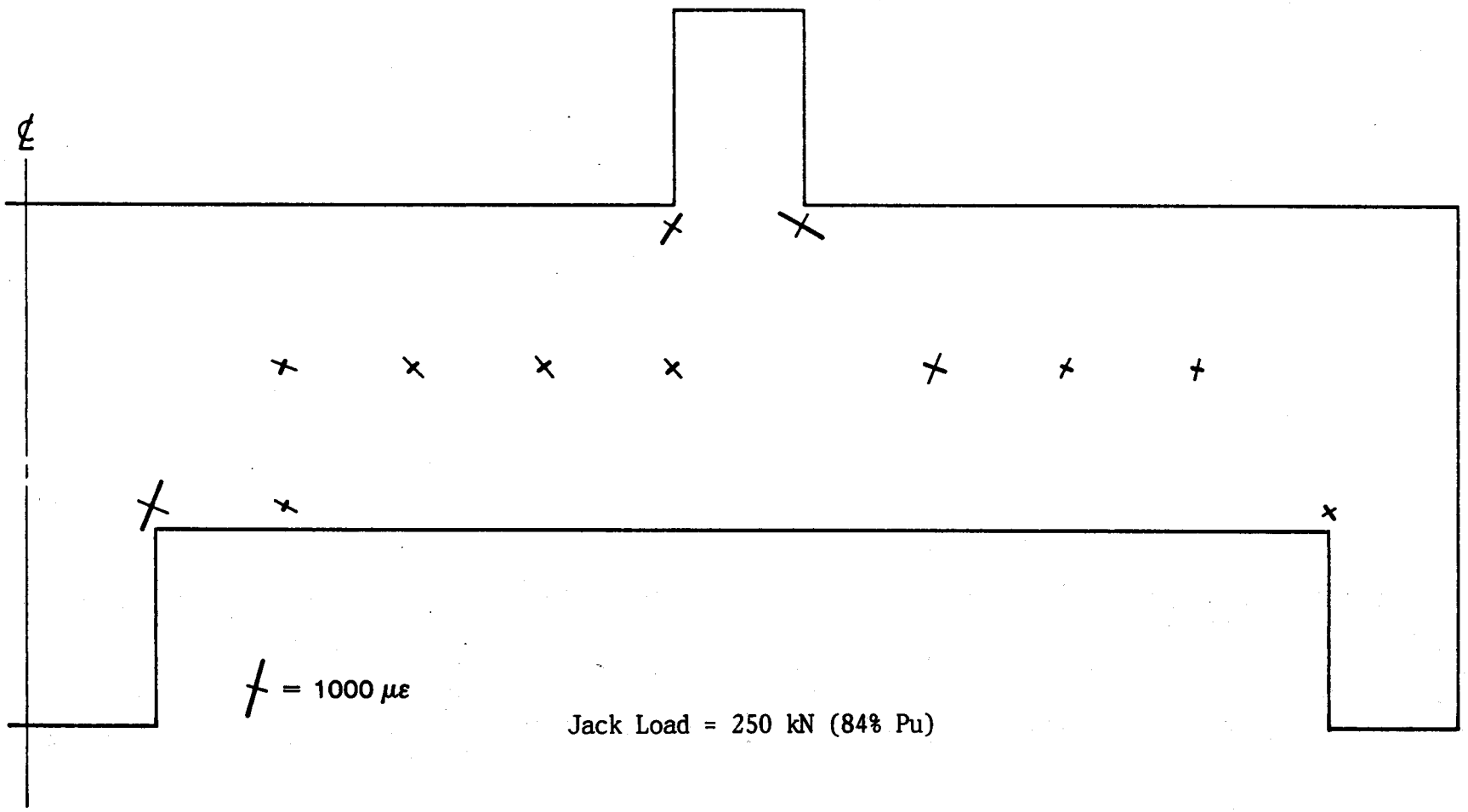

Figure 6.89 Beam 7/2.0 Concrete Compressive Strains

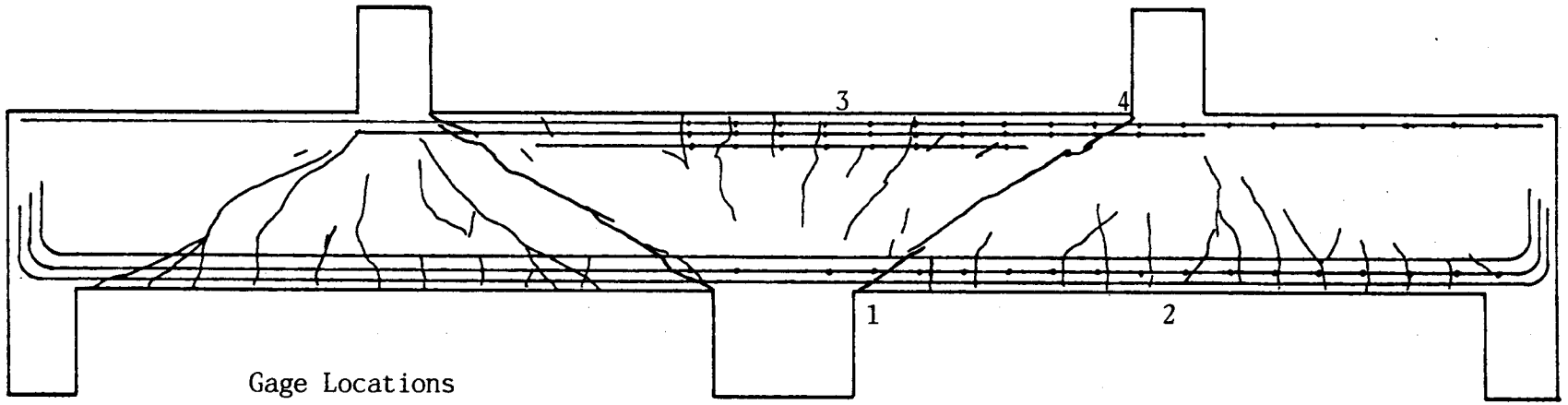

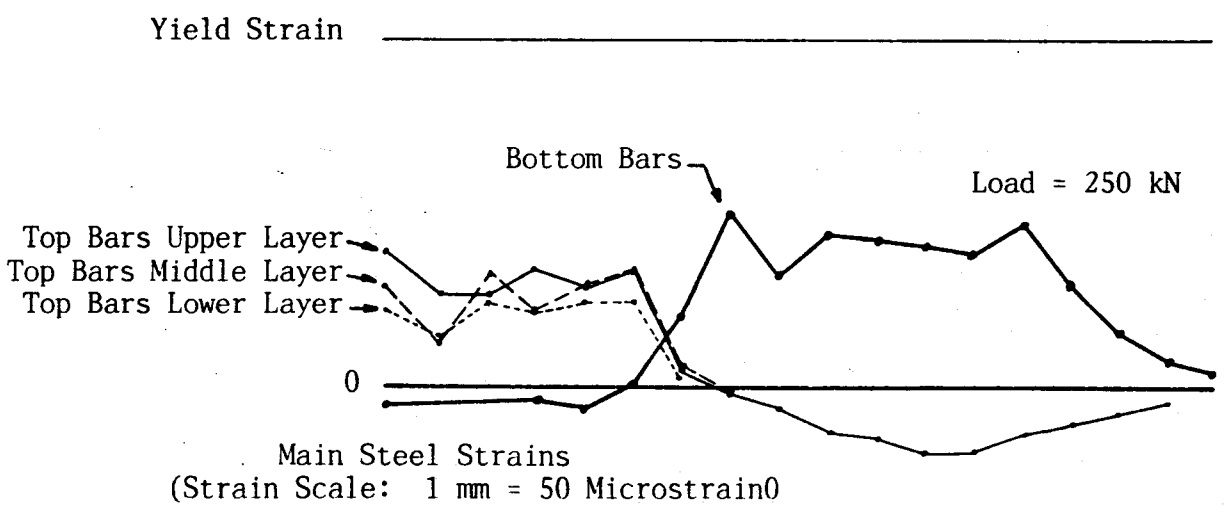

Figure 6.90 Beam 7/2.0 Steel Strains

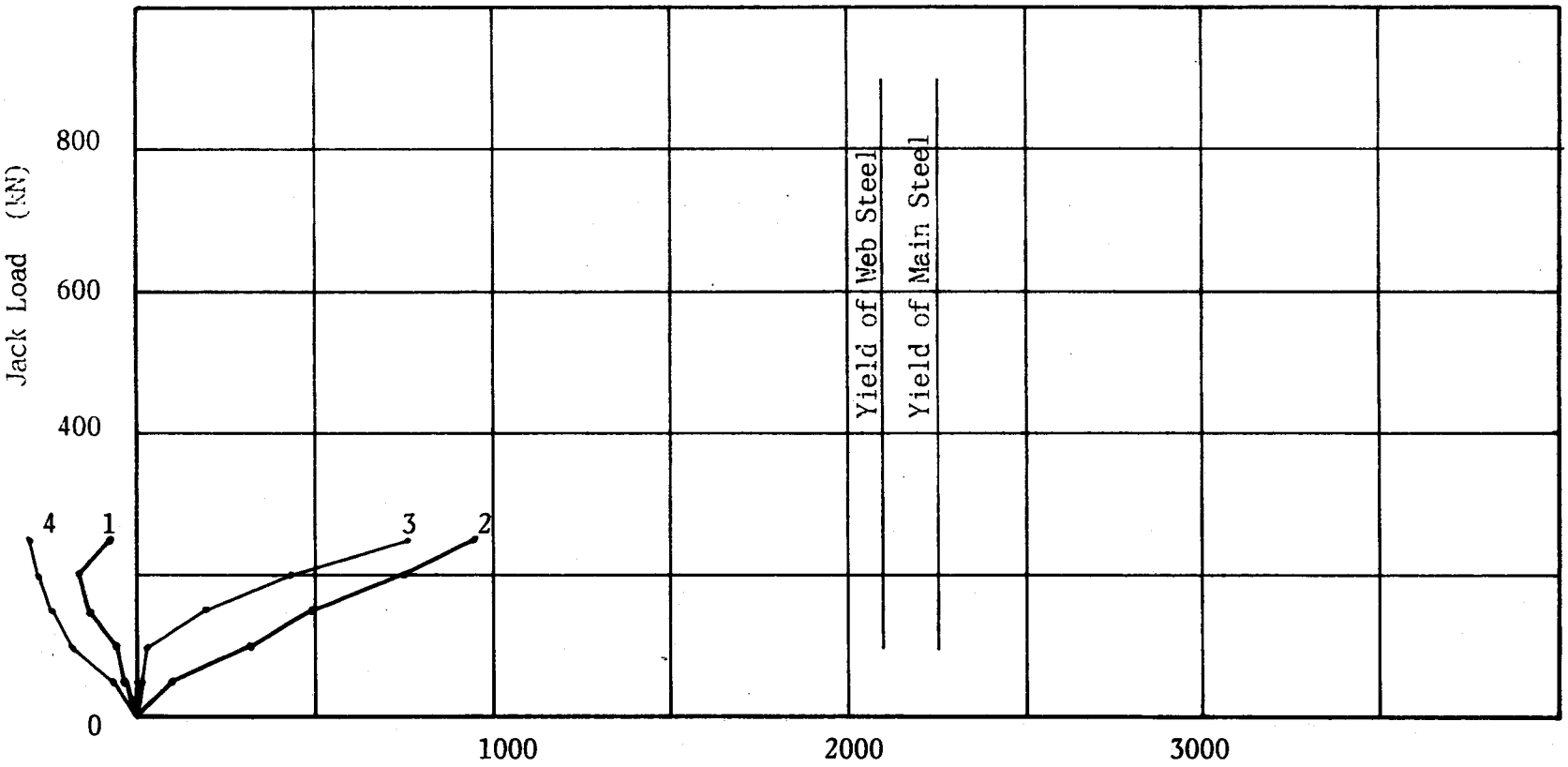

Figure 6.91 Beam 7/2.0 Load vs. Steel Strain

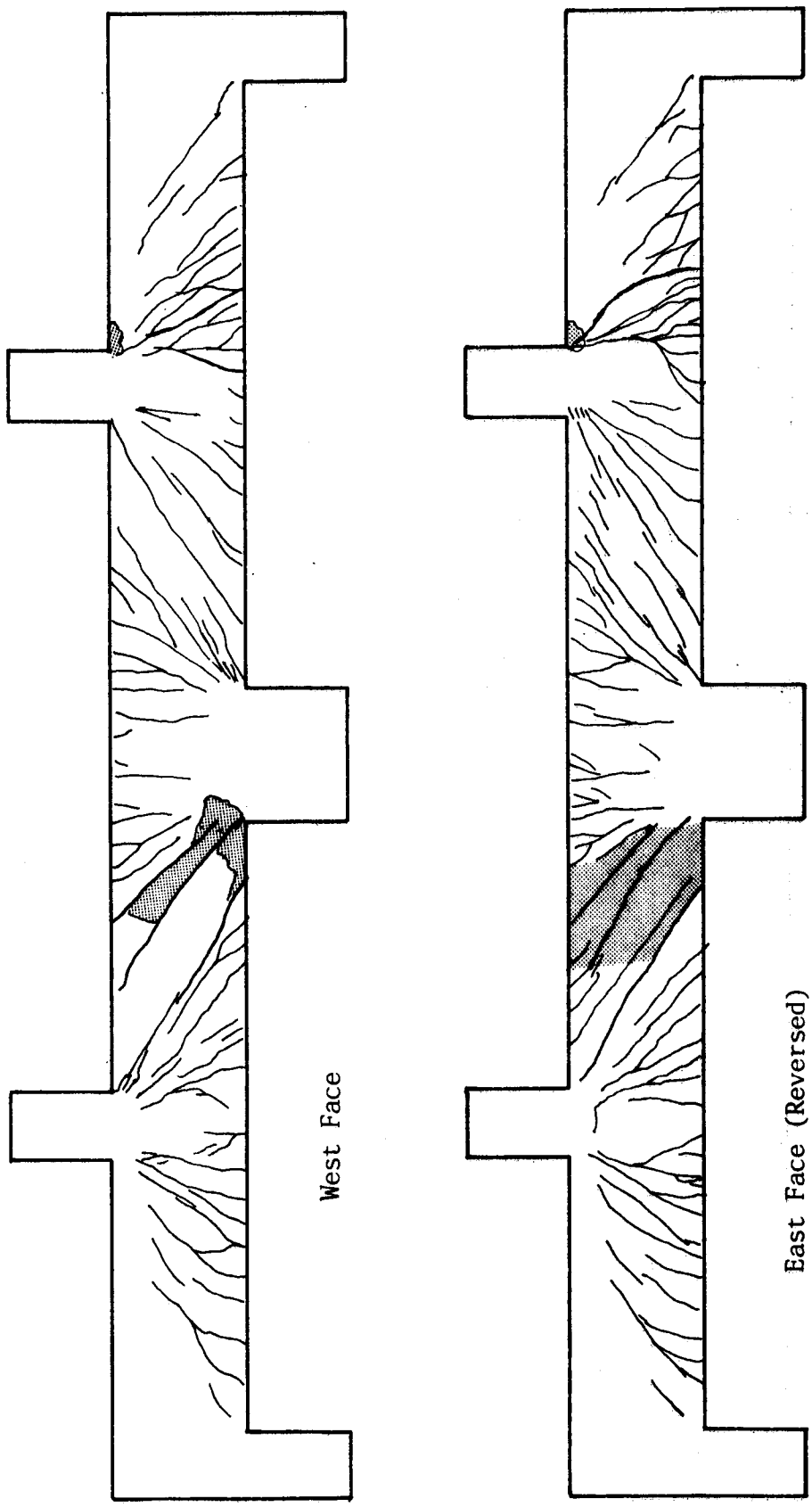

Figure 6.92 Beam 5/2.5 Crack Patterns

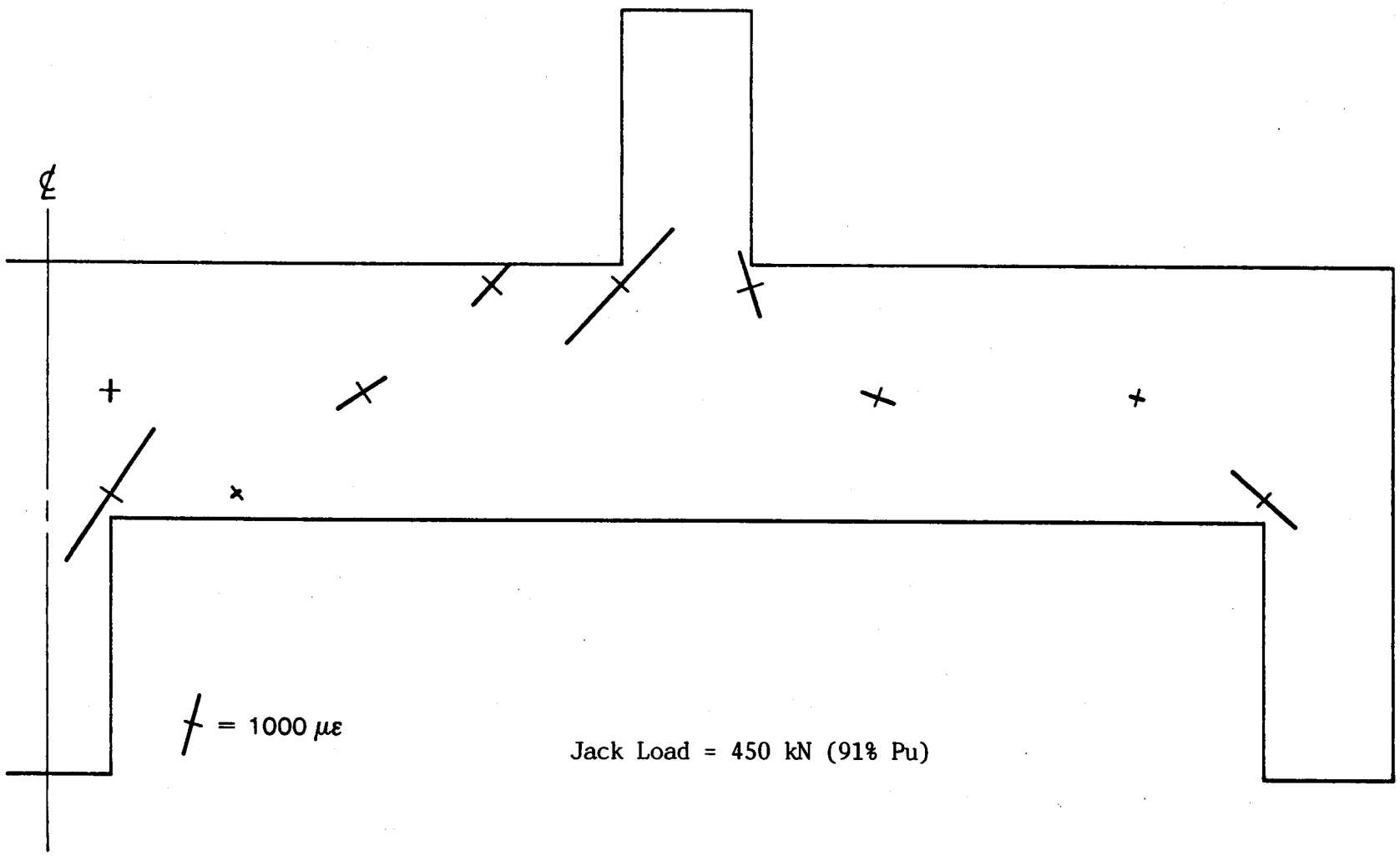

Figure 6.93 Beam 5/2.5 Concrete Compressive Strains

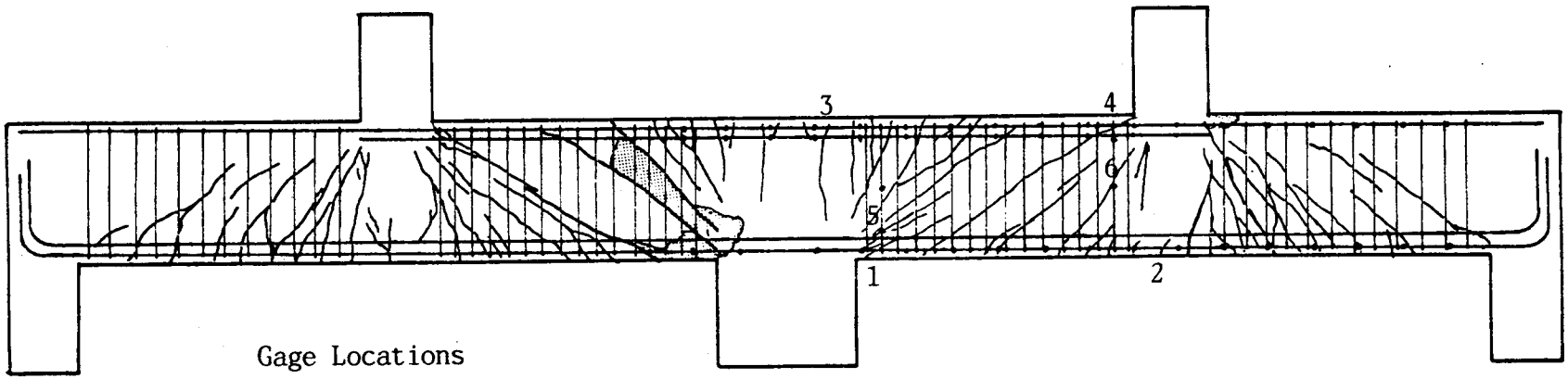

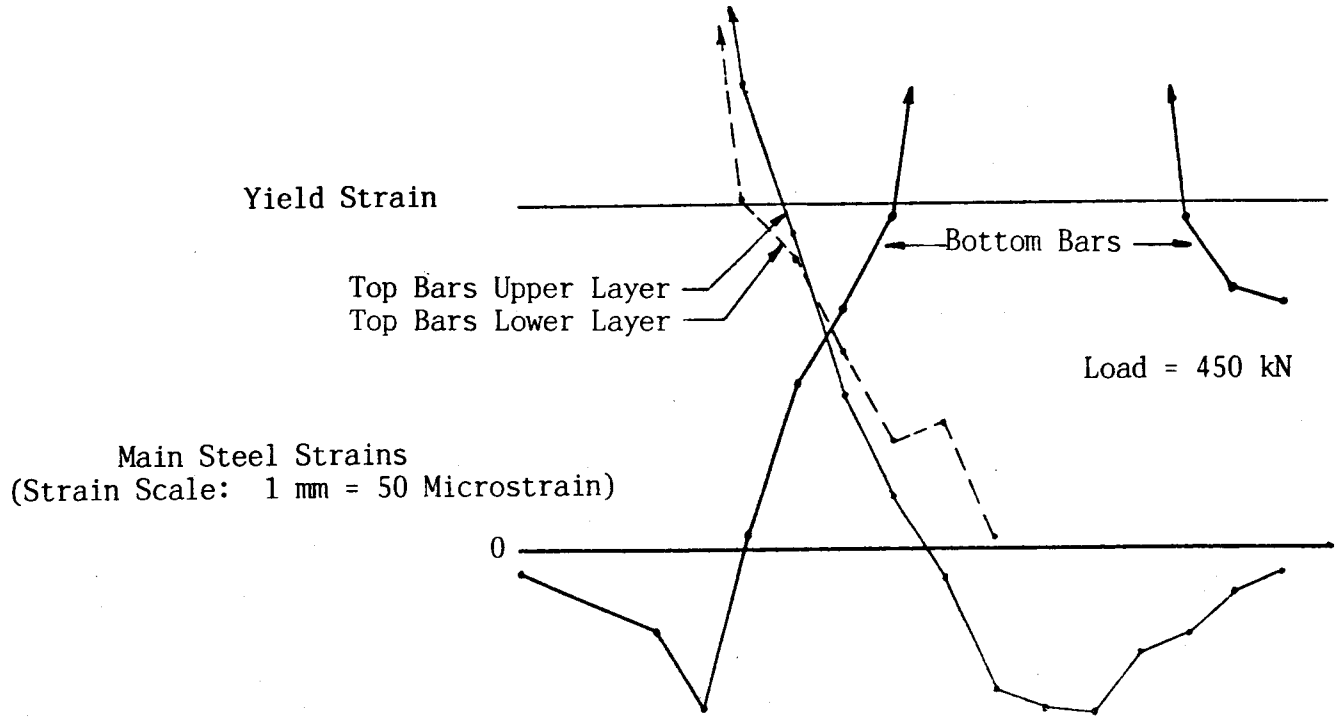

Figure 6.94 Beam 5/2.5 Steel Strains

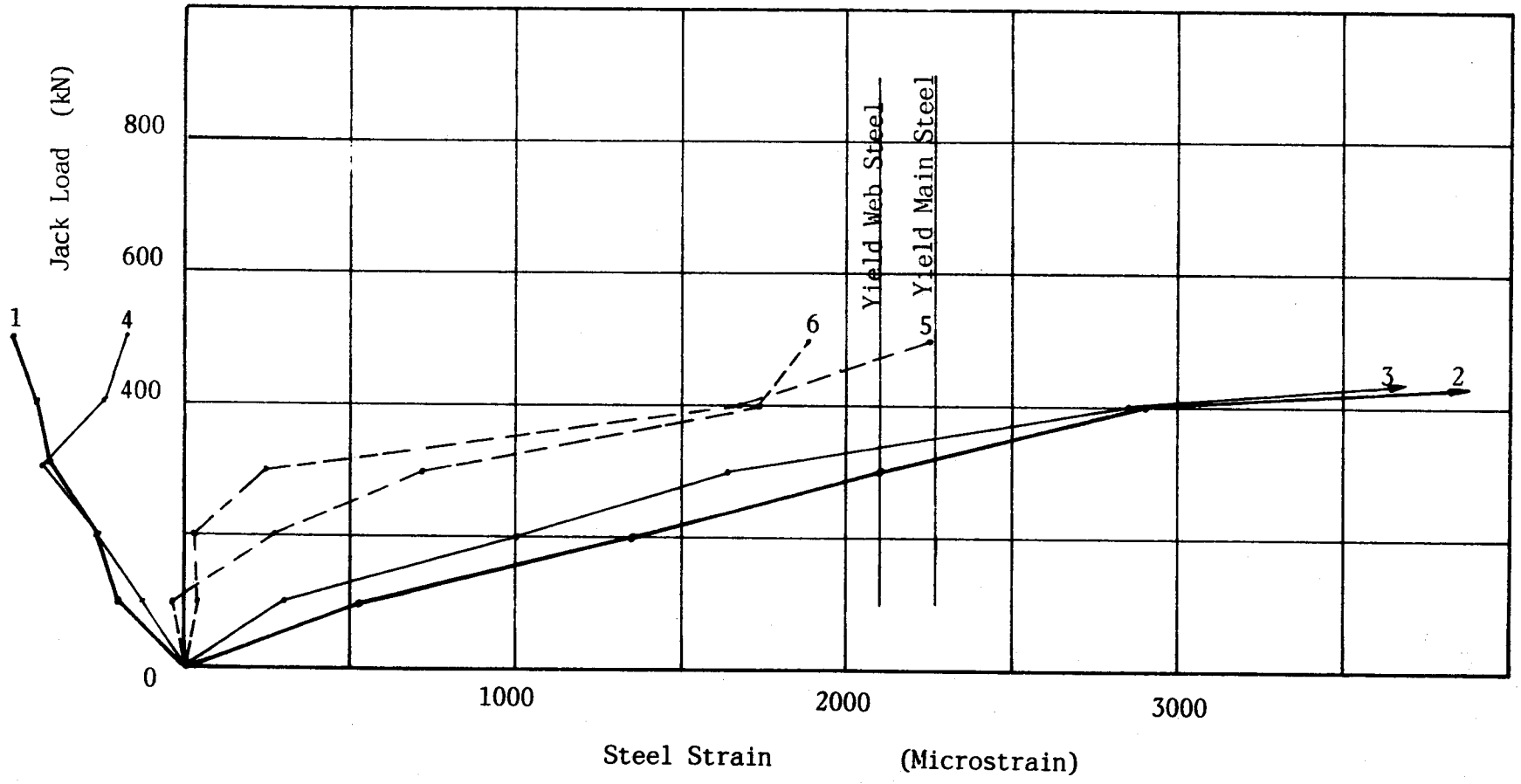

Figure 6.95 Beam 5/2.5 Loads vs. Steel Strain

obtained in the south interior shear span. As with other beams which had maximum stirrups, the side cover delaminated from this beam along the plane of the stirrups.

7. Summary and Conclusions

While the results of any single test should not be given too much statistical significance, some general observations can be made by considering all of the specimens together. The formation of cracks started with flexural cracks originating at the bottom reinforcement (positive flexural cracks). In the continuous beams this was followed by the development of negative flexural cracks over the interior support. The flexural cracks started small and grew with increased load. The beams tested developed very distinctive inclined cracks. These cracks formed very suddenly. Their formation was usually accompanied by a loud "thud". The entire inclined crack formed immediately and did not grow in length with subsequent increases in load. In the deepest beams, these inclined cracks formed well before failure. The inclined cracks delineated concrete compression struts which carried load directly to the support. Ultimate failure was usually due to shear-compression or crushing at the end of one of these struts.

The data presented in this report is analysed in Rogowsky and MacGregor, "Shear Strength of Deep Reinforced Concrete Continuous Beams", Structural Engineering Report No. 110, Department of Civil Engineering, University of Alberta, 1983.